BNL-52574
Formal Report

Proceedings of RIKEN BNL Research Center Workshop Volume 17

HARD PARTON PHYSICS IN HIGH-ENERGY NUCLEAR COLLISIONS

March 1–5, 1999

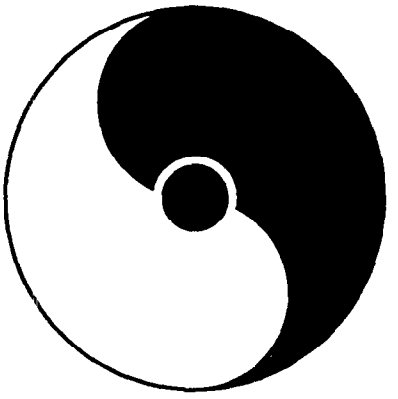

Organizers

Jim Carroll, Charles Gale, Mike Tannenbaum and Raju Venugopalan

RIKEN BNL Research Center

Building 510, Brookhaven National Laboratory, Upton, NY 11973, USA

Other RIKEN BNL Research Center Proceedings Volumes:

Volume 16 - RIKEN Winter School — Structure of Hadrons —Introduction to QCD Hard Processes— BNL-

Volume 15 - QCD Phase Transitions - BNL-52561

Volume 14 - Quantum Fields In and Out of Equilibrium - BNL-52560

Volume 13 - Physics of the 1 Teraflop RIKEN-BNL-Columbia QCD Project First Anniversary Celebration - BNL-66299

Volume 12 - Quarkonium Production in Relativistic Nuclear Collisions - BNL-52559

Volume 11 - Event Generator for RHIC Spin Physics - BNL-66116

Volume 10 - Physics of Polarimetry at RHIC - BNL-65926

Volume 9 - High Density Matter in AGS, SPS and RHIC Collisions - BNL-65762

Volume 8 - Fermion Frontiers in Vector Lattice Gauge Theories - BNL-65634

Volume 7 - RHIC Spin Physics - BNL-65615

Volume 6 - Quarks and Gluons in the Nucleon - BNL-65234

Volume 5 - Color Superconductivity, Instantons and Parity (Non?)-Conservation at High Baryon Density - BNL-65105

Volume 4 - Inauguration Ceremony, September 22 and Non-Equilibrium Many Body Dynamics - BNL- 64912

Volume 3 - Hadron Spin-Flip at RHIC Energies - BNL-64724

Volume 2 - Perturbative QCD as a Probe of Hadron Structure - BNL-64723

Volume 1 - Open Standards for Cascade Models for RHIC - BNL-64722

Preface to the Series

The RIKEN BNL Research Center was established this April at Brookhaven National Laboratory. It is funded by the "Rikagaku Kenkysho" (Institute of Physical and Chemical Research) of Japan. The Center is dedicated to the study of strong interactions, including hard QCD/spin physics, lattice QCD and RHIC physics through nurturing of a new generation of young physicists.

For the first year, the Center will have only a Theory Group, with an Experimental Group to be structured later. The Theory Group will consist of about 12-15 Postdocs and Fellows, and plans to have an active Visiting Scientist program. A 0.6 teraflop parallel processor will be completed at the Center by the end of this year. In addition, the Center organizes workshops centered on specific problems in strong interactions.

Each workshop speaker is encouraged to select a few of the most important transparencies from his or her presentation, accompanied by a page of explanation. This material is collected at the end of the workshop by the organizer to form a proceedings, which can therefore be available within a short time.

T.D. Lee
July 4, 1997

*Work performed under the auspices of U.S.D.O.E. Contract no. DE-AC02-98CH10886.

CONTENTS

Introduction

The RIKEN-BNL center workshop on "Hard parton physics in high energy nuclear collisions" was held at BNL from March 1st–5th, 1999. The focus of the workshop was on hard probes of nucleus-nucleus collisions that will be measured at RHIC with the PHENIX and STAR detectors. There were about 45 speakers and over 70 registered participants at the workshop, with roughly a quarter of the speakers from overseas.

About 60% of the talks were theory talks. A nice overview of theory for RHIC was provided by George Sterman. The theoretical talks were on a wide range of topics in QCD which can be classified under the following:

a) energy loss and the Landau–Pomeranchuk–Migdal effect,
b) minijet production and equilibration,
c) small x physics and initial conditions,
d) nuclear parton distributions and shadowing,
e) spin physics,
f) photon, di–lepton, and charm production,
g) hadronization, and simulations of high pt physics in event generators.

Several of the experimental talks discussed the capabilities of the PHENIX and STAR detectors at RHIC in measuring high pt particles in heavy ion collisions. In general, these talks were included in the relevant theory sessions. A session was set aside to discuss the spin program at RHIC with polarized proton beams. In addition, there were speakers from $D\emptyset$, HERA, the fixed target experiments at Fermilab, and the CERN fixed target Pb+Pb program, who provided additional perspective on a range of issues of relevance to RHIC; from jets at the Tevatron, to saturation of parton distributions at HERA, and recent puzzling data on direct photon production in fixed target experiments, among others.

The breadth and depth of the topics discussed, as well as the close interaction between experiment and theory, made for a very stimulating atmosphere. The idea for such a workshop originated with Klaus Kinder–Geiger, who passed away tragically in the crash of Swissair Flt. 111. Klaus's idea was to have equal numbers of particle and nuclear physicists, theorists and experimentalists, get together and thrash out the various QCD issues relevant to RHIC. It was a very idealistic vision, and in practice it may have worked out somewhat differently from what he had planned. Nevertheless, we believe the atmosphere of the workshop was one he would have enjoyed, and enhanced with his lively spirit. The workshop and these proceedings are dedicated to the memory of Klaus Kinder–Geiger.

Jim Carroll
Charles Gale
Mike Tannenbaum
Raju Venugopalan

Overview of Hard Partons for RHIC

George Sterman

Institute for Theoretical Physics
State University of New York at Stony Brook
Stony Brook, NY 11794-3840, USA

Perturbative Quantum Chromodynamics (pQCD) is the appropriate tool to describe QCD dynamics at short distances. It allows us to treat quantities that are dominated by short-distance physics and are yet observable, directly or indirectly. Hard scattering at RHIC requires a reevaluation of pQCD formalism, appropriate to propagation through a dense, potentially hot, final-state medium. The basic pQCD observables are the total and jet cross sections in e^+e^- annihilation, $\hat{\sigma}(Q) = \sum_{n\geq 0} c_n(Q/\mu)\,\alpha_s(\mu)$. An even richer class of observables can be expressed as factorized *convolutions* of short-distance quantities with long-distance, non-perturbative matrix elements. Examples are hard-scattering cross sections in hadron-hadron, including nucleus-nucleus scattering,

$$\sigma^{\rm phys}_{hh'\to F}(M) = \sum_{ii'} \phi_{i/h}(\mu) \otimes \hat{\sigma}_{ii'\to F}(M/\mu, \alpha_s(\mu)) \otimes \phi_{i'/h'}(\mu)\,, \tag{1}$$

relevant to a large class of final states F, characterized by heavy masses (or high momentum transfers) M, that will be observable at RHIC, including jet, high-p_T hadron, heavy-quark, weak vector boson and direct photon production. The sums are over parton types i and i', with convolutions usually over their fractional momenta. The factorization scale μ separates perturbative dynamics from the long-distance functions ϕ, describing the distributions of partons in hadrons or nuclei, and/or the fragmetation of partons into hadrons. DGLAP evolution equations, of the form $\mu d\phi(\mu)/d\mu = P(\alpha_s(\mu))\otimes\phi$, follow from the independence of the physical cross section from μ, assuming that μ is large enough that $\alpha_s(\mu)$ and $\Lambda_{\rm QCD}/\mu$ are small. With its polarization capability, RHIC will make possible the measurement of spin-dependent distributions. Nuclear collisions will promote corrections to (1) associated with multiple scatterings, which are generally small corrections for nucleons, to prominence.

Of special interest are final states characterized by a hierarchy of hard scales, such as for the production of heavy quarks or of geometrically narrow, but energetic jets. Denoting the induced ratios by r, corrections of the form $\alpha_s^n(\mu)\ \ln^k r$ can arise at each order, with $n \leq k \leq 2n+1$, depending on the dynamics. Resummation techniques typically allows us to organize, and often explicitly to sum, infinite series of such logarithms. Resummation is intimately related to the same factorization properties that lead to Eq. (1), and, in a wider context, to *effective field theory* descriptions of QCD dynamics. In effective field theories, evolution is manifested in the renormalization of composite operators, often path-ordered exponentials, that act as sources of soft gluons, associated with fast-moving partons, $W_\beta = {\rm P}\exp[-ig\int_0^\infty dy\,\beta\cdot A(y\beta)]$.

Relativistic effects translate perturbative dynamics over long distances. For pp collisions, the evolution is between the scattered partons and the surrounding vacuum. In pA collisions, nuclear media modify high-energy final states, typically through modest changes in single-particle spectra or relative transverse momenta. Hard partons in the AA collisions of RHIC may be sensitive probes of early evolution of the produced hot system. The comparison of high-p_T photons and hadrons, studies of jet fragmentation, spectra, rates and correlations each offer information on the distribution of energy in the expanding hadronic matter. The evolution of off-shell partons through hot matter will also serve to test the hadronization process itself.

Factorization at Nonleading Power

(1)

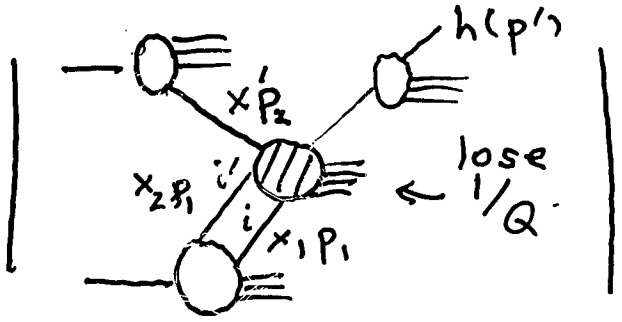

$\sim \sigma_4$

(2)

$$\omega \frac{d\sigma_4}{d^3p'} = \sum_{(ii')jk} \int \frac{dx'}{x'} f_{j/P_2}(x') \int \frac{dz}{z^2} D_{h/k}(z)$$

$$\times \int dx_1 dx_2 dx_3 T_{(ii')/P_1}(x_1, x_2, x_3) \times \hat{\sigma}^{(4)}_{(ii')+j\to k}$$

(3)

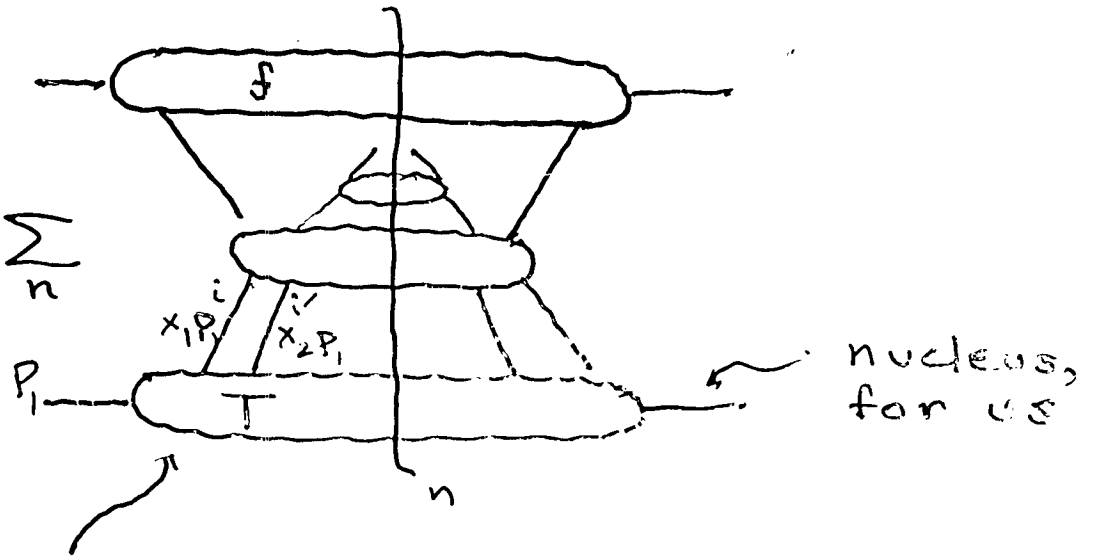

(4)

$$T(x_i) = \int \frac{dy_1^- dy_2^- dy_3^-}{(2\pi)^3} e^{ip^+(x_1y_1^- + x_2y_2^- + x_3y_3^-)}$$

$$\times t_{\alpha\beta\gamma\delta} \langle P | B^\dagger_{i\alpha}(0) \hat{B}^\dagger_{i'\beta}(y_3) B_{i'\gamma}(y_2) B_{i\delta}(y_1) |$$

R. Ellis, Furmanski, Petronzio (82) } DIS
R. Jaffe (82), J. Qiu (90)

- Why?

Formal arguments: J. Qiu, G.S. (1991)

Heuristic:

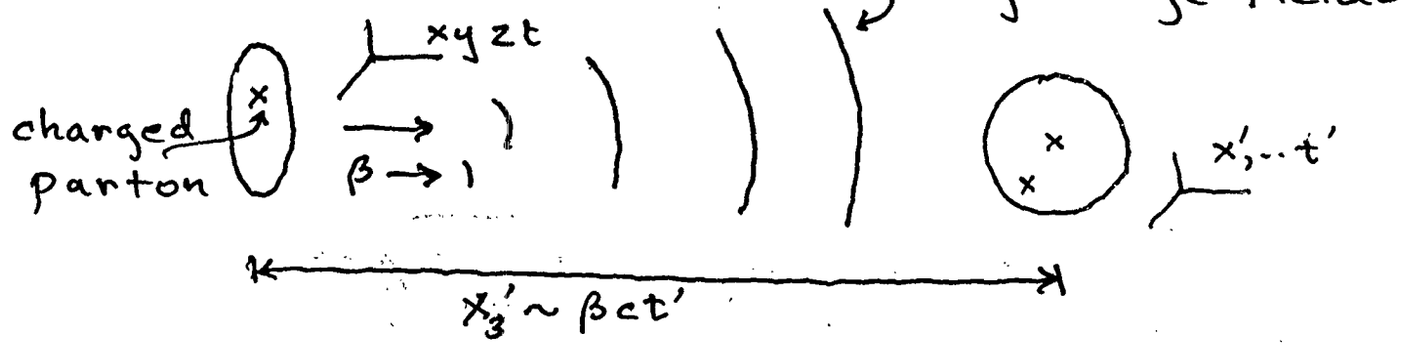

Lorentz Contractions: $\Delta \equiv \beta c t' - x_3'$

field	x frame	x' frame
scalar	$V(x) = \frac{e}{\lvert\vec{x}\rvert}$	$V'(x') = \frac{e}{(x_T^2 + \gamma^2\Delta^2)^{1/2}}$
		$\to 1/\gamma$
		$\sim$ "ruler"
gauge	$A^-(x) = \frac{e}{\lvert\vec{x}\rvert}$	$A'^-(x') = \frac{e\gamma(1+\beta)}{(x_T^2 + \gamma^2\Delta^2)^{1/}}$
		$\to 1 \gg$ "ruler
field strength	$E_3(x) = \frac{e}{\lvert\vec{x}\rvert^2}$	$E_3'(x') = \frac{-e\gamma\Delta}{(x_T^2 + \gamma^2\Delta^2)^{3/2}}$
		$\to 1/\gamma^2 \ll$ "ruler

Suggests: Factorization to $O(1/Q^2)$ (not a $1/Q$ in)
(R. Basu, A. Ramalho, G.S. '84)

(Consistent w/ Doria, Frenkel, Taylor noncancellation in QCD)

57

- Stretching out short distances

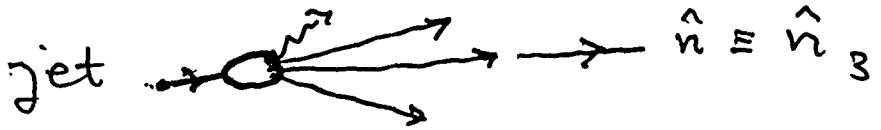

when are particles emitted?

'splitting time'

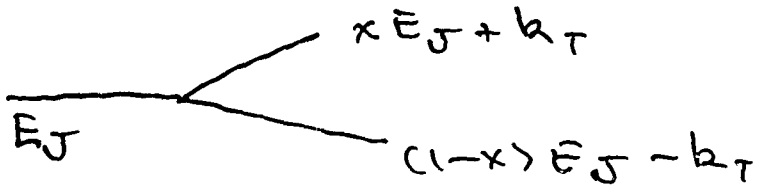

$$\Delta E \simeq \frac{1}{\Delta t(x)} = \sqrt{x^2 E_J^2 + k_T^2} + \sqrt{(1-x)^2 E_J^2 + k_T^2} - E$$

$$\simeq \frac{k_T^2}{2xE_J} + \frac{k_T^2}{2(1-x)E_J}$$

$$= \frac{k_T^2}{2x(1-x)E_J}$$

$$\Delta t(x) = \frac{2x(1-x)E_J}{k_T^2}$$

- lifetimes $\propto E_J$
- soft, wide-angle particles emitted <u>early</u>
- "leading" particles <u>late</u>

HARD PARTONS IN NUCLEAR COLLISIONS

- AA collision in "target" rest fram
  - Cole

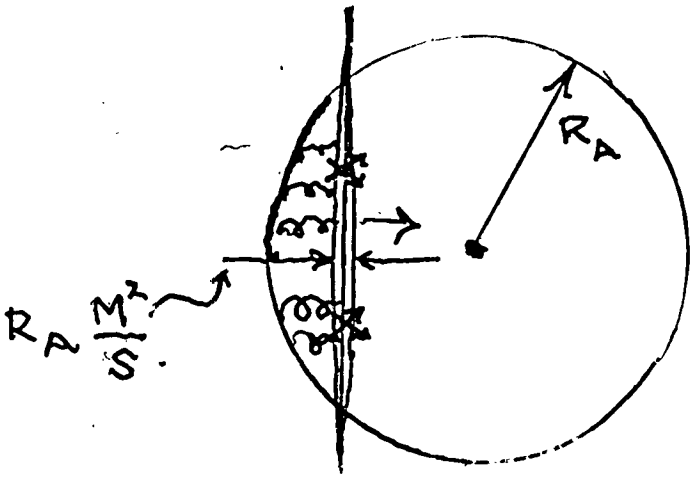

'burn-through'

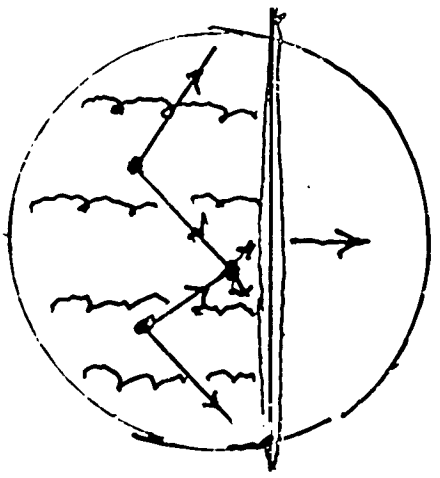

'cascade'

- Gustafsou
- Wang
- Longacre
- Sorge
- Steinberg

- The 'small-x' connection
  - a single G-exchange 'frees' an entire ladder:
  - B-ladder in A-rest:

- Mueller
- Sarcevic
- Leonidov
- Guo
- Frankfurt
- Jalilian-Marian
- Kovner
- Kovchegov
- Vogt

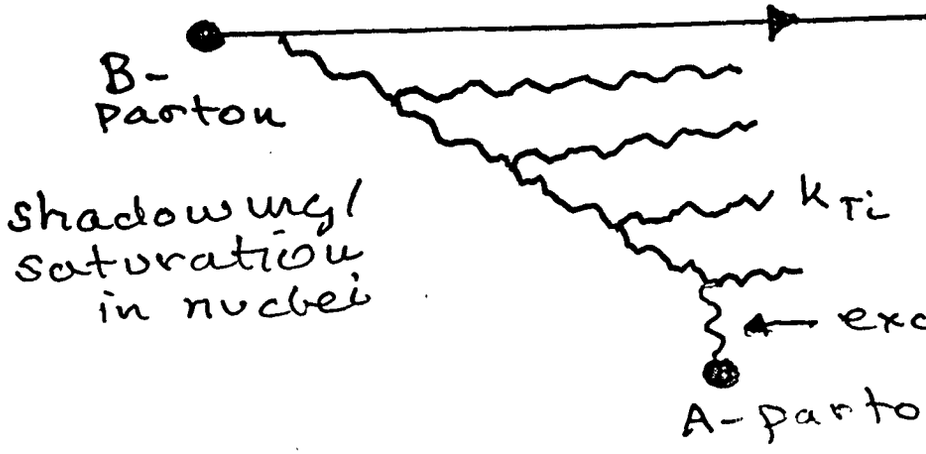

- Nonuniqueness of exchange c.m. frame

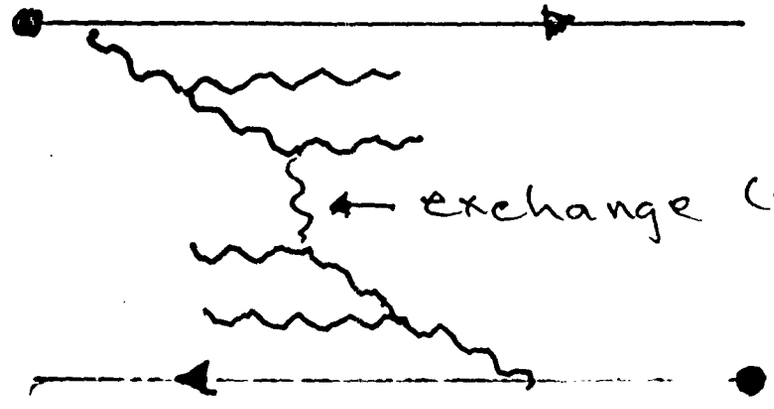

- $\sigma_{minijet} \sim F_A(x) F_B(x)$

  $x \hookrightarrow$ factorization scale

Resummation $\hookrightarrow$ Renormalization in effective FT (BFKL)

- Nuclei as superpositions of sources on the light cone

McLerran-Venugopalan
Kovner, Jalilian-Marian, Wiegert; Kovchegov
- Kovner
- Balitsky

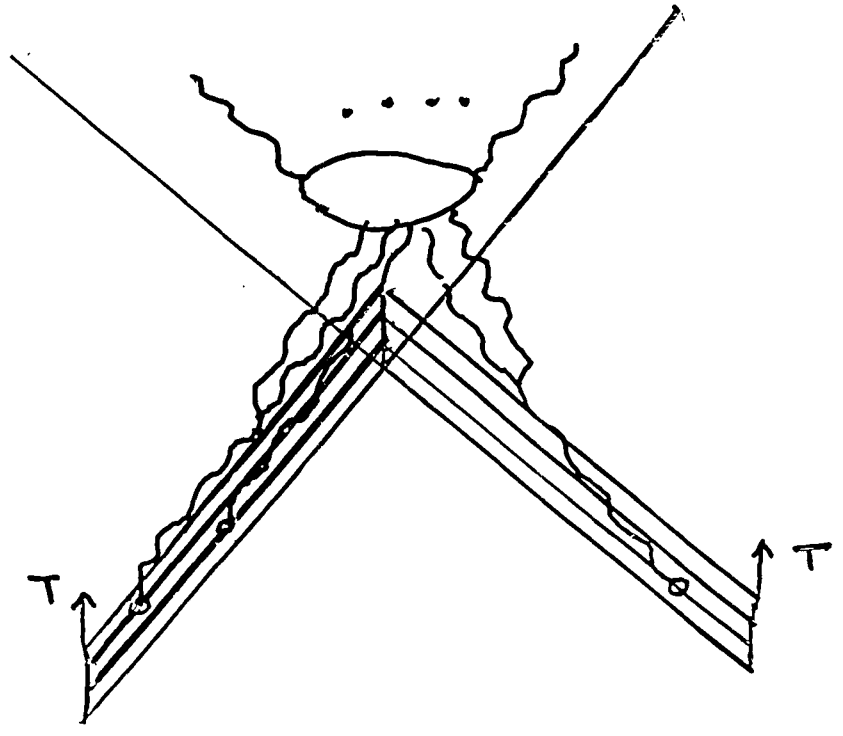

- Coherent 'cascade'
- Model for minijets
- Alternate EFT: Lipatov (Schaefer et al)

- Medium diagnostics
  - dijets (and or leading particles)
    - Tannenbaum
    - Kharzeev
    - Ogilvie
    - Christie
    - Awes

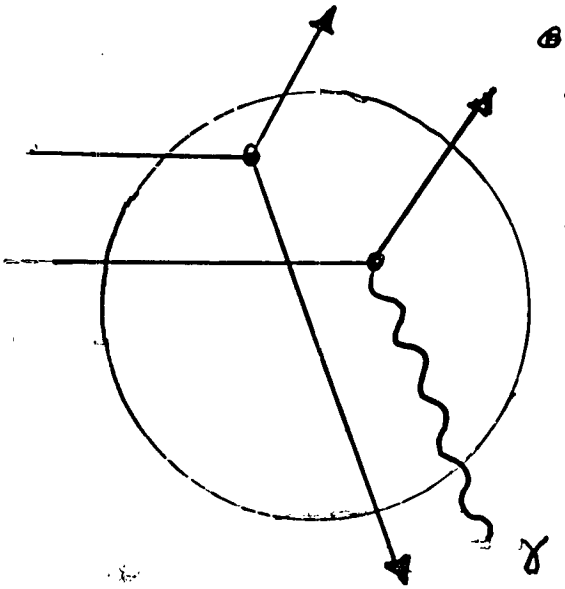

    - Kunde
  - and direct γ/jet pairs
  - Drell-Yan dileptons (initial state) • Peng

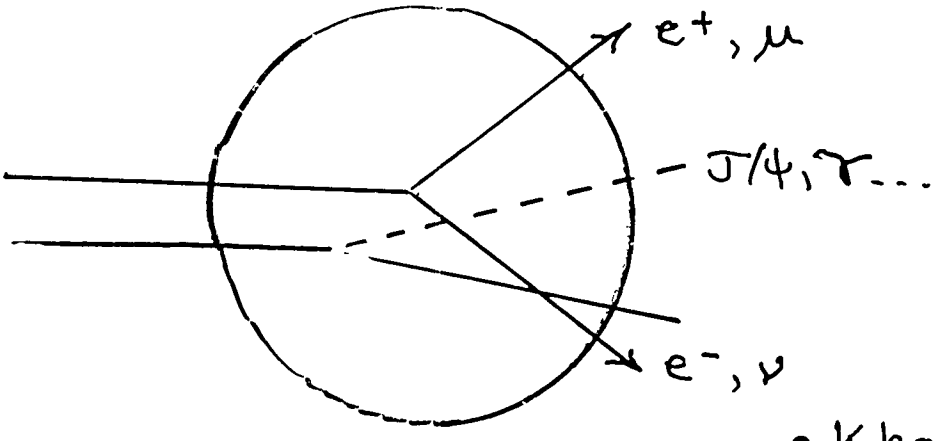

    - Kharzeev
  - Quarkonia (color evolution in medium)

collisional: $\nu_{min} = \mu_D^2 / 2M_0$

$\nu_{max} = min(2M_0/\tan^2\theta_0, E/4)$

radiative: $\omega_{min} = E_{LPM} = \chi_g \mu_D^2$

$\omega_{max} = E$

$\bar{\omega} \lesssim E_{LPM} (\theta_M/\theta_0)^{4/3}$

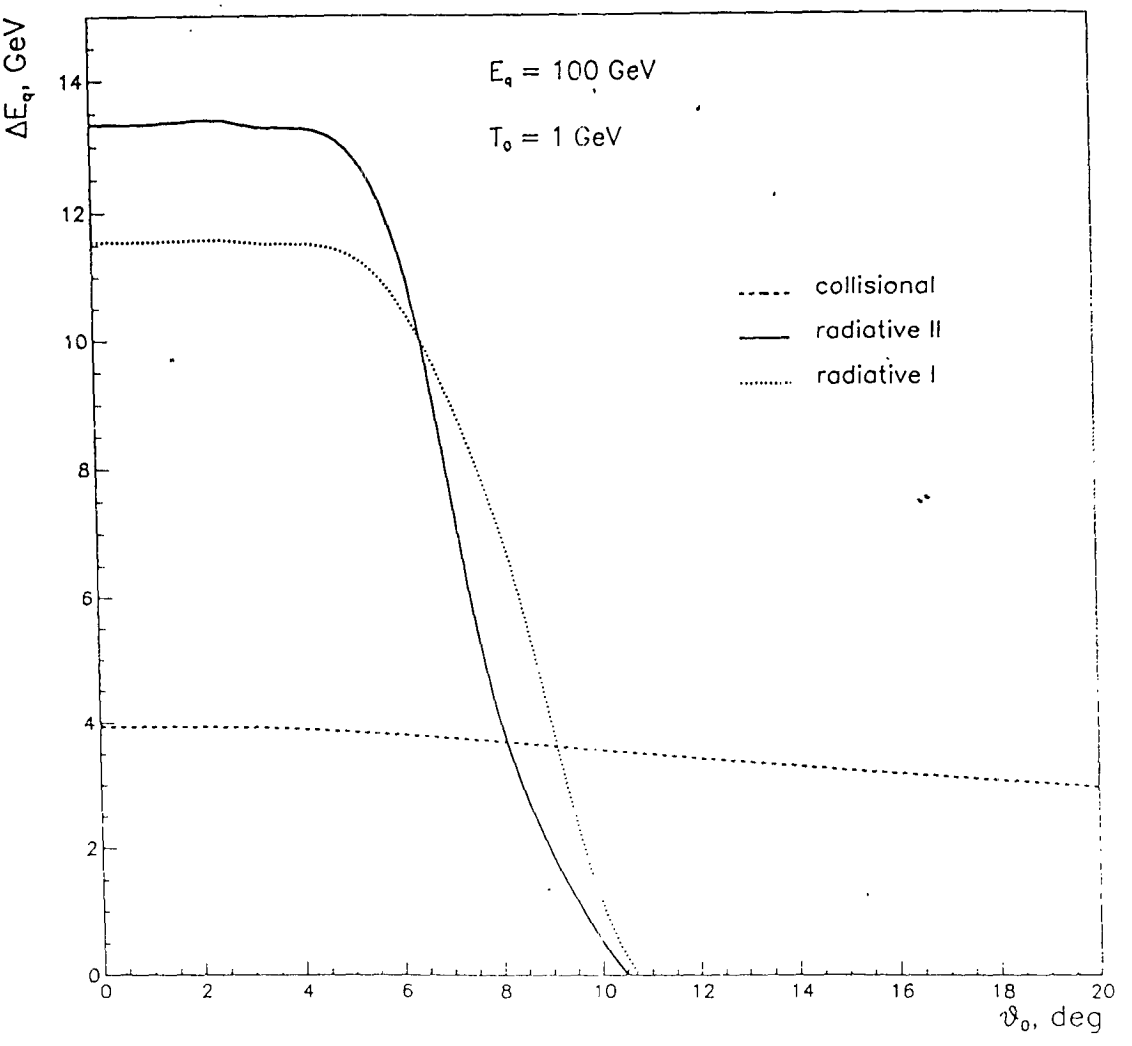

I.P. Lokhtin, A.M. Snigirev. Phys. Lett. B440 (1998) 163

The average radiative (coherent medium-dependent part, the dotted and solid curves for models I and II respectively) and collisional (dashed curves) energy losses of quark-initiated jet ΔE_q with initial energy $E = 100$ GeV in the central rapidity region $y = 0$ as a function of the parameter θ_0 of a jet cone size. $R_A = 7$ fm.

$T = T_0 (\tau_0/\tau)^{1/3}$, $\tau_0 \simeq 0.9\ fm/c$

$\Lambda_{QCD} \sim C$

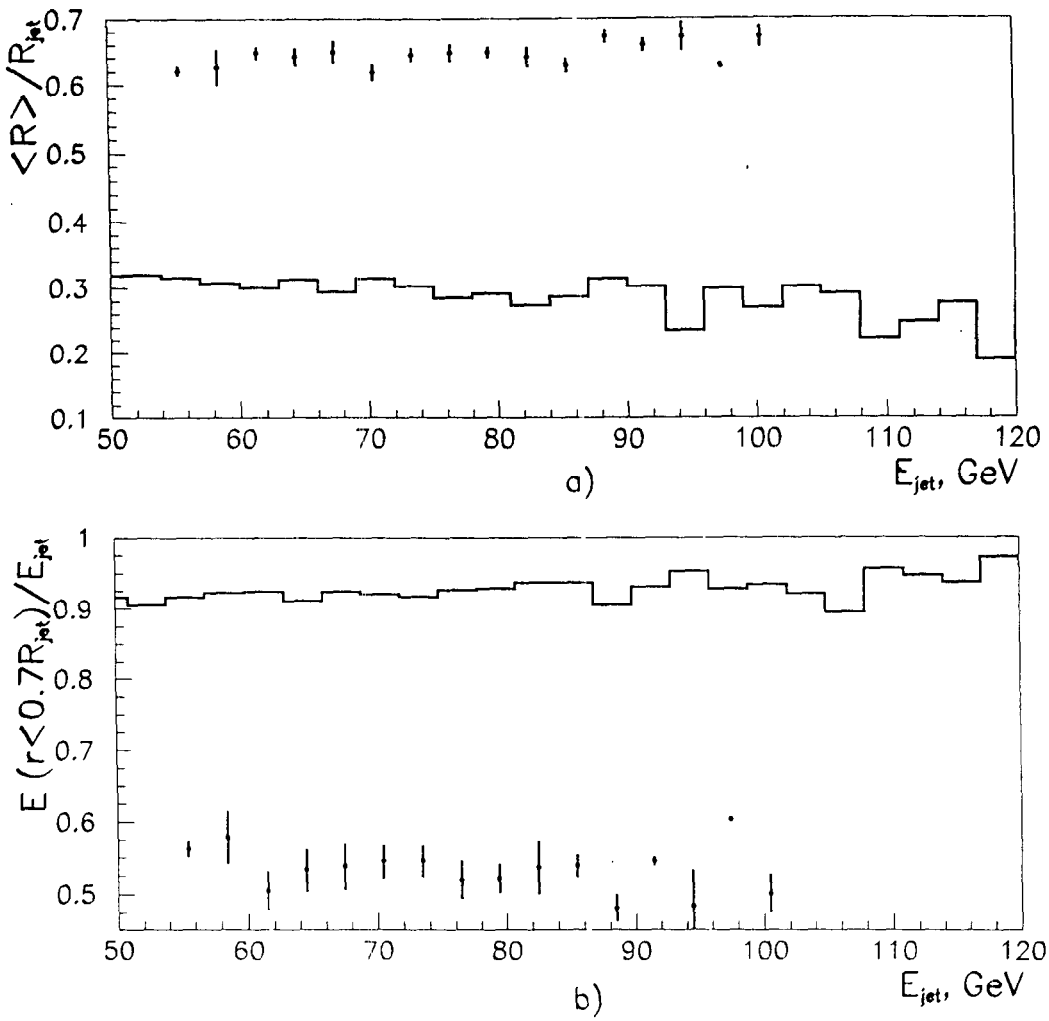

The average radius $< R >= \Sigma_i R_{i0} \cdot (E_i - \overline{E_i})/E_{jet}$ (a) and the energy density $E\ (r < 0.7R_{jet})/E_{jet}$ (b) of "true" hard jet (histogram) and "false" jet (points) versus jet energy E_T^{jet}, $R_{jet} = 0.5$.

CERN CMS NOTE 1998/005

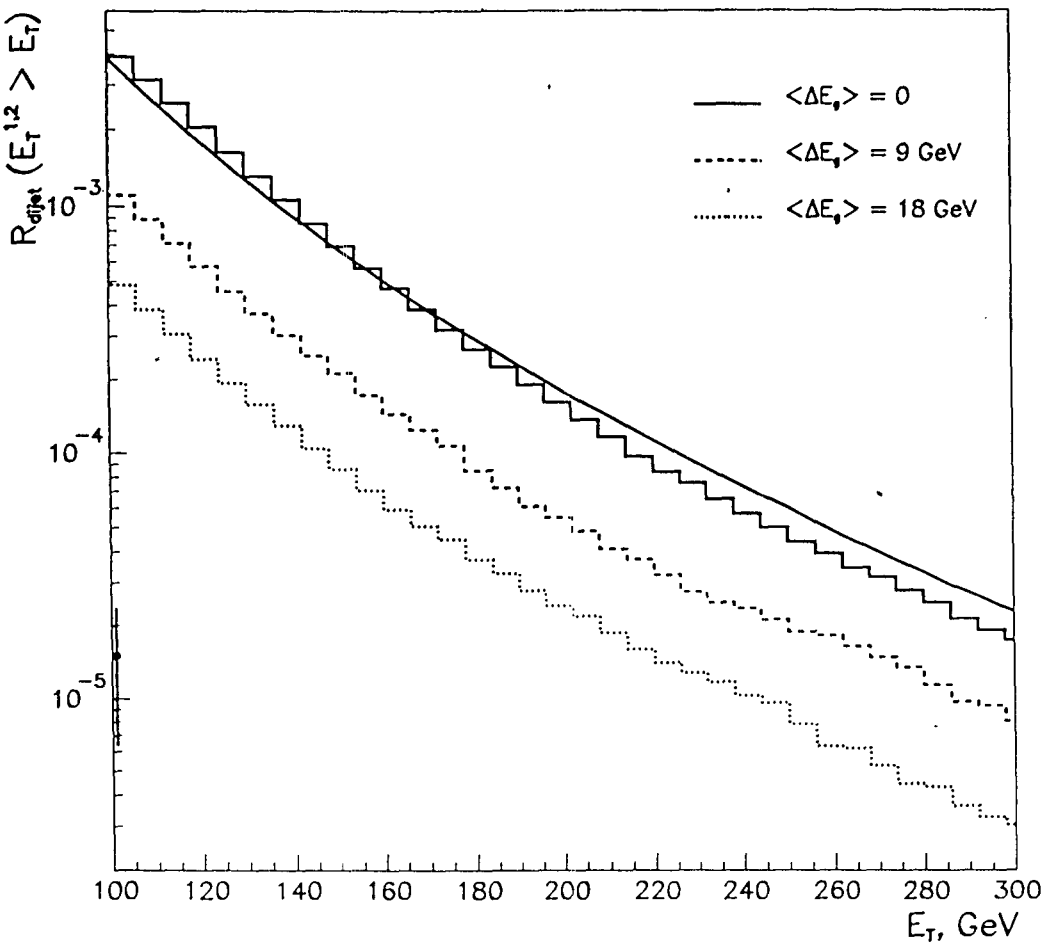

The probability R_{dijet} of dijets with transverse energy $E_T^{1,2} > E_T$ in central $Pb-Pb$ collisions for different quenching scenarios: "true" hard (histograms) and "false" (point, the dashed line presents the Gaussian fit) dijets. Additional criterion on average radius of a jet $< R > /R_{jet} < 0.5$ is used ($R_{jet} = 0.5$). Solid curve shows the result for dijet spectrum at parton level as calculated with PYTHIA (initial state gluon radiation is taken into account).

$E_T \approx 100$ GeV: $gg \to gg$ ($\approx 60\%$)
$qg \to qg$ ($\approx 30\%$)
$qq \to qq$, $q\bar{q} \to q\bar{q}$ ($\approx 10\%$)

CERN CMS NOTE 1998/063

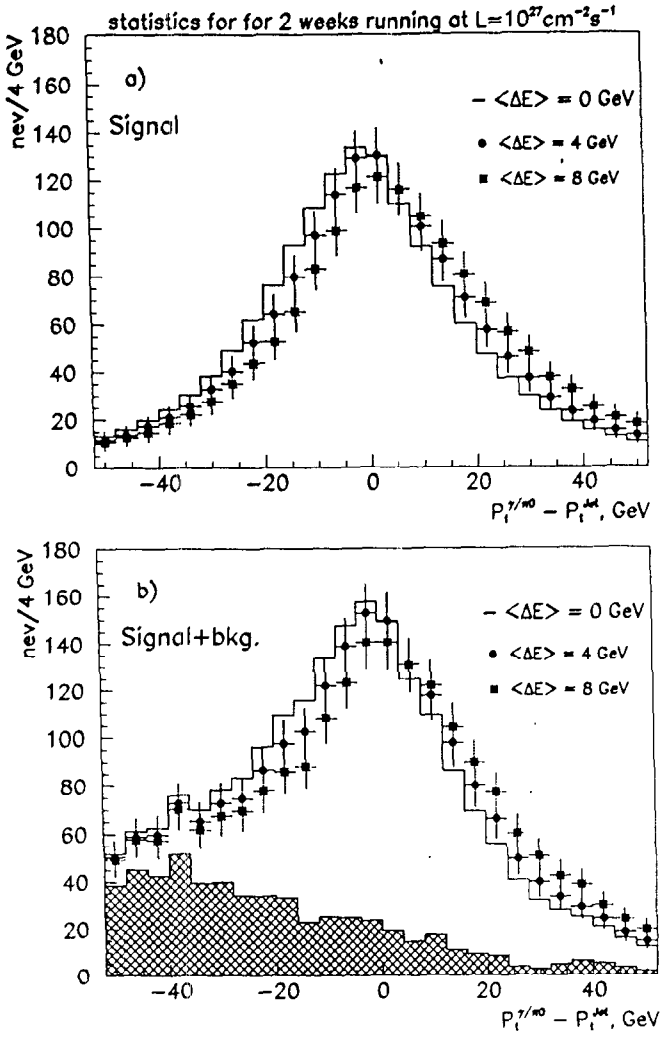

The distributions of differences in transverse energy between the γ and jet with $p_T^{\gamma,\ jet} > 120$ GeV/c for two weeks LHC running (a) without (π^0 + jet) background counting; b) with (π^0 + jet) background counting) in the rapidity region $\mid y^{\gamma,\ jet} \mid < 1.5$ for different values of jet energy losses (initial state gluon radiation and finite jet energy resolution are taken into account).

CONCLUSIONS

Although the radiative energy losses of a high energy projectile parton dominate over the collisional energy losses, the angular distribution of energy losses is essentially different for two mechanisms:

- Due to coherent effects, the radiative energy loss decreases with increasing the angular size the jet. It becomes comparable with the collisional energy loss for $\theta_0 \gtrsim 5^0 - 10^0$.
- The bulk of "thermal" particles knocked out of the dense matter by elastic scatterings emerges outside the narrow jet cone and thus cause the "jet energy loss".

"True" hard QCD-jets vs. "false" thermal jets:

- The striking distinction in the properties of "false" and QCD-jets (energy spectrum and intrinsic structure) allows us to optimize jet-finding algorithm in ultra-relativistic heavy ion collisions.

$jet + jet$ production:

- sensitive to the energy losses
- good efficiency
- high statistics
- normalization on pp by $Z(\to \mu^+\mu^-)$
- nuclear shadowing is not strong ($x \gtrsim 0.03$)

$\gamma + jet$ production:

- direct observation of energy losses by $E_T^\gamma - E_T^{jet}$ distribution
- not high statistics
- large background from $jet + jet(\to \pi_0 \to 2\gamma)$

$Z(\to \mu^+\mu^-) + jet$ production:

- direct observation of energy losses by $P_T^Z - E_T^{jet}$ distribution
- very low statistics
- small background

Is it possible to observe the medium-induced energy losses of hard quarks and gluons measuring hadronic jets in ultra-relativistic collisions of nuclei?

presented by *I.P.Lokhtin*

Moscow State University, Nuclear Physics Institute, Moscow, Russia

1. Angular structure of collisional and radiative energy losses of hard jet in dense QCD-matter

2. Jet recognition in heavy ion collisions at LHC (CMS)

3. The observation of jet energy losses using $jet + jet$, $\gamma + jet$ and $Z(\to \mu^+\mu^-) + jet$ production

Where is the Energy Loss?

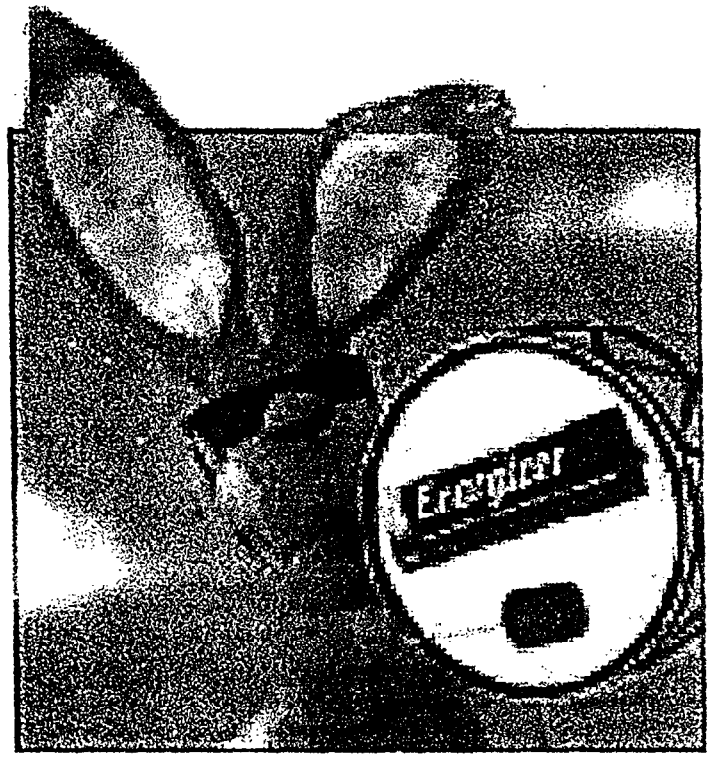

- A brief history of energy loss theory
- How to measure dE/dx?
- What to expect at RHIC?
- What is the situation at SPS?
- What can we conclude?

Prospects for RHIC

- **Hard processes more accessible, i.e., direct γ**

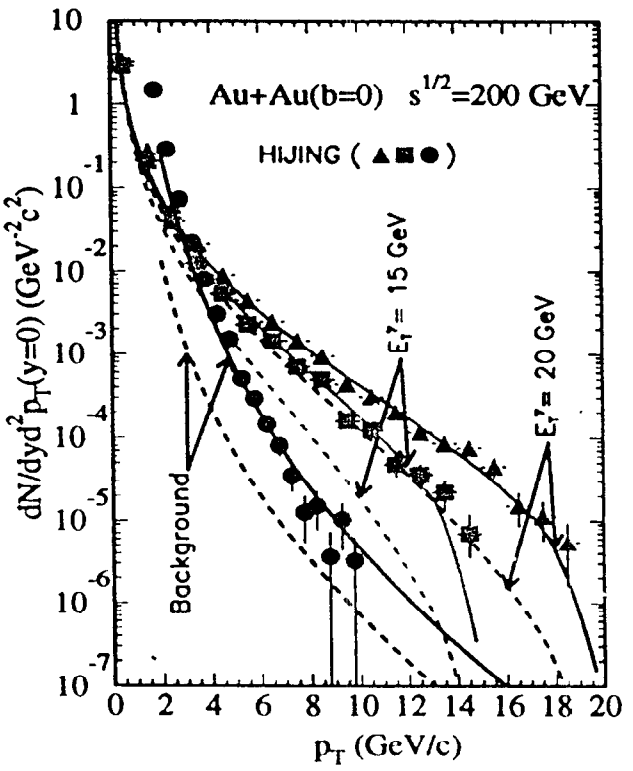

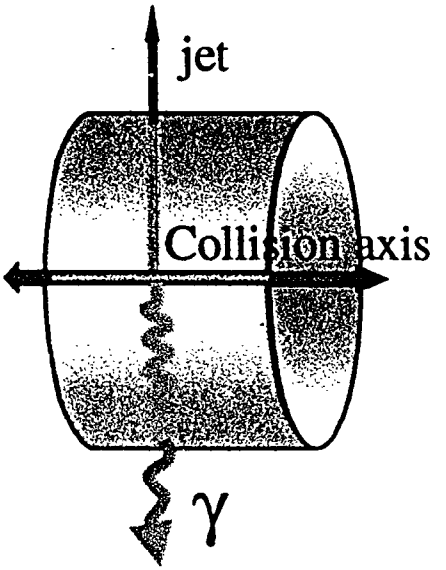

X.-N.W. Huang
Sarcevic
PRL 77(96)

X.-N.Wang
PRC55(97)

10 GeV γ
3500/year
Not quite year-
1 physics

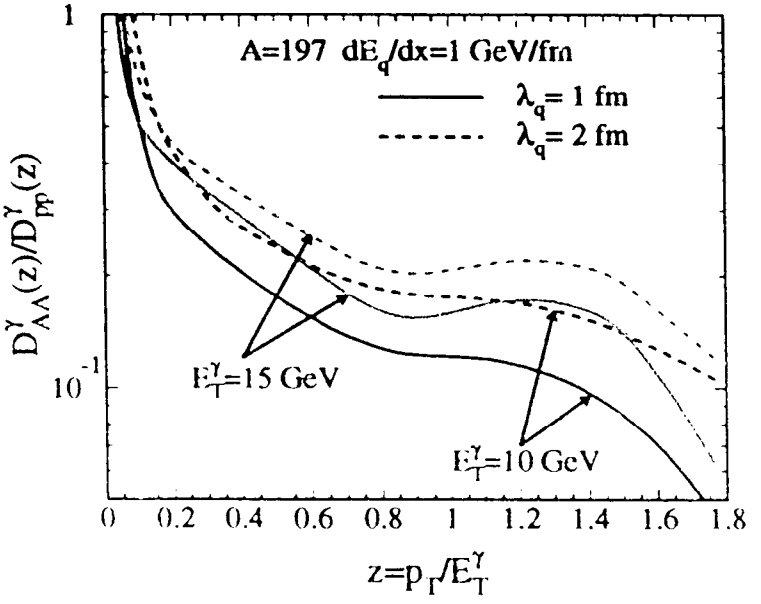

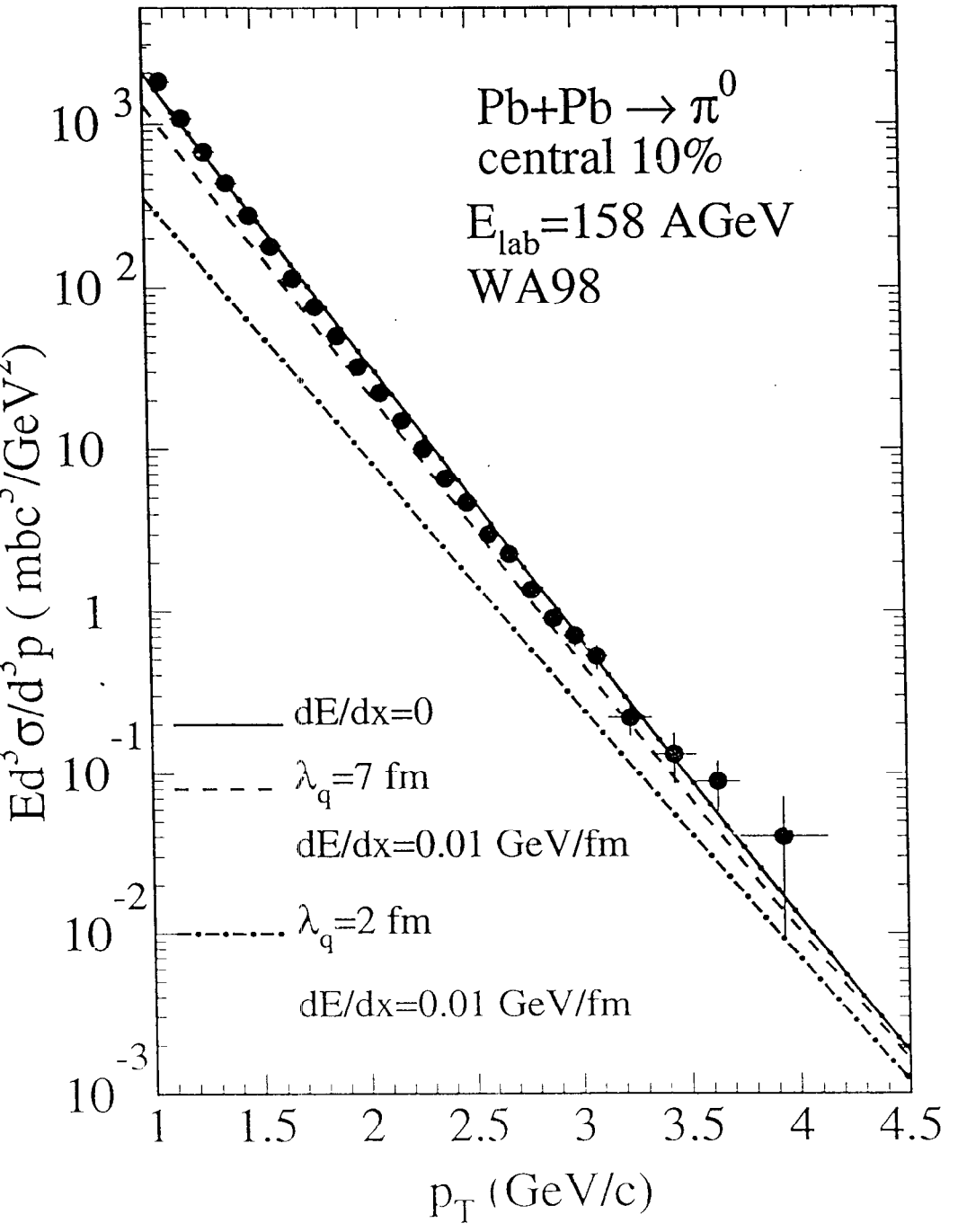
Pb+Pb → π0
central 10%
Elab=158 AGeV
WA98
dE/dx=0
λq=7 fm
dE/dx=0.01 GeV/fm
λq=2 fm
dE/dx=0.01 GeV/fm
Ed3σ/d3p (mbc3/GeV2)
pT (GeV/c)
10 3
10 2
10
1
10-1
10-2
10-3
1
1.5
2
2.5
3
3.5
4
4.5

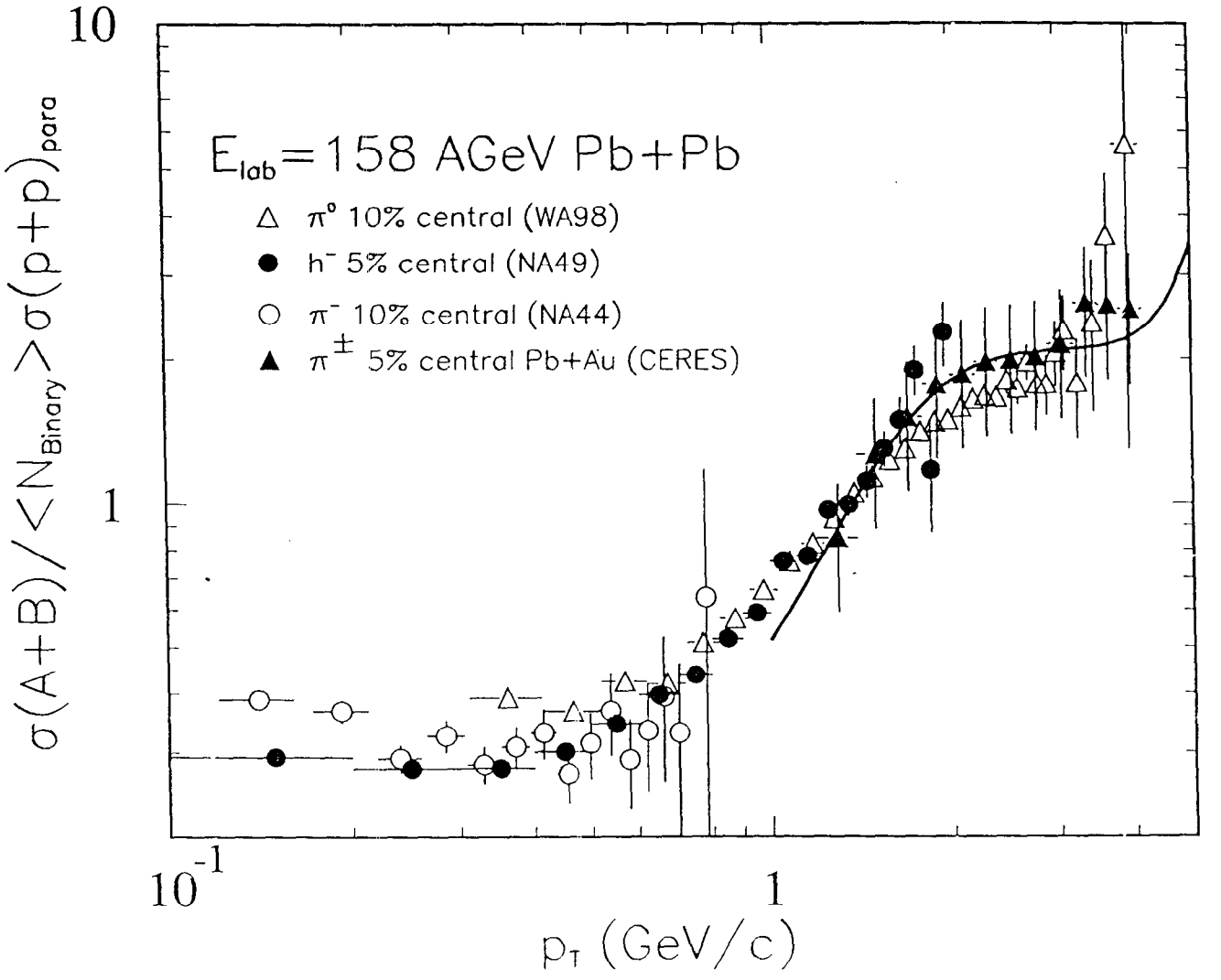
10
1
10^{-1}
1
$\sigma(A+B)/\langle N_{Binary}\rangle\sigma(p+p)_{para}$
p_T (GeV/c)
E_{lab}=158 AGeV Pb+Pb
π^0 10% central (WA98)
h^- 5% central (NA49)
π^- 10% central (NA44)
$\pi^\pm$ 5% central Pb+Au (CERES)

Single Particle Spectra at RHIC

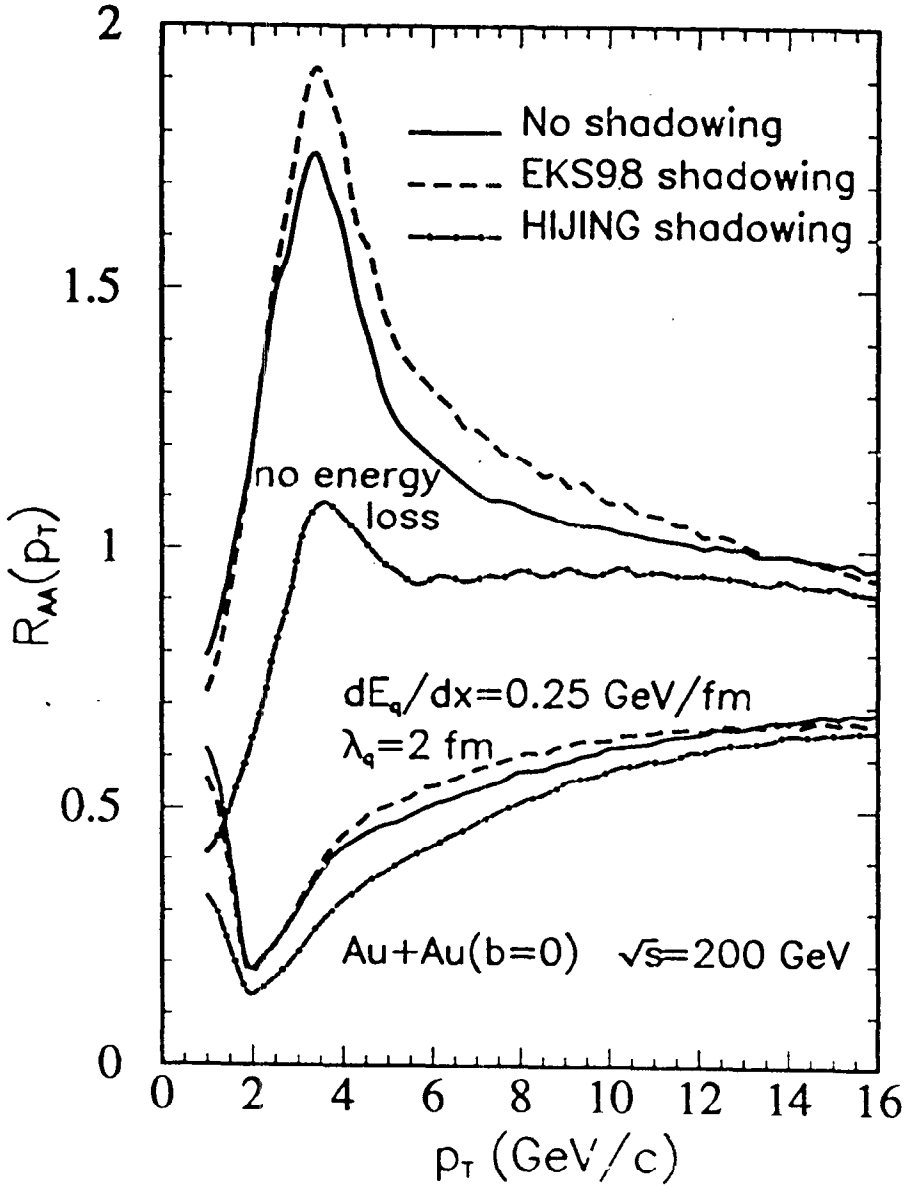

Please don't use $A^{\alpha(p_T)}$ parametrization !!!

[e.g. A vs $(1+A)/2$]

What we can conclude so far?

- **Large p_T >1 GeV/c spectra: Hard Scattering**

- **Shape of spectra in pA (AA?) in p_T<1 GeV/c: interplay between hard and soft (shadowing)**

- **No evidence of energy loss:**
  - short life time of QGP?
  - Or QGP does not cause dE/dx? (inconsistent with QGP formation)
  - Complete thermalization? (the A-scaling is just a miracle)

- **Hadronic stage does not contribute to jet quenching**

Light cone formalism for bremsstrahlung in multiple scattering

Boris Kopeliovich

Max-Plank-Institut für Kernphysik, Heidelberg

Outlook

- Light-cone formalism for radiation of prompt photons and Drell-Yan lepton pairs
- Transverse momentum distribution
- Nuclear effects: shadowing or antishadowing?
- Gluon radiation
- Multiple interactions and effects of coherence in gluon bremsstrahlung.
- Nonperturbative effects in production of $q\bar{q}$ pairs and radiation of gluons

Light-cone formalism for radiation: prompt photons and Drell-Yan pairs

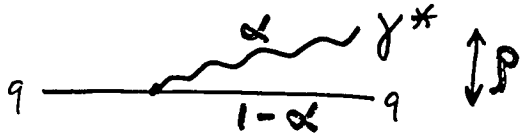

B. K. 1994
S. Brodsky, A. Hebecker & E. Quack, 1996
B. Zakharov 1996
A. Schäfer, A. Tarasov & B. K. 1998

$$\frac{d\sigma(qN\to\gamma^* qN)}{d(\ln\alpha)} = \int d^2\vec{\rho}\,|\Psi_{\gamma^* q}|^2\,\sigma_{q\bar{q}}(\alpha\rho)$$

★ Why the $q\bar{q}$ dipole cross section?

The impact parameters of the initial and final quarks are shifted

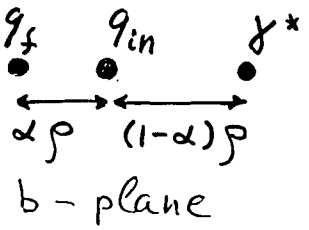

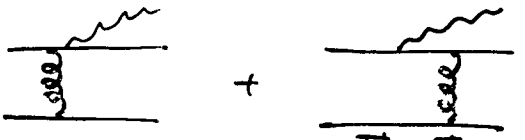

$$1 - e^{i\vec{k}\alpha\vec{\rho}}$$

In other words: $|q\rangle = |q\rangle_0 + |q\gamma^*\rangle + \dots$

In order to produce a new state the Fock states $|q\rangle_0$ and $|q\gamma\rangle$ have to interact differently

$$A(q\to q\gamma) \propto A_q^{el} - A_{q\gamma}^{el}$$

The quark-photon distribution function

$$\Psi^{T,L}_{\gamma^* q}(\vec{\rho},\alpha) = \frac{\sqrt{\alpha_{em}}}{2\pi}\,\bar{\chi}_f\,\hat{\Gamma}^{T,L}\chi_i\,K_0(\varepsilon\rho)$$

$$\varepsilon^2 = (1-\alpha)Q^2 + \alpha^2 m_q^2$$ different from ε^2 in DIS

The vertex operator $\hat{\Gamma}^{T,L}$ is also different from DIS

$$\hat{\Gamma}^T = i m_q \alpha^2 \vec{e}^*(\vec{n}\times\vec{\sigma}) + \alpha\,\vec{e}^*(\vec{\sigma}\times\vec{\nabla}_\rho) - i(2-\alpha)\vec{e}^*\cdot\vec{\nabla}_\rho$$

$$\hat{\Gamma}^L = 2Q(1-\alpha)$$

A. Schäfer, A. Tarasov & B.K. 1998

The transverse momentum distribution

$$\frac{d^3\sigma(qN\to q\gamma^* N)}{d(\ln\alpha)\,d^2k_T} = \frac{1}{(2\pi)^2}\int d^2\rho_1 d^2\rho_2\, e^{i\vec{k}_T(\vec{\rho}_1-\vec{\rho}_2)}\,\Psi^*_{\gamma q}(\alpha,\rho_1)\,\Psi_{\gamma q}(\alpha,\rho_2)$$

$$\times\frac{1}{2}\left\{\sigma_{q\bar{q}}(\alpha\rho_1)+\sigma_{q\bar{q}}(\alpha\rho_2)-\sigma_{q\bar{q}}[\alpha(\vec{\rho}_1-\vec{\rho}_2)]\right\}$$

Integrating over $\vec{k}_T$ we arrive at the original factorized formula

Interplay of nuclear shadowing/antishadowing

$$\sigma^A \equiv \frac{d\sigma^A}{d(\ln\alpha)d^2k_T} \approx A^{n(k_T,\alpha)}$$

$$n(k_T,\alpha) = \frac{d(\ln\sigma^A)}{d(\ln A)}$$

antishadowing (LP enhancement)

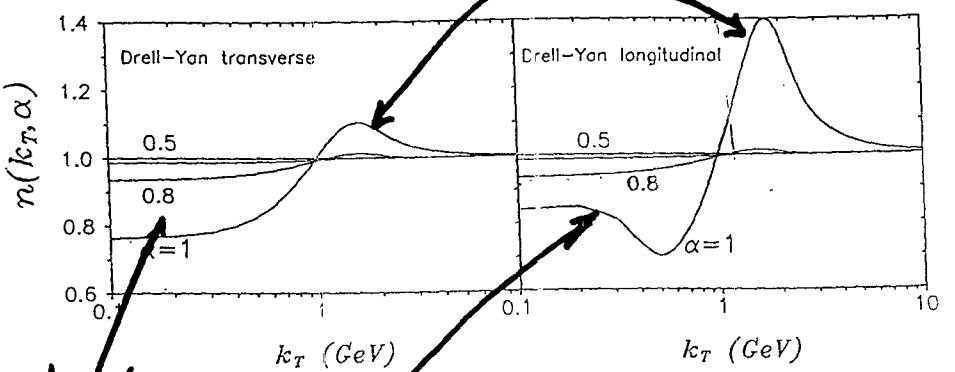

shadowing (LP suppression)

$$\langle \rho^2 \rangle \sim \frac{1}{Q^2(1-\alpha)}$$

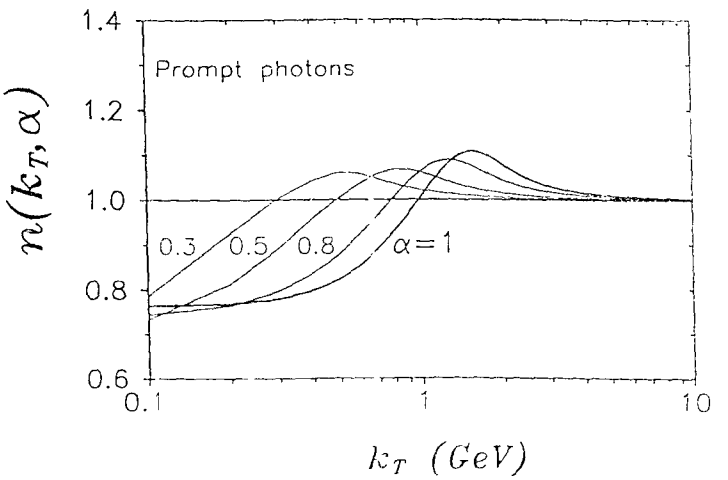

★ Gluon radiation

Factorized formula for integrated X-section

$$\frac{d\sigma(qN\to qGN)}{d(\ln\alpha)} = \int d^2\rho \left|\Psi_{Gq}(\alpha,\vec{\rho})\right|^2 \sigma_{q\bar{q}G}(\alpha,\rho)$$

B. K. 1994

B. Zakharov 1996

- $\Psi_{Gq}(\alpha,\vec{\rho})$ looks the same as $\Psi_{\gamma^* q}(\alpha,\vec{\rho})$ up to replacement $\alpha_{em} \Rightarrow \frac{4}{3}\alpha_s$

- $\sigma_{q\bar{q}G}(\alpha,\rho)$ is the dipole cross section for a colorless system $q\bar{q}G$ with a nucleon

$$\sigma_{q\bar{q}G}(\rho_1,\rho_2) = \frac{9}{8}\left[\sigma_{q\bar{q}}(\rho_1)+\sigma_{q\bar{q}}(\rho_2)\right] - \frac{1}{8}\sigma_{q\bar{q}}(\vec{\rho}_1-\vec{\rho}_2)$$

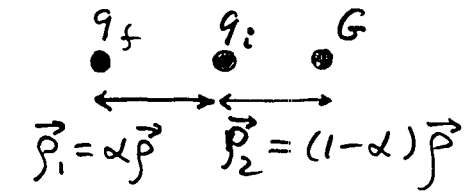

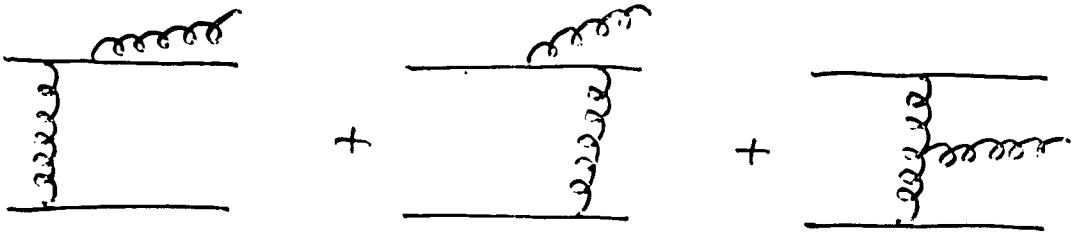

If $t_c = \frac{2E_q \alpha(1-\alpha)}{\varepsilon^2 + k_T^2} \lesssim R_A$ one should calculate the Green function of the $\gamma^* q$ system propagating through a medium

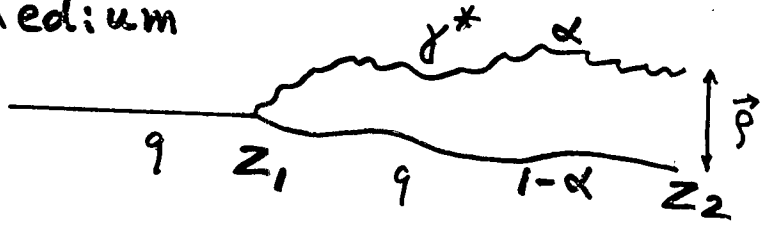

a more intuitive definition of the distribution function $\Psi_{\gamma q}(\vec{\rho}, \alpha)$

$$\Psi_{\gamma q}^{T,L}(\vec{\rho}, \alpha) = \frac{iZ_q\sqrt{\alpha_{em}}}{4\pi E_q \alpha(1-\alpha)} \int_{-\infty}^{z_2} dz_1 \, \bar{\chi} \hat{\Gamma}^{T,L} \chi \, G_{\gamma q}(z_1, \vec{\rho}_1; z_2, \rho_2)$$

The Green function describes the propagation of the $\gamma^* q$ pair from the creation point $z = z_1$, $\rho_1 = 0$ up to $z = z_2$, $\vec{\rho} = \vec{\rho}_2$.

It obeys the evolution (Schrödinger) equation

$$i \frac{d}{dz_2} G_{\gamma q}(z_1, \rho_1 = 0; z_2, \vec{\rho}_2 = \vec{\rho}) =$$

$$\left[\frac{\varepsilon^2 - \Delta_\rho}{2E_q \alpha(1-\alpha)} + V(z_2, \vec{\rho}, \alpha) \right] G_{\gamma q}(z_1, 0; z_2, \rho)$$

Boundary condition $G_{\gamma q}(z_2, \vec{\rho}_2, z_1, \vec{\rho}_1)\Big|_{z_2 = z_1} = \delta(\vec{\rho}_2 - \vec{\rho}_1)$

Summary

- There is much in common between DIS and radiation of photons & gluons in the light-cone representation
- Advantages of the light-cone approach:
  - more intuitive space-time pattern
  - all multiple interactions of the quark and the radiated gluons are taken into account by a simple eikonalization
  - nonperturbative interaction between quarks ($\gamma^* \to q\bar{q}$) and gluons ($q \to qG$) is included using the Green function formalism.
  - Explicit inclusion of the nonperturbative effect allows to get rid of "effective" quark/gluon mass
- Nuclear shadowing/antishadowing is found to depend on k_T. Inteference not only suppresses, but can also enhance radiation.
- Nuclear broadening of transverse momentum results from color filtering, rather than from initial state rescattering

Why Leading Particles Can Be used to Measure Hard-Scattering at RHIC

M.J.Tannenbaum
BNL/PHENIX
March 1, 1999

• Hard Scattering in p-p collisions was discovered at the CERN ISR in 1972 by the method of leading particles.

• A very large flux of high p_T pions was observed with a power-law tail which varied systematically with $\sqrt{s}$, the c.m. energy of the collision.

• The huge flux of high p_T particles proved that the partons of DIS strongly interacted with each other.

• Scaling arguments allowed the form of the force law between 'partons' to be determined but there was some early confusion caused by initial transverse momentum k_T which distorted the spectra.

• Further ISR measurements utilizing inclusive single or pairs of hadrons established that high transverse momentum particles are produced from states with two roughly back-to-back jets which are the result of scattering of constituents of the nucleons as described by Quantum Chromodynamics.

• These measurements are illustrated on the following pages.

http://www.rhic.bnl.gov/phenix/WWW/publish/sapin/conferences/hardscat99/

My Best Bet on Discovering QGP
Utilizes semi-Inclusive π^0 or $\pi^{\pm}$ production

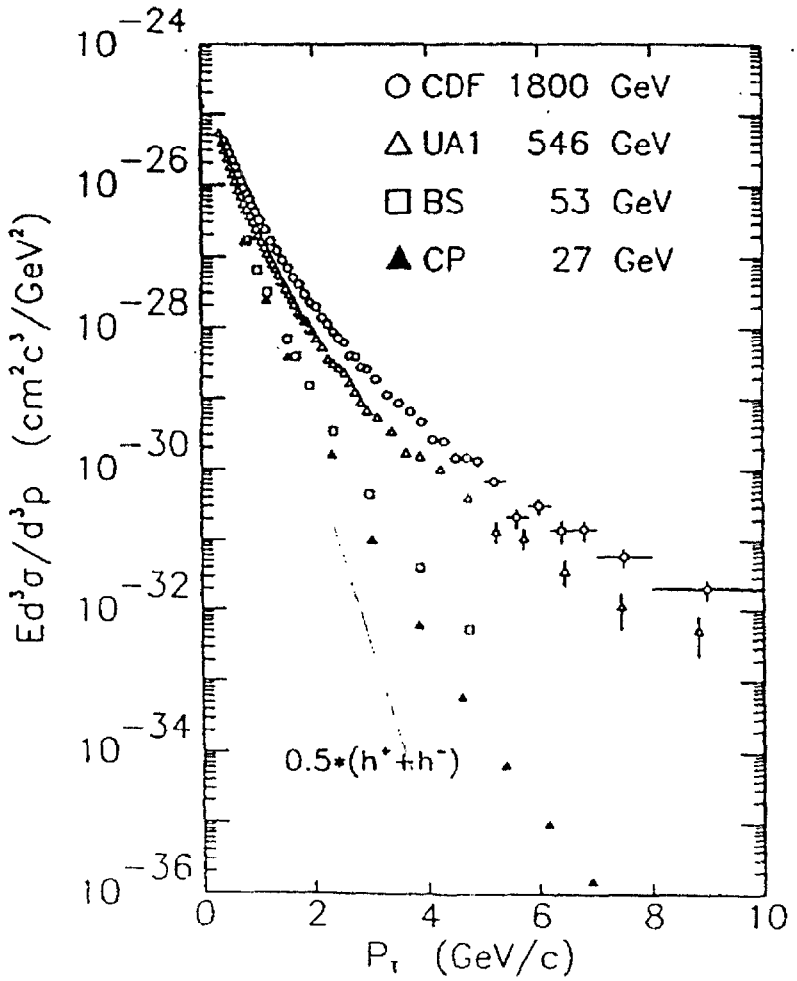

Invariant cross section for non-identified charged-averaged hadron production at 90° in the c.m. system as a function of the transverse momentum p_T tablulated by CDF for a range of C.M. energies $\sqrt{s}$. There is an exponential tail (e^{-6p_T}) at low p_T, which depends very little on $\sqrt{s}$. This is the soft physics region, where the hadrons are fragments of 'beam jets'. At higher p_T there is a power-law tail which depends very strongly on $\sqrt{s}$. This is the hard-scattering region, where the hadrons are fragments of the high p_T QCD jets from constituent-scattering. My hope is that the QGP causes the high p_T quarks to lose all their energy and stop, so that the high p_T tail will 'vanish' for central Au + Au collisions

In RHI central collisions, leading particles are the only way to find jets because in one unit of Δr there is $\pi \times \frac{1}{2\pi}\frac{dE_T}{d\eta} \sim 375$ GeV !!!.

How Everything You Want To Know about JETS can be done in PHENIX with leading particles in each arm c.f. CCOR

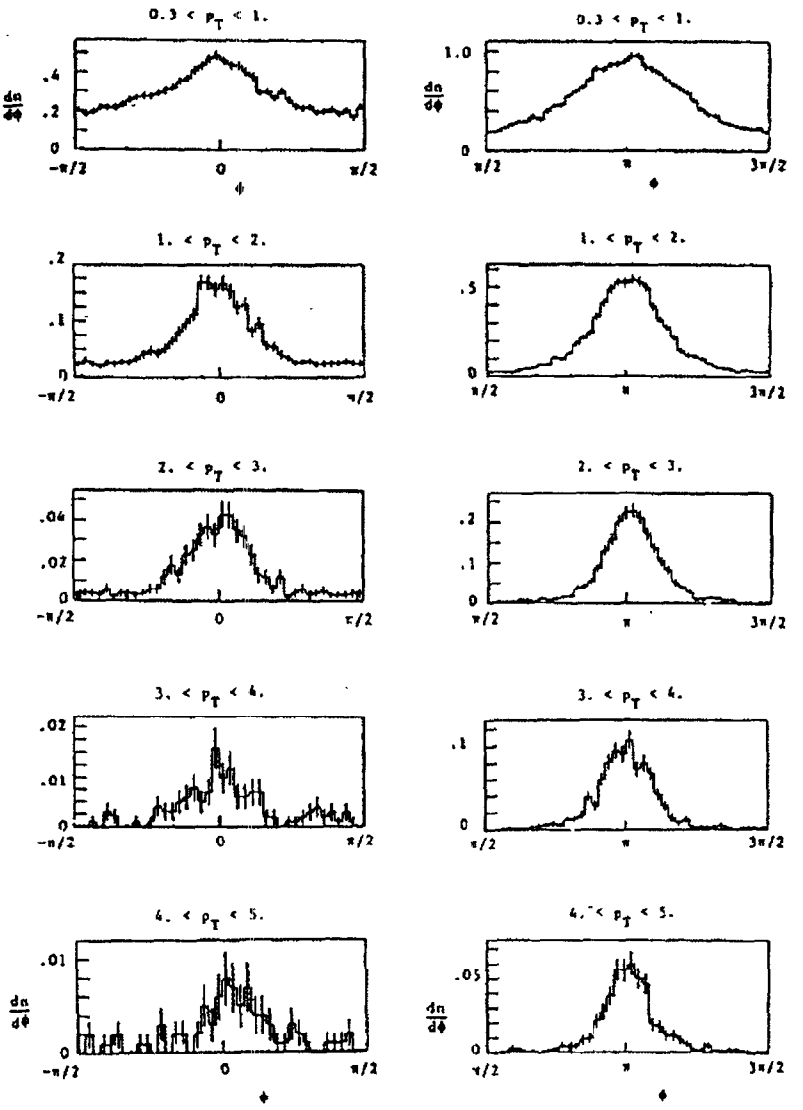

Two particle correlation in azimuth of charged particles relative to a triggering neutral with transverse momentum $p_{Tt} \geq 7.0$ GeV/c which defines the zero of azimuth, $\phi = 0$. Charged particles with $|\eta| < 0.7$ in the same 'arm' as the trigger are on the left and opposite 'arm' to the trigger on the right. As the p_T of the observed charged particle increases, the width of the away side peak (plots on the right) narrows. This effect clearly shows that the jets **are not collinear in azimuth** (they have a net transverse momentum k_T. If there were only fragmentation transverse momentum, then $p_T \times \Delta\phi$ would remain constant which would equal to $< j_T >$, the mean transverse momentum of fragmentation. [See PL 97B (1980) 163 for details]

Measurement of fragmentation function with the same data

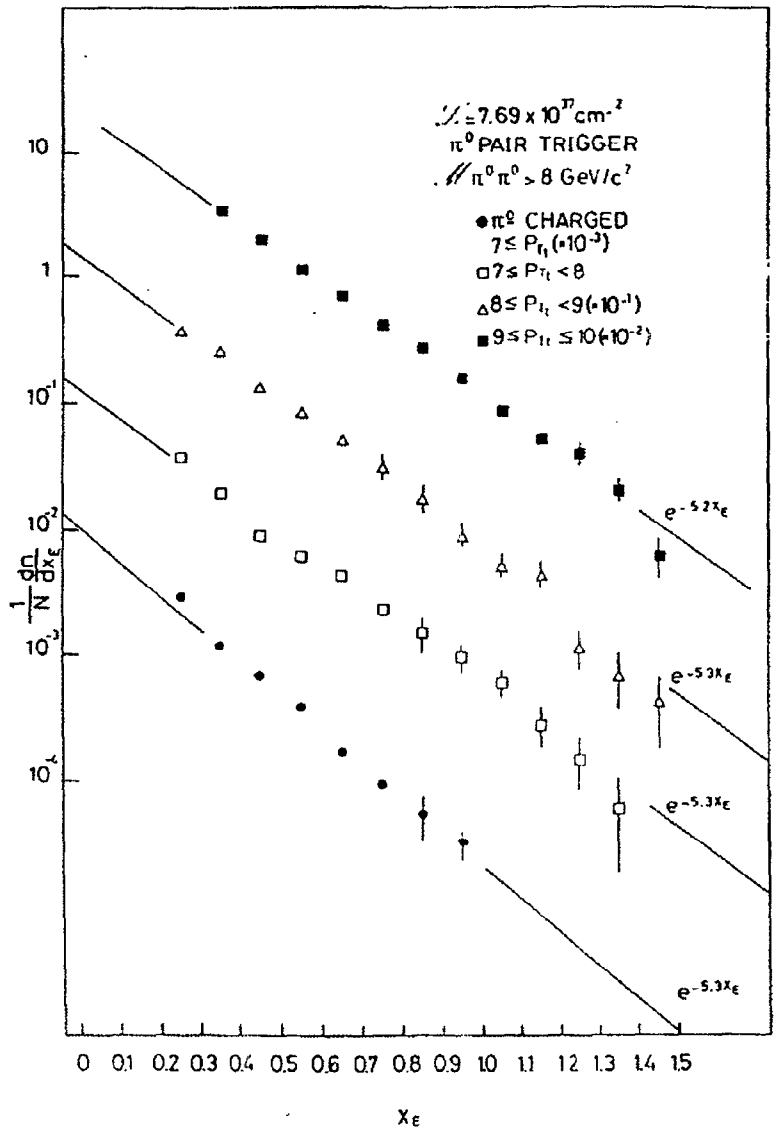

Distribution in x_E for a charged pion (or π^0) observed roughly back-to-back to a triggering π^0 of transverse momentum p_{Tt}, where both pions have $|\eta| < 0.5$ in the c.m. system. x_E is the ratio of the component of the p_T of the second pion, opposite in azimuth to the triggering pion, divided by p_{Tt}. **Exercise for students:** What do you have to know about the leading trigger particle to convert from $e^{-5.3x_E}$ to the jet fragmentation variable z $[e^{-6z}]$.

Same Data Set measures k_T

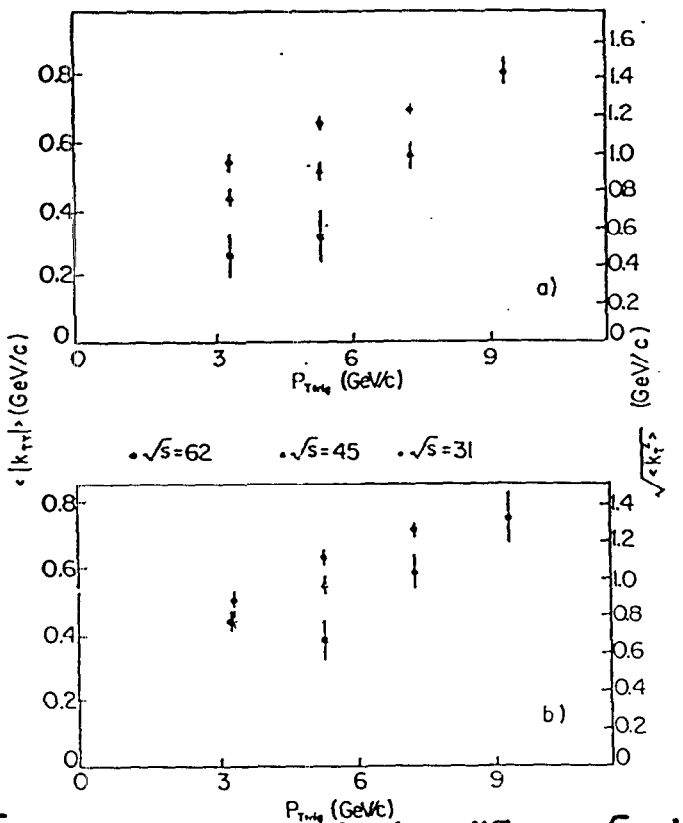

(a) $<|k_{Ty}|>$ and $\sqrt{(<k_T^2>)}$ as a function of p_{Ttrig} for three different $\sqrt{s}$ values, optained from back-back correlations. (b) The same using events where the sum of charged paricle transverse momenta on the away side balances p_{Ttrig} [see Phys Lett 97B (1980) 163].

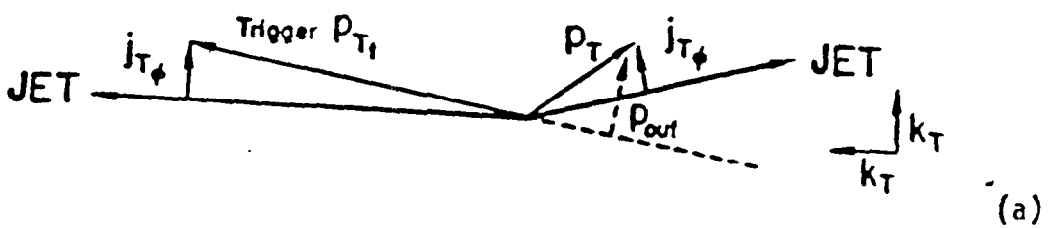

(a)

$$<|p_{out}|>^2 = <|j_{T\phi}|>^2 + x_E^2\,(<|j_{T\phi}|>^2 + <|k_T|>^2)$$

Same Data Set— First measurement of QCD subprocess angular distributions

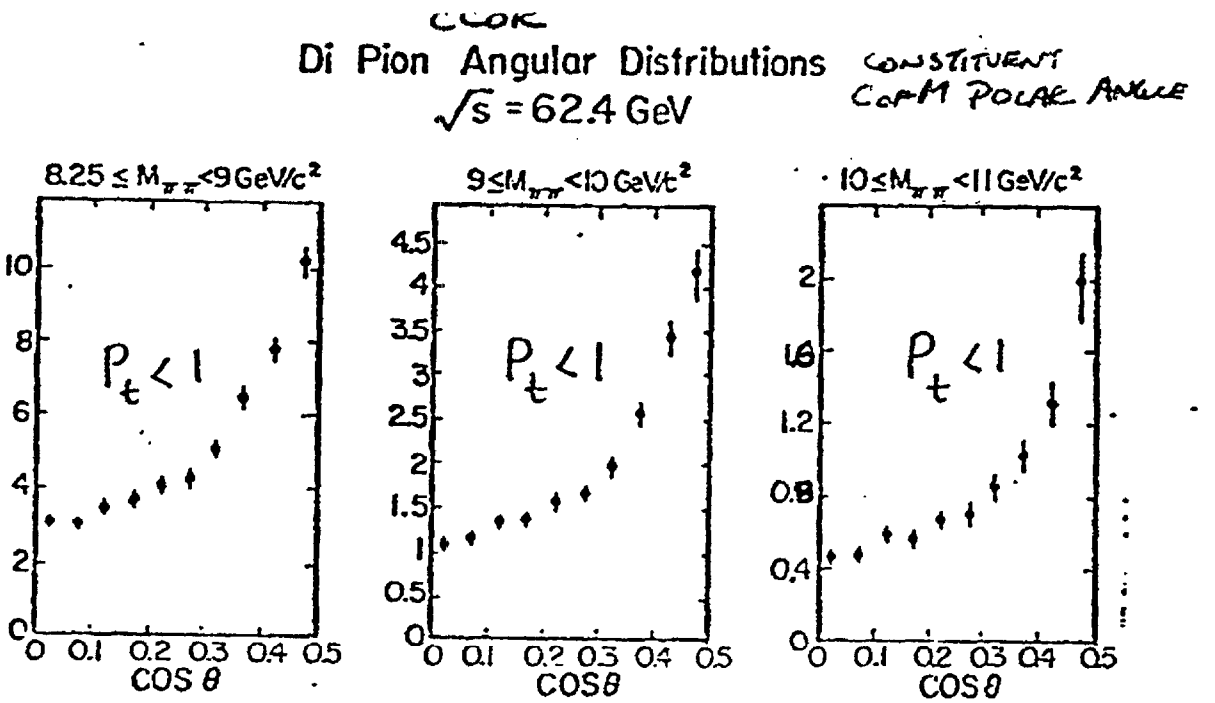

QCD Subprocess predictions normalized at 90°

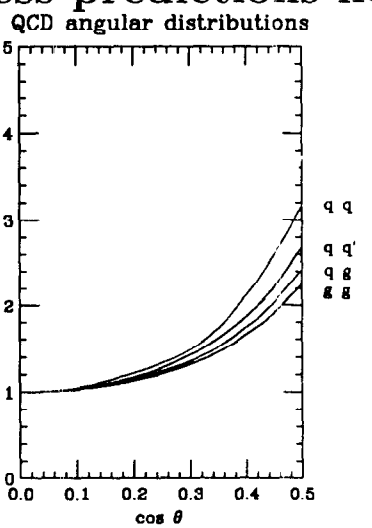

Angular distributions of pairs of nearly back-to-back π^0 as a function of the invariant mass $M_{\pi\pi}$ of the pair. The net P_t of the pion pair is restricted as indicated on the figure and the net rapidity of the di-pion system is restricted to $|Y_{\pi\pi}| < 0.35$. The distribution plotted is the polar angular distribution of the dipion axis in the frame with zero net longitudinal momentum. The important feature of the analysis in these variables, which are more typically used for lepton pairs, is that the di-pion angular distribution at fixed mass corresponds closely to the distribution of scattered partons at fixed $\hat{s}$, thus the data and QCD prediction at the parton level can be directly compared without recourse to a Monte Carlo. [see Nucl Phys **B209** (1982) 284].

Jets at HERA

Mieczyslaw Witold Krasny
Paris University & Oxford University

RIKEN Workshop - March 1999

- Introduction
- Universality of the quark fragmentation
- Jet finding and jet properties
- Reconstruction of partonic momenta using jets
- Inclusive jet spectra
- Jets as measurement tools - an example
- Summary and outlook

HERA future

Two options for HERA operation beyond 2005 are being considered:

- Collisions of electrons with nuclei
- Collisions of electrons with polarized protons

Studies of the physics potential of the eA option:

- 1995 eA physics introduced to the DIS95 workshop held in Paris
- 1996 DESY workshop. Rapport of the working group on eA scattering published in "Future Physics at HERA", ed. G.Ingelman, A. DeRoeck, R. Klanner (DESY 1996)
- 1997 Joint GSI-DESY workshop in Seeheim
- 1998 Trento workshop
- 1999 "Physics with HERA as eA collider" workshop at DESY Hamburg, 25-26 May (for more info: http://www.desy.de/heraea)

Selected physics highlights

of the eA option

- Study of the large density partonic systems. Search for non-linear QCD phenomena.
- Study of partonic structure of the large distance strong interactions. How universal is the concept of Pomeron?
- Nucleus as a tool for filtering out soft from hard processes. Perturbative QCD studies of hard processes.
- Nucleus as a femtovertex detector to study the space-time structure of strong interactions.
- Physics of luminous photon-photon scattering.

...in addition:

- Precision measurement of partonic distributions in nuclei in the x_{Bj} range 10^{-4} - 10^{-1}.
- Study of propagation of partons through the nucleus. High E_T jets as densometer of of the medium.

... both of potential use in interpreting the forthcoming RHIC and the LHC-AA data

The accelerator requirements

Preliminary studies (Willeke 1997) show that with relatively modest investment ions can be accelerated and stored at HERA providing luminosities of e.g.:

- $L = 6 \times 10^{30} cm^{-2} s^{-1}$ for electron - carbon collisions
- $L = 2 \times 10^{28} cm^{-2} s^{-1}$ for electron - lead collisions

The optimal choice of ions , required for studies of hard partonic processes in electron- nucleus collisions, covers uniformly the $A^{1/3}$ range (e.g D_2 O_{16}, Ca_{40}, Sn_{120} and Pb_{207}) with 1/A scaling of the corresponding collected luminosities

Already with luminosities of 1/A pb^{-1} a significant physics output is expected.
Example: for electron-lead collisions - one month of running with the upgraded HERA machine.

Precision measurements require 10 times larger luminosities (10/A pb^{-1}). Simultaneous storage of two or three types of isoscalar nuclei allows one to drastically reduce the systematic uncertainties of several important measurements (e.g. nuclear ratios of partonic densities) (to $\approx$ 1 % level). Such running mode is considered possible by the machine experts.

Summary and outlook

- High energy electron beam provides a precise surgery tool to eject, from hadronic matter, quarks with experimentally calibrated momenta and angles
  (contrary to "coloured tools" the radiation of QED quanta can be precisely monitored).

- Observables controlling universal fragmentation of quarks:
  - energy flow in the (η, ϕ) plane within and outside jets
  - charged particle spectra
  - particle multiplicities

  are well understood for large Q^2 electron-proton scattering at HERA ($Q^2 \geq 100$ GeV ^{2}).

- Experimental studies of these observables in electron-nucleus collisions using quark jets with tagged energies and angles could allow one to "calibrate" , with high accuracy, the size nuclear effects and thus significantly improve the precision with which hard partons can be used as medium densometers in AA collisions.

- The NLO perturbative QCD describes successfully jet production processes observed at HERA (note small deviations at the highest E_T values). The Monte Carlo models based on the perturbative QCD provide satisfactory description of the internal structure of jets.

- For $E_T \geq 25$ GeV jets the detector effects and hadronisation effects are small and the jet kinematical variables approximate very closely those of the corresponding partonic system.

- Measurement of di-jets produced in electron-nucleus collisions enables one to directly measure the distribution of gluons in the nucleus (hopefully as a function of impact parameter using wounded nucleon tagging). This method is less biased with respect to structure function analysis method, in particular for nuclear target).

Conclusions

- **Most precise measurement to date of jet cross-sections.**
- **Extensive effort went into**
  - **1) Data Accumulation (2 years)**
  - **2) Jet Energy Calibration(4 years)**
    - **Offset**
    - **Showering**
    - **Response**
  - **3) Event Selection (1 year)**
  - **3) Resolution Unsmearing (1 year)**
- **QCD in excellent agreement with observed cross sections.**

More results from Dr. Turner...

JBlazey NIU '99

A moment discussing three conceptual levels of jets ....

Jet Definition

Consider factorized $p\bar{p}$ interaction:

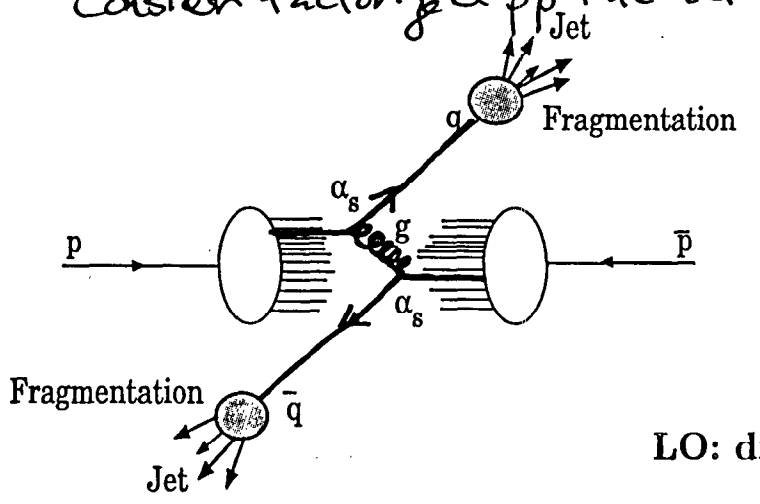

- ⋆ Hard scattering
- ⋆ Parton shower
- ⋆ Fragmentation/Hadronization

LO: dijet event ($\sigma \sim \alpha_s^2$)

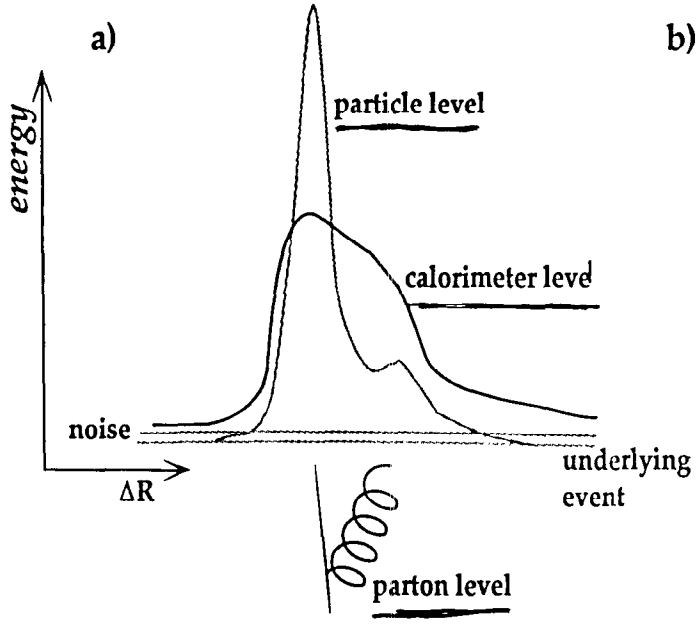

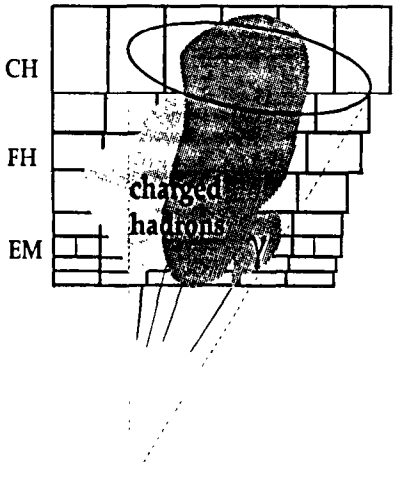

- **Parton Level Jet:** composed of quarks and gluons (before hadronization)
- **Particle Level Jet:** composed of final state particles (after hadronization)
- **Calorimeter Level Jet:** measured object (after calorimeter shower)

Use algorithm for jet reconstruction

JBlazey NIU '9

The reality must deal with cells, merging, splitting...

D0 Algorithm

- Iterate using Snowmass algorithm.
- $E_t = \Sigma E_{Ti}$, $E_{Ti} = (E^2_{x\,i} + E^2_{y\,i})^{1/2}$
- $E_x = \Sigma E_{x\,i}$, $E_y = \Sigma E_{y\,i}$, $E_z = \Sigma E_{z\,i}$

  $\cos\theta_0 = E_z/(E^2_x + E^2_y + E^2_z)^{1/2}$

  $\eta = -\ln(\tan\theta_0/2)$

A feature of cone-alg's

- Two jets are merged if they share >50% of the smaller jet E_t
- Two jets are split if the share <50% of the smaller jet E_t. Cells are assigned to the closest jet.

J Blazey NIU '99

Jet Energy Scale Correction

No central magnetic field ⇒ data based calibration

- **ADC-to-GeV and Layer-to-Layer calibration done during RECONSTRUCTION based on Test Beam e and π data)**
- **Jet Energy Scale performs second step calibration**

Measured jet energy back to the

PARTICLE LEVEL

$$E_{jet}^{ptcl} = \frac{(E^{meas} - O)}{[(R_{cone} R_{jet}]}$$

- **O: energy offset due to Ur noise, pileup and underlying event.**
- **R_{jet}: energy response (uninstrumented regions, differences between nuclear and EM interacting particles, module-to-module inhomogeneities).**
- **R_{cone}: fraction of the particle jet energy that is deposited inside the algorithm cone.**

Unimportant for $\phi.7$ Cone.

D0 Inclusive Jet Cross Section 1800 GeV, $|\eta| < 0.5$, 92 pb^{-1} (Submitted to PRL, hep-ex/9807018)

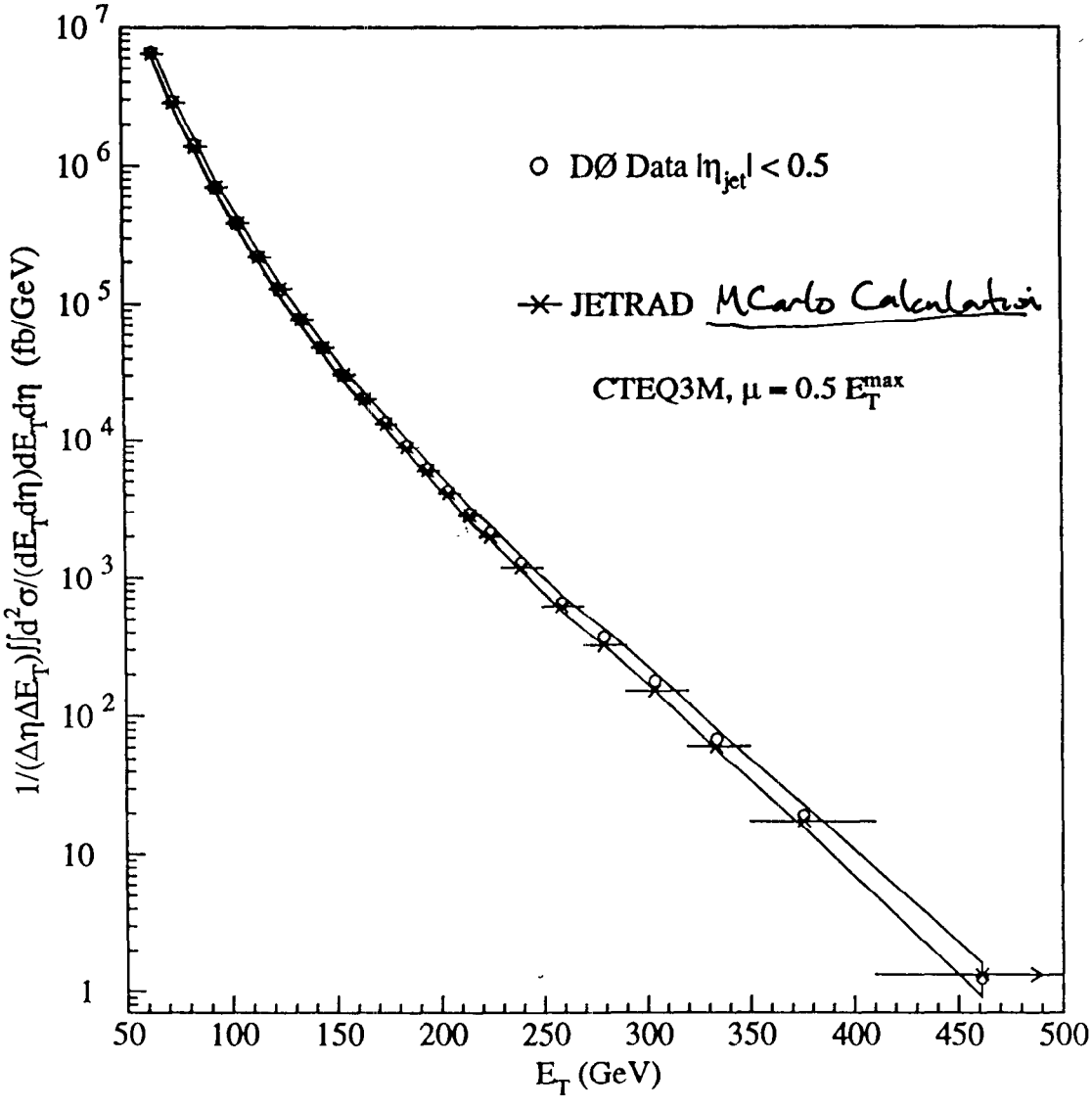

- **Good agreement over seven orders of magnitude.**

To be qualitative requires ... theory and data uncertainties

Cross Section
Ratio

Visual Comparisons

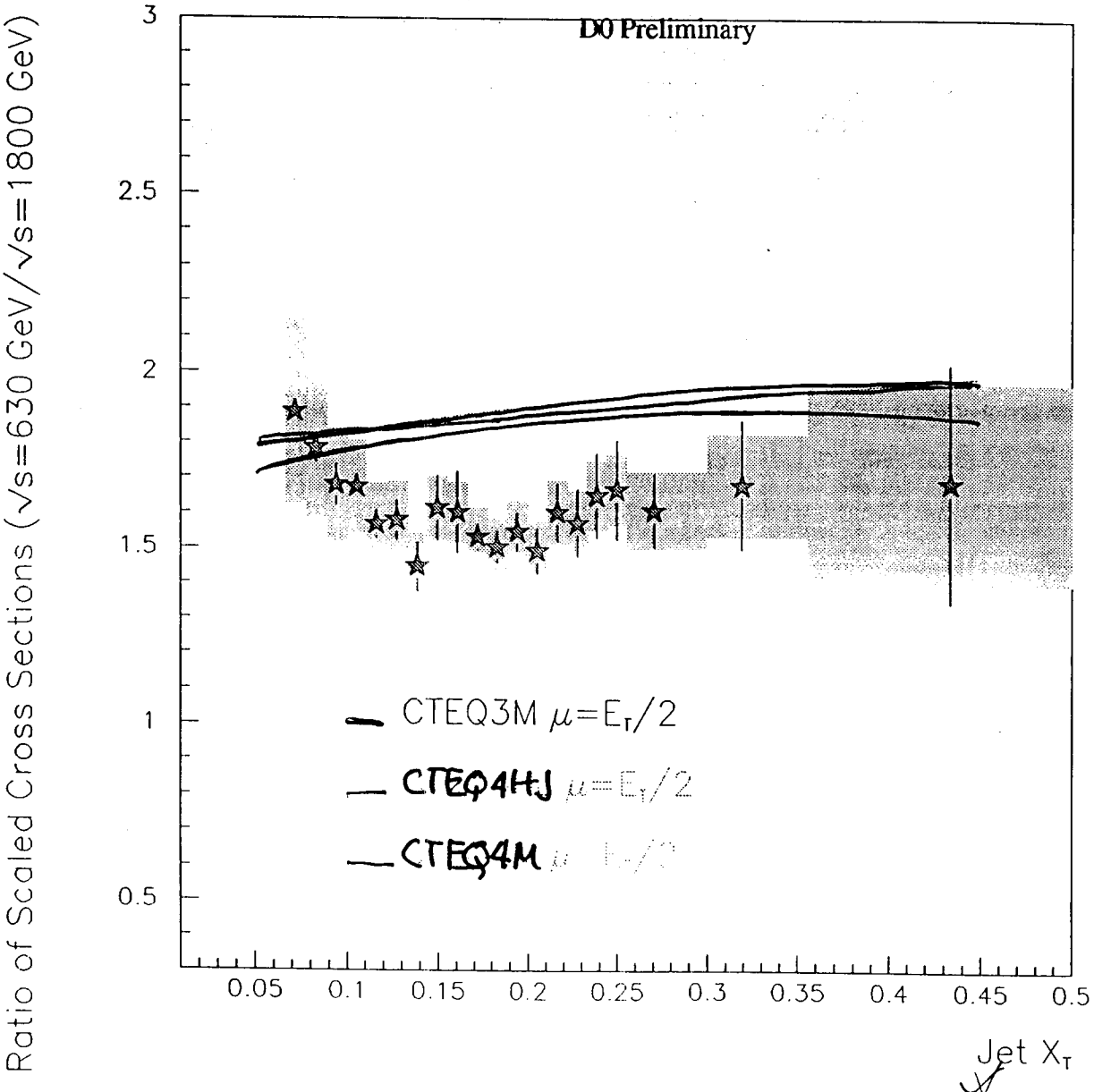

⇒ PDF's not important

JBlazey NDM

Kathy Turner, BNL (kathy@bnl.gov)
Riken-BNL Workshop on Hard Parton Physics in High-Energy Nuclear Collisions
March 1,1999

Hard Parton Physics at the Tevatron $\longrightarrow$ Results from DØ

The focus of this talk was to show Run 1 results from the DØ experiment at Fermilab that may be applicable to RHIC. The analyses discussed are tests of QCD and are summarized below. The full talk is available at http : //www.rhic.bnl.gov/afs/rhic/star/doc/www/conf/index.html. All the results shown are either published or can be obtained from the DØ results pages at http : //www − d0.fnal.gov/public/d0_physics_v2.html and then go to "Publications","Summer 98 Results" or to Physics Groups "QCD" (then either "Approved Plots" or the "Working Groups"). The preceding talk by Prof. G. Blazey should be consulted for details on jet triggering, algorithms, corrections, and calibrations.

Dijet Angular and Mass Distributions:

The dijet angular distribution provides a direct test of QCD is insensitive to parton distribution functions (pdf). The value measured is $\frac{1}{N}\frac{dN}{d\chi}$ where $\chi = e^{2|\eta^*|}$ and η^* is η of c.o.m. system. This variable flattens out the distribution to facilitate comparison with NLO QCD predictions, which were done using Jetrad (Nucl Phys. B**403** (1993) 633). The data are also compared to a prediction with a compositeness scale Λ_c, and lead to a limit on quark compositeness of $\Lambda_c > 1.9$ TeV. See Fig. 1.

The dijet mass spectrum provides constraints on the pdfs and limits on quark compositeness. The dijet mass is calculated assuming the jets are massless. The 95% lower limits on the compositeness mass scale obtained are $\Lambda^+ > 2.7$ TeV and $\Lambda^- > 2.4$ TeV. See Fig. 2.

Jet Shapes:

Jets have structure due to gluon radiation and fragmentation. We measure the radial E_T distribution in jets with cone-size $R = 1.0$, $\rho(r) = 1/N[\Sigma(E_T(r)/E_T(R))]$, as a function of the distance r from the jet axis and compare to NLO QCD predictions at the parton level. This is the first order a jet shape prediction can be made. The run 1A analysis was published (PLB **357** (1995) 500) and there was a subsequent theory paper (hep-ph/9510420). The data show that jets narrow with increasing jet E_T and going from central to forward jets and are insensitive to differences in axis definitions. Herwig Monte Carlo describes the data well whereas the NLO QCD predictions vary considerably with jet axis and clustering definitions. See Figs. 3 and 4.

Color Coherence:

In QCD theory, there is interference of soft gluon radiation emitted along color connected particles. This color coherence is studied to determine the details of hadronic final state to see if these effects can survive hadronization. Also the relative importance of perturbative vs. non-perturbative contributions is measured. In the multijets analysis (PLB **414** (1997) 419), events with 3 or more jets are chosen and the angular distribution of the softer 3rd jet is measured around the 2nd highest E_T jet. The data show a clear enhancement of events in the event plane (i.e. plane defined by direction of 2nd jet and beam axis, $\beta = 0, \pi$) and a depletion in the transverse plane ($\beta = \pi/2$). The data differ from Isajet, which has no color coherence (CC) effects, and from Pythia when angular ordering (AO) is turned off. The NLO QCD prediction from Jetrad and Herwig (has CC) agree best with the data. See Fig. 5.

In the W+ jets analysis (preliminary), the leading E_T jet opposite in ϕ to the W is selected in the event. The multiplicity of calorimeter towers above 250 MeV in a ring around the jet and W from $.7 < R < 1.5$ is measured. Around the W the angular distribution of soft gluons is expected to to be uniform, whereas around the jet there is expected to be structure. This enhancement of multiplicity around the jet compared to the W is seen in the data. Monte Carlo models which include CC effects and QCD predictions (hep-ph/9612351) in which the parton cascade is evolved much further than traditional QCD (MLLA calculation) agree well with the data. See Fig. 6.

Direct Photons:

Direct photons can be used as probes for hard parton interactions w/o fragmentation effects. Used as a test of NLO QCD, they give information on the contribution from higher order corrections, especially multiple soft gluon emission (i.e. k_T effects)
gluon pdfs and also matrix elements. The analysis based on Run 1A data sample is published (PRL **77** (1996) 5001) and the Run 1B results are preliminary. The inclusive cross section is consistent with QCD predictions (PRD **42** (1990) 61), but data from all experiments show a trend away from predictions - especially at low p_T. The γ-jet angular distribution agrees well with the same NLO predictions. The di-photon p_T spectrum shows deviation from NLO (PRD **46** (1992) 2018) at low p_T. Predictions which add in multiple gluon emission, Pythia or resummed-QCD (hep-ph/9701258), are consistent with data. See Fig. 7 and 8.

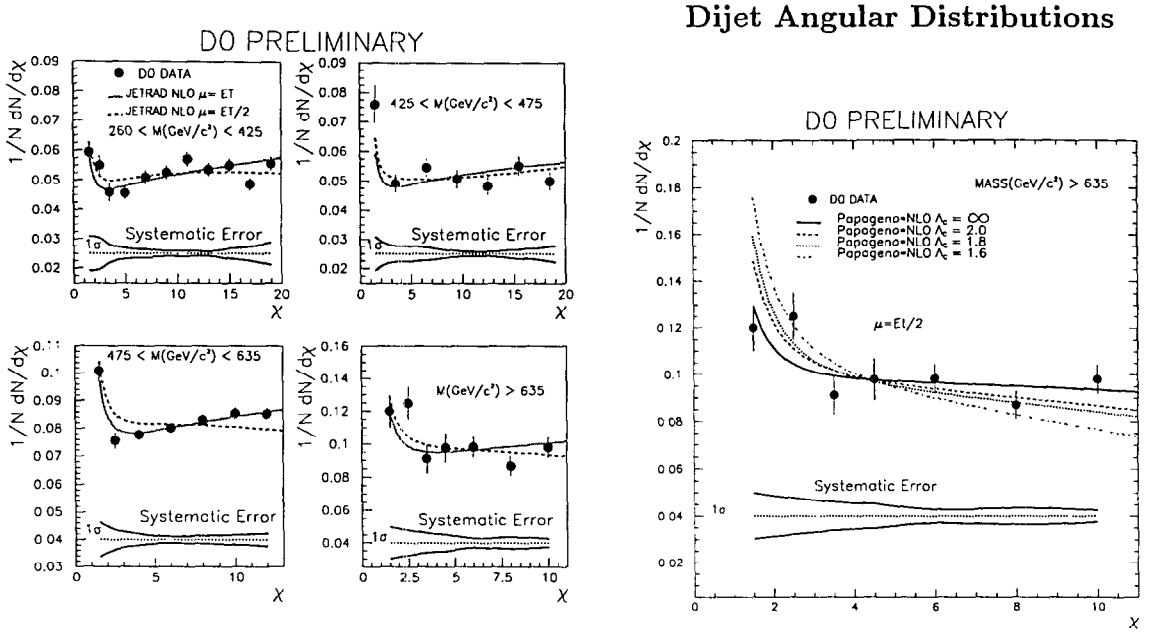

Figure 1: (A) The dijet angular distribution vs. χ is shown over 4 regions of dijet mass and compared to NLO QCD predictions using JETRAD. (B) The data are shown compared to predictions with various values of the compositeness scale, Λ_c.

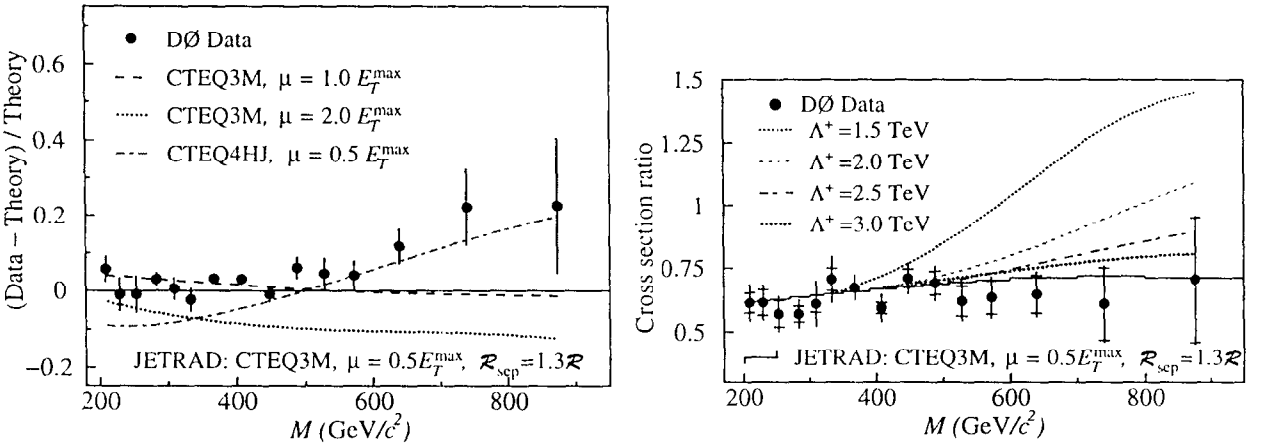

Figure 2: (A) The difference between the dijet mass distribution data and theory are shown vs. the dijet mass. Also shown are the differences between the nominal pdf and μ-scale and other settings (lines). The shaded region indicated the errors on the data. (B) The ratio of the dijet mass spectra for $|\eta|_{jet} < 0.5$ and $0.5 < |\eta|_{jet} < 1.0$ and the NLO prediction at the nominal settings and scaled to different compositeness values.

D0 Jet Shape - CENTRAL

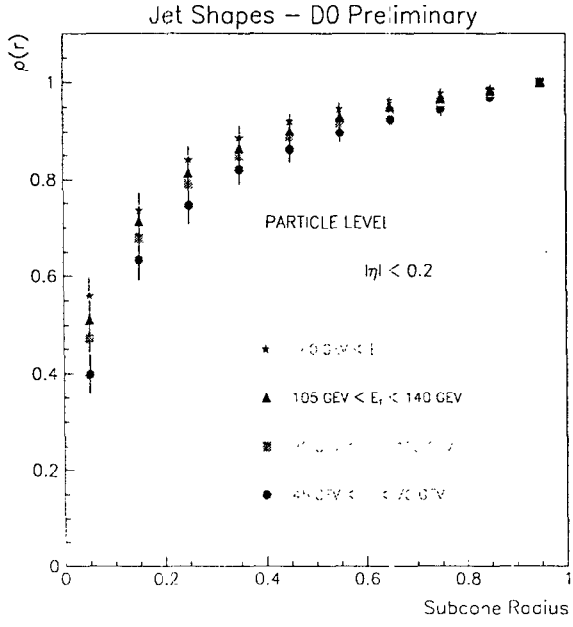

Slide 9

Figure 3: The measured integrated jet E_T as a function of distance from jet axis, corrected for detector effects, is shown in the central region for 4 values of jet E_T.

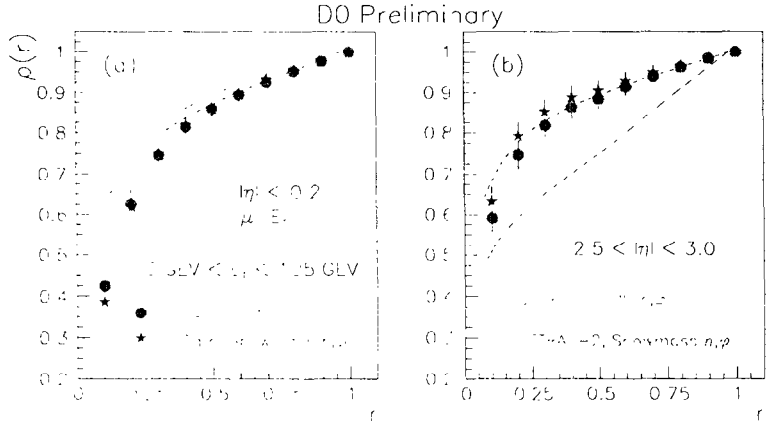

Figure 4: The data are shown for jets in the central (a) and forward (b) regions, using two different jet axis definitions, compared to the NLO prediction using the two different definitions.

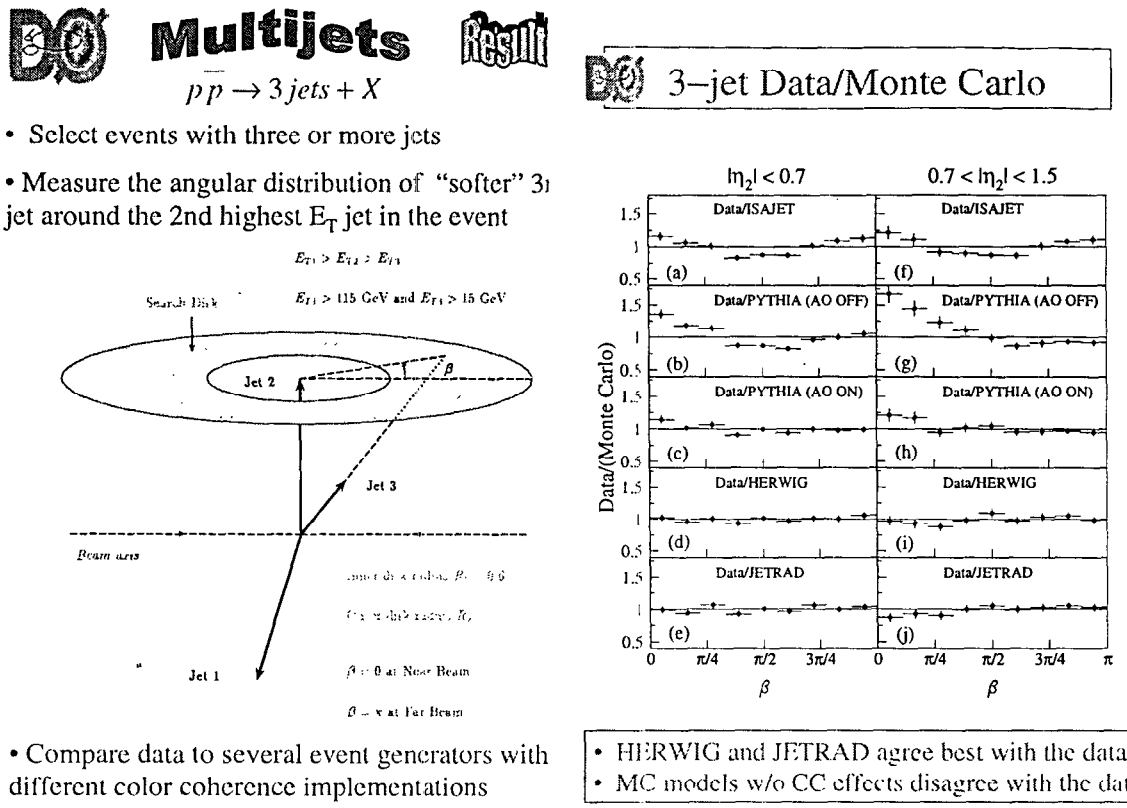

Figure 5: (A) Explanation of coordinate system used in analysis. (B) Ratio of observed β distributions relative to the MC predictions for two η regions. MC models that don't have color coherence effects are seen to disagree with the data.

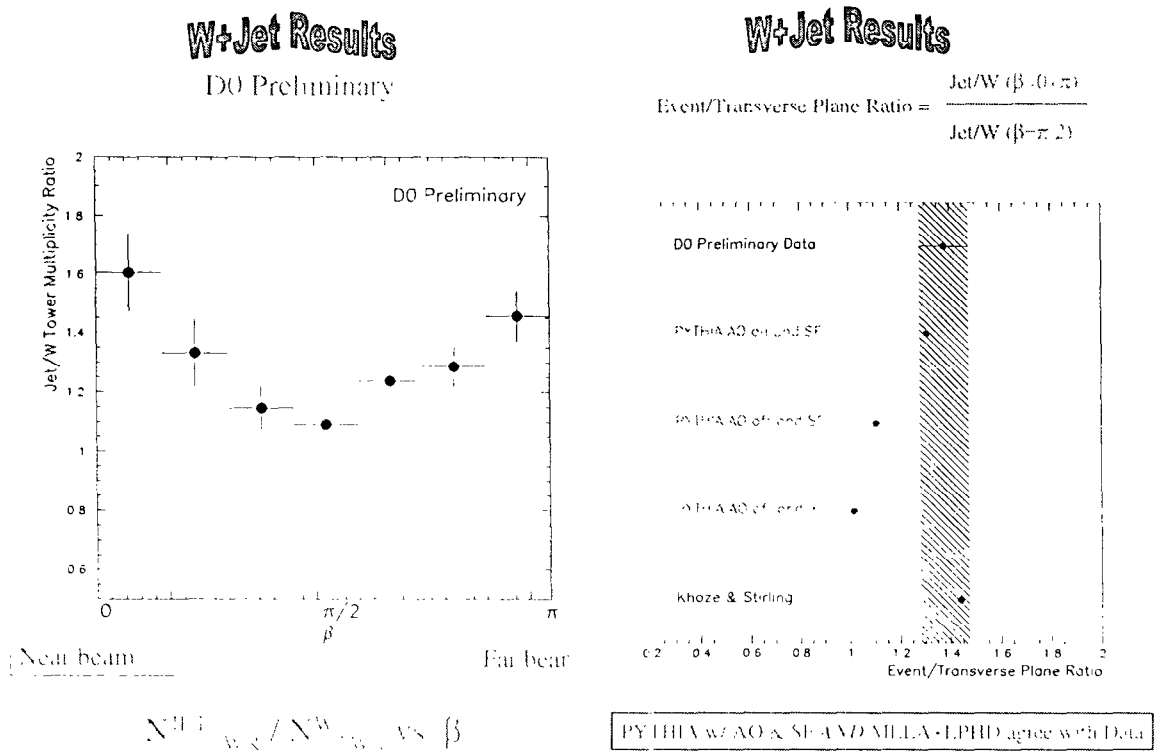

Figure 6: (A) The ratio of calorimeter tower multiplicity around the jet and the W as a function of the angle β. (B) The ratio of event plane to transverse plane of jet/W tower multiplicity for the data, Pythia with various color coherence implementations and for a MLLA QCD calculation.

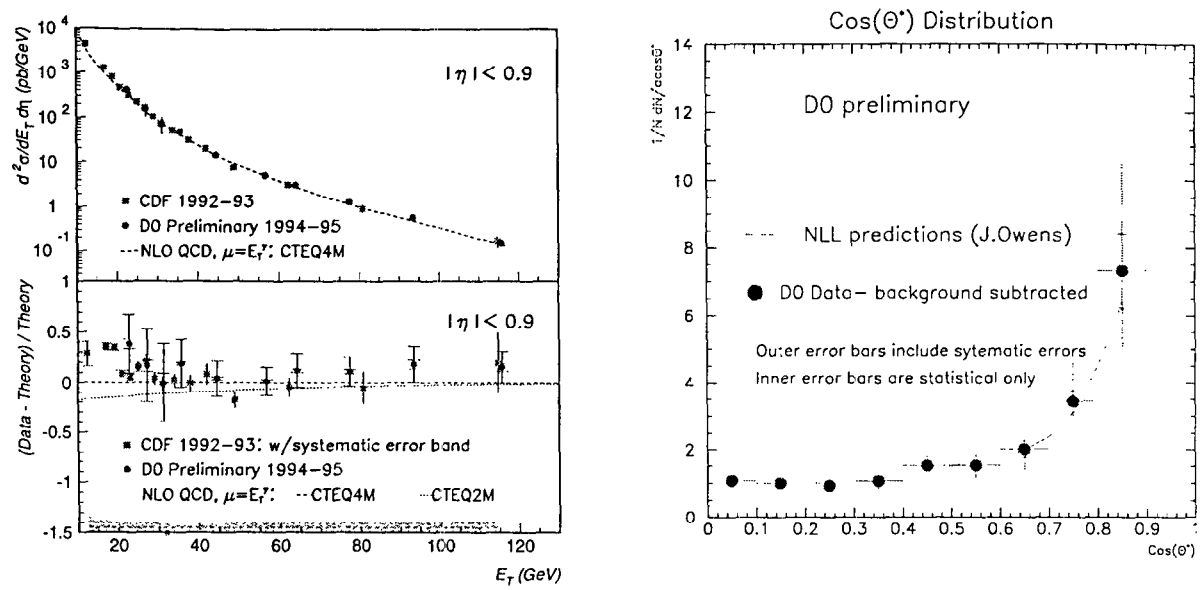

Figure 7: (A) The direct-γ cross section from DØ and CDF, compared to NLO QCD (Baer *et al*). (B) The γ+jet angular distribution (Run 1A).

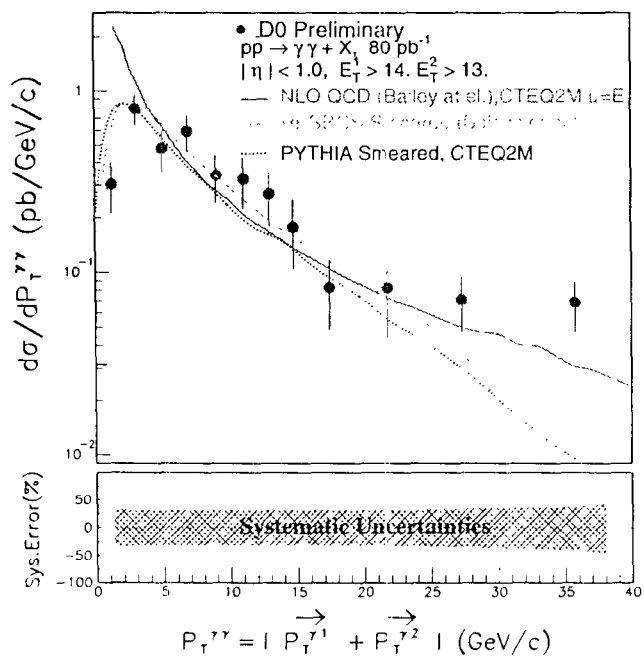

Figure 8. The di-photon p_T spectrum (Run 1B).

Partons in A+A Collisions at RHIC with PHENIX

Paul Stankus
Workshop on Hard Parton Physics
Mar 2, BNL

Theme: The goal of RHI physics is to diagnose the state of very hot, dense nuclear matter, particularly seeking novel QCD effects such as the predicted QGP.

Hard-scattered partons are potentially very useful probes of the earliest stages of RHI collisions once collider energies become available.

1. (not much) Physics
2. A pallet of measurements in the PHENIX experiment
3. Some questions I have for smarter people
4. Conclusions

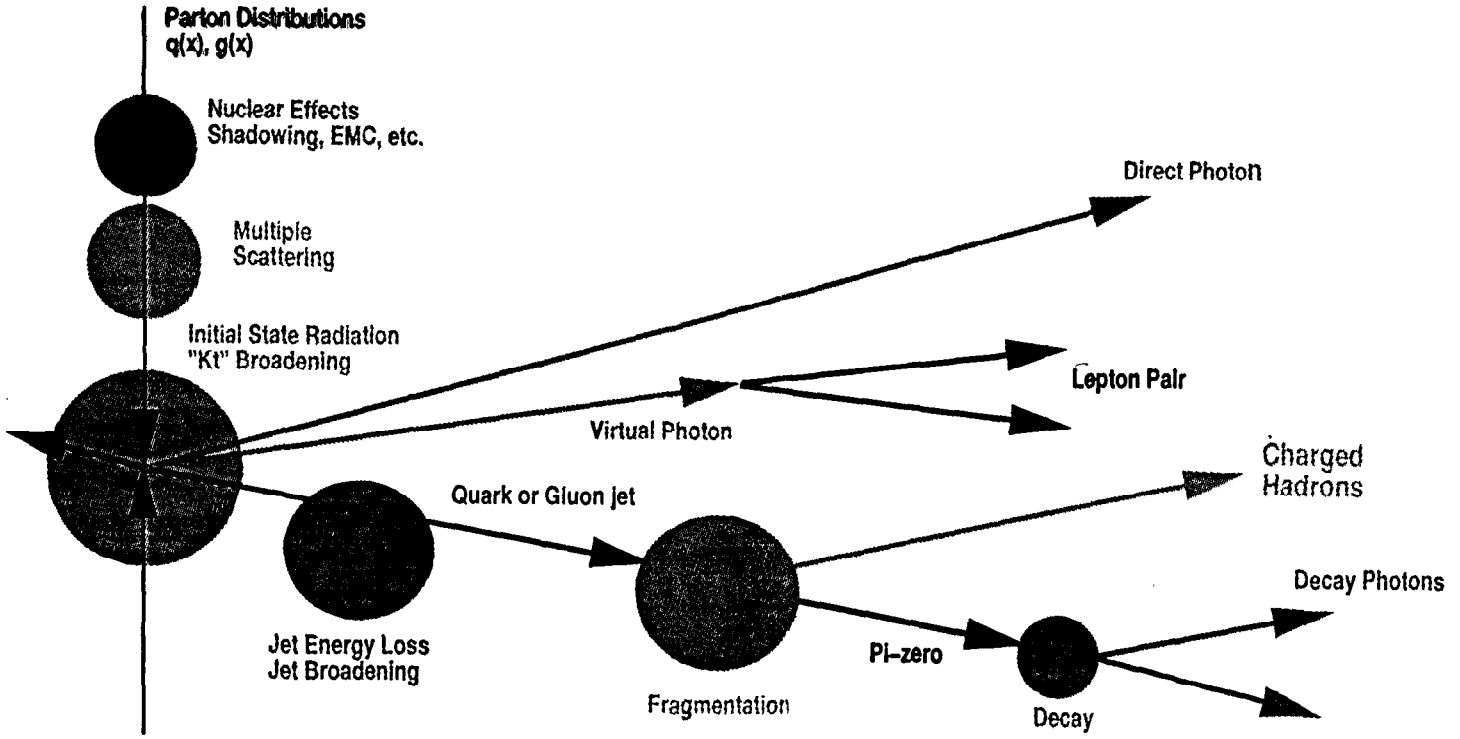

	Parton Distributions q(x), g(x)	Nuclear PDF Effects	Multiple Scattering	Initial State Radiation "Kt" Broadening	Jet Energy Loss, Broadening	Fragmentation	Decay
A+A							
Inclusive Photons	✔	✔	✔	✔	✔	✔	✔
Inclusive Hadrons, π^0	✔	✔	✔	✔	✔	✔	
Direct Photons and Lepton Pairs	✔	✔	✔	✔			
Hadron–Hadron Back to Back	✔	✔			✔	✔	
Photon–Hadron Back to Back			✔	✔	✔	✔	
Photon–Photon Back to Back			✔	✔			
p+p							
Inclusive Hadrons	✔			✔		✔	
Direct Photons	✔			✔			
p+A							
Direct Photons	✔	✔	✔	✔			

Inclusive Photons into PHENIX EMCal

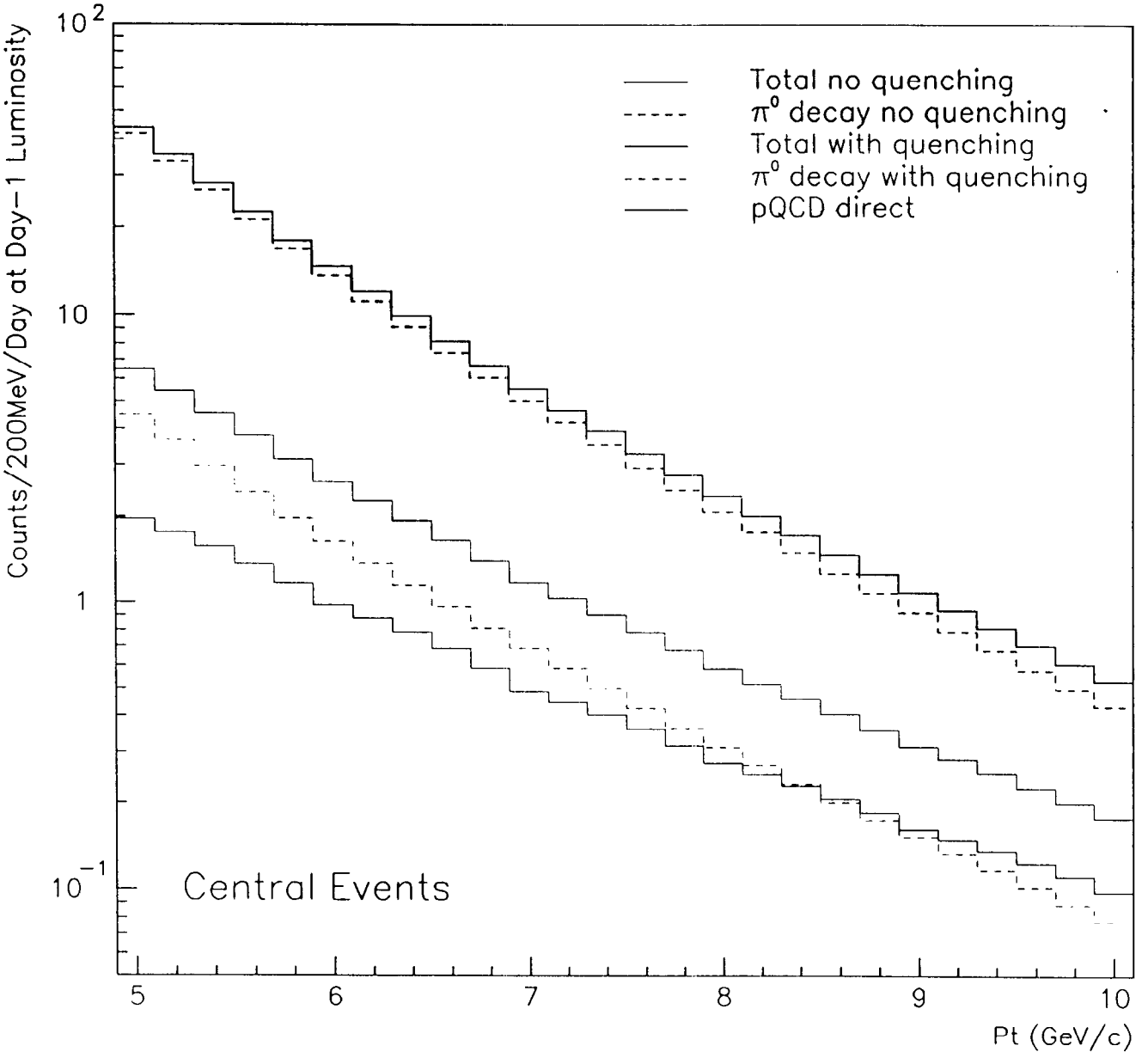

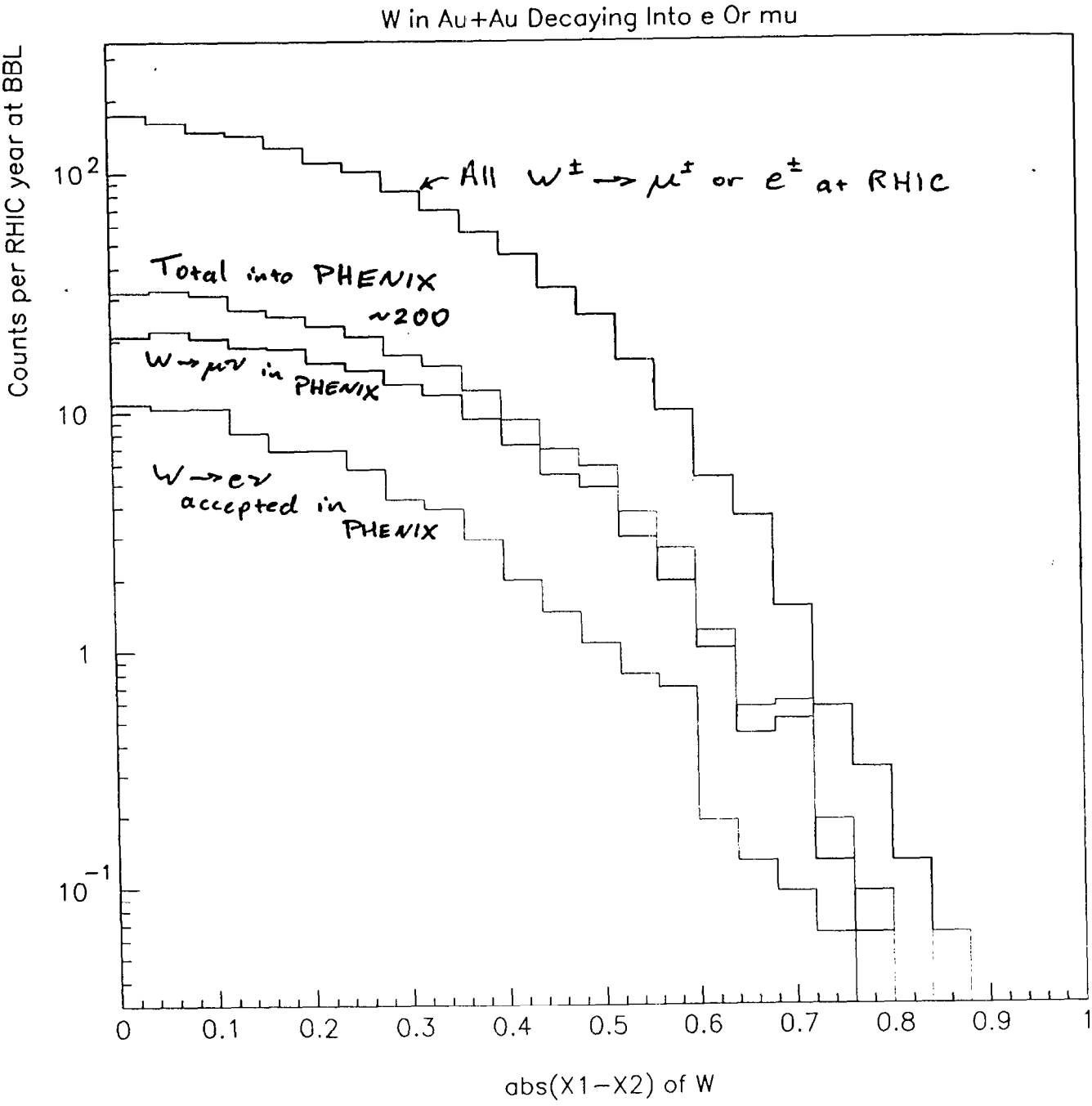
W in Au+Au Decaying Into e Or mu
Counts per RHIC year at BBL
10^2
10
1
10^{-1}
All $W^{\pm} \to \mu^{\pm}$ or $e^{\pm}$ at RHIC
Total into PHENIX
~200
$W \to \mu\nu$ in PHENIX
$W \to e\nu$
accepted in
PHENIX
0
0.1
0.2
0.3
0.4
0.5
0.6
0.7
0.8
0.9
1
abs(X1−X2) of W

4a Nuclear Charge Symmetry Violation: A "Boutique" Measurement at RHIC

(Suggestion: J. Moss, LANL)

Nuclear charge symmetry – the proton is the isospin mirror of the neutron – can be expressed in terms of PDF's as:

$u^p(x) = d^n(x), u^n(x) = d^p(x)$

$\bar{u}^p(x) = \bar{d}^n(x), \bar{u}^n(x) = \bar{d}^p(x)$

Though known to be broken in static limit, $m_n \neq m_p$, expression in PDF's not well known (see recent Boros, Londergan, Thomas, Phys.Rev.Lett. 81 (1998)).

If isospin balanced nuclei were run in RHIC (e.g. α, ^{40}Ca, etc.) then CSV would manifest an imbalance between the processess $u + \bar{d} \rightarrow W^+$ and $\bar{u} + d \rightarrow W^-$. So, a simple measurement of the W^+/W^- rate ratio could yield a "precision" measurement of CSV in the nucleon.

Very preliminary work suggests $\approx$4000 $W^{\pm}$ accepted into PHENIX per year in O+O at $\sqrt{S}$=250 GeV and B.B.L. – right on the edge of possibility. Clearly, more work is needed.

Questions For the Luminaries:

(1) We believe that medium effects will distinguish medium from vacuum; but will they ever distinguish QGP from HG from Other? or is -dE/dx at best a "densitometer"?

(2) My picture of "factorizing" production, medium effects and fragmentation is certainly naive. How am I to picture a string with it's tail in the QGP? what does it attach to? Do I need an (entirely?) new picture for fragmentation?

(3) Can un-interacted partons ever "see" an early pile-up of thermalized QGP material?

Angular Correlations at High-p_t

Craig Ogilvie, for the STAR Collaboration

To first discover, then study the properties of the QGP requires a probe that is both sensitive to correlations in the plasma and retains its information during the intense hadronic scattering in the exit phase of the reaction. One class of signatures that may satisfy these requirements is the yield and correlations of particles at high transverse momenta (pt). As partons from hard-scattering collisions travel through the dense, hot, early stage of the collision, they are predicted to lose energy due to increased radiation of gluons. One experimental consequence of this energy-loss may be a reduction in the yield of high-pt hadrons. Given the complexity of heavy-ion reactions, and also that pt-distributions depend on many other factors, e.g. the currently unknown gluon distributions in Au, it is important to find complentary experimental probes of energy-loss physics. An alternative probe of energy-loss may be how two-particle correlations in angle change as a function of pt and centrality.

After a hard scattering in p+p reactions, the hadrons from the fragmenting parton appears as a jet. This can be characterised by the energy within a jet cone, and by the distribution of energy and particles within the cone. Given that fluctuations in the large number of soft hadrons at RHIC make it hard to impossible find jets in Au+Au reactions, an interesting alternative may be to measure the correlation of two high-pt particles as a function of relative angle. The key idea is that if a hard-parton travels through a plasma, then the nearly collinear-gluons radiated from the fast parton would produce a broader angular distribution of emitted hadrons

In this talk correlation functions in two different relative angles are explored: the relative angle α between two tracks, and the difference in azimuthal angle, $\Delta\Phi$. To begin to develop our algorithms for these observables in STAR we have simulated Au+Au reactions with the HIJING event generator, through STAR's GEANT and simulation of the TPC response and finally through the tracking and analysis chain. In Au+Au reactions the simulated correlations in α are strong, but may be more difficult to interpret given the uncertainty of the correct parton-parton reference frame and that other sources of correlation exist. The correlation in $\Delta\Phi$ is weaker and may be difficult to observe above the combinatorical background. Both will be measured in STAR during the first year of RHIC operation.

The small-angle rise in the correlation functions can be fitted with a gaussian. The width and amplictude of these gaussians characterises each correlation function. In HIJING energy-loss of hard partons is modeled as a transfer of energy from the parton to nearby strings. By comparing the simualtions with energy-loss off , the correlation functions both broaden and become weaker if the parton loses energy in the HIJING simulation. To search for this effect in RHIC we plan to measure the correlation functions as a function of centrality in Au+Au. Peripheral reactions provide a baseline behavior for the correlation functions. The effects of energy-loss should be largest in the most central reactions. These correlation functions will be measured for different transverse momenta of the pair of particles.

Measuring two-particle correlation functions at RHIC has the potential to probe the propagation of a fast parton through a QGP. If the gluon radiation from such a parton increases in a plasma, then both the momemtum and angular distributions of the hadrons will be changed. The angular distribution of the hadrons can be characterized by two-particle angular correlation functions. These measurements are complementary to the high-pt spectra of hadrons and may offer the calculational advantage of being insensitive to the unknown gluon-distribution in Au. In addition experimental effects such as acceptance and tracking efficienies will cancel. Angular correlations may therefore provide robust, early information on the propagation of a fast parton through a possible QGP.

Angular Correlations at High-p_t

- Basic idea
  - hard scattering produces two high-pt partons
  - hadrons from fragmenting parton emitted in tight cone
  - any two of these hadrons are strongly correlated in angle
    - » 2-particle angular correlation function in Au+Au
      - X.N Wang Phys. Rev. D47, 2754 (93)
    - » sensitive to energy-loss of fast parton within QGP?
    - » not sensitive to shadowing of structure functions?
    - » complementary to change in high-pt spectra
- Preliminary simulations for STAR
- Next steps

Angular Correlations Between Two Final Hadrons

$$\alpha = \cos^{-1}(\hat{p}_1 \cdot \hat{p}_2)$$

$$\Delta\phi = |\phi_1 - \phi_2|$$

$$C(\text{angle}, pt_1, pt_2) = \frac{N_{real}(\text{angle}, pt_1, pt_2)}{N_{\text{mixed events}}(\text{angle}, pt_1, pt_2)}$$

1) Correlations less sensitive to rate of initial hard-scattering than high-pt spectra of hadrons
   => less sensitive to shadowing of structure functions in Au
2) Use both angles, α frame dependence, ϕ worse combinatorics
3) Instrumental effects cancel, e.g. acceptance, track efficiency (apply 2-track acceptance-cut)
   => early, robust measurement in year 1 @ RHIC

Do Correlations Probe Energy-loss ?

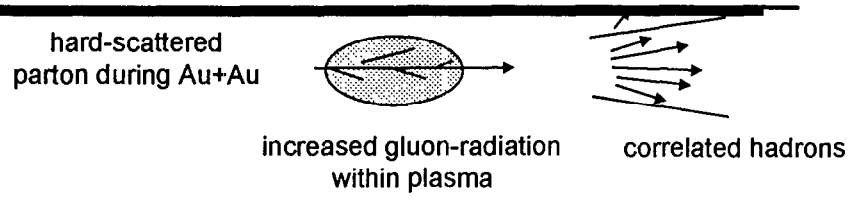

- How does the redistribution of energy change the correlation of hadrons?
  - nearly-collinear bremstrahlung gluons
    - » maintain but broaden angular correlation ?
  - energy given to nearby "string" (HIJING)
    - » little angular correlation between string, fast parton ?

Pythia: p+p $s^{1/2}$ 200 GeV/c in STAR's Acceptance

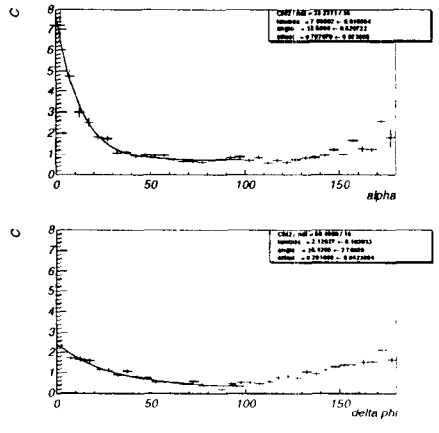

$pt_1, pt_2 > 1$ GeV $\quad |\eta|<1.7$

$$C = \text{offset} + \text{lambda} \times e^{-\alpha/\text{fit\_angle}}$$

$$C = \text{offset} + \text{lambda} \times e^{-\Delta\phi/\text{fit\_angle}}$$

Correlation in α much tighter than $\Delta\phi$

Correlations Can be Measured in Au+Au

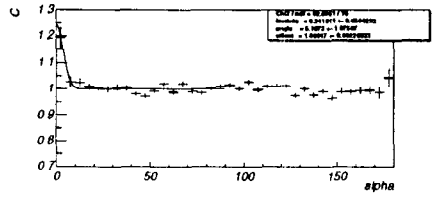

α

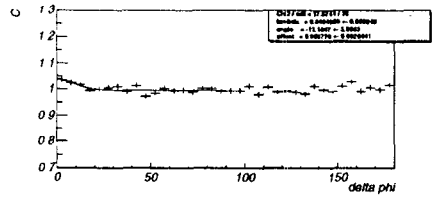

Δϕ

HIJING : Au+Au 200 AGeV
b<10fm: Jet Quenching ON

$p_\perp^1, p_\perp^2 > 1.0\text{GeV/c}$ $|\eta|<1.7$

$C = \text{offset} + \text{lambda} \times e^{-(\Delta\phi/\text{fit\_angle})^2}$

Correlation in α much tighter than Δϕ
Correlation in Δϕ very weak in central reactions

HIJING : Au+Au $s^{1/2}$=200 AGeV, central

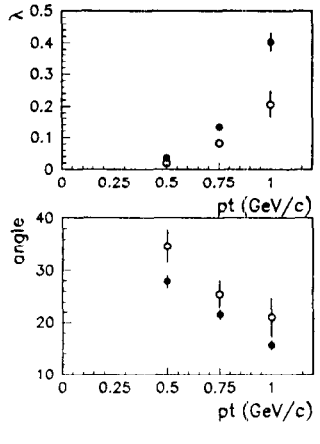

$C = \text{offset} + \lambda \times e^{-(\alpha/\text{fit\_angle})^2}$

- ● 'jet quenching' off
- ○ 'jet quenching' on

- HIJING high-pt partons lose energy to nearby strings
- => broadens and weakens angular correlation

- How to search for this at RHIC?
- study correlations vs centrality

Centrality Dependence of Angular Correlations

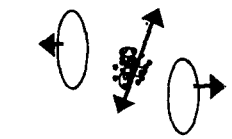

Angular correlations in peripheral reactions ~ p+p

Steadily increase centrality

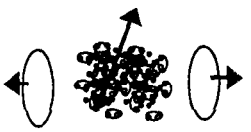

Steadily increase the average length hard partons travel through plasma

HIJING : Au+Au $s^{1/2}$=200 AGeV: Quenching ON

0<M<250

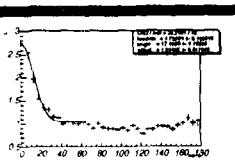

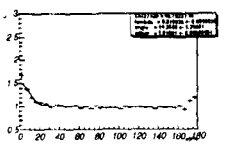

250<M<750

750<M<1250

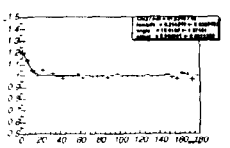

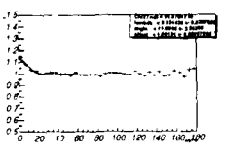

1250<M<1750

1750<M<2250

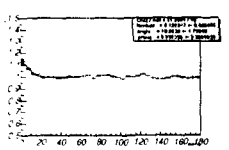

M= event multiplicity
correlation function
tracks in TPC
$pt_1, pt_2 > 1$ GeV/c, $|\eta|<1.7$

HIJING: Jet-Quenching ON

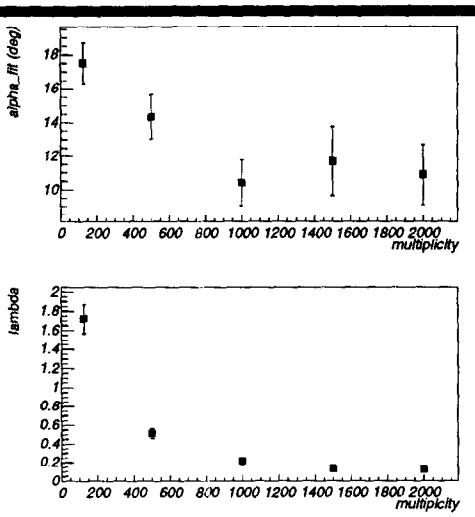

Correlation functions
tracks in TPC
$pt_1, pt_2 > 1$ GeV/c, $|\eta|<1.7$

Decrease in λ due to increasing combinatorics

but why does alpha_fit decrease with multiplicity?

Questions and Plans

- How do other treatments of energy-loss change angular correlations? e.g. medium-induced bremstrahlung
- Are correlations insensitive to initial gluon shadowing?
- Choice of relative angle α or $\Delta\phi$
- Explore
  - tighten η-cut, select on total transverse momentum of pair
- Technical : two-track acceptance cut, resolution vs pt, ghosts

Angular correlations - feasible, complementary probe of energy loss in a plasma

Early robust, observable : many instrumental effects cancel, e.g. acceptance, track efficiency

Data Sets for High P_t Physics with the STAR Detector

W.B. Christie, BNL

Presented at the RIKEN-BNL Workshop on

Hard parton physics in high energy nuclear collisions

March 2, 1999.

Outline

- Brief Physics Introduction
- Measurements necessary
- Brief Intro. to STAR Detector
- Schedule Considerations
- Summary

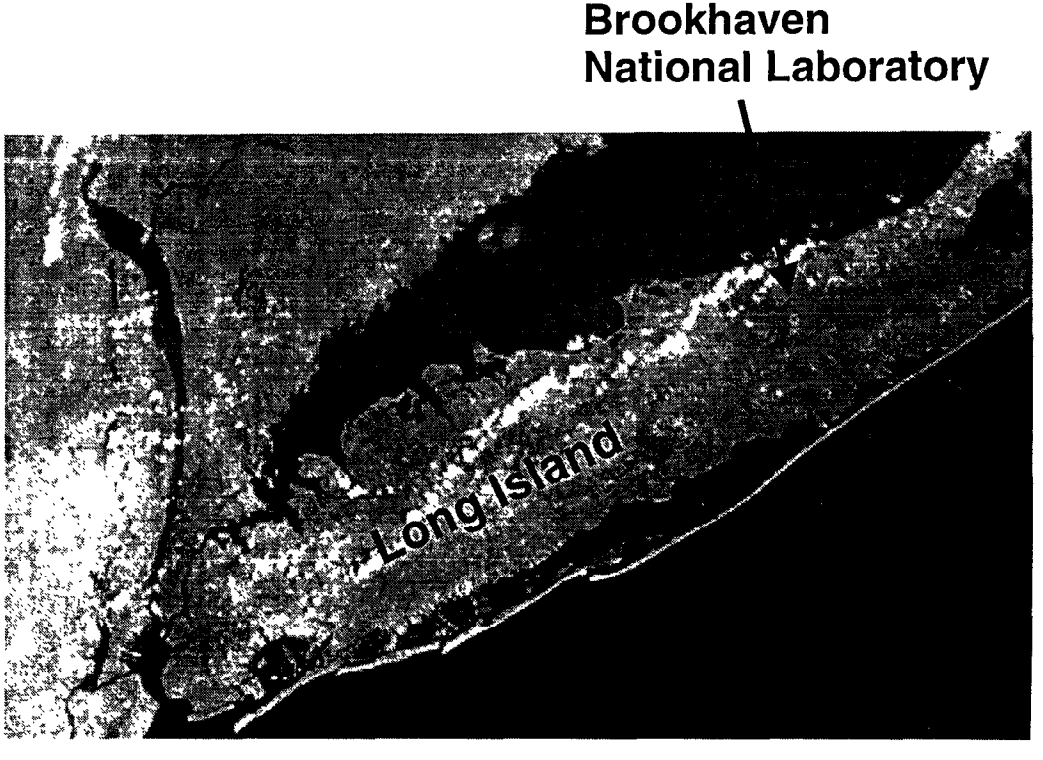

Measurements to be made

- Inclusive particle spectra
  - pp, pA (various A), and AA
- Quark and gluon distributions (structure functions) in the proton
  - pp data set at $\sqrt{s}$ = 200 GeV, select γ-jet final state
- Nuclear Shadowing (modification of structure ftns for bound nucleons)
  - pA data set, select γ-jet final state
- Jet Fragmentation functions
  - pp data set at $\sqrt{s}$ = 200 GeV, select γ-jet final state
  - pA data set, select γ-jet final state
  - AA data sets, select events with "tagged" photon (tough)

STAR from the Inside - Out

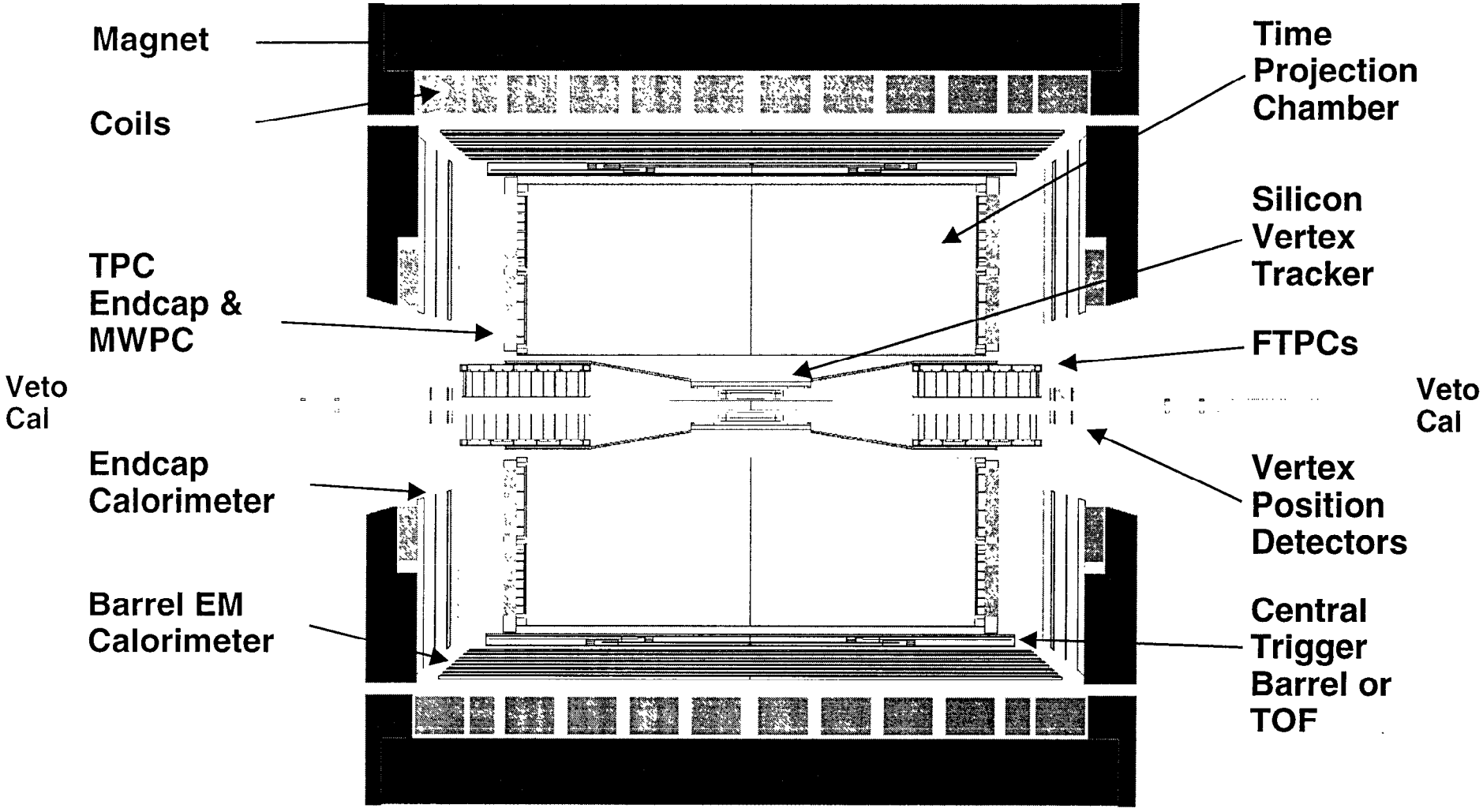

99

Schedule considerations

STAR Barrel Electromagnetic Calorimeter (BEMC) Construction and Installation

Year	1999	2000	2001	2002	2003
Module	12	30	32	32	14

STAR Endcap Electromagnetic Calorimeter (EEMC) Schedule

present schedule has EEMC installed in summer of 2002.

⇛ **STAR will be fully instrumented to take High Statistics pp and pA data sets in Physics run starting Fall of 2002** (assumes last 14 BEMC modules installed early)

Take Spin data set in Fall 2002 Physics run?

- **~ 10 weeks of polarized pp at $\sqrt{s}$ = 200 GeV**
- **~ 10 weeks of polarized pp at $\sqrt{s}$ = 500 GeV**
- **~ 10 weeks of pA**

Summary

- The use of hard probes to study the matter produced at RHIC looks promising

- The data sets that one needs to persue this analysis includes:

  - pp, pA, and AA.

- The measurements one needs to make are the gluon structure functions and the fragmentation functions

- The STAR detector will have the capability to make these measurements

- The time scale to have the Barrel and Endcap Calorimeters fully instrumented is the summer of 2002.

- STAR will start working on this Physics in the first (1999) run

Gluon minijet production in high energy nuclear collisions

XIAOFENG GUO
Department of Physica and Astronomy, Universitu of Kentucky
Lexington, KY 40506

In ultra-relativistic heavy ion collisions, physical observables sensitive to a few GeV momentum scale, such as the mini-jet production, will be dominated by scattering of soft gluons from both heavy ion beams. Understanding the distribution of soft gluons formed in the initial stage of the collision is particularly interesting and important. McLerran and Venugopalan (MV) developed a new formalism for calculation of the soft gluon distribution for very large nuclei. In this approach, the valence quarks in the nuclei are treated as the classical source of the color charges, and the gluon distribution function for very large nuclei may be obtained by solving the classical Yang-Mills Equation. Using the classical glue field generated by a single nucleus obtained in the MV formalism as the basic input, Kovner, McLerran, and Weigert (KMW) computed the soft gluon production in a collision of two ultra-relativistic heavy nuclei by solving the classical Yang-Mills equations with the iteration to the second order.

Through explicit calculation of soft gluon production in partonic process $qq \to qqg$, I show that at the leading order, McLerran-Venugopalan formalism is consistent with QCD perturbation theory. I also demonstrate that the key logarithm in KMW's result represents the logarithm in DGLAP evolution equations.

(continue McLerren-Venugopalan model:)

For soft gluon production in heavy ion collisions

— valence quarks in nuclei
= two infinitely thin sheets of color charges moving at the speed of light in $+\hat{z}$ & $-\hat{z}$ directions : $J^{\nu}_{1,2} = \delta^{\nu\pm}\,\delta(x^{\pm})\,\rho_{1,2}(x_T)$

— using the classical gluon field generated by a single nucleus as input

— solve classical Yang-Mills eq.

⇒ obtain the leading soft gluon production in heavy ion collisions

Lowest order non-trivial solution:
(Kovner, McLerran, & Weigert)

$$\frac{d\sigma}{dy\,d\vec{p}_T^{\,2}} = \frac{2g^6}{(2\pi)^4}\left(\frac{N_q}{2N_c}\right)^2 N_c(N_c^2-1)\frac{1}{p_T^4}\ln\left(\frac{p_T^2}{\Lambda_{cutoff}}\right)$$

with $\frac{N_q}{2N_c} = S_T\,\mu^2$ $\quad\mu^2$ — averaged color charge density

S_T — transverse area of nulei

N_q — total number of valence q

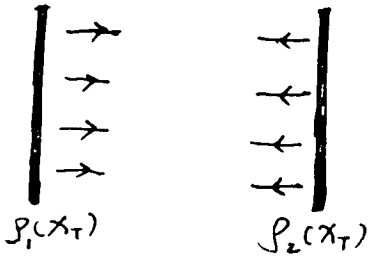

How does it work ?

- $\frac{d\sigma}{dy\,dp_T^2} = \frac{1}{2s}|M|^2\,dps$ $\qquad |M^2| \propto$

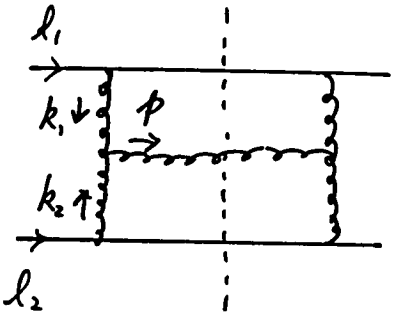

$$poles = \frac{1}{k_1^2+i\epsilon}\cdot\frac{1}{k_1^2-i\epsilon}\cdot\frac{1}{k_2^2+i\epsilon}\cdot\frac{1}{k_2^2-i\epsilon}$$

$$dps = \frac{d^4k_1}{(2\pi)^4}\cdot\frac{d^4k_2}{(2\pi)^4}\cdot(2\pi)\,\delta((l_1-k_1)^2)\cdot(2\pi)\,\delta((l_2-k_2)^2)$$

$\Rightarrow$ Leading contribution : when $k_1^2 \to 0$ Limit
or $k_2^2=(p-k_1)^2 \to 0$

Note: k_1^2 & k_2^2 can not $\to 0$ at the same time

$\because p^2=(k_1+k_2)^2=0$, and k_1 & k_2 are along different direction

- Applying factorization theorem :

at $k_1^2 \to 0$ limit (k_1 on-shell),

collinear expansion : $k_1 \approx x\,l_1 + o(k_{1T})$

with $k_{1T} \sim \Lambda_{cutoff} << P_T$

(all P_T come from k_2)

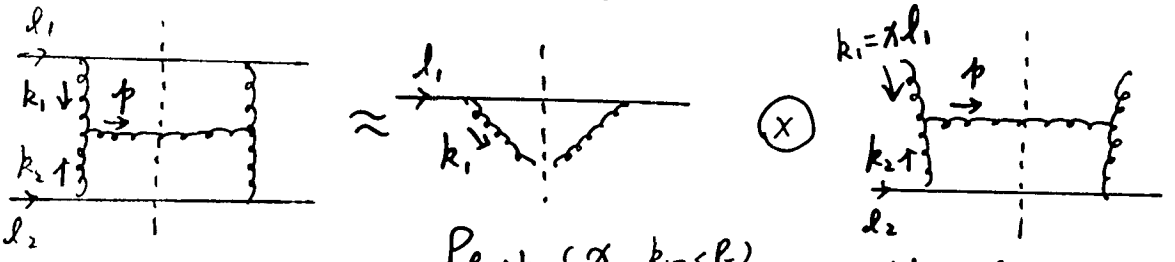

$P_{l_1\to k_1}(x,\ k_{1T}<P_T)$ $\qquad$ $H(xl_1,\ l_2,\ p)$

$\uparrow$ $\qquad$ $\uparrow$

quark splitting $\qquad$ partonic $2\to 2$ process

similary for $k_2^2 \to 0$ limit

Gauge invariance ?

For $qq \to qqg$ process. also need to include:

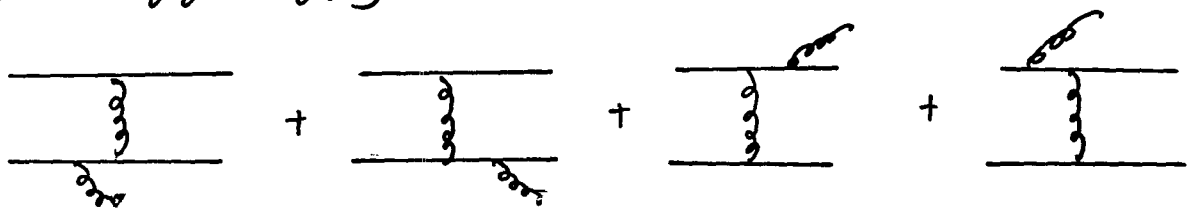

when taking the leading contribution at $k_i^2 \to 0$ Limit:

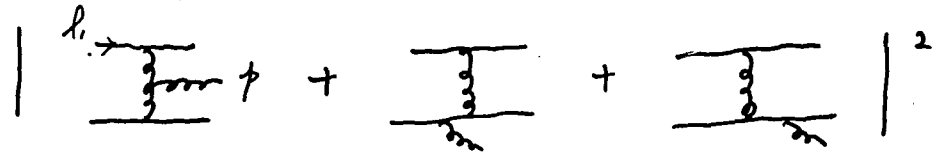

$\to$

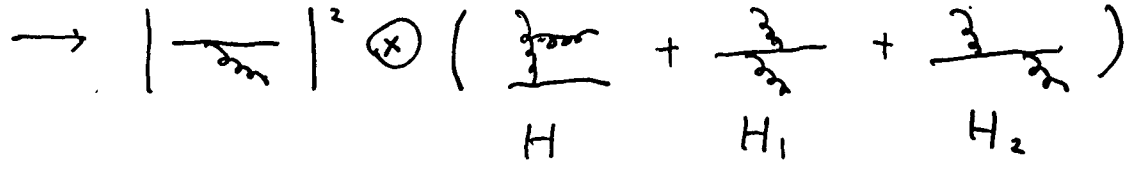

$\frac{H_1}{H} \sim \frac{H_2}{H} \sim \frac{p_\perp}{l_\perp}$, at soft gluon limit $\frac{p_\perp}{l_\perp} \to 0$

(in $\bar{n}\cdot A = 0$ gauge

$\Rightarrow$ H_1 & H_2 contribution to the leading soft gluon production can be neglected!

similarly, the other two diagrams are also suppressed!

Final result:

$P_{l_1 \to k_1}$: 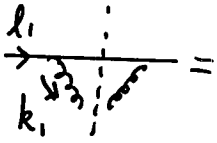 $= \frac{N_c^2-1}{2N_c}\left(\frac{g^2}{8\pi^2}\cdot\frac{1+(1-x)^2}{x}\right)\ln\frac{p_T^2}{\Lambda^2_{cutoff}}$

— quark splitting function in DGLAP parton evolution eq.

$H(x, l_1, l_2, p)$: 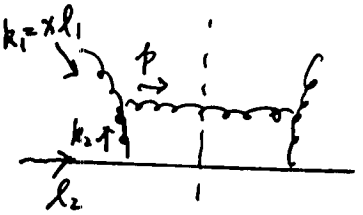

$s=(l_1+l_2)^2=2l_+l_-$

$$= (8\pi)g^4\left(\frac{1}{2}\right)\left(\frac{p_+}{xl_+}\right)^2\frac{1}{p_T^4}\frac{1}{s-2l_+p_-}\delta\left(x-\frac{2p_+l_-}{s-2l_+p_-}\right)$$
$$\cdot\left[(xs-2xl_+p_-)^2+(2xl_+p_-)(2p_+p_-)\right]$$

$\frac{d\sigma_{gg\to g}}{dy\,dp_T^2}$ = 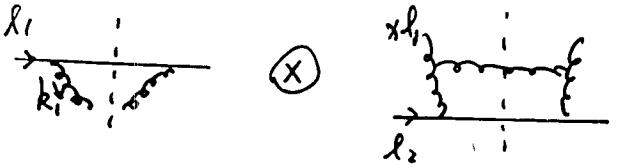

$$= 2\left(\frac{1}{2(2\pi)^3}\cdot\frac{1}{2s}\right)\int\frac{dx}{x}\cdot P_{l_1-k_1}(x)\cdot H(xl_1, l_2, p)$$

$$= \frac{2g^6}{(2\pi)^4}\cdot\left(\frac{1}{2N_c}\right)^2 N_c(N_c^2-1)\left(\frac{1}{p_T^4}\right)\ln\frac{p_T^2}{\Lambda^2_{cutoff}}$$

after taking the soft gluon limit $x=\frac{p_T}{l_+}<<1$

reproduce KMW's result at $N_f=1$

In pQCD, use quark distribution $f_{q/A}(x, Q^2 = p_T^2)$ to replace N_q in KMW formula

$$\frac{d\sigma_{AB\to g}}{dy\, dp_T^2} = \int dz_1\, dz_2\; f_{q/A}(z_1)\, f_{g/B}(z_2) \cdot \left(\frac{d\sigma_{qg\to g}}{dy\, dp_T^2}\right)$$

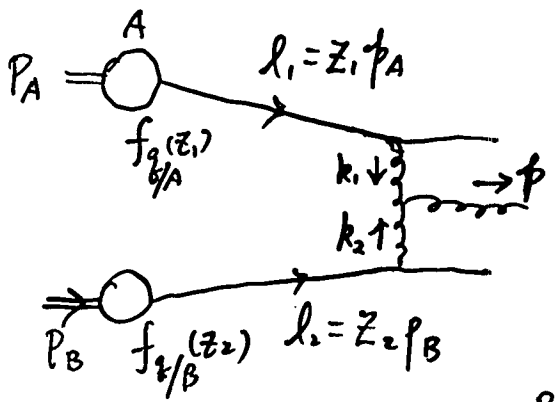

$\doteq$

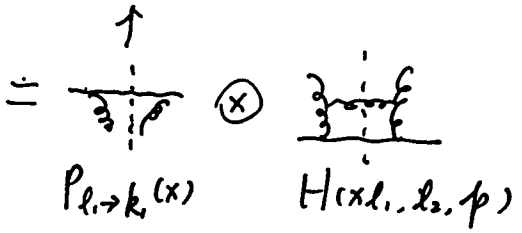

$\approx$

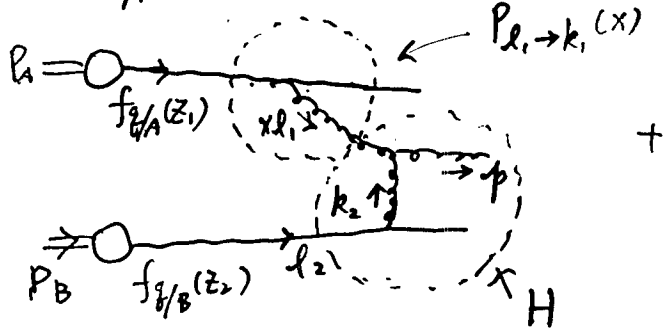

+

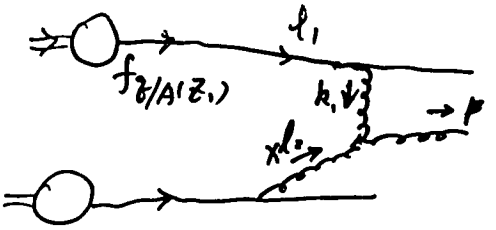

DGLAP evolution eq.:

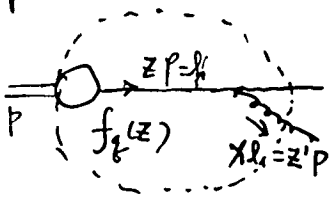

+

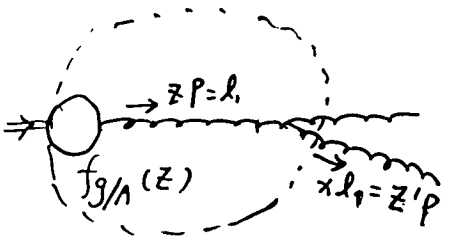

$f_q(z) \otimes P_{q\to g}\left(\frac{z'}{z}\right)$ + $f_{g/A}(z) \otimes P_{g\to g}\left(\frac{z'}{z}\right)$

(gluon splitting neglected in KMW model)

$= f_{g/A}(z')$

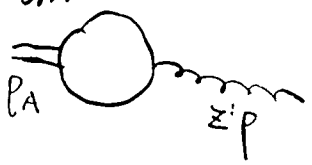

Transverse Momentum Dependence of the Landau - Pomeranchuk - Migdal Effect

U.A. Wiedemann + M. Gyulassy

Columbia University

Theory

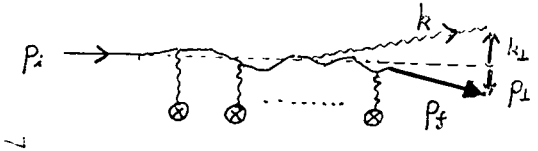

Experiment

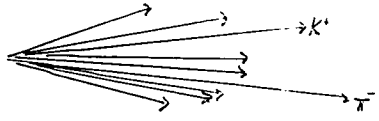

needed: $\dfrac{d^5\sigma}{d(\ln x)\, d^2p_\perp\, d^2k_\perp}$

LPM effect in QED

- L.D. Landau, I.J. Pomeranchuk, Dokl. Acad. Nauk SSSR 92 (1953) 92
- A.B. Migdal Phys. Rev. 103 (1956) 1811

recent interest:

- R. Blankenbecler, S.D. Drell, PRD 53 (1996) 6265
  R. Blankenbecler, PRD 55 (1997) 190; 2441
- V.N. Baier, V.M. Katkov, PRD 57 (1998) 3146 + hep-ph/9805231
- BDMPS, Nucl. Phys. B 478 (1996) 577
- B.G. Zakharov, JETP Lett. 63 (1996) 952; 64 (1996) 781
  + hep-ph/9807540 Phys. Atom. Nucl. 61 (1998) 838

fuelled by:

- data SLAC E-146 PRL 75 (1995) 1949
  PRL 76 (1996) 3550, PRD 56 (1997) 137.
- QCD - analogue

LPM effect in QCD

- J.F. Gunion, G. Bertsch PRD 25 (1982) 746
- M. Gyulassy, X-N. Wang PRD 51 (1995) 3436
- BDMPS NPB 483 (1997) 291
  484 (1997) 265
  531 (1998) 403
- B.G. Zakharov JETP Lett 63 (1996) 952
  65 (1997) 615
- M. Gyulassy, P. Levai, I. Vitev in preparation

here: Extension of Zakharov's formalism to $\frac{d\sigma}{dln x\, dp_\perp\, dk_\perp}$.

Method of Kopeliovich, Schäfer, Tarasov hep-ph/9808378

Kopeliovich, Schäfer, Tarasov

Furry approximation for QED

$$M_{fi} = \int d^4x\ \bar{\Psi}^+_{(x,p_2)}\ \alpha\cdot\varepsilon\ e^{ik\cdot x}\ \Psi^+_{(x,p_1)}$$ radiation amplitude

Ψ^-, Ψ^+: solutions of Dirac equation in external potential

$$U(x) = \sum_{i=1}^{N} U_0(\underbrace{r-r_i}_{\text{transverse}}, \underbrace{z-z_i}_{\text{longitudinal coordinates}})$$

$$\Psi^+_{(x,p_1)} = e^{-iE_1 t + ip_1 z}\, D_1\, F^+_{(x,p_1)}\, \frac{u(p_1)}{\sqrt{2E_1}} + O\left(\frac{U}{E_1}\right) + O\left(\frac{1}{E_1^2}\right)$$

$$D_1 = 1 - i\frac{\alpha_z \nabla}{2E_1} - \frac{\alpha\cdot(p_1 - n|p_1|)}{2E_1} \quad ; n = \frac{k}{k}$$

$$F^+_{(x,p_1)} = \int d^2r_1\ G(z, r; z_-, r_1 | p_1)\ e^{ip_{1\perp}\cdot r_1}$$

$$G(z', r'; z, r | p) = \int D_{r(\xi)}\ \exp\left\{\frac{ip}{2}\int_z^{z'} d\xi \left[\dot{r}^2(\xi) - iU(r(\xi),\xi)\right]\right\}$$

this is exact to $O(\frac{U}{E^2})$, $O(\frac{1}{E^2})$

the radiation probability reads

$$\langle |M_{fi}|^2 \rangle = 2\mathrm{Re} \int d\underline{r}_1\, dz\, d\underline{\rho}\, d\underline{r}_2\, d\underline{r}_1'\, dz'\, d\underline{\rho}'\, d\underline{r}_2' \; \frac{1}{4p_1^2(1-x)^2}$$

$$\times \int dz \int_z^\infty dz'\, e^{-i\underline{p}_{21}\cdot(\underline{r}_2-\underline{r}_2') + i\underline{p}_{11}\cdot(\underline{r}_1-\underline{r}_1') - iq(z'-z)}$$

$$\left\langle G(z_+,\underline{r}_2;z',\underline{\rho}|p_2)\, G^*(z_+,\underline{r}_2';z',\underline{r}'|p_2) \right\rangle$$

$$\hat{\Gamma}_r \hat{\Gamma}_{r'}^* \left\langle G(z',\underline{\rho};z,\underline{r}|p_2) G^*(z',\underline{r}';z,\underline{\rho}'|p_1) \right\rangle$$

$$\left\langle G(z,\underline{r};z_-,\underline{r}_1|p_1)\, G^*(z,\underline{\rho}';z_-,\underline{r}_1'|p_1) \right\rangle$$

vertex function:

$$\hat{\Gamma}_r = \underbrace{\sqrt{1-x}\; u^*(p_2)\, \mathcal{D}_2^*}\; \overbrace{\underline{\alpha}\cdot\underline{\xi}}^{\text{interaction vertex}}\; \underbrace{\mathcal{D}_1\, u(p_1)}$$

spinor structure of wavefunctions $\psi^+\psi^-$

spin and helicity - averaged

$$\hat{\Gamma}_r \hat{\Gamma}_{r'}^* = \underbrace{(4-4x+2x^2)\frac{\partial}{\partial \underline{r}}\cdot\frac{\partial}{\partial \underline{r}'}}_{q_{nf}} + \underbrace{2m_e^2 x^2}_{q_{sf}}$$

q_{nf}: spin non-flip contribution; q_{sf}: spin flip contribution

Averaging over the medium

$$\langle f \rangle \equiv \left(\prod_{i=1}^N \int \frac{dz_i\, d\underline{r}_i}{\pi R^2 \Delta z} \right) f(\underline{r}_1,\dots,\underline{r}_N; z_1,\dots,z_N)$$

$(\underline{r}_i, z_i)$ centers of external potentials

In $\langle GG^* \rangle$, we have to average over: $e^{-i\int_z^{z'}(U(\underline{r})-U(\underline{r}'))}$

building block

$$W_i(\underline{r},\underline{r}';z',z) = i\int_z^{z'} d\bar{z}\left[U_0(\underline{r}-\underline{r}_i;\bar{z}-z_i) - U_0(\underline{r}'-\underline{r}_i;\bar{z}-z_i)\right]$$

$$\left\langle \exp\left\{\sum_i W_i\right\}\right\rangle = \prod_{i=1}^N \langle e^{W_i}\rangle = \left(\frac{1}{N}\int dz_i\, d\underline{r}_i \underbrace{n(z_i,\underline{r}_i)}_{=\frac{N}{\pi R^2\Delta z},\ \text{density}} e^{W_i}\right)^N$$

$$\equiv \left(1+\frac{\bar{V}}{N}\right)^N \xrightarrow{N\to\infty} = e^{\bar{V}}$$

$$\bar{V} = \int dz_i\, d\underline{r}_i\; n(z_i,\underline{r}_i)\left(e^{W_i(\underline{r},\underline{r}';z',z)} - 1\right)$$

crucial: $\bar{V}$ depends only on $\hat{\rho} = \underline{r}-\underline{r}'$

not on $\bar{\rho} = \underline{r}+\underline{r}'$

see this in explicit calculation $\longrightarrow$

Explicit calculation for Yukawa potential

$$U_0(\underline{x}) = \frac{Z e^2}{4\pi} \frac{e^{-Mx}}{|\underline{x}|}$$

$$\Rightarrow \boxed{\bar{V}[\hat{\underline{\rho}}] = -\int_{\underline{z}}^{\underline{z}'} d\underline{\xi}\; n(\underline{\xi})\; \sigma(\hat{\underline{\rho}}(\underline{\xi}))} \qquad \sigma = \text{"Dipol cross section"}$$

$$\sigma(\underline{\rho}) = \frac{Z^2 \alpha_{em}^2}{M^2} 4\pi \left(1 - (M\rho) K_1(M\rho)\right)$$

This dipol cross section is the Mott cross section:

$$\int \frac{d\underline{\rho}}{(2\pi)^2} \sigma(\underline{\rho})\, e^{i \underline{q}_\perp \cdot \underline{\rho}} = \frac{4 Z^2 \alpha_{em}^2}{(M^2 + \underline{q}_\perp^2)^2} - \frac{4\pi Z^2 \alpha_{em}^2}{M^2} \delta^{(2)}(\underline{q}_\perp)$$

$$\Rightarrow \left\langle \exp\left\{\sum_i W_i\right\}\right\rangle = e^{\bar{V}[\hat{\underline{\rho}}]} \qquad \text{use this to} \longrightarrow$$

Simplifying path integrals

$$I_1 = \langle G(\underline{z}', \underline{r}(z'); \underline{z}, \underline{r}(z)|p)\, G^*(\underline{z}', \underline{r}'(z'); \underline{z}, \underline{r}'(z)|p)\rangle$$

$$= \int D\bar{\underline{\rho}}\, D\hat{\underline{\rho}}\, \exp\left\{\frac{i\rho}{2} \int_{\underline{z}}^{\underline{z}'} \dot{\hat{\underline{\rho}}} \cdot \dot{\bar{\underline{\rho}}}\right\} e^{\bar{V}[\hat{\underline{\rho}}]} \qquad \hat{\underline{\rho}}(\underline{\xi}) = \underline{r}(\underline{\xi}) - \underline{r}'(\underline{\xi})$$
$$\bar{\underline{\rho}}(\underline{\xi}) = \underline{r}(\underline{\xi}) + \underline{r}'(\underline{\xi})$$

- $D\bar{\underline{\rho}}$ - integration $\Rightarrow$ δ-function
- The path $\hat{\underline{\rho}}(\underline{\xi})$ is fixed to a straight line

$$\hat{\underline{\rho}}_s(\underline{\xi}) = \hat{\underline{\rho}}(\underline{z}') \frac{\underline{\xi} - \underline{z}}{\underline{z}' - \underline{z}} + \hat{\underline{\rho}}(\underline{z}) \frac{\underline{z}' - \underline{\xi}}{\underline{z}' - \underline{z}}$$

- $$\boxed{\int d\underline{r}_2\, d\underline{r}_2'\, e^{-i\underline{p}_{2\perp} \cdot (\underline{r}_2 - \underline{r}_2')} I_1 = \exp\left[-i\underline{p}_{2\perp} \cdot \underline{\rho}_2 - \int_{\underline{z}}^{\underline{z}_+} n(\underline{\xi})\, \sigma(\underline{\rho}_2)\right]}$$

- How to simplify $\langle G(\underline{z}', \underline{r}(z'); \underline{z}, \underline{r}(z)|p(1-x)|G^*(\underline{z}', \underline{r}'(z'); \underline{z}, \underline{r}'(z)|p)\rangle$

$$= \int D\underline{r}\, D\underline{r}'\, \exp\left\{\frac{i\rho}{2} \int_{\underline{z}}^{\underline{z}'} \left[(1-x)\dot{\underline{r}}^2 - \dot{\underline{r}}'^2\right]\right\} e^{\bar{V}[\underline{r} - \underline{r}']} \quad ?$$

introduce identity

$$1 = \mathcal{N} \int D\underline{r}_e\, \exp\left\{\frac{i\rho}{2} x \int_{\underline{z}}^{\underline{z}'} \underline{r}_e'^2\, d\underline{\xi}\right\}$$

the radiation cross section is: Kopeliovich Schäfer Terasov

$$\frac{d^5\sigma}{d\ln x\, d\rho_1\, dk_\perp} = \frac{\alpha_{em}}{(2\pi)^4}\frac{2x^2}{\rho_1^2(1-x)^2}\,\mathrm{Re}\int d\rho_2\, d\rho_1 \times \int_{-\infty}^{\infty} dz \int_z^{\infty} dz'\, e^{-iq(z'-z) - \int_{-\infty}^{z} n(\bar z)\sigma(x\rho_1)d\bar z - \int_{z'}^{\infty} n(\bar z)\sigma(x\rho_2)d\bar z}$$

transverse momentum dependence

$$\times \left\{ \times \exp\left\{-ix\left(p_\perp - \frac{1-x}{x}k_\perp\right)\cdot\rho_2 - ik_\perp\cdot\rho_1\right\} \times \left[-\frac{4-4x+2x^2}{4x^2}\frac{\partial}{\partial\rho_1}\cdot\frac{\partial}{\partial\rho_2} + \frac{m_e^2x^2}{2}\right]\right\} K(z',\rho_2;z,\rho_1|\mu)$$

interaction vertex

where $q = \frac{xm_e^2}{2(1-x)p_1}$, $\mu = p_1(1-x)x$

$$K(z',\rho_2;z,\rho_1|\mu) = \int \mathcal{D}r\, \exp\left\{i\int_z^{z'} d\bar z\left[\frac{\mu}{2}\dot r^2 + i n(\bar z)\sigma(xr)\right]\right\}$$

expand using free Green's function:

$$K_v(z',\rho_2;z,\rho_1|\mu) = \frac{\mu}{2\pi i(z'-z)}\exp\left\{\frac{i\mu}{2(z'-z)}(\rho_2-\rho_1)^2\right\}$$

Limiting case:

Zakharov's energy loss formula

$$\frac{d\sigma}{d(\ln x)} = \int d^2\rho_1 d^2k_\perp \frac{d^5\sigma}{d\ln x\, d^2\rho_1 d^2k_\perp} \qquad \text{Zakharov}$$

$$= \frac{\alpha_{em}}{p_1^2(1-x)^2}\,2\mathrm{Re}\int dz\int_z dz'\, e^{iq(z'-z)}\, g(z';z)\, K(z',\rho_2;z,\rho_1)\Big|_{\rho_1=\rho_2=0} \quad \circledast$$

vertex function: $g(z';z) = -\frac{4-4x+2x^2}{4x^2}\frac{\partial}{\partial\rho_1}\cdot\frac{\partial}{\partial\rho_2} + \frac{m_e^2x^2}{2}$

In the dipol approximation $\sigma(\rho) \approx \frac{1}{2}C\rho_1^2$

$K(z',\rho_2;z,\rho_1)$ is the Green's function of a harmonic oscillator;

$$K_{osz}(z',\rho_2;z,\rho_1) = \frac{\mu\Omega}{2\pi i\sin(\Omega\Delta z)}\exp\left\{\frac{i\mu\Omega}{2\sin(\Omega\Delta z)}\left[(\rho_1^2+\rho_2^2)\cos(\Omega\Delta z) - 2\rho_1\cdot\rho_2\right]\right\}$$

$$\Omega = \frac{1-i}{\sqrt{2}}\sqrt{\frac{nCx^2}{\mu}}$$

in dipol approximation, Zakharov showed that $\circledast$

agrees with Migdal's energy loss formula for infinite medium

An Accurate Measurement of the Landau-Pomeranchuk-Migdal Effect

P. L. Anthony,[1] R. Becker-Szendy,[1] P. E. Bosted,[2] M. Cavalli-Sforza,[3,*] L. P. Keller,[1] L. A. Kelley,[3] S. R. Klein,[3,4] G. Niemi,[1] M. L. Perl,[1] L. S. Rochester,[1] and J. L. White[1,2]

[1]*Stanford Linear Accelerator Center, Stanford, California 94309*

[2]*The American University, Washington, D.C. 20016*

[3]*Santa Cruz Institute for Particle Physics, University of California, Santa Cruz, California 95064*

[4]*Lawrence Berkeley Laboratory, Berkeley, California 94720*

(Received 1 May 1995)

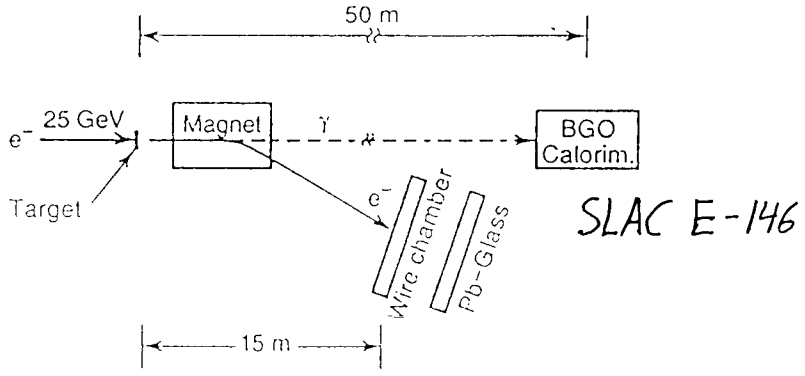

FIG. 2. Schematic picture of the experiment.

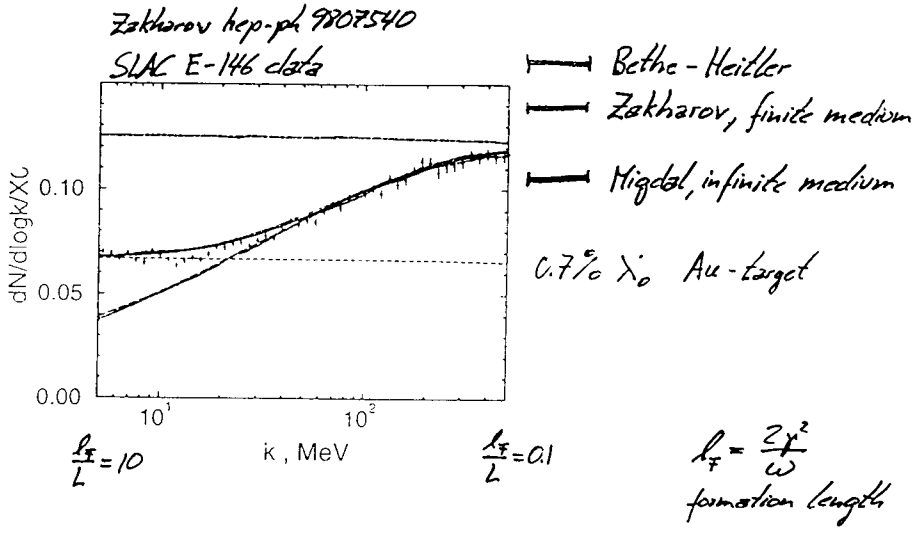

The Bethe-Heitler Limit

$$K(z',\rho_2;z,\rho_1) = K_v(z',\rho_2;z,\rho_1) - \int_z^{z'} n(\bar{z}) \int d\rho\, K_v(z',\rho_2;\bar{z},\rho)\,\sigma(x\rho)\,K_v(\bar{z},\rho;z,\rho_1) + O(n^2\alpha_{em}^2)$$

expanding $\frac{d^5\sigma}{dlnx\,d^2p_\perp d^2k_\perp}$ to leading order in $n\alpha_{em}$:

$$\left.\frac{d^5\sigma}{dlnx\,d^2p_\perp\,d^2k_\perp}\right|_{nf} = \frac{Z^2\alpha_{em}^2}{(2\pi)^2}\,\frac{16}{(M^2+q_\perp^2)^2}\,\chi^2\frac{(p_\perp+k_\perp)^2}{k_\perp^2(k_\perp-x(p_\perp+k_\perp))^2}\,T$$

This is Bethe-Heitler to $O(\frac{1}{E})$.

Physics of dipol cross section

projectile = $|q\rangle + |qg\rangle + \ldots$

if all components interact with same amplitude, then coherence is not disturbed, bremsstrahlung not generated

radiation amplitude $\propto$ difference between elastic scattering amplitudes of different fluctuations.

take: ϱ = size of $\bar{q}$-g

same picture leads to $q\bar{q}g$ interaction cross section when "photon" is charged.

Summary

⚠ this is a first report on work in progress

- $\frac{d\sigma}{d\ln x\, d^2p_\perp d^2k_\perp}$

  → extends Zakharov's formalism to include angular dependence

  → satisfies important limiting cases

  → can be extended to QCD

  → will be applied to "realistic" scenarios.

BNL, 1995

New results on minijet production in hadron and nuclear collisions.

Andrei Leonidov.

- The next-to-leading order contributions to transverse energy production in wide acceptance were computed in QCD parton model.

- The collinear factorization was shown to break down at $E_\perp \sim 55$ GeV in describing transverse energy production in $p\bar{p}$ collisions at $\sqrt{s} = 540$ GeV.

- The initial minijet system in hadron and nuclear collisions is characterized by substantial angular asymmetry

Next-to leading order calculation of minijet induced transverse energy production

- jet  observable collimated transverse energy flow

- minijet computable contribution to overall transverse energy production, but not observable as separate jet

Computable: $\alpha_s(p_\perp) \ll 1$ -> PQCD valid

LO 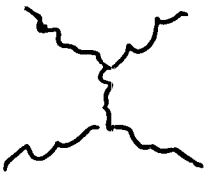 + ... $2 \to 2$ $\sigma \sim O(\alpha_s^2)$

NLO 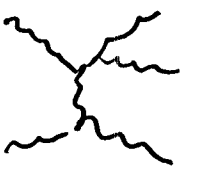 + ... $2 \to 3$ $\sigma \sim O(\alpha_s^3)$

 + ... $2 \to 2$

 + ... $\sigma \sim O(\alpha_s^3)$

Infrared stability

- The produced partons have to convert themselves into observable hadrons. Infrared stable quantities are those that do not depend on what happens to partons after they are produced, i.e. calculable exclusively in terms of produced quarks and gluons. (And structure functions).

- Transverse energy spectrum calculated in full azimuth and some <u>finite</u> rapidity acceptanse <u>is infrared stable</u>

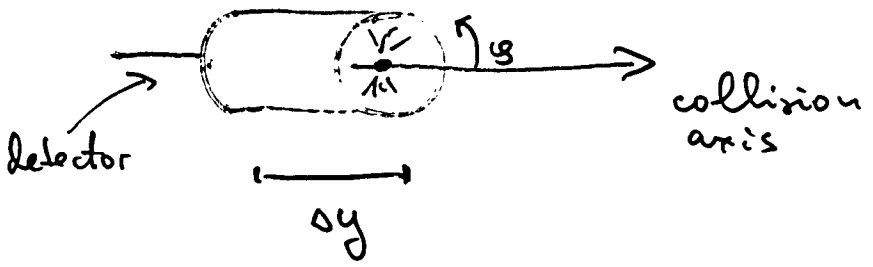

$$\frac{d\sigma^{NLO}}{dE_\perp} = \int D^2PS \; \frac{d\sigma}{d^4p_1 d^4p_2} \delta\left(E_\perp - \sum_{i=1}^{2} |p_{\perp i}|\right) \theta(y_{min} < y_i < y_{max})$$

(2 → 2)

$$+ \int D^3PS \; \frac{d\sigma}{d^4p_1 d^4p_2 d^4p_3} \delta\left(E_\perp - \sum_{i=1}^{3} |p_{\perp i}|\right) \theta(y_{min} < y_i < y_{max})$$

(2 → 3)

A.L., D.Ostrovsky hep-ph/9811417

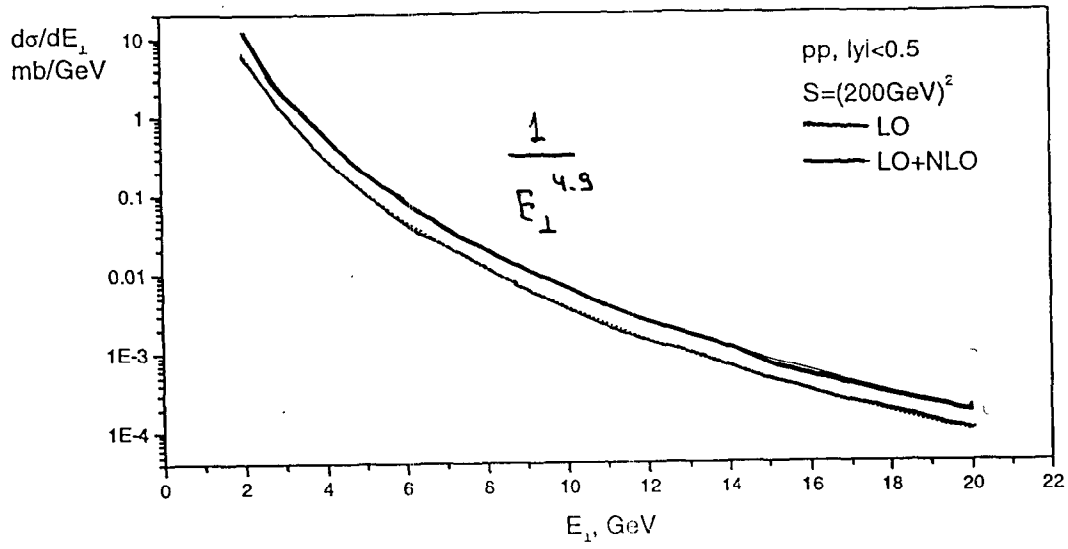

Figure 1: NLO (solid line) and LO (dashed line) transverse energy spectrum in a unit central rapidity window for pp collisions at RHIC energy $\sqrt{s} = 200$ GeV

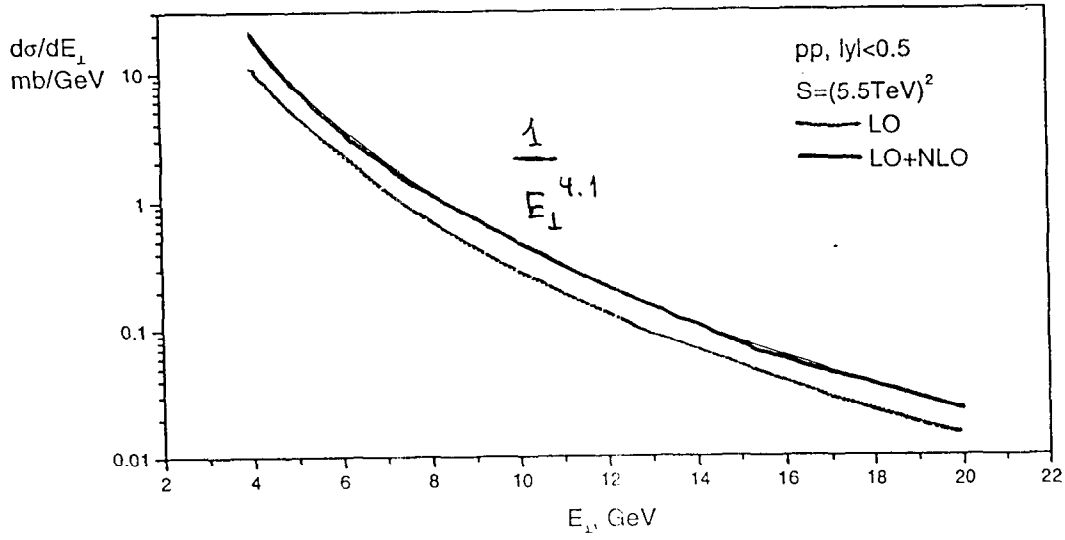

Figure 2: NLO (solid line) and LO (dashed line) transverse energy spectrum in a unit central rapidity window for pp collisions at LHC energy $\sqrt{s} = 5500$ GeV

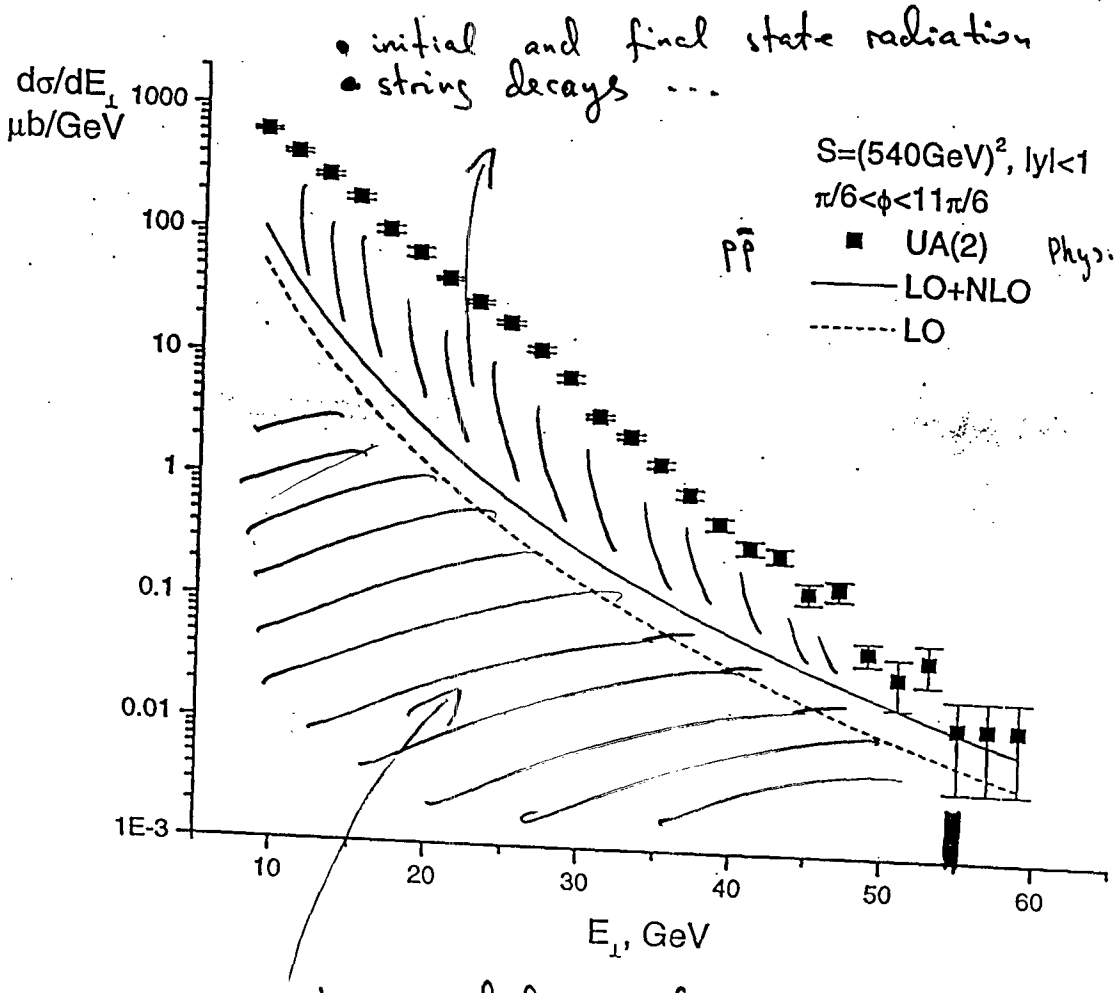

QCD parton model predictions, NLO accuracy, collinear factorization.

- Up to the transverse energy ~ 55 GeV collinearly factorized QCD parton model does not describe the data.

- Higher order corrections and higher twist effects important (as realized e.g. in HIJING)

- Absolute lower bound on the scale of transverse energy production in QCD parton model.

- $\int dy \int_{E_0} dE_\perp \frac{d\sigma^{(hard)}}{dy\, dE_\perp} = \sigma_{in}^{(hard)}$

- $\sigma_{in}^{(hard)} = \sigma_{in}(\sqrt{s}) - \sigma_{in}^{(soft)}$

  32 mb

	RHIC	LHC
LO	2.35	6
LO + NLO	2.74	7.1

E_0 [GeV]

- In nuclear collisions one expects

$$E_\perp\Big|_{AA} \sim A^{\frac{1}{6}} \cdot E_\perp\Big|_{pp}$$

~ 2.4 for $A = 200$

Studying Parton Propagation Dynamics in STAR: High P_T π^0's in Year-1

T.M. Cormier, Wayne State University
for the STAR Collaboration

The STAR detector will be well suited to the study of parton propagation dynamics in the dense hadronic or quark-gluonic matter produced in AA collisions at RHIC. With the large acceptance of STAR's time projection chamber, the final states resulting from hard partonic scattering will be characterized in great detail. However, even with the substantial power of the TPC, the complexity of AA final states at RHIC will narrow the list of robust observables, or the applicable P_T range, for the study of hard process at RHIC. As a simple example we note that a typical 0.7 jet cone in central AuAu collisions will contain over 100 GeV of transverse energy from the underlying event. Fluctuations in this background energy, event by event, will clearly preclude any straightforward measurements of jet E_T distributions with acceptable energy resolution at any reasonable E_T.

In AA collisions, the observable signatures of hard partonic process which are likely to survive in the presence of the underlying event, will include high P_T single particle (i.e. leading particle) and direct photon inclusive spectra, correlations of these leading particles and direct photons with next-to-leading particles in the same jet and/or leading particles in the away-side jet. (For the purposes of the present discussion, I ignore charmonium and open charm production.) These correlations, compared directly to the corresponding measurements for pp reactions, may provide more direct insight into the jet attenuation mechanism.

In STAR, where the TPC readout strongly limits the total event rate, an efficient trigger is required for the most interesting high P_T probes. The STAR detector accomplishes this with an electromagnetic calorimeter and consequently the greatest reach in P_T in STAR will be for those events which contain a high P_T π^0 or direct photon (or electron). As an illustration, this talk focuses on the observation of the inclusive high P_T π^0 spectrum, with some emphasis on the year-1 capability as a first window on jet quenching phenomena at RHIC. The ultimate prospects for leading particle-correlations and direct photons will also be discussed.

Figure 1 shows the di-photon invariant mass spectrum of π^0 's and η's at various P_T thresholds illustrating the capability of the STAR calorimeter even at low P_T where the combinatoric background is very large. Measurements at lower PT will be important to map out the transition from hard process to the soft physics regime. Figure 2 shows the corresponding mass spectrum for the P_T range of 5 to 6 GeV/c assuming the year-1 configuration of the calorimeter and an integrated luminosity corresponding to approximately 1 month at nominal RHIC luminosity (i.e. an optimistic year-1 scenario). Beginning in this P_T range, X. N. Wang (hep-ph/9804357) predicts jet attenuation in the single particle spectrum which is not complicated by the much larger yield of thermal pions which dominate at slightly lower P_T. The predicted attenuation at 5 GeV/c (not included in figure 2) is approximately an order of magnitude and will be readily observable with the statistics in figure 2.

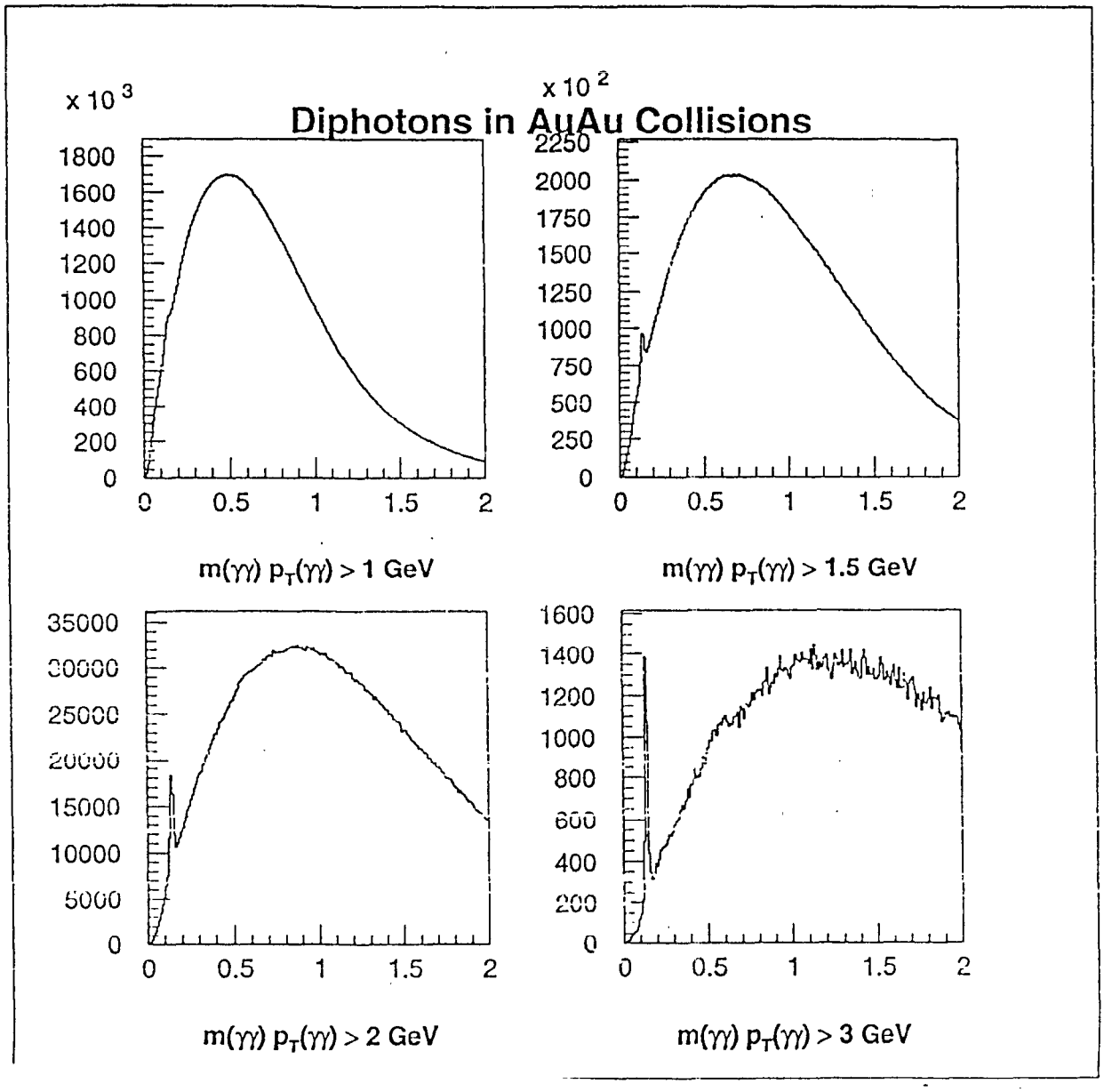
Diphotons in AuAu Collisions
x 10 3
1800
1600
1400
1200
1000
800
600
400
200
0
0 0.5 1 1.5 2
m(γγ) p_T(γγ) > 1 GeV
x 10 2
2250
2000
1750
1500
1250
1000
750
500
250
0
0 0.5 1 1.5 2
m(γγ) p_T(γγ) > 1.5 GeV
35000
30000
25000
20000
15000
10000
5000
0
0 0.5 1 1.5 2
m(γγ) p_T(γγ) > 2 GeV
1600
1400
1200
1000
800
600
400
200
0
0 0.5 1 1.5 2
m(γγ) p_T(γγ) > 3 GeV

Figure 1.

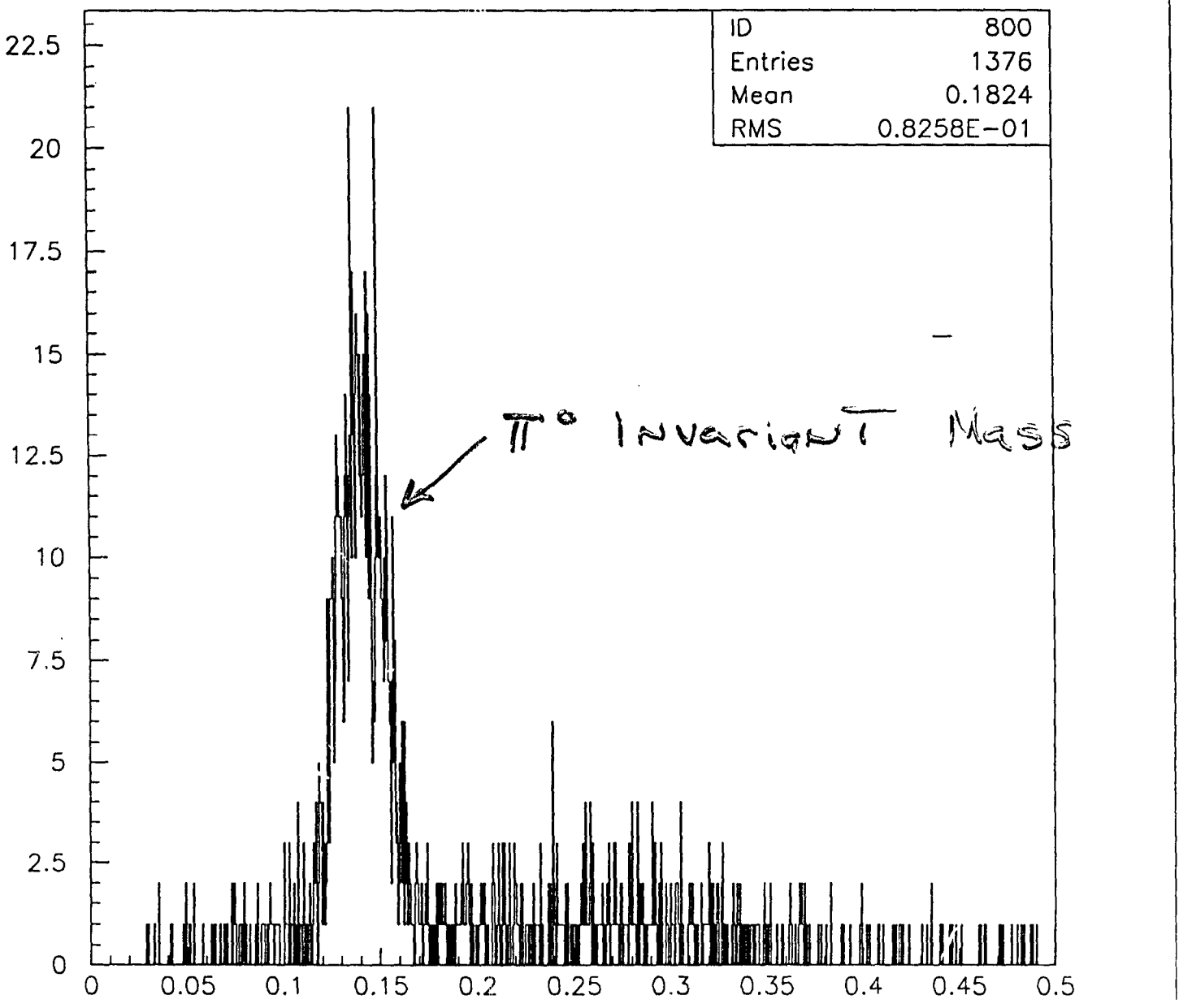
ID 800
Entries 1376
Mean 0.1824
RMS 0.8258E-01
π° Invariant Mass
22.5
20
17.5
15
12.5
10
7.5
5
2.5
0
0 0.05 0.1 0.15 0.2 0.25 0.3 0.35 0.4 0.45 0.5

Figure 2.

Partonic Picture of Nuclear Shadowing at Small x*

Ina Sarcevic
University of Arizona
ina@gluon.physics.arizona.edu

Small-x parton distributions in nuclei are essential for:

- Studying semihard processes which play an important role in ultrarelativistic heavy-ion collisions at $\sqrt{s} \geq 200$GeV, such as
  - ⋆ Minijet production
  - ⋆ Charm production
  - ⋆ Dilepton production
  - ⋆ Direct photon production
  - ⋆ J/Ψ suppression

- For determining the initial condition for possible formation of QGP

Z. Huang, H.J. Lu and I. Sarcevic, Nucl. Phys. A637, 79 (1998).

Partonic Picture of Nuclear Shadowing Effect: the Glauber-Gribov Multiple Scattering Model

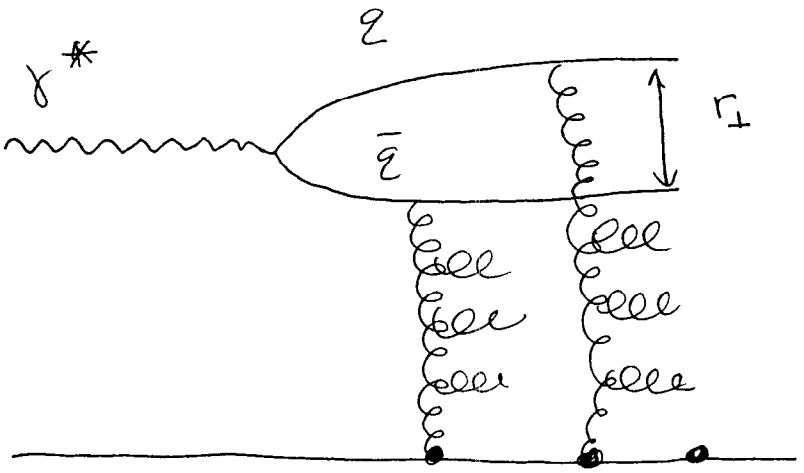

A.H. Mueller, Nucl. Phys. B335 (1990)
Ayala et al., Nucl. Phys. B493 (1997)
Huang, Lu, Sarcevic, Nucl. Phys. A637 (1998) 79

$$\tau_{\gamma^\star} \sim 1/mx$$

- If $\tau_{\gamma^\star}$ (or l_c)$< R_{NN}, \longrightarrow \sigma(\gamma^\star A) = A\sigma(\gamma^\star N)$ large-x region (no shadowing)
- If $R_{NN} < \tau_{\gamma^\star} < R_A$, vector meson ($\rho$, ω or ϕ) or $q\bar{q}$-pair interacts with the fraction of nucleons coherently (shadowing effect)
- If $\tau_{\gamma^\star} > R_A$, vector meson or $q\bar{q}$-pair interacts with all nucleons in a nucleus coherently (small-x region)

The total hadron-nucleus cross section is given by

$$\sigma(hA) = \int d^2b\ 2(1 - e^{-\sigma_{hN}T_A(b)/2})$$

Assuming Gaussian form for the nucleus thickness function, $T_A(b)$, impact-parameter integration can be done analytically,

$$\begin{aligned}\sigma_{hA} &= 2\pi R_A^2 \left[\kappa_h - \frac{1}{4}\kappa_h^2 + \cdots + (-1)^{n-1}\frac{\kappa_h^n}{nn!} + \cdots\right] \\ &= 2\pi R_A^2 \left[\gamma + \ln \kappa_h + E_1(\kappa_h)\right] \ ,\end{aligned}$$

where

$$\kappa_h = A\sigma_{hN}/(2\pi R_A^2)$$

is the effective number of $h - N$ scatterings (averaged over the impact parameter)

- For $\kappa_h << 1$, $\qquad\qquad \sigma_{hA} \to 2\pi R_A^2 \kappa_h = A\sigma_{hN}.$

i.e. the destructive interference between multiple scattering amplitudes reduces the cross section and it approaches the geometric limit $2\pi R_A^2$, a surface term which varies roughly as $A^{2/3}$.

Predictions for Gluon Shadowing

- Similarly to the quark case,

$$xg_N(x,Q^2) = \frac{2}{\pi^3}\int_0^1 dz \int d^2\mathbf{r}|\psi(z,\mathbf{r})|^2\sigma_{ggN}(\mathbf{r}) \ ,$$

where the wave function squared for a gg pair is

$$|\psi(z,\mathbf{r})|^2 = \frac{1}{z(1-z)}\left[(a^2K_2(a\mathbf{r}) - aK_1(a\mathbf{r})/\mathbf{r})^2 + a^2K_1(a\mathbf{r})^2/\mathbf{r^2}\right] \stackrel{a\mathbf{r}\ll 1}{\Longrightarrow} \frac{2}{z\mathbf{r}^4} \ ,$$

and the cross section in the DLA is

$$\sigma_{ggN}(\mathbf{r}) = \frac{9}{4}\sigma_{q\bar{q}N} = \frac{3\pi^2}{4}\mathbf{r^2}\alpha_s(4/\mathbf{r^2})x'g_N^{\rm DLA}(x',4/\mathbf{r^2}) \ .$$

- Gluon distribution in a nucleon is given by

$$g_N(x,Q^2) = g_N(x,Q_0^2) + \int_x^1 \frac{dx'}{x'}\int_{Q_0^2}^{Q^2}\frac{dQ'^2}{Q'^2}\frac{\alpha_s(Q'^2)}{2\pi}\left(6\frac{x'}{x}\right)g_N(x',Q')$$

In the small-x limit splitting function in the DLA can be easily identified: $P_{gg}(z) \simeq 6/z$ where $z = x/x'$. Due to the different splitting function, the gluon density increases as Q^2 increases by an amount 12 times bigger than that for the quark density, leading to a much stronger scaling violation.

- The nuclear gluon distribution in the Glauber-Gribov model is given by the evolution equation

$$xg_A(x,Q^2) = xg_A(x,Q_0^2) + \frac{2R_A^2}{\pi^2}\int_x^1 \frac{dx'}{x'}\int_{Q_0^2}^{Q^2} dQ'^2 \left[\gamma + \ln(\kappa_g) + E_1(\kappa_g)\right]$$

where

$$\kappa_g = \frac{9}{4}\kappa_q = \frac{3\pi A}{2R_A^2 Q'^2}\alpha_s(Q'^2) xg_N^{DLA}(x,Q'^2)$$

- In the region of small-x and for $Q^2 \geq 3$ GeV^2, κ_g is large and gluon distribution is driven by the perturbative part:

$$R_g(x,Q^2) \to \frac{xg_A^{pert}(x,Q^2)}{Axg_N^{pert}(x,Q^2)}$$

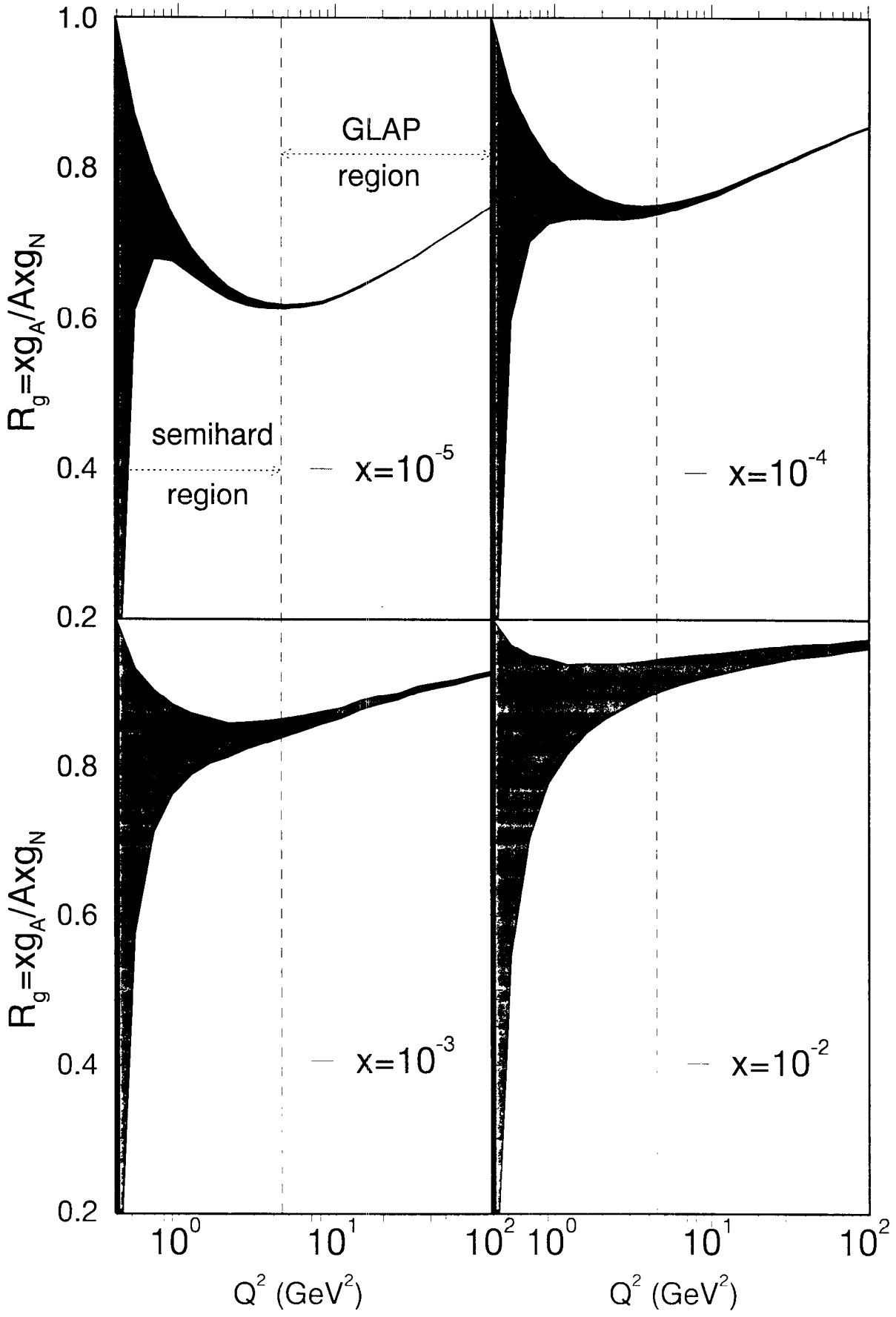
1.0
0.8
0.6
0.4
0.2
$R_g=xg_A/Axg_N$
GLAP
region
semihard
region
$x=10^{-5}$
$x=10^{-4}$
$x=10^{-3}$
$x=10^{-2}$
10^0
10^1
10^2
Q^2 (GeV^2)

Conclusions

- Nuclear shadowing effect is due to the coherent scatterings of the color-singlet $q\bar{q}$ fluctuations of the virtual photon off the nucleons inside the nucleus.
- Shadowing effect is not a higher-twist effect, i.e. it persists even at relatively large Q^2. This is due to the strong scaling violation of the gluon distribution, $g_N(x, Q^2)$, at small x.
- Quark shadowing at semi-hard scale, $Q^2 \sim 3\text{GeV}^2$, has a large contribution from non-perturbative effects.
- However, gluon shadowing at small x and for $Q^2 \geq 3\text{GeV}^2$ is perturbative in nature and it does not depend on the initial, non-perturbative input at Q_0^2.
- Gluon shadowing at small x and at semi-hard scale, $Q^2 \sim 3\text{GeV}^2$, is stronger than for the quarks, and the shadowing ratio does not exhibit saturation at small x.
- Impact parameter dependence of gluon distribution in a nucleus is not factorizable.

DILEPTON PRODUCTION AT FERMILAB AND RHIC

J. C. Peng, P. L. McGaughey, and J. M. Moss
Physics Division, Los Alamos National Laboratory, Los Alamos, NM 87545

Some highlights from a series of fixed-target dimuon production experiments at Fermilab are presented. Future prospects for several dilepton experiments at RHIC are discussed.

1. Introduction

The first dilepton production experiment was performed at the AGS almost 30 years ago [1]. Over the years, hadron-induced dilepton production experiments have led to the discoveries of various vector bosons (J/Ψ, Υ, and Z^0). They also provided important and often unique informations on parton distributions in nucleons, nuclei, and mesons.

A series of fixed-target dimuon production experiments (E772, E789, E866) have been carried out at Fermilab in the last 10 years. Some highlights from these experiments are presented here. In addition, the prospect for performing several dilepton production experiments at RHIC is discussed.

2. Scaling Violation in Drell-Yan Process

In the "Naive" Drell-Yan (DY) model, the differential cross section, $m^3 d^2\sigma/dx_F dm$, has an expression showing its scaling property as follows:

$$M^3 \frac{d^2\sigma}{dM dx_F} = \frac{8\pi\alpha^2}{9} \frac{x_1 x_2}{x_1 + x_2} \times \sum_a e_a^2 [q_a(x_1)\bar{q}_a(x_2) + \bar{q}_a(x_1) q_a(x_2)]. \quad (1)$$

The right-hand side of Eq. (1) is only a function of x_1, x_2 and is independent of the beam energies. This scaling property no longer holds when QCD corrections to the DY are taken into account.

While logarithmic scaling violation is well established in Deep-Inelastic Scattering (DIS) experiments, it is not well confirmed in DY experiments at all. As an example, Figure 1 compares the NA3 data [2] at 400 GeV with the E605 [3] and E772 [4] data at 800 GeV. The solid curve in Figure 1 corresponds to NLO calculation for 800 GeV $p+d$ ($\sqrt{s} = 38.9$ GeV) and it describes the NA3/E605/E772 data well. No evidence for scaling violation is seen. As discussed in a recent review [5], there are mainly two reasons for this. First, unlike the DIS, the DY cross section is a convolution of two structure functions. Scaling violation implies that the structure functions rise for $x \leq 0.1$ and drop for $x \geq 0.1$ as Q^2 increases. For proton-induced DY, one often involves a beam quark with $x_1 > 0.1$ and a target antiquark with $x_2 < 0.1$. Hence the effects of scaling violation are partially cancelled. Second, unlike the DIS, the DY experiment can only probe relatively large Q^2, namely, $Q^2 > 16$ GeV^2 for a mass cut of 4 GeV. This makes it more difficult to observe the logarithmic variation of the structure functions in DY experiments.

Possible indications of scaling violation in DY process have been reported in two pion-induced experiments, E326 [6] at Fermilab and NA10 [7] at CERN. E326 collaboration compared their 225 GeV $\pi^- + W$ DY cross sections against calculations with and without scaling violation. They observed better agreement when scaling violation is included. This analysis is subject to the uncertainties associated with the pion structure functions, as well as the nuclear effects of the W target. The NA10 collaboration measured $\pi^- + W$ DY cross sections at three beam energies, namely, 140, 194, and 286 GeV. By checking the ratios of the cross sections at three different energies, NA10 largely avoids the uncertainty of the pion structure functions. However, the relatively small span in $\sqrt{s}$, together with the complication of nuclear effects, make the NA10 result less than conclusive.

RHIC provides an interesting opportunity for unambiguously establishing scaling violation in the DY process. Figure 1 shows the predictions for $p+d$ at $\sqrt{s} =$ 500 GeV. The scaling-violation accounts for a factor of two drop in the DY cross sections when $\sqrt{s}$ is increased from 38.9 GeV to 500 GeV. It appears quite feasible to establish scaling violation in DY with future dilepton production experiments at RHIC.

3. Flavor-Asymmetry and Charge-Symmetry-Violation of the Nucleon Sea

The DY process complements DIS as a tool to probe parton distributions in nucleons and nuclei. This is well illustrated in the recent progress in the study of flavor-asymmetry in the nucleon sea.

Until recently, it had been assumed that the distributions of $\bar{u}$ and $\bar{d}$ quarks in the proton were identical. While the equality of $\bar{u}$ and $\bar{d}$ is not required by any known symmetry, it is a plausible assumption for sea quarks generated by gluon splitting. As the masses of the up and down quarks are small compared to the confinement scale, nearly equal number of up and down sea quarks should result.

The assumption of $\bar{u}(x) = \bar{d}(x)$ can be tested by measurements of the Gottfried integral [8], defined as

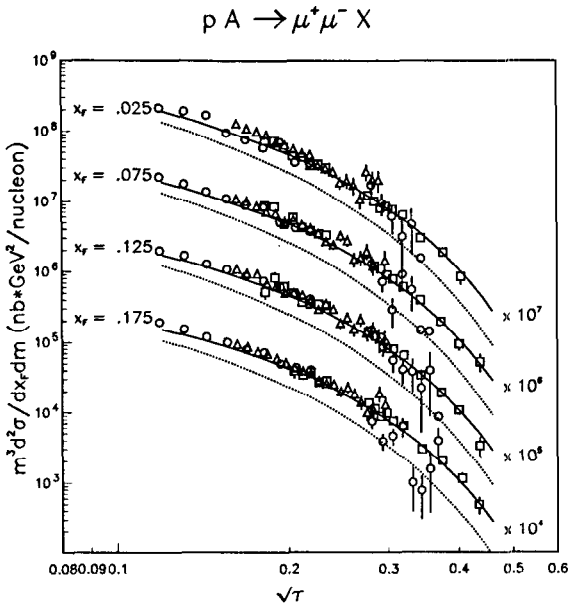

FIG. 1. Comparison of DY cross section data with NLO calculations using MRST [15] structure functions. Note that $\tau = x_1 x_2$. The E772 [4], E605 [3], and NA3 [2] data points are shown as circles, squares, and triangles, respectively. The solid curve corresponds to fixed-target p+d collision at 800 GeV, while the dotted curve is for p+d collision at $\sqrt{s} = 500$ GeV.

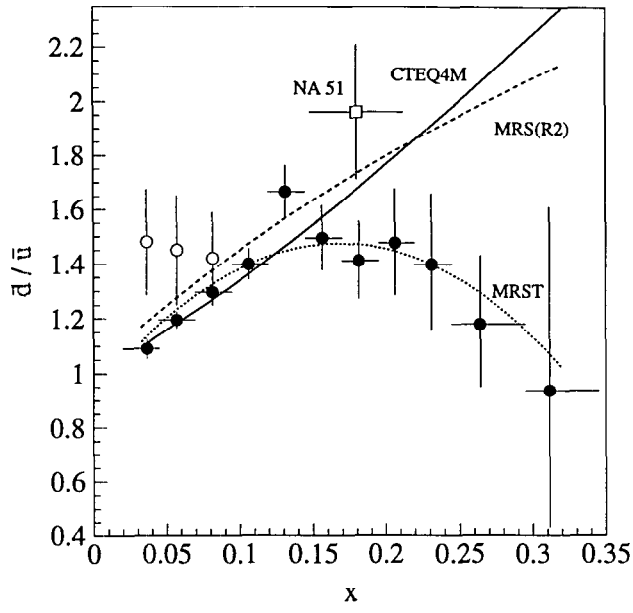

FIG. 2. The ratio of $\bar{d}/\bar{u}$ in the proton as a function of x extracted from the Fermilab E866 cross section ratio. The curves are from various parton distributions. The error bars indicate statistical errors only. An additional systematic uncertainty of ± 0.032 is not shown. Also shown is the result from NA51, plotted as an open box. The open circles correspond to $\bar{d}/\bar{u}$ values extracted with the assumption of the CSV effect reported in ref. [19].

$$I_G = \int_0^1 \left[F_2^p(x,Q^2) - F_2^n(x,Q^2)\right]/x \; dx = \frac{1}{3} + \frac{2}{3}\int_0^1 \left[\bar{u}_p(x) - \bar{d}_p(x)\right] dx, \qquad (2)$$

where F_2^p and F_2^n are the proton and neutron structure functions measured in DIS experiments. The second step in Eq. 2 follows from the assumption of charge symmetry. Under the assumption of a symmetric sea, $\bar{u}_p = \bar{d}_p$, the Gottfried Sum Rule (GSR) [8], $I_G = 1/3$, is obtained.

The most accurate test of the GSR was reported by the New Muon Collaboration (NMC) [9], which measured F_2^p and F_2^n over the region $0.004 \leq x \leq 0.8$. They determined the Gottfried integral to be 0.235 ± 0.026, significantly below 1/3. This result implies that the integral of $\bar{d} - \bar{u}$ is nonzero. However, the x-dependence of $\bar{d} - \bar{u}$ remained unspecified.

The proton-induced DY process provides an independent means to probe the flavor asymmetry of the nucleon sea [10]. An important advantage of the Drell-Yan process is that the x-dependence of $\bar{d}/\bar{u}$ can be determined. The NA51 [11] and the E866 [12] collaborations have compared the proton-induced DY dimuon yields from hydrogen and deuterium targets, and they deduced the ratios of $\bar{d}/\bar{u}$ as shown in Figure 2. For $x < 0.15$, $\bar{d}/\bar{u}$ increases linearly with x and is in good agreement with the CTEQ4M [13] and MRS(R2) [14] parameterizations. However, a distinct feature of the data, not seen in either parameterization, is the rapid decrease towards unity of $\bar{d}/\bar{u}$ beyond $x_2 = 0.2$. The E866 data clearly affect the current parameterization of the nucleon sea. The most recent structure functions of Martin et al. [15](MRST) included the E866 data in its global fit and its parametrization of $\bar{d}/\bar{u}$ is shown in Figure 2.

Many papers have considered virtual mesons as the origin for the observed $\bar{d}/\bar{u}$ asymmetry (see recent review of Kumano [16]). Here the $\pi^+(\bar{d}u)$ cloud, dominant in the process, $p \to \pi^+ n$, leads to an excess of $\bar{d}$ sea. Comparison of the E866 data with various theoretical models has also been made [17].

It should be emphasized that the extraction of $\bar{d}/\bar{u}$ values from the NA51 and E866 DY experiments required the assumption of charge symmetry, namely, $\bar{d}_n = \bar{u}_p, \bar{u}_n = \bar{d}_p$, etc. Evidence for a surprisingly large charge-symmetry-violation (CSV) effect was recently reported by Boros et al. [18,19] based on an analysis of F_2 structure functions determined from muon and neutrino DIS experiments. A large asymmetry, $\bar{d}_n(x) \approx 1.25\bar{u}_p(x)$ for $0.008 < x < 0.1$, is apparently needed to bring the muon and neutrino DIS data into agreement. How would this finding, if confirmed by further studies, affect the E866 analysis of the flavor asymmetry? First, CSV alone could

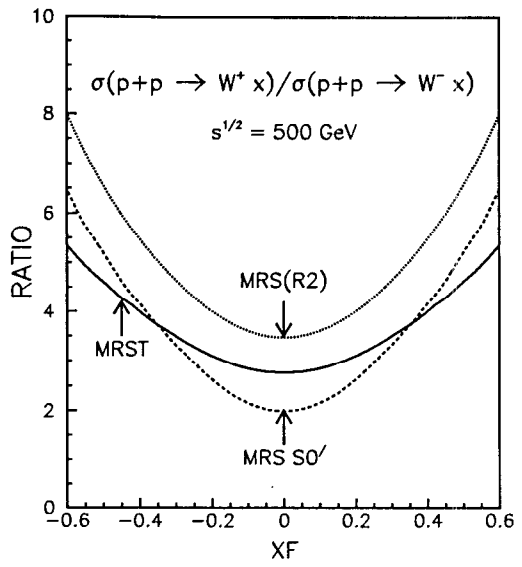

FIG. 3. Predictions of $\sigma(p+p \to W^+x)/\sigma(p+p \to W^-x)$ as a function of x_F at $\sqrt{s} = 500$ GeV. The dashed curve corresponds to the $\bar{d}/\bar{u}$ symmetric MRS S0′ structure functions, while the solid and dotted curves are for the $\bar{d}/\bar{u}$ asymmetric structure function MRST and MRS(R2), respectively.

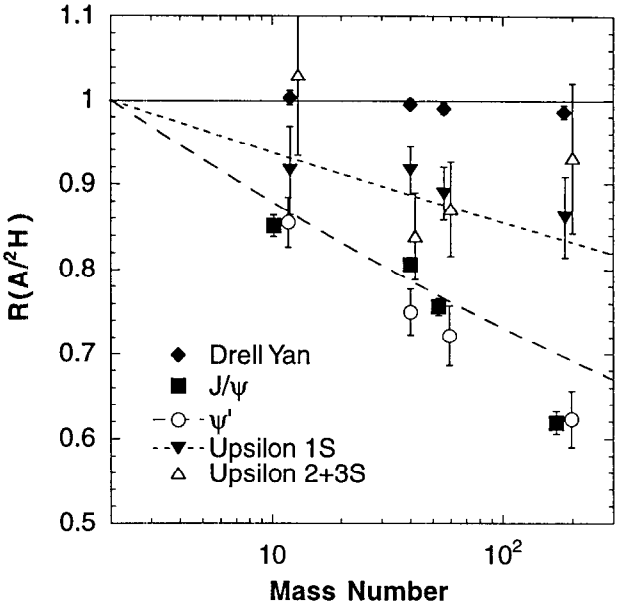

FIG. 4. Ratios of heavy-nucleus to deuterium integrated yields per nucleon for 800 GeV proton production of dimuons from the Drell-Yan process and from decays of the J/ψ, ψ', $\Upsilon(1S)$, and $\Upsilon(2S+3S)$ states [5]. The short dash and long dash curves represent the approximate nuclear dependences for the $b\bar{b}$ and $c\bar{c}$ states, $A^{0.96}$ and $A^{0.92}$, respectively.

not account for the E866 data. In fact, an even larger amount of flavor asymmetry is required to compensate the possible CSV effect [19]. This is illustrated in Figure 2, where the open circles correspond to the $\bar{d}/\bar{u}$ values one would have obtained if the CSV effect reported by Boros et al. is assumed. Second, there has been no indication of CSV for $x > 0.1$. Thus the large $\bar{d}/\bar{u}$ asymmetry from E866 for $x > 0.1$ is not affected.

To disentangle the $\bar{d}/\bar{u}$ asymmetry from the possible CSV effect, one could consider W boson production, a generalized DY process, in $p+p$ collision at RHIC. An interesting quantity to be measured is the ratio of the $p+p \to W^+ + x$ and $p+p \to W^- + x$ cross sections [20]. It can be shown that this ratio is very sensitive to $\bar{d}/\bar{u}$. An important feature of the W production asymmetry in $p+p$ collision is that it is completely free from the assumption of charge symmetry. Figure 3 shows the predictions for $p+p$ collision at $\sqrt{s} = 500$ GeV. The dashed curve corresponds to the $\bar{d}/\bar{u}$ symmetric MRS S0′ [21] structure functions, while the solid and dotted curves are for the $\bar{d}/\bar{u}$ asymmetric structure function MRST and MRS(R2), respectively. Figure 3 clearly shows that W asymmetry measurements at RHIC could provide an independent determination of $\bar{d}/\bar{u}$.

4. Nuclear Medium Effects of Dilepton Production

From a high-statistics measurement of dilepton production in 800 GeV proton-nucleus interaction, the target-mass dependence of DY, J/Ψ, Ψ', and Υ productions have been determined in E772 [22–24]. As shown in Figure 4, different nuclear dependences are observed for different dilepton processes. While the DY process shows almost no nuclear dependence, pronounced nuclear effects are seen for the production of heavy quarkonium states. E772 found that J/Ψ and Ψ' have similar nuclear dependence. The nuclear dependences for Υ, Υ' and Υ'' are less than that observed for the J/Ψ and Ψ'. Within statistics, the various Υ resonances also have very similar nuclear dependences.

Although the integrated DY yields in E772 show little nuclear dependence, it is instructive to examine the DY nuclear dependences on various kinematic variables. Using the simple A^α expression to fit the DY nuclear dependence, the values of α are shown in Figure 5 as a function of $x_T(x_2)$, M, x_F, and p_t. Several features are observed:

1. A suppression of the DY yields from heavy nuclear targets is seen at small x_2. This is consistent with the shadowing effect observed in DIS. In fact, E772 provides the only experimental evidence for shadowing in hadronic reactions. The reach of small x_2 in E772 is limited by the mass cut ($M \geq 4$ GeV) and by the relatively small center-of-mass energy

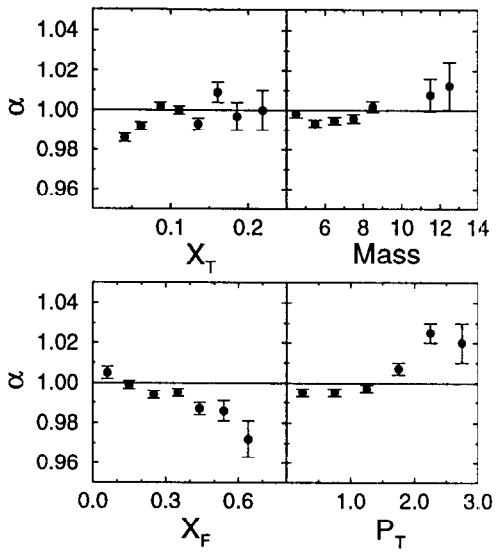

FIG. 5. Nuclear dependence coefficient α for 800 GeV p+A Drell-Yan process versus various kinematic variables [22].

(recall that $x_1 x_2 = M^2/s$). p-A collisions at RHIC clearly offer the exciting opportunity to extend the study of shadowing to much smaller x.

2. $\alpha(x_F)$ shows an interesting trend, namely, it decreases as x_F increases. It is tempting to attribute this behavior to initial-state energy-loss effect. However, there is a strong correlation between x_F and x_2 ($x_F = x_1 - x_2$), and it is essential to separate the x_F energy-loss effect from the x_2 shadowing effect. Figure 6 shows α versus x_F for two bins of x_2, one in the shadowing region ($x_2 \leq 0.075$) and one outside of it ($x_2 \geq 0.075$). There is no discernible x_F dependence for α once one stays outside of the shadowing region. Therefore, the apparent suppression at large x_F in Figure 5 reflects the shadowing effect at small x_2 rather than the energy-loss effect.

3. $\alpha(p_t)$ shows an enhancement at large p_t. This is reminiscent of the Cronin Effect [25] where the broadening in p_t distribution is attributed to multiple parton-nucleon scatterings. It is instructive to compare the p_t broadening for DY process and quarkonium production. Figure 7 shows $\Delta\langle p_t^2\rangle$, the difference of mean p_t^2 between p-A and p-D interactions, as a function of A for DY, J/Ψ, and $\Upsilon(1S)$ productions at 800 GeV. The DY and Υ data are from E772 [26], while the J/Ψ results are from E789 [27], E771 [28], and preliminary E866 analysis [29]. More details on this analysis will be presented elsewhere [26]. Figure 7 shows that $\langle p_t^2\rangle$ is well described by the simple expression $a + bA^{1/3}$. It also shows that the p_t broadening for J/Ψ is similar to Υ, but significantly larger (by a factor of 3 to 4) than the DY. A factor of 9/4 could be attributed to the color factor of the initial gluon in the quarkonium production versus the quark in the DY process. The remaining difference could come from the final-state multiple scattering effect which is absent in the DY process.

Baier et al. [30] have recently derived a relationship between the partonic energy-loss due to gluon bremsstrahlung and the mean p_t^2 broadening accumulated via multiple parton-nucleon scattering:

$$-dE/dz = \frac{3}{4}\,\alpha_s\,\Delta\langle p_t^2\rangle. \qquad (3)$$

This non-intuitive result states that the total energy loss is proportional to square of the path length traversed by the incident partons. From Figure 7 and Eq. 3, we deduce that the mean total energy loss, ΔE, for the p+W DY process is $\approx$ 0.5 GeV. Such an energy-loss is too small to cause any discernible effect in the x_F (or x_1) nuclear dependence. As shown in Figure 6, the dashed curve corresponds to ΔE = 16 GeV (for p+W), and the E772 data are consistent with Eq. 3. A much more sensitive test for Eq. 3 could be done at RHIC, where the energy-loss effect is expected to be much enhanced in A-A collision [31].

[1] J.H. Christenson *et al.*, Phys. Rev. Lett. **25**, 1523 (1970).
[2] J. Badier *et al.*, Z. Phys. C **26**, 489 (1984).
[3] G. Moreno *et al.*, Phys. Rev. D **43**, 2815 (1991).
[4] P.L. McGaughey *et al.*, Phys. Rev. D **50**, 3038 (1994); to be published (1999).
[5] P.L. McGaughey, J.M. Moss and J.C. Peng, to be published in Annu. Rev. Nucl. Part. Sci. (1999).
[6] H.B. Greenlee *et al.*, Phys. Rev. Lett. **55**, 1555 (1985).
[7] K. Freudenreich, Int. J. Mod. Phys. A **5**, 3643 (1990).
[8] K. Gottfried, Phys. Rev. Lett. **18**, 1174 (1967).
[9] P. Amaudruz *et al.*, Phys. Rev. Lett. **66**, 2712 (1991); M. Arneodo *et al.*, Phys. Rev. D **50**, R1 (1994).
[10] S.D. Ellis and W.J. Stirling, Phys. Lett. B **256**, 258 (1991).
[11] A. Baldit *et al.*, Phys. Lett. B **332**, 244 (1994).
[12] E.A. Hawker *et al.*, Phys. Rev. Lett. **80**, 3715 (1998).
[13] H.L. Lai *et al.*, Phys. Rev. D **55**, 1280 (1997).
[14] A.D. Martin, R.G. Roberts and W.J. Stirling, Phys. Lett. B **387**, 419 (1996).
[15] A.D. Martin *et al.*, Eur. Phys. J. C **4**, 463 (1998).
[16] S. Kumano, Phys. Rept. **303**, 183 (1998).

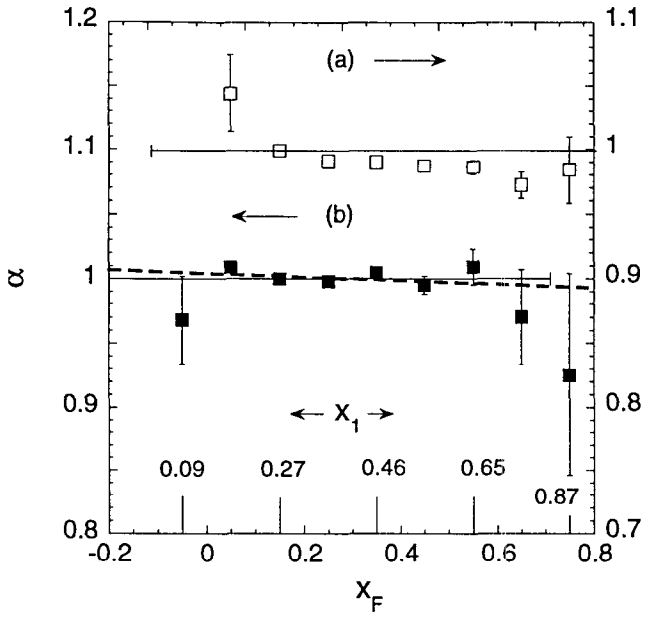

FIG. 6. Nuclear dependence coefficient α for the Drell-Yan process [22] versus x_F for (a) $x_2 \leq 0.075$, right scale, and (b) $x_2 \geq 0.075$, left scale. The thin solid lines show $\alpha = 1$. The dashed line is a linear least-squares fit to the lower points. Also shown is the mean value of x_1 for (b).

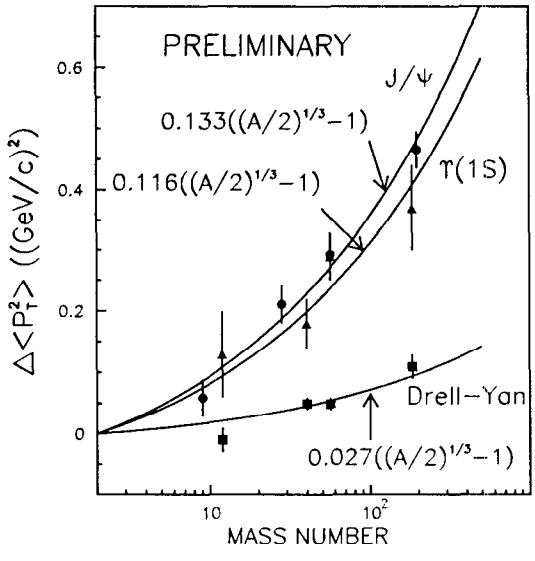

FIG. 7. The change of mean p_t^2 for nuclear target, $\Delta\langle p_t^2\rangle = \langle p_t^2\rangle(A) - \langle p_t^2\rangle(D)$, for 800 GeV p+A Drell-Yan process and J/Ψ and $\Upsilon(1S)$ productions.

[17] J.C. Peng *et al.*, Phys. Rev. D **58**, 092004 (1998).
[18] C. Boros, J.T. Londergan and A.W. Thomas, Phys. Rev. Lett. **81**, 4075 (1998).
[19] C. Boros, J.T. Londergan, and Thomas AW, Phys. Rev. D **59**, 074021 (1999).
[20] J.C. Peng, D.M. Jansen, Phys. Lett. B **354** 460 (1995).
[21] A.D. Martin, W.J. Stirling and R.G.Roberts, Phys. Lett. B **306**, 145 (1993).
[22] D.A. Alde *et al.*, Phys. Rev. Lett. **64**, 2479 (1990).
[23] D.A. Alde *et al.*, Phys. Rev. Lett. **66** 133 (1991).
[24] D.A. Alde *et al.*, Phys. Rev. Lett. **66** 2285 (1991).
[25] J.W. Cronin *et al.*, Phys. Rev. D **11**, 3105 (1975).
[26] P.L. McGaughey, J.M. Moss and J.C. Peng, to be published (1999).
[27] M.H. Schub *et al.*, Phys. Rev. D **52**, 1307 (1995).
[28] T. Alexopoulos *et al.*, Phys. Rev. D **55**, 3927 (1997).
[29] M. J. Leitch, in Proceedings of "Quarkonium Production in Relativistic Nuclear Collisions", Institute for Nuclear Theory, Seattle, WA, May 1998.
[30] R. Baier *et al.*, Nucl. Phys. B **484**, 265 (1997); R. Baier *et al.*, Nucl. Phys. B **531**, 403 (1994).
[31] R. Baier *et al.*, Nucl. Phys. B **483**, 291 (1997).

Unpolarized and Polarized Parton Distributions in Nuclei

S. Kumano *

Department of Physics
Saga University
Saga 840-8502
Japan

ABSTRACT

We discuss parton distributions in nuclei. First, F_2 structure functions are explained in a rescaling model with a recombination mechanism [1]. Then, the model is applied to other quantities such as valence-quark [2], sea-quark, and gluon [3] distributions in nuclei. In particular, the nuclear gluon distributions are important in connection with various phenomena in heavy-ion physics. Nuclear dependence of Q^2 evolution is not very clear at this stage [4]; however, higher-twist effects in nuclear interactions could be tested if accurate experimental data are taken. It is also interesting to study the flavor asymmetric distribution $\bar{u} - \bar{d}$ in nuclei because it is expected to be modified due to the nuclear interactions [5]. Furthermore, we point out that it is important to study the spin structure of spin-1 nuclei such as the deuteron in order to shed light on a new aspect of spin physics [6].

References

[1] SK and F. E. Close, Phys. Rev. C41, 1855 (1990); SK, Phys. Rev. C48, 2016 (1993); C50, 1247 (1994).

[2] R. Kobayashi, SK, and M. Miyama, Phys. Lett. B354, 465 (1995).

[3] SK, Phys. Lett. B298, 171 (1993).

[4] SK and M. Miyama, Phys. Lett. B378 (1996) 267; M. Miyama and SK, Comput. Phys. Commun. 94 (1996) 185; M. Hirai, SK, and M. Miyama, CPC 108 (1998) 38; 111 (1998) 150.

[5] SK, Phys. Lett. B342, 339 (1995); Phys. Rep. 303 (1998) 183.

[6] F. E. Close and SK, Phys. Rev. D42, 2377 (1990); S. Hino and SK, SAGA-HE-136 (Phys. Rev. D in press); SAGA-HE-139.

* kumanos@cc.saga-u.ac.jp.
http://www2.cc.saga-u.ac.jp/saga-u/riko/physics/quantum1/structure.html.

Gluons in nuclei

NMC $\mu^- + A \rightarrow \mu^- + J/\psi + X$

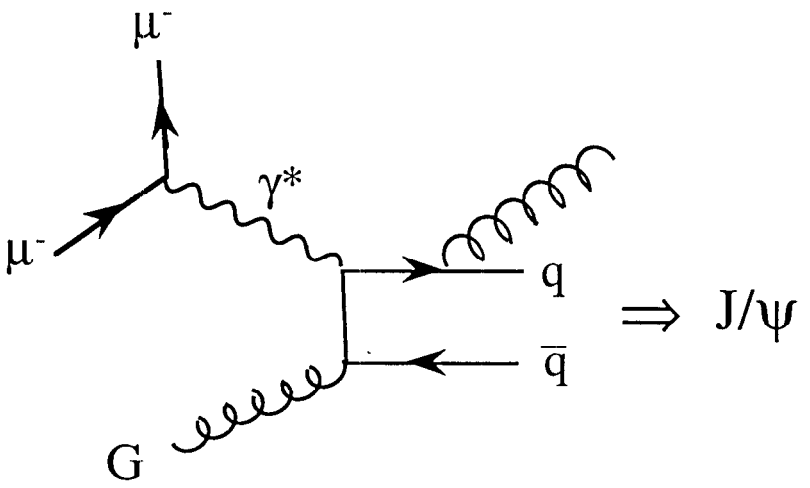

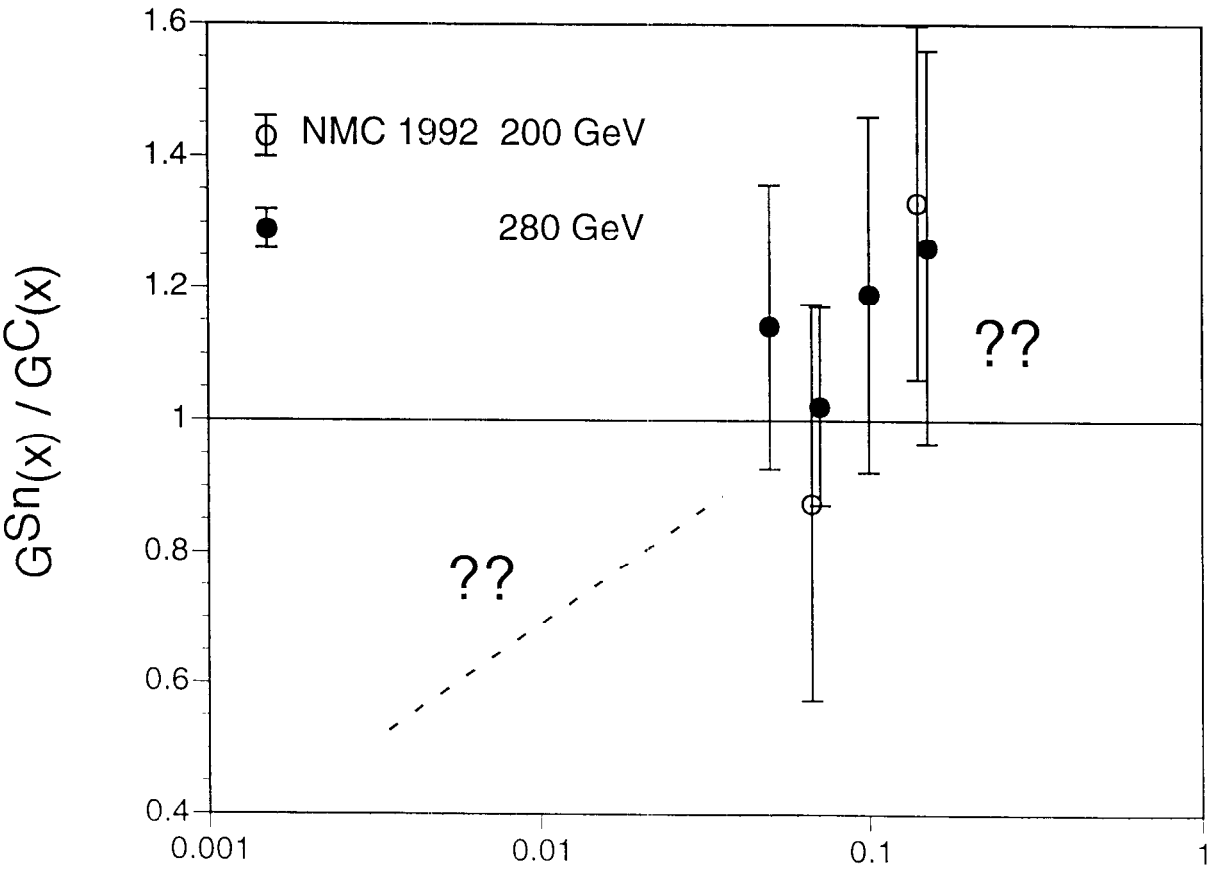

Nuclear modification of

$$x\,[\bar{u}(x) - \bar{d}(x)] \quad \text{in} \quad {}^{184}_{74}W_{110}$$

input parton distributions = MRS-1993

several % modification effects

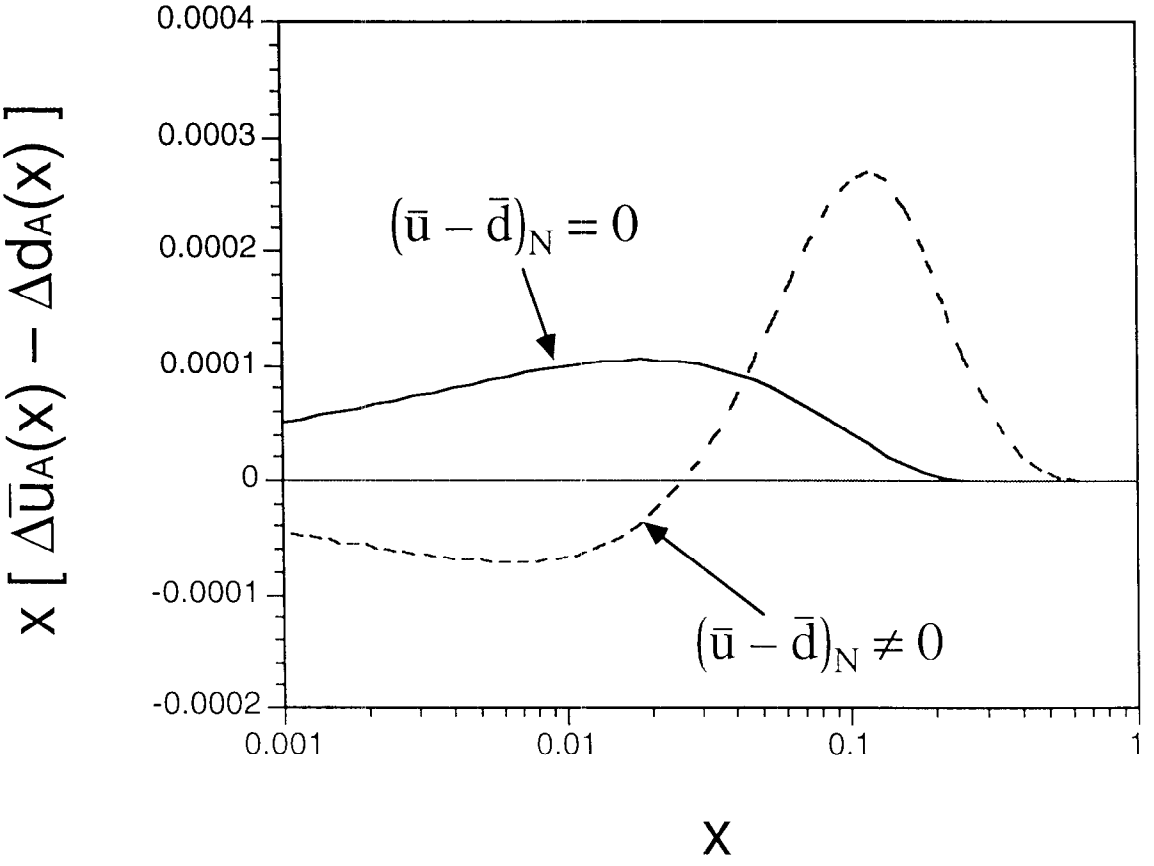

Nuclear dependence

$$\frac{\partial \left(F_2^{Sn}/F_2^{C}\right)}{\partial\left(\ln Q^2\right)}$$

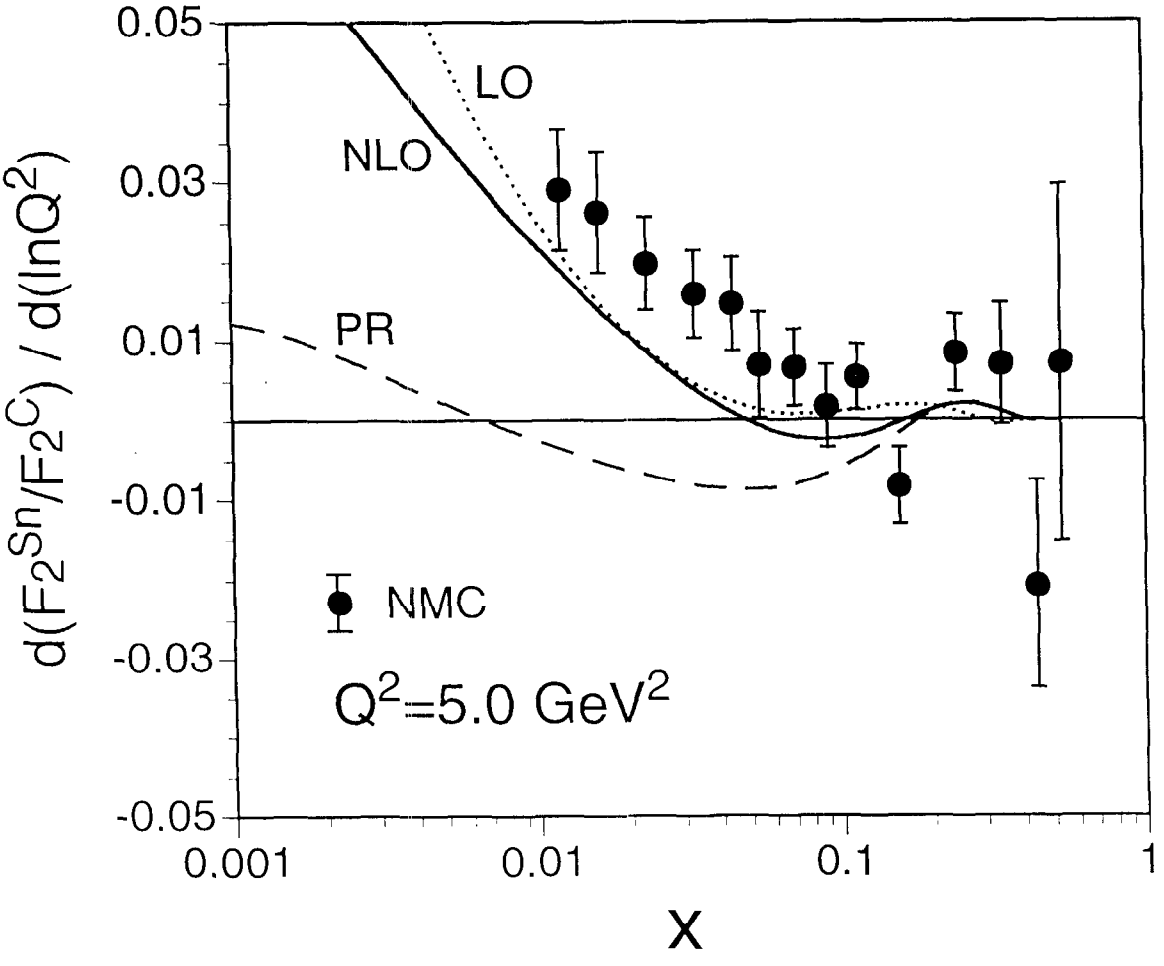

$$\int dx\, b_1^D(x) = \frac{5}{6}\left[\Gamma_{0,0} - \frac{1}{2}(\Gamma_{1,1} + \Gamma_{-1,-1})\right] + \frac{1}{9}(\delta Q + \delta\bar{Q})_{sea}$$

macroscopically

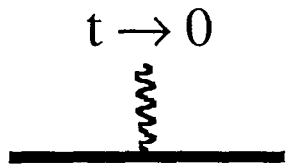

$$\Gamma_{0,0} = \lim_{t\to 0}\left[F_C(t) - \frac{t}{3M^2}F_Q(t)\right]$$

$$\Gamma_{+1,+1} = \Gamma_{-1,-1} = \lim_{t\to 0}\left[F_C(t) + \frac{t}{6M^2}F_Q(t)\right]$$

$$\int dx\, b_1^D(x) = \lim_{t\to 0} -\frac{5}{12}\frac{t}{M^2}F_Q(t) + \frac{1}{9}(\delta Q + \delta\bar{Q})_{sea}$$

$$\Rightarrow \lim_{t\to 0} -\frac{5}{12}\frac{t}{M^2}F_Q(t)$$

Gottfried sum rule

$$\int \frac{dx}{x}\left[F_2^p(x) - F_2^n(x)\right] = \frac{1}{3}\int dx\left[u_v - d_v\right] + \frac{2}{3}\int dx\left[\bar{u} - \bar{d}\right]$$

Experimental possibilities

HERA, ELFE ?, RHIC ?

Summary on $\vec{\mathbf{p}} + \vec{\mathbf{d}} \to \mu^+\mu^- + \mathbf{X}$

- Hermiticity, Parity, Time-reversal $\to$ 108 (48) structure functions exit in the pd (pp) Drell-Yan.
- 22 (11) structure functions by the $\vec{Q}_T$ integration or by the $Q_T \to 0$ limit.
- New spin dependent structure functions $\to$ associated with tensor structure.
- Structure functions for the intermediate polarization ($\beta = \pi/4$). They do not contribute to the cross section in the longitudinally ($\beta = 0$) and transversely ($\beta = \pi/2$) polarized reactions.
- Quadrupole polarizations: Q_0, Q_1, Q_2 and the spin asymmetries.
- Only 4 structure functions are finite in the naive parton model.
- The tensor distributions δq and $\delta\bar{q}$ can be measured by A_{UQ_0} measurements.
- The pd Drell-Yan is suitable for measuring $\delta\bar{q}$.
- Possibility at the RHIC-Spin project.

High-p_T Direct Photon and π^0 Production from E706

Michael Begel
FOR THE E706 COLLABORATION

Direct-photon production has long been viewed as an ideal process for measuring the gluon distribution in the proton and has been calculated to next-to-leading order (NLO) [1]. The quark–gluon Compton scattering subprocess ($gq \rightarrow \gamma q$) provides a large contribution to inclusive γ production. The gluon distribution is relatively well constrained for $x < 0.1$ by deep-inelastic scattering and Drell-Yan data, but less so at larger x. Direct-photon data constrains the fits at large x, and consequently has been incorporated in several modern global parton distribution analyses.

A pattern of deviation between measured direct-photon cross sections and NLO calculations has been observed [2]. The suspected origin of the disagreements is the effects of initial-state soft-gluon radiation, referred to here as k_T effects. Kinematic distributions for high-mass pairs of particles directly probe the transverse momentum of incident partons in hard-scattering events. Evidence of significant k_T has been observed in measurements of dimuon, diphoton, and dijet pairs [3].

Fermilab E706 is a fixed-target experiment designed to measure the production of direct-photons, neutral mesons, and associated particles at high-p_T [4]. The apparatus features a large lead and liquid argon electromagnetic calorimeter [5] and a charged particle spectrometer [6]. The experiment accumulated data with 530 GeV/c and 800 GeV/c proton beams and a 515 GeV/c π^- beam incident upon Be, Cu, and H_2 targets. Event selection triggers, sensitive to high-p_T showers, were employed to accumulate data over a broad p_T range.

Several kinematic distributions of direct-photon pairs are shown in Fig. 1 for 515 GeV/c π^-Be interactions. Overlayed on the data are the results from both NLO [7] and resummed [8] pQCD calculations. The resummed calculation (RESBOS), which incorporates the effects of multiple soft-gluon emission, provides a reasonable match to the shape of the data. Also shown are the $\gamma\gamma$ distributions from PYTHIA which approximates k_T effects by a Gaussian smearing technique. Analyses of π^0 pairs [4], as well as studies of the distribution of the fractional momentum carried by charged particles in jets recoiling against isolated photons, also show evidence of substantial k_T, as do our comparisons of the measured high-p_T charged-D cross section to NLO pQCD [6]. All these results suggest a supplemental $\langle k_T \rangle$ of order 1 GeV/c. Similar soft-gluon effects may be expected in other hard-scattering processes, such as the inclusive production of jets or direct-photons [9].

Invariant cross sections for inclusive direct-photon and π^0 production are displayed in Figs. 2—4 with theory overlays. Discrepancies between the NLO theory and the data are particularly striking. Resummed pQCD calculations for single direct-photon production are anticipated [10]. In the meantime, we employed a phenomenological model to incorporate k_T effects in pQCD calculations of direct-photon and π^0 production [4, 3]. We use leading-order (LO) pQCD calculations [11] which include k_T smearing to create K-factors; we then apply these K-factors to the NLO calculations.

The experimental consequences of k_T smearing are expected to depend on $\sqrt{s}$. At the Tevatron collider [12], where p_T is large compared to k_T, only the lowest end of the p_T spectrum is modified (Fig. 5). For the E706 data, the k_T-enhancements (using values consistent with the high-mass pair data) are successful in describing both the shape and normalization of both the direct-photon and π^0 cross sections (Figs. 2—4). Comparisons are also shown for the lower energy WA70 [13] and UA6 [14] data (Fig. 5). The k_T-enhanced theory compares well with the π^0 cross sections and with the CDF, DØ, E706, UA6, and π^- beam WA70 direct-photon cross sections.

[1] P. Aurenche *et al.*, Phys. Lett. **140B**, 87 (1984).
[2] J. Huston *et al.*, Phys. Rev. **D51**, 6139 (1995).
[3] L. Apanasevich *et al.*, Phys. Rev. **D59**, 074007 (1999).
[4] L. Apanasevich *et al.*, Phys. Rev. Lett. **81**, 2642 (1998).
[5] L. Apanasevich *et al.*, Nucl. Instrum. Meth. **A417**, 50 (1998).
[6] L. Apanasevich *et al.*, Phys. Rev. **D56**, 1391 (1997).
[7] B. Bailey *et al.*, Phys. Rev. **D46**, 2018 (1992).
[8] C. Balázs *et al.*, Phys. Rev. **D57**, 6934 (1998).
[9] R. Feynman *et al.*, Phys. Rev. **D18**, 3320 (1978); A. P. Contogouris, Nucl. Phys. **B179**, 461 (1981); A. P. Contogouris, Phys. Rev. **D32**, 1134 (1985).
[10] H.-L. Lai and H.-n. Li, Phys. Rev. **D58**, 114020 (1998).
[11] J. F. Owens, Rev. Mod. Phys. **59**, 465 (1987).
[12] See, e.g., S. Linn at the ICHEP conference in Vancouver, July 1998.
[13] M. Bonesini *et al.*, Z. Phys. **C38**, 371 (1988); *ibid.* **37**, 535 (1988); *ibid.* **37**, 39 (1987).
[14] G. Ballocchi *et al.*, Phys. Lett. **B436**, 222 (1998).

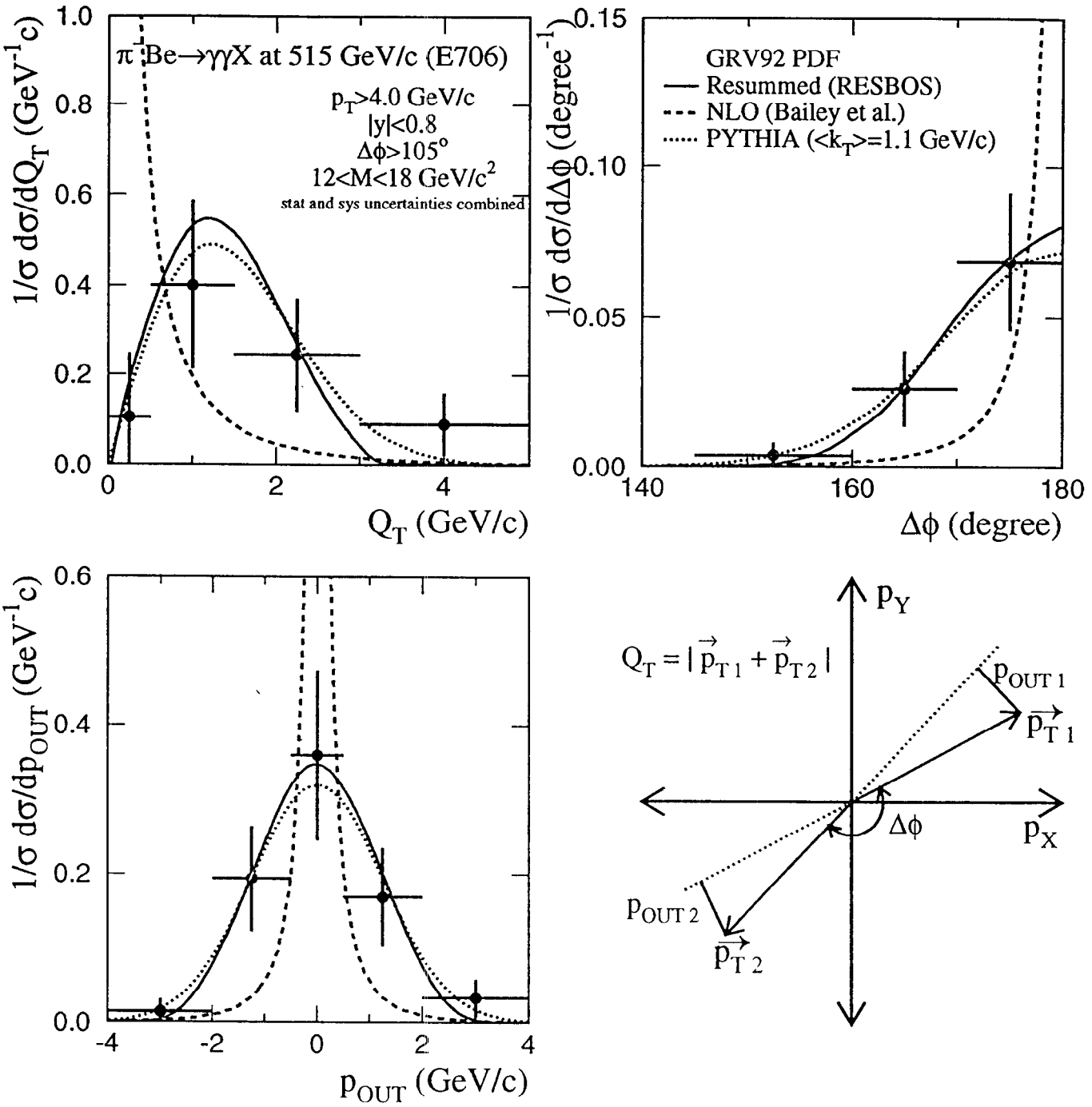

Figure 1 Kinematic distributions for high-mass direct-photon pairs produced in 515 GeV/c π^-Be interactions. Overlayed on the data are the results from NLO (dashed) and resummed (solid) calculations. PYTHIA results (dotted) with $\langle k_T \rangle$ = 1.1 GeV/c are also shown. The various kinematic quantities are illustrated in the vector diagram.

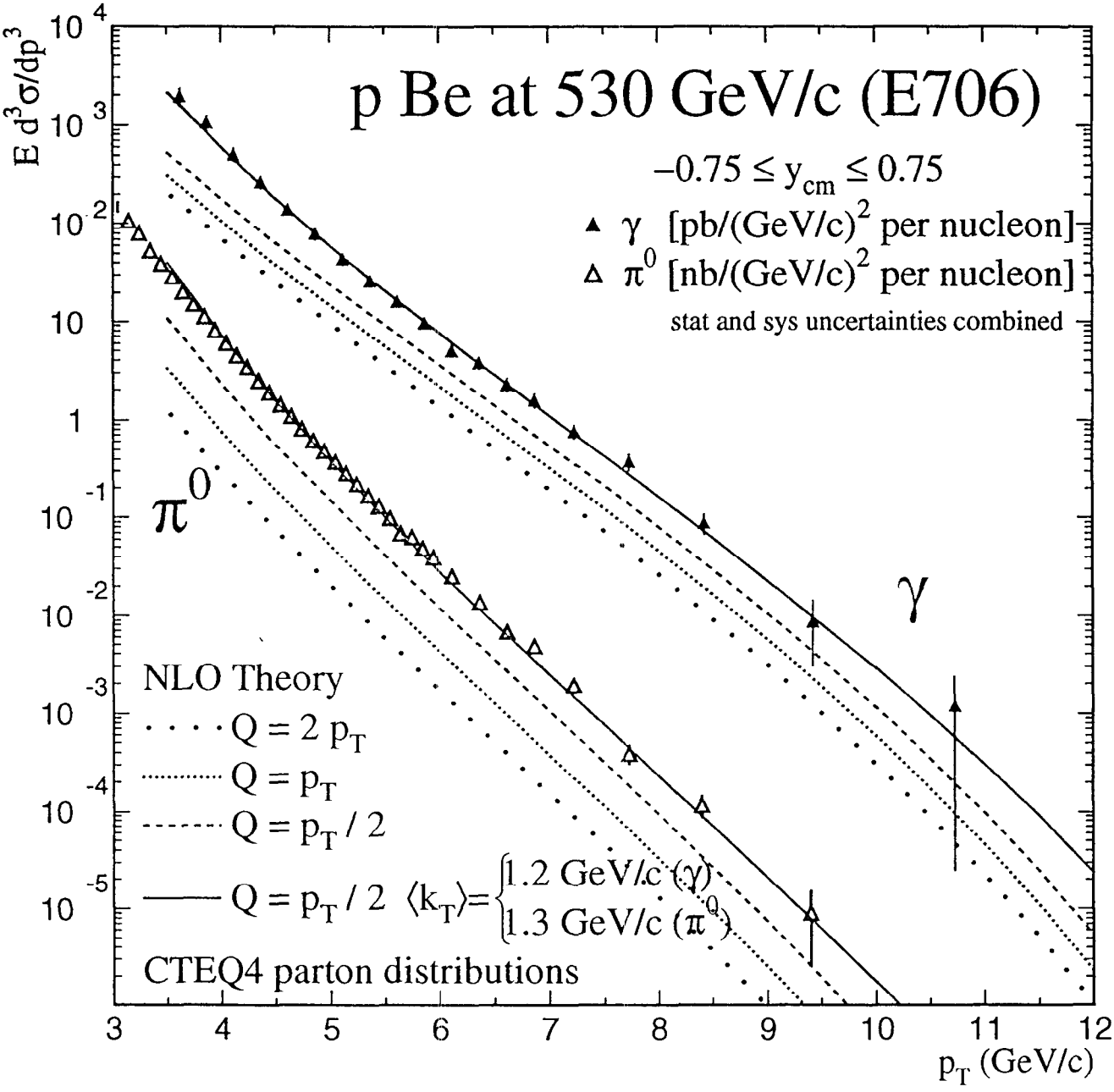

Figure 2 Invariant cross section (per nucleon) for direct-photon and π^0 production in pBe interactions at 530 GeV/c. Cross sections are shown as a function of p_T averaged over the full rapidity range, $-0.75 \leq y_{cm} \leq 0.75$. Curves represent NLO QCD calculations for scale choices of $Q = 2p_T$ (wide dots), $Q = p_T$ (dotted), and $Q = p_T/2$ (dashed), and a k_T-enhanced NLO result with scale $Q = p_T/2$ (solid).

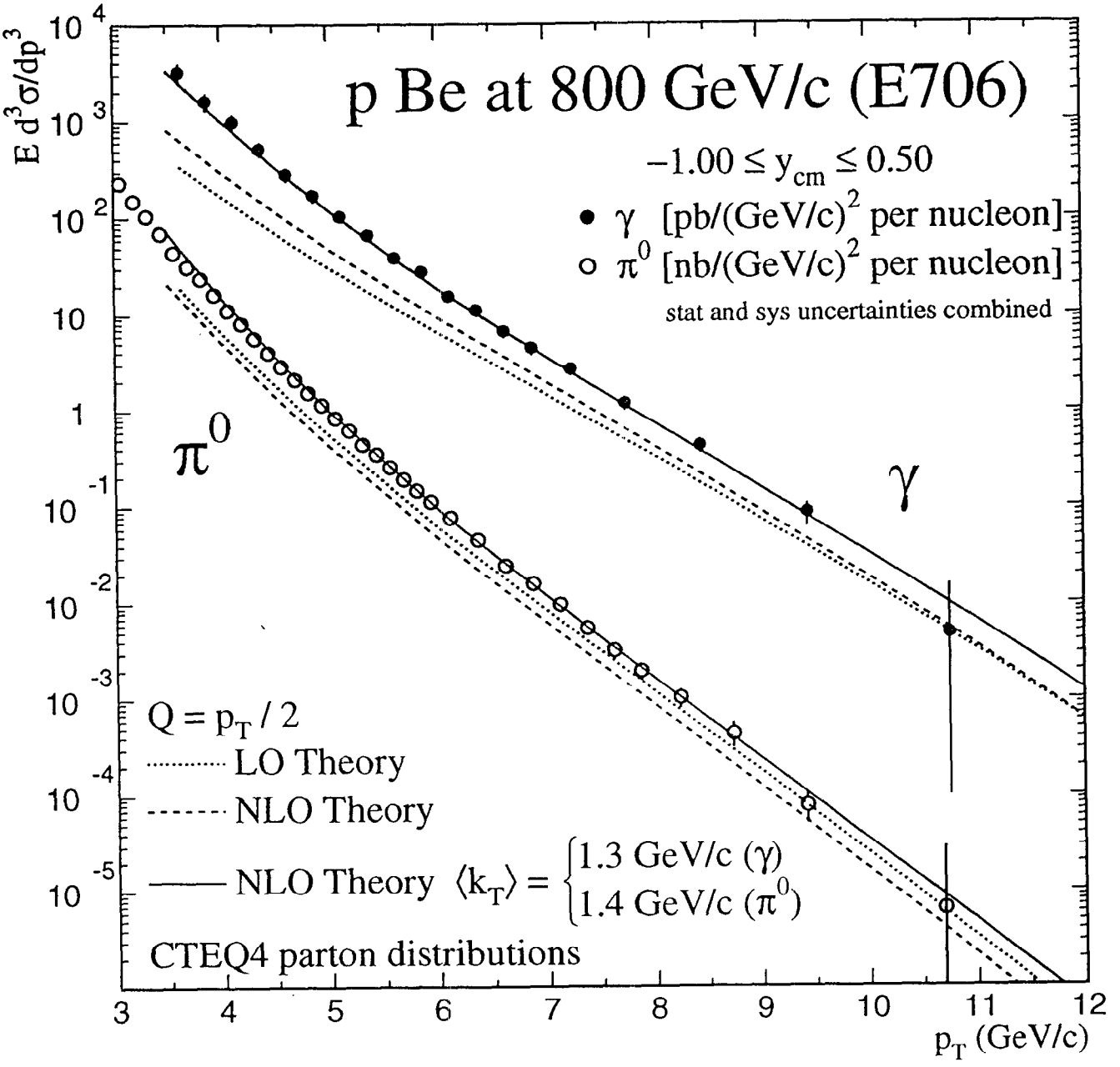

Figure 3 Invariant cross section (per nucleon) for direct-photon and π^0 production in pBe interactions at 800 GeV/c. Cross sections are shown as a function of p_T averaged over the full rapidity range, $-1.0 \leq y_{cm} \leq 0.5$. Curves represent LO (dotted) and NLO (dashed) pQCD calculations and a k_T-enhanced NLO result (solid) for scale $Q = p_T/2$.

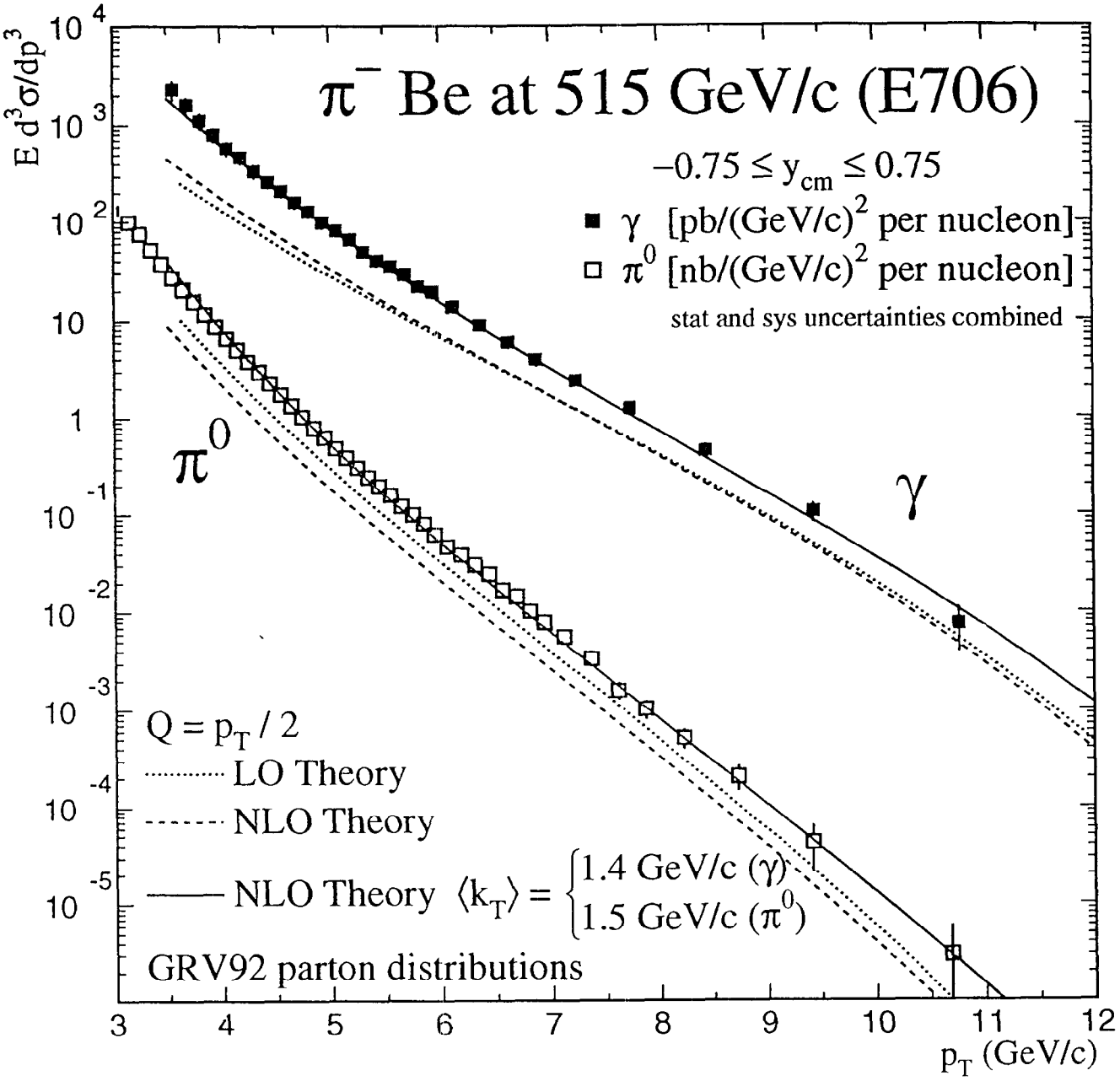

Figure 4 Invariant cross section (per nucleon) for direct-photon and π^0 production in π^-Be interactions at 515 GeV/c. Cross sections are shown as a function of p_T averaged over the full rapidity range, $-0.75 \leq y_{cm} \leq 0.75$. Curves represent LO (dotted) and NLO (dashed) pQCD calculations and a k_T-enhanced NLO result (solid) for scale $Q = p_T/2$.

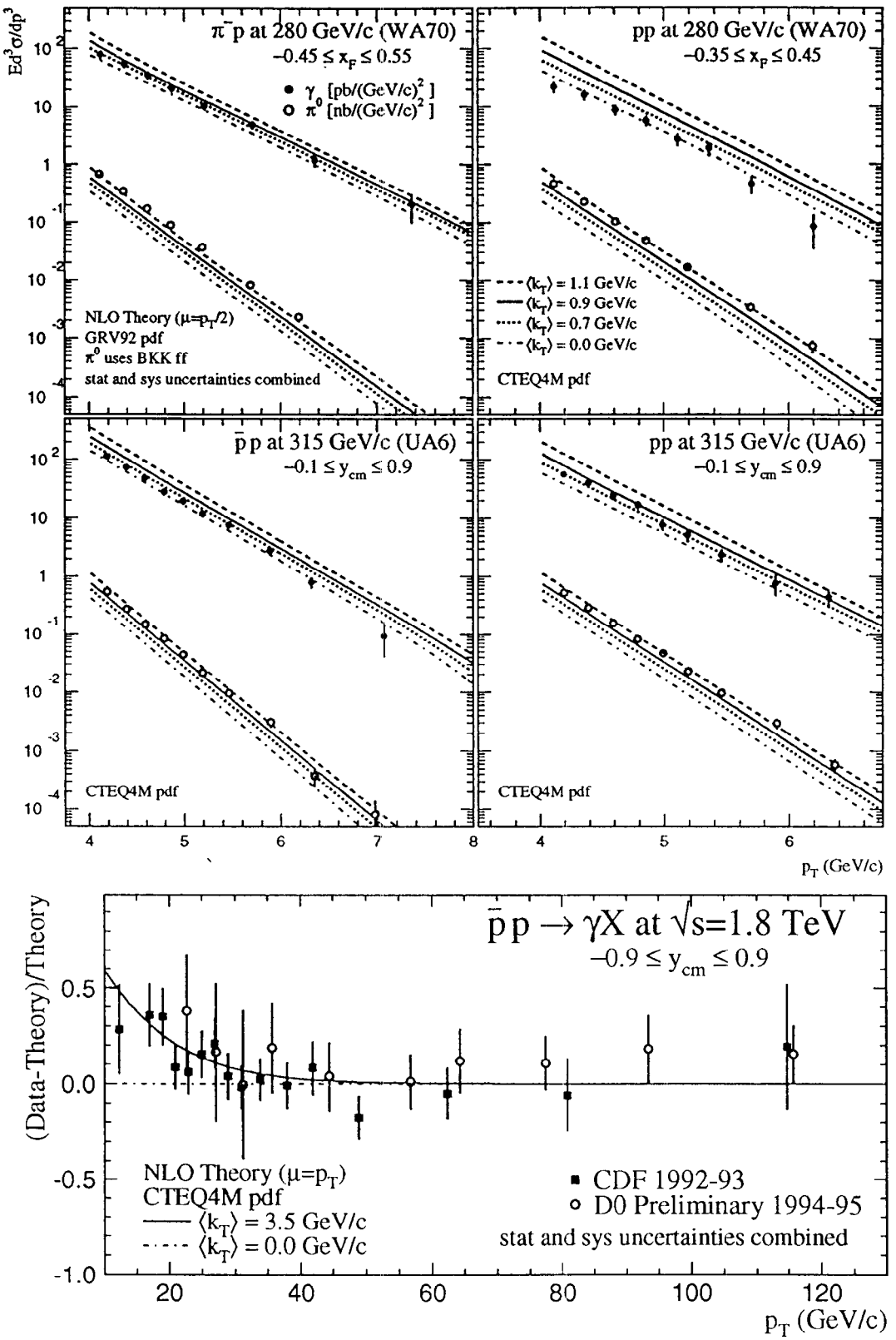

Figure 5 Top: Invariant cross sections for direct-photon and π^0 production for WA70 and UA6. Overlayed on the data are the results of the NLO calculation with k_T enhancements for several values of $\langle k_T \rangle$.
Bottom: The quantity (Data-Theory)/Theory (for NLO theory without k_T adjustment) for the CDF and DØ isolated direct-photon cross sections, overlayed with the expected effect from k_T-enhancement for $\langle k_T \rangle = 3.5$ GeV/c (solid curve).

A critical phenomenological study of inclusive γ production

P. Aurenche

M. Fontannaz
J.Ph Guillet
B. Kniehl
E. Pilon
M. Werlen

hep-ph/9811388

I THEORETICAL AMBIGUITIES

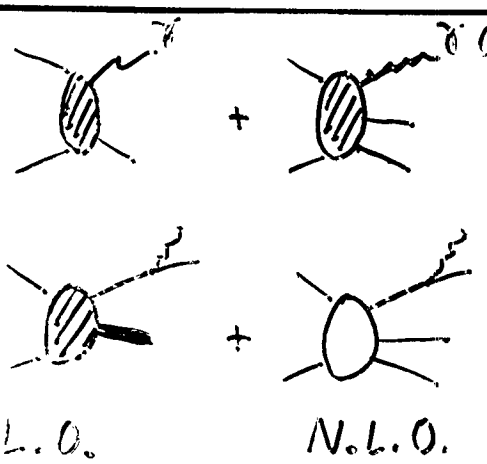

Inclusive γ produced at large $\vec{p}_T$ in hard collision: $d\sigma^{dir}$

or

via bremsstahlung from q, G produced at larg $\vec{p}_T$: $d\sigma^{brems.}$

$$\frac{d\sigma^{\gamma}}{d\vec{p}_T\, d\eta}(\mu, M, M_F) = \frac{d\sigma^{dir}}{d\vec{p}_T\, d\eta}(\mu, M, M_F) + \frac{d\sigma^{brems}}{d\vec{p}_T\, d\eta}(\mu, M, M_F$$

Residual sensitivity of N.L.O. perturbative predictions to μ, renormal. scale ; M, factoriz. scale ; M_F fragment. scale

- p_T large enough (4 - 5 GeV/c) : stability in μ, M (Figure 1)
  weak dependence in M_F
- p_T smaller : no stability in any scale.

⇒ N.L.O. predictions useful for $p_T \gtrsim 4$ or 5 GeV/c

In pheno. studies : use $\mu = M = M_F = p_T/2$ or $p_T/4$

II [illegible]

- data : WA70, UA6, E706, R806, R110, AFS : $20 \leq \sqrt{s}[\text{GeV}] \leq 63$
- [illegible] ⇒ same pheno.

Fig. II

CTEQ4M
($P_T/2$)

Fig. II

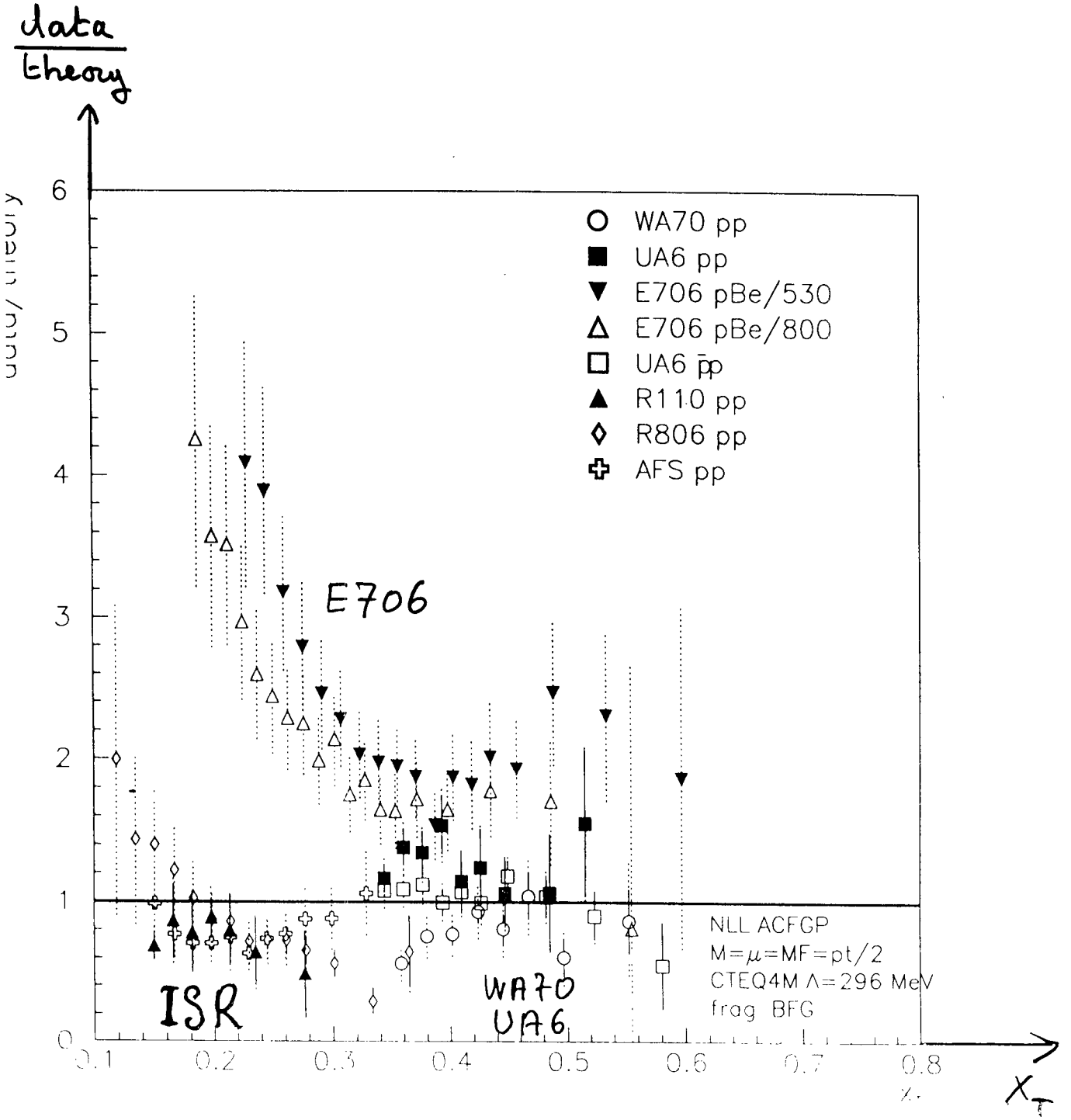

Fig. III

CTEQ 4M
($P_T/3$)

condition: $(P_T/3)^2 > Q_0^2 = 2.56\ GeV^2$

cuts off low P_T points

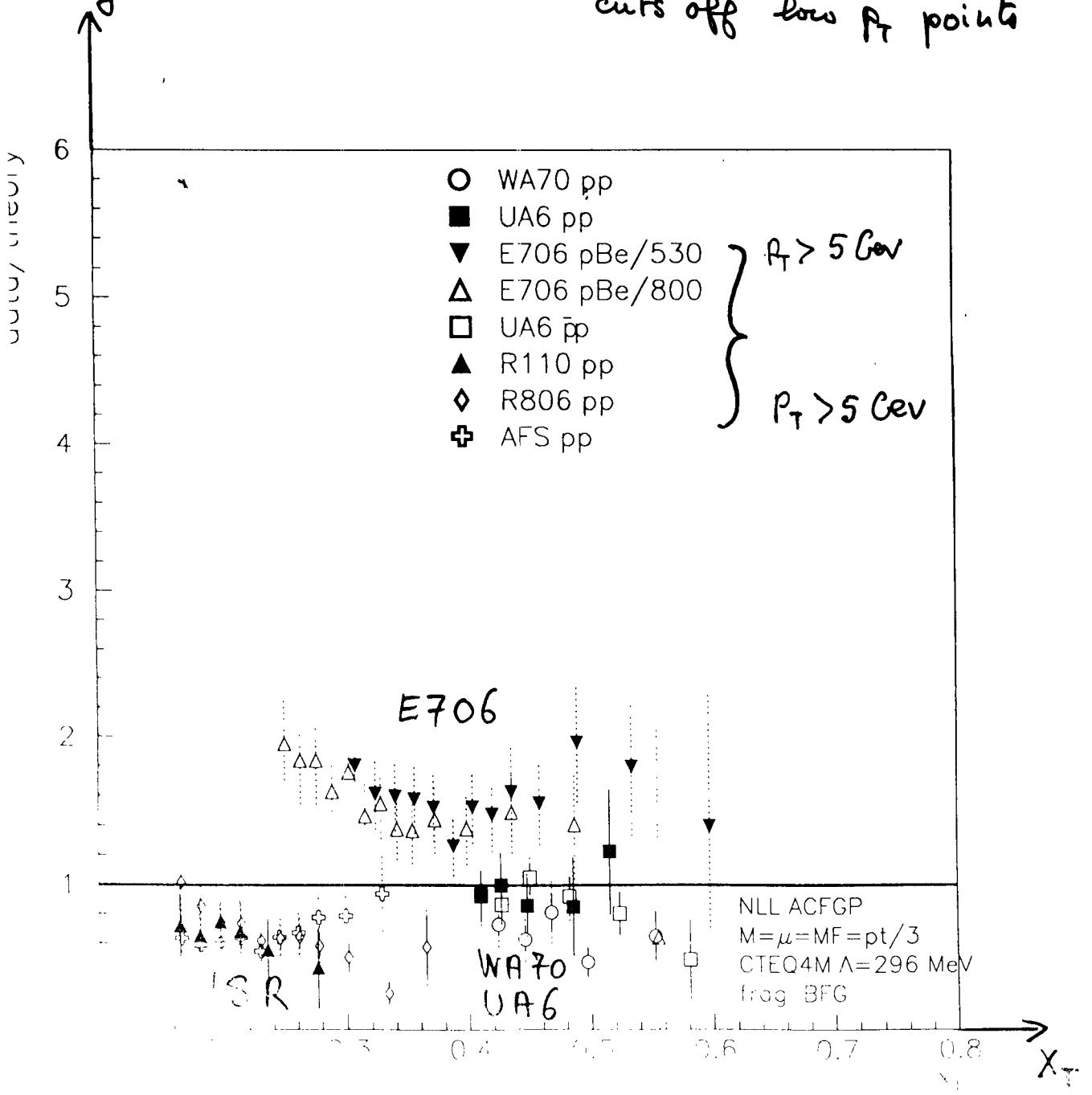

Fig. I

Theoretical ambiguities

for pBe (800 GeV), $p_T = 6.12$ GeV/c

Variation of $\frac{d\sigma^\gamma}{d\vec{p}_T d\eta}$ vs M and M_F

Fig.

μ : $\frac{d\sigma}{d\mu} = 0$

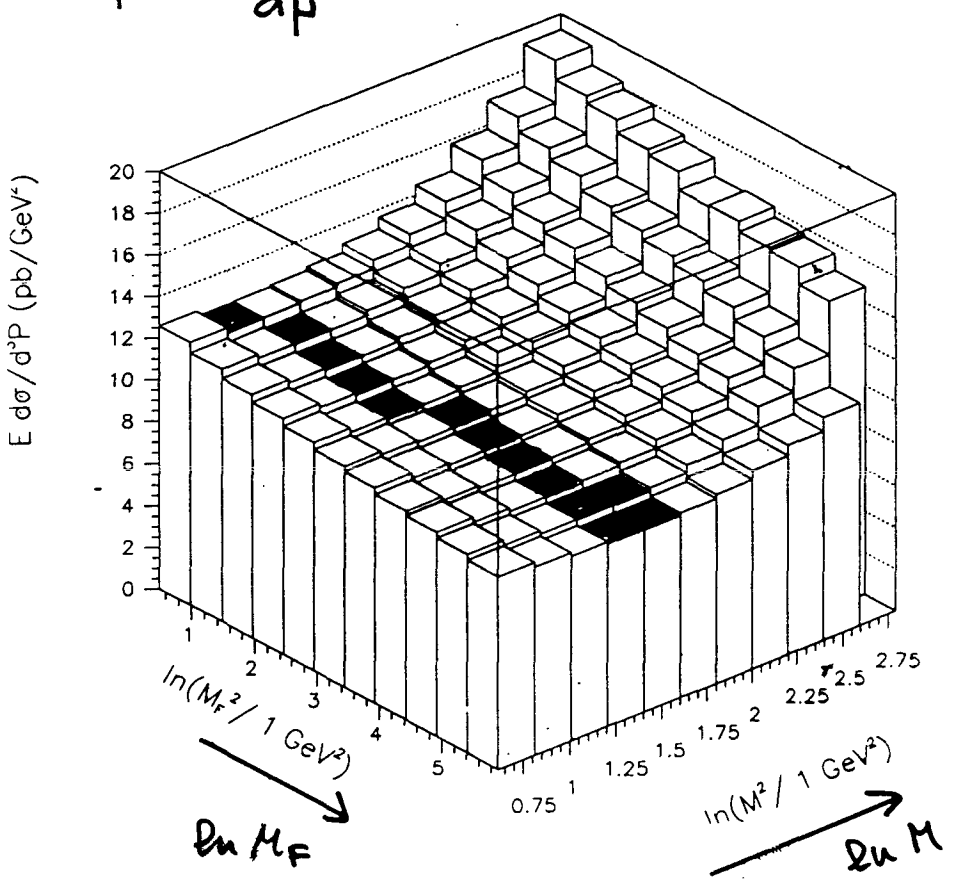

$M = \mu$

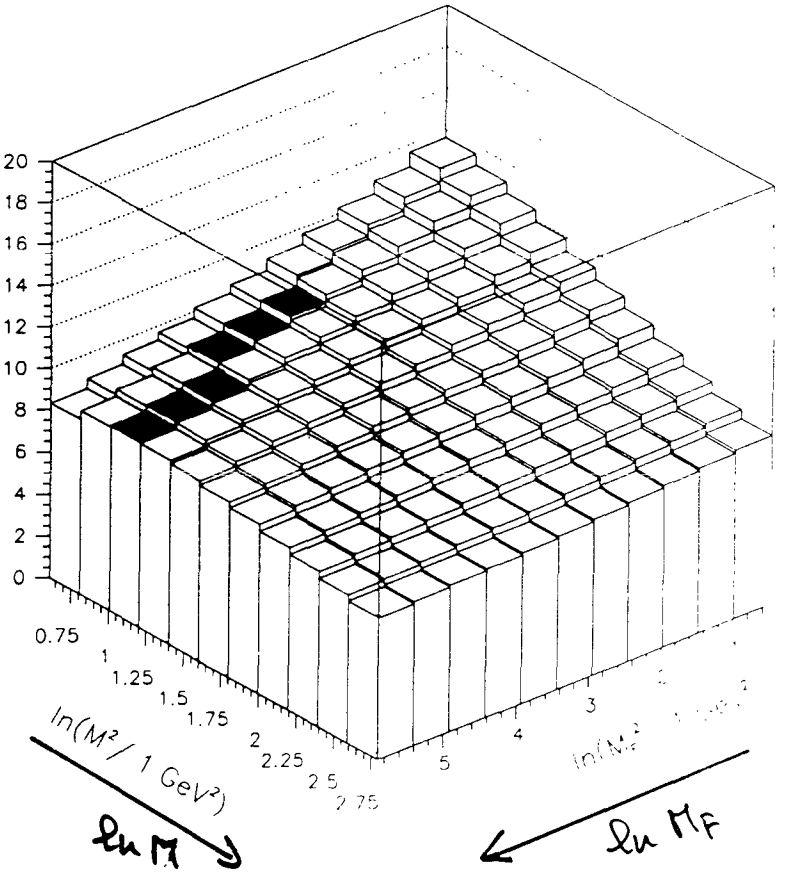

- **Strict N.L.O. predictions:**
  - scale = $P_T/2$: data/theory ~ 1 for WA70, UA6, ISR.
    " ~ 2 to 4 for E706
  - scales = $P_T/3$: data/theory < 1 for WA70, ISR
    ~ 1 for UA6
    ~ 1.5 to 2 for E706

  Figs: II, III

  - E706 : higher than other data
  - E706, ISR : incompatible in overlapping $x_T = \frac{2P_T}{\sqrt{s}}$ range

- **Primordial $\langle k_T \rangle$ * N.L.O. predictions**

  Introduced $\langle k_T \rangle$ smearing; $\langle k_T \rangle$ measured in $\frac{d^2\sigma}{dq_T^2}$, ...
  - Excellent agreement with E706 : $\langle k_T \rangle$ = 1.2 / 1.3 GeV/c
  - good agreement with UA6 pp : $\langle k_T \rangle$ = .7 / .9 GeV/c
  - disagreement with UA6 $\bar{p}p$, WA70
  - would obtain violent disagreement with ISR

- conclusions: No theory can accomodate all data!
  Are inclusive γ data compatible.

III π^0 HADROPRODUCTION

- Data from same expts as above
- Theory not reliable for normalisation (scale, fragm. function) but good enough to interpolate in P_T, $\sqrt{s}$
- WA70, UA6, E706, R806 could be made to agree with theory within error bars.

CONCLUSIONS: Problems with experimental $\frac{\gamma}{\pi}$?

HARD PHOTON & PION PRODUCTION AT RHIC ENERGIES

G. PAPP, P. LEVAI, G. FAI
KSU/ELTE/RMKI

High-p_T particle production at RHIC:

e.g. $A + A \longrightarrow \gamma + X$
$A + A \longrightarrow \pi^0 + X$

Systematic studies of

$p + A \longrightarrow \gamma + X$
$p + A \longrightarrow \pi^0 + X$ are needed in pQCD

Nuclear effects
- — initial state multiple collisions;
- — final state radiation;
- — shadowing;
- — jet-quenching;
- — ...

One of the basic questions is

$p + p \longrightarrow \gamma + X$
$p + p \longrightarrow \pi^0 + X$ in pQCD

nucl-th/9903012, KSUCNR-102-99

PION PRODUCTION IN pp COLLISION IN pQCD:

$$E_\pi \frac{d\sigma_\pi^{pp}}{d^3p} = \sum_{abcd} \int dx_1 dx_2 \; f_{a/p}(x_1, Q^2) \; f_{b/p}(x_2, Q^2) \times K \frac{d\sigma}{d\hat{t}}(ab \to cd) \frac{D_{\pi/c}(z_c, \widehat{Q}^2)}{\pi z_c}$$

TWO METHODS:

1. Additional (non-perturbative) parameter:
intrinsic k_T

$$dx \; f_{a/p}(x, Q^2) \to dx \; d^2k_T \; g(\vec{k}_T) \; f_{a/p}(x, Q^2)$$

$$g(\vec{k}_T) = \frac{\exp(-k_T^2/\langle k_T^2 \rangle)}{\pi \langle k_T^2 \rangle}$$

$\langle k_T^2 \rangle$: 2D width of the k_T distribution
$\langle k_T^2 \rangle = 4\langle k_T \rangle^2 / \pi$

J.F. Owens, Rev.Mod.Phys. 59, 465 (1987)
J. Huston et al. Phys.Rev. D51, 6139 (1995)
M. Begel, these Proceedings

2. Improved NLO (NNLO) calculations:
adjusted (optimized) scale parameters

P. Aurenche, et al., hep-ph/9811382
P. Aurenche, these Proceedings

Basic elements of our pQCD calculation with $\langle k_T \rangle$:

a, Parton Disribution Function: MRST-98 — NLO

$Q = p_T/2$, $\Lambda_{\overline{MS}}(n_f = 4) = 300$ MeV

A.D. Martin, et al., Eur. Phys. J. C4 (1998) 463.

b, Fragmentation Functions: BKK — NLO

$\widehat{Q} = p_T/z_c$ J. Binnewies, et al., Phys. Rev. D52 (1995) 4947.

c, Partonic Cross Sections: Field-Feynman — LO

$K = 2$ C.Y. Wong, H. Wang, Phys. Rev. C58 (1998) 376.

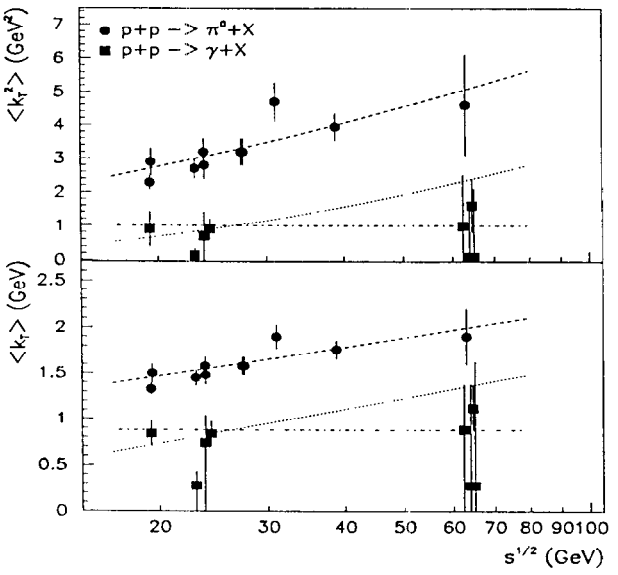

Figure 1: The best fit values of $\langle k_T^2 \rangle$ in $pp \to \pi^0 X$ and $pp \to \gamma X$ reactions (upper panel), and a calculated $\langle k_T \rangle$ (lower panel).

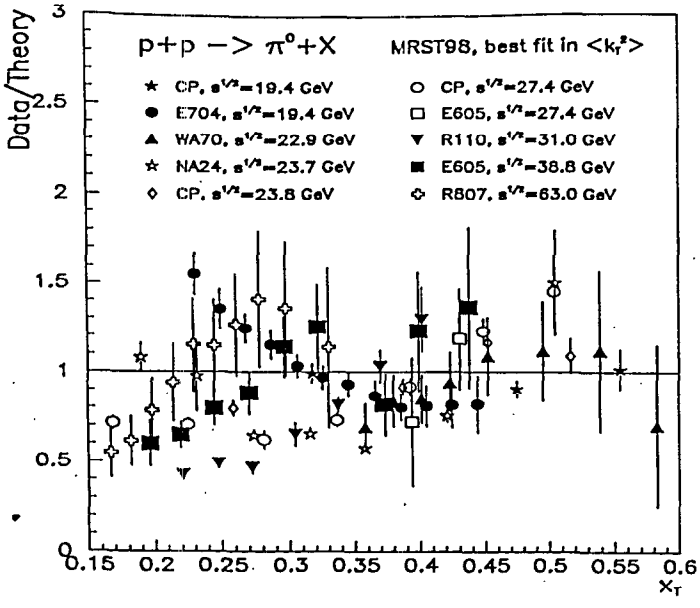

Figure 2: Data to theory ratios for $pp \to \pi^0 X$ reactions applying the best fit for $\langle k_T^2 \rangle$, $x_T = 2p_T/\sqrt{s}$.

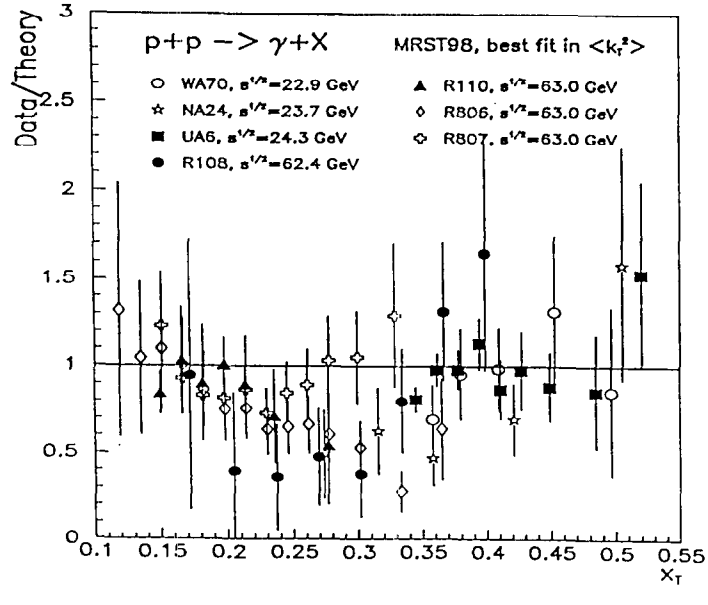

Figure 3: Data to theory ratios for $pp \to \gamma X$ reactions applying the best fit for $\langle k_T^2 \rangle$, $x_T = 2p_T/\sqrt{s}$.

PION PRODUCTION IN pA COLLISION BY pQCD:

$$E_\pi \frac{d\sigma_\pi^{pA}}{d^3p} = \sum_{abcd} \int d^2b t_A(b) \int d^2k_{T,1} g(\vec{k}_{T,1}) \int d^2k_{T,2} g(\vec{k}_{T,2})$$
$$\int dx_1 dx_2 \; f_{a/p}(x_1, Q^2) \; f_{b/p}(x_2, Q^2) \; K \; \frac{d\sigma}{d\hat{t}}(ab \to cd) \; \frac{D_{\pi/c}(z_c, \widehat{Q}^2)}{\pi z_c}$$

NUCLEAR EFFECT: $\langle k_T^2 \rangle_{pA} = \langle k_T^2 \rangle_{pp} + C \cdot h_{pA}(b)$

1. All possible collisions

$$h_{pA}^{all}(b) = \nu_A(b) - 1 \qquad C_{pBe}^{all} = 0.8 \pm 0.2 GeV^2$$
$$\nu_A(b) = \sigma_{NN} \; t_A(b) \qquad C_{pTi}^{all} = 0.4 \pm 0.2 GeV^2$$
$$C_{pW}^{all} = 0.3 \pm 0.2 GeV^2$$

2. Saturation:

$$h_{pA}^{sat}(b) = \begin{cases} 0 & \text{if } \nu_A(b) < 1 \\ \nu_A(b) - 1 & \text{if } 1 \le \nu_A(b) < 2 \\ 1 & \text{if } 2 \le \nu_A(b) \end{cases}$$

$$\Longrightarrow \quad C^{sat} = 0.8 \text{ GeV}^2$$

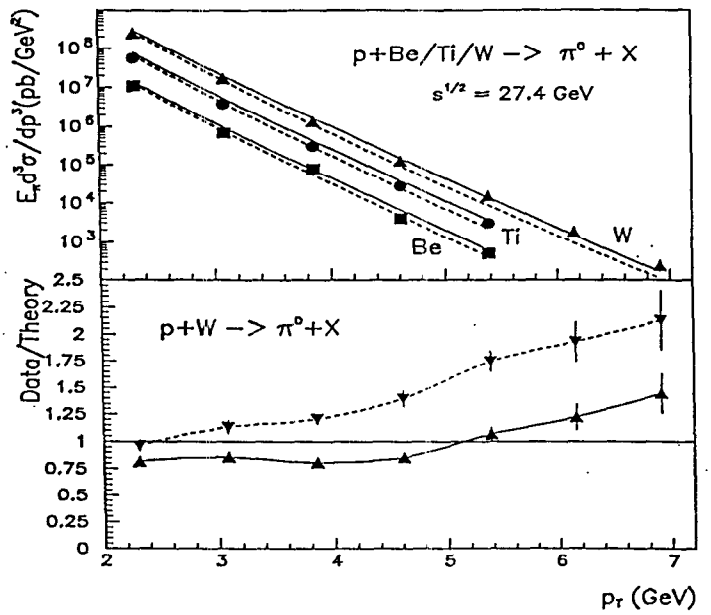

Figure 4: Cross section per nucleon in $pA \to \pi^0 X$ reactions ($A = Be, Ti, W$), data from D. Antreasyan et al. (PRD19,764,1979). We show $C^{sat} = 0.8$ GeV^2 (full lines) and $C^{sat} = 0$ (dashed lines).

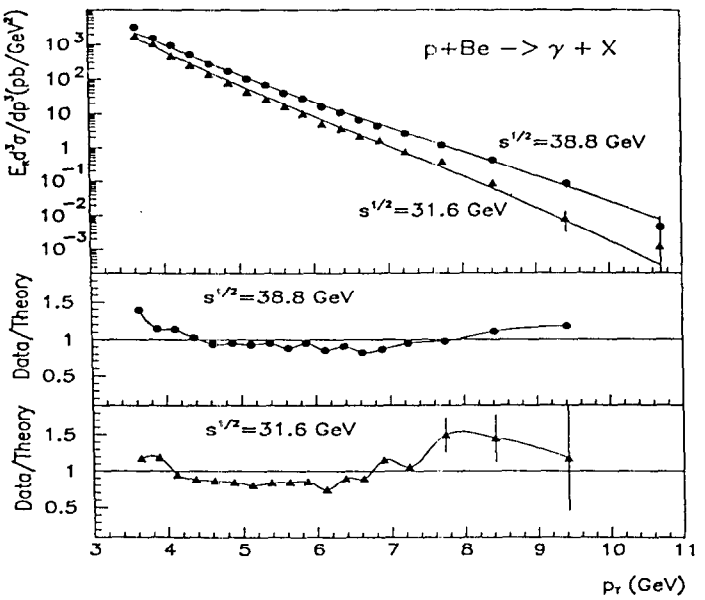

Figure 5: Cross section per nucleon in the $pBe \to \gamma X$ reaction at $\sqrt{s} = 38.8$ GeV (dots) and at $\sqrt{s} = 31.6$ GeV (full up triangles) from E706 Coll. Solid lines indicate $C^{sat} = 0.8$ GeV^2.

Pion and Direct Photon Production in Nuclear Collisions

Terry Awes
Oak Ridge National Laboratory
for the **WA98 Collaboration**

Outline:

- Motivation
- Scaling of Particle Production (Energy Density - Thermalization).
- Direct Photon Analysis Method
- Preliminary Pb + Pb Direct Photon Result
- Summary

Acknowledge: Christoph Blume, Damian Bucher, Thomas Peitzmann, Sergei Fokin, Sasha Lebedev, Paul Stankus.

"Hard Parton Physics in High-Energy Nuclear Collisions"
BNL
March 1-5, 1999

Centrality Dependence of N_γ:

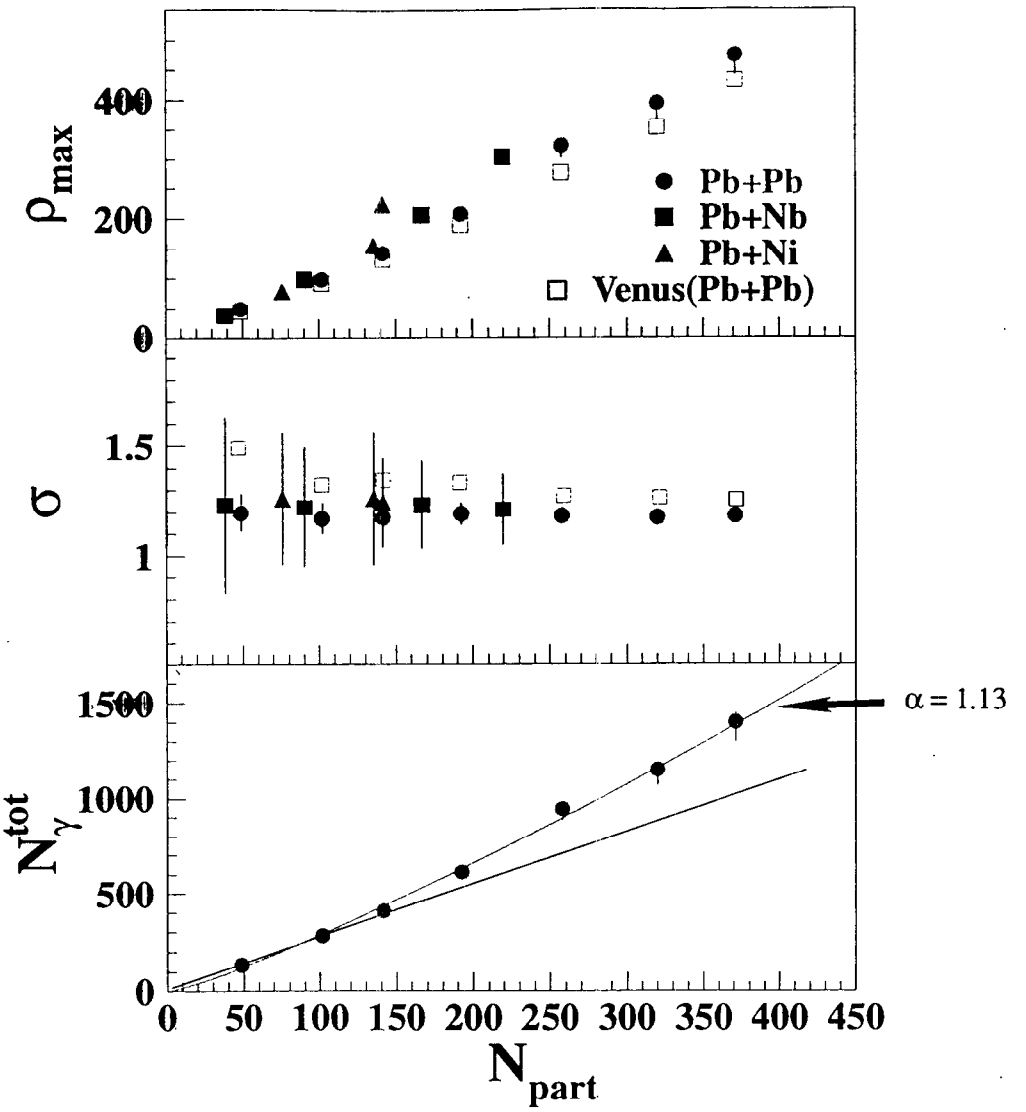

- N_γ^{tot} and $\rho_{max}(\equiv dN_\gamma/d\eta|_{max})$ increase like $\approx N_{part}^{1.1}$
- Width σ of $dN_\gamma/d\eta$ distribution remains constant.

WA98 π^0 Central Pb+Pb

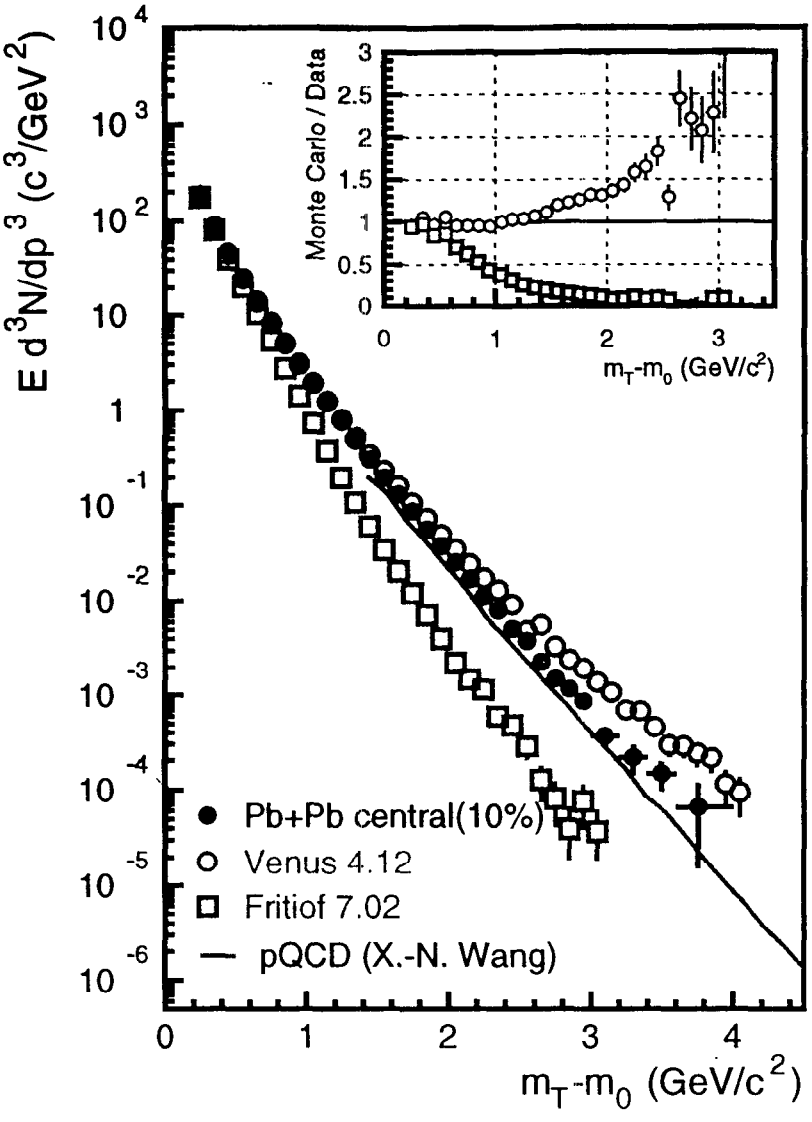

- Models give good/poor/lousy description of data.
- Study Centrality Dependence to investigate Nuclear Effects.
- Use Model Independent Analysis.

Centrality Dependence of Mean p_T:

WA80/WA98 π^0 Results

Truncated Mean p_T:

$$\langle p_T(p_T^{min})\rangle = \left(\frac{\int_{p_T^{min}}^{\infty} p_T \frac{dN}{dp_T} dp_T}{\int_{p_T^{min}}^{\infty} \frac{dN}{dp_T} dp_T} \right) - p_T^{min}$$

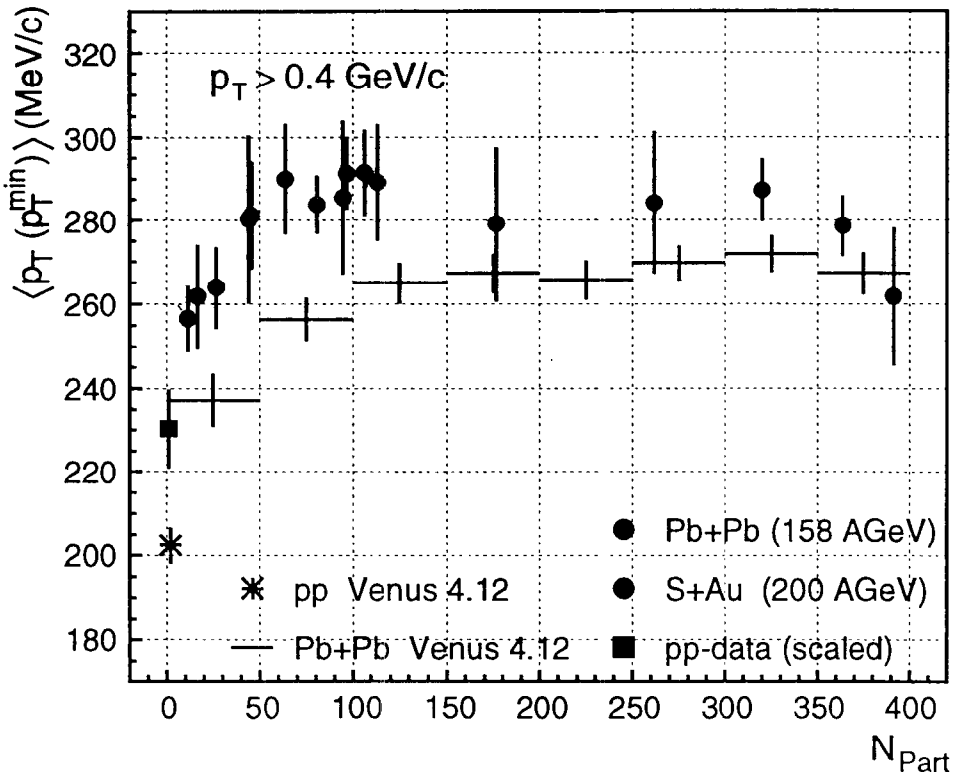

WA98, PRL 81 (1998) 4087.

Mean p_T saturates for systems larger than $N_{Part.} \approx 50$.

p_T Dependence of N_{part}-scaling

WA98 π^0 Results

$$E\frac{dN}{d^3p}(N_{part}) = N_{part}^{\alpha(p_T)} \cdot \sigma(N^0_{part})$$

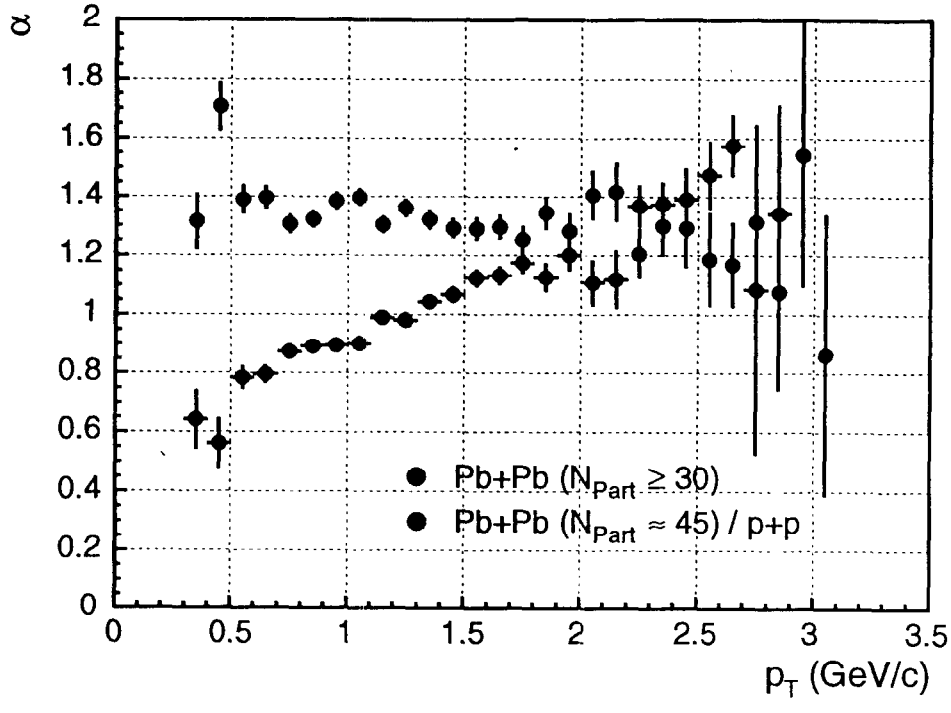

WA98, PRL 81 (1998) 4087.

- π^0 yield scales as $\approx N_{part}^{4/3}$ at all p_T for $N_{part} > 30$
  $\rightarrow$ Shape does not change.

- But, shape is different from $p - p$ at all p_T.

Evidence of Thermalization

Summary

At SPS energies:

- **Soft particle production scales $\simeq N_{Part}^{1.1}$ (or $\simeq N_{Coll}^{0.8}$).**
  - Naive Wounded Nucleon Model not valid
  - Secondary rescattering contributes to net particle production
- **Mean $< p_T >_{\pi^0}$ (or E_T/N_{Ch}) saturates for centralities with $N_{Part} > 50$.**
  - In thermal picture $\rightarrow$ T=constant
- **π^0 spectral shape is invariant and scales $\simeq N_{Part}^{1.3}$ for centralities with $N_{Part} > 50$ ($p_T > 0.5$ GeV/c).**
  - Thermalization would explain naturally
- **Thermal direct photon production is small! (Observable?!).**
  - Initial Temperature is "low"
  - "Large" number of degrees of freedom
- **Preliminary indication for observation of "hard" direct photons.**
  - Nuclear k_T effects
  - Improved $T_{Initial}$ limits

Physics with the STAR RICH

G.J.Kunde

for the Yale/Cern/Bari

RICH-Collaboration

Ring Imaging Cherenkov Detector I

- PID for Kaon/Pion/Proton
- Momentum from TPC
- Located at y=0

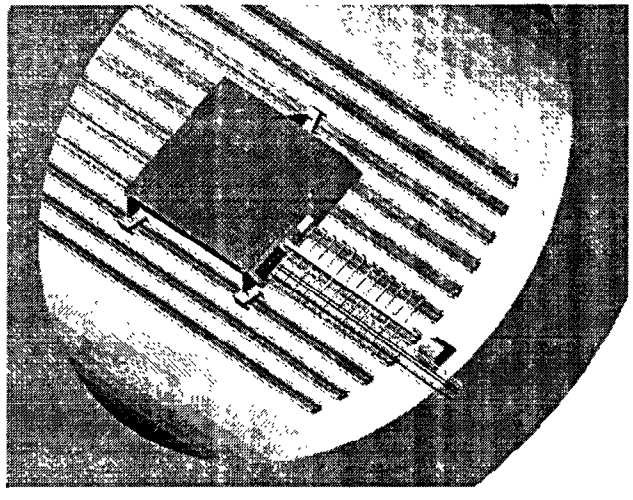

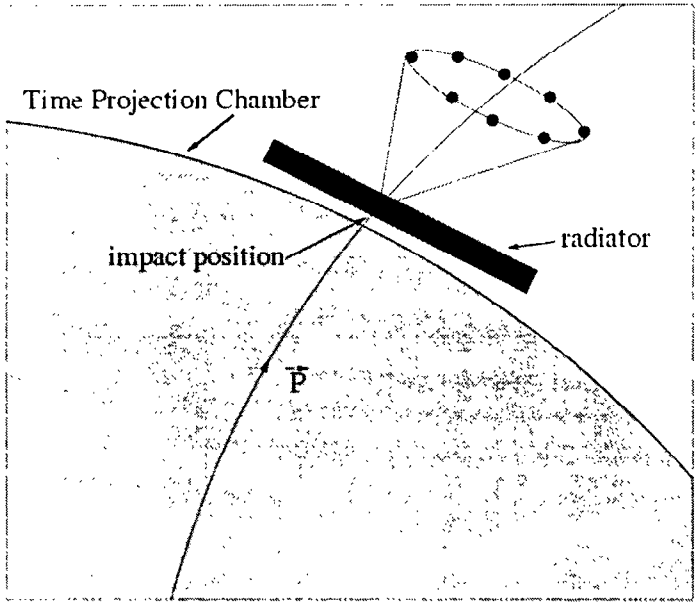

- PID-Ranges:
- 1-3 GeV/c for K/pi
- 1.5-5 GeV/c for p/anti-p

Ring Imaging Cherenkov Detector II

- TPC gives PID for Majority of Particles
- RICH adds Inclusive PID for High-Pt

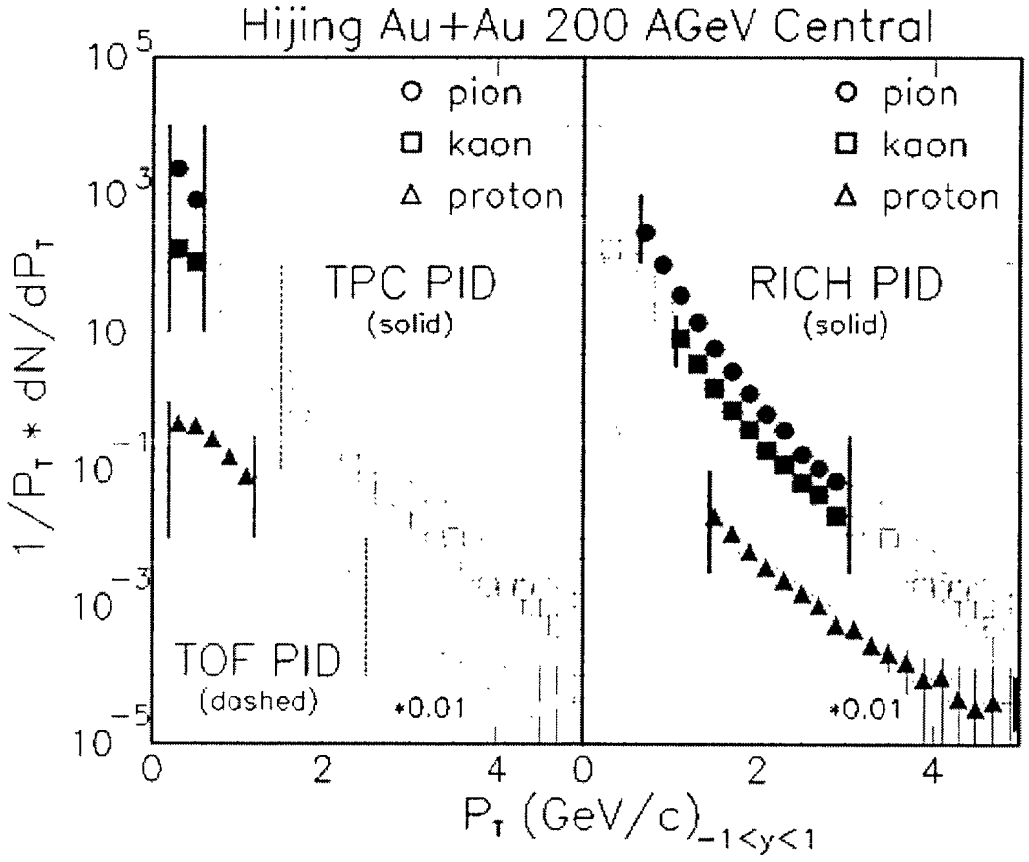

Ring Imaging Cherenkov Detector III

RICH: small phi acc.

Courtesy of P.Jacobs

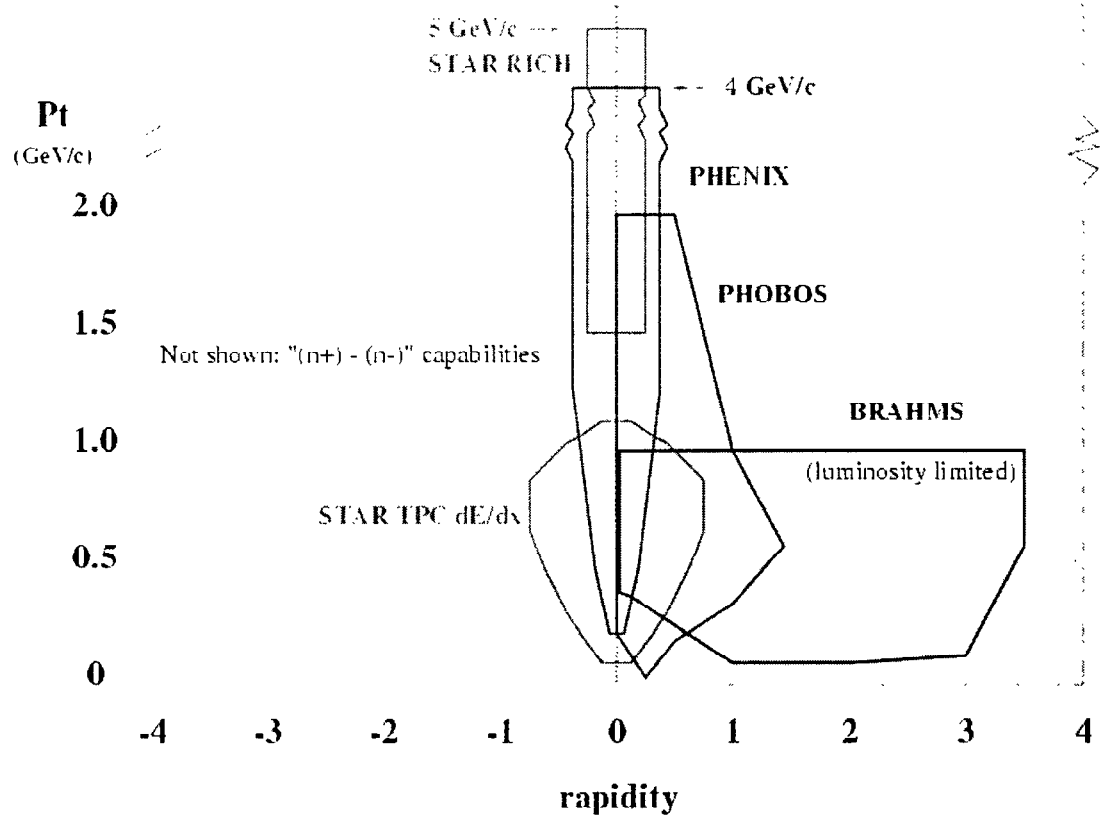

- Tagging of Spectra

Partonic Energy Loss VII

- Tagging of Spectra
  - Hard photon
  - Fast particle
- Hard photon
  - Very small cross section
  - Possible with EMC
- Fast Particle
  - Possible with TPC/EMC

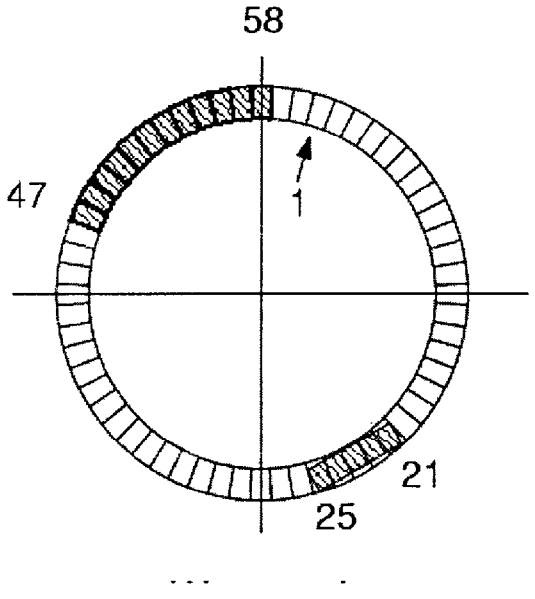

EMC Configuration 1st Year

Partonic Energy Loss VIII

- Fast Particle Tagging
  - Require that there is one particle with high Pt in 10 degree cone on opposite side
- Small Effect for 3 GeV/c. Study in Progress ...

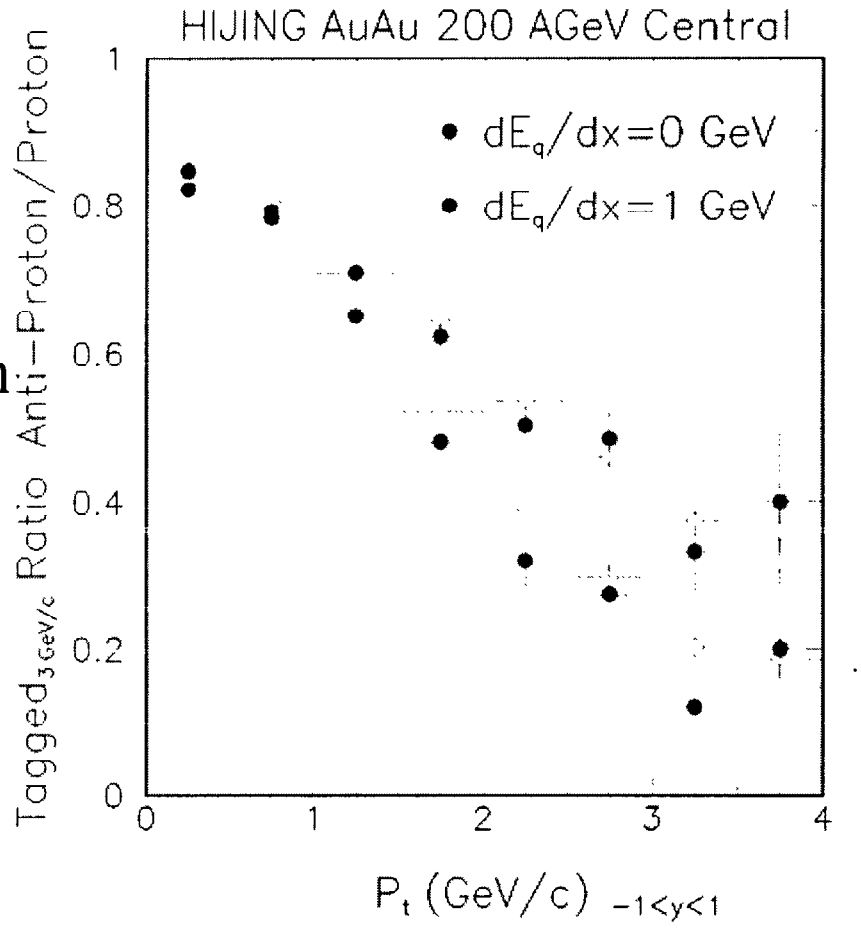

Summary

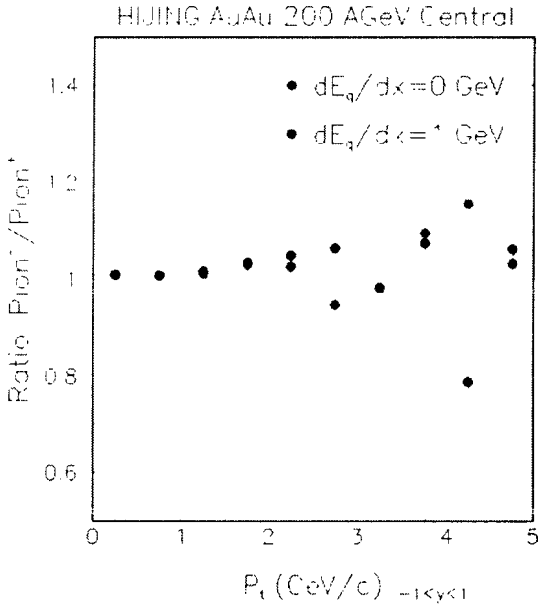

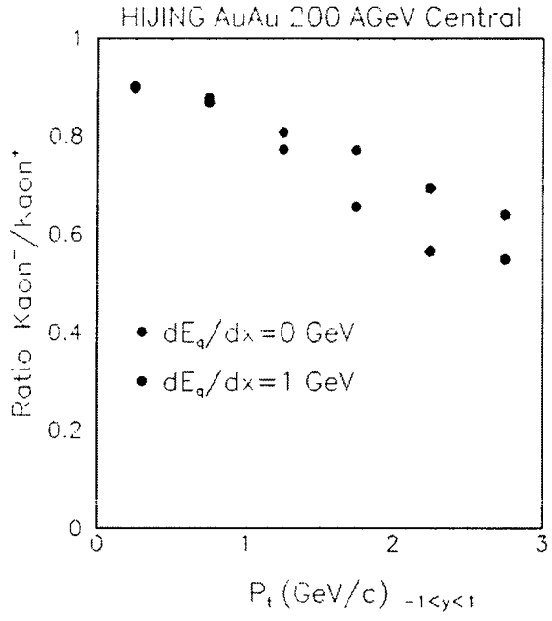

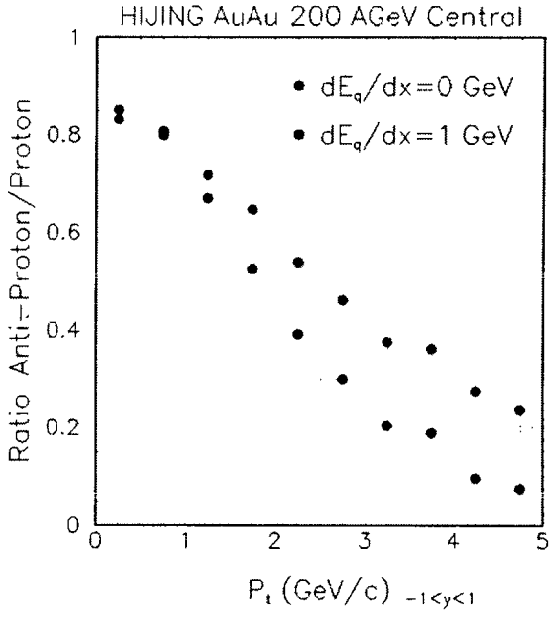

- Partionic Energy Loss Via Identified Particle Ratios

GLUON SHADOWING AND RELATED QCD PHENOMENA

L. Frankfurt

1. QCD interaction should be different at different scales → variety of factorization theorems.

2. Nuclear shadowing in DIS is leading twist phenomenon calculable in the approximation of small nuclear density in terms of cross section of „soft" diffraction in DIS and in the black body approximation

3. HERA data on diffraction in DIS imply ... significant shadowing of gluon distributions in nuclei at $Q^2 = Q_0^2 \sim 4\ GeV^2$ and $x \sim 10^{-3}$

4. Important role in DIS of the interaction of compact system with a nuclear target. Calculable in QCD as the consequence of QCD factorization theorem.

5. Color Coherent Hard diffractive processes, CT have been observed at HERA and at FNAL

Nuclear shadowing phenomenon is much better understood in the nucleus rest frame.

DICTIONARY

IMF description	Rest frame description
Large k_t of a parton.	Small transverse distances between partons $b^2 \sim 1/k_t^2$
QCD evolution	Ordering over transverse distance between partons
QCD evolution equation	$\sigma_{q\bar{q}T} = \frac{\pi^2}{3} b^2 \alpha_s\left(\frac{6b^2}{b^2}\right) \times G_T\left(x, \frac{6b^2}{b^2}\right)$
Gribov diffusion presents but often ignored.	V. Gribov diffusion in impact parameter space. Increase of $\langle b^2 \rangle$ with $\ln 1/x$ as a result of randomness of radiation. Approximation of frozen configurations is in variance with QCD

Structure function of D for $\frac{1}{2m_N x} >> r_D$

$$f_{j/D}(x,Q^2) = f_{j/p}(x,Q^2) + f_{j/n}(x,Q^2) -$$

$$-\eta/4\pi \int dx_{IP}\, dt\, S(4t)\, \frac{d f_{j/N}}{dx_{IP}\, dt}\left(\frac{x}{x_{IP}}, Q^2, t\right)$$

$S(t)$ is e.m. form factor of deuteron.

$$\eta = \left(1 - \left(\mathrm{Re}\,A_{diff}/\mathrm{Im}\,A_{diff}\right)^2\right) \Big/ \left[1 + \left(\frac{\mathrm{Re}\,A_{diff}}{\mathrm{Im}\,A_{diff}}\right)^2\right]$$

$\frac{d f_{j/N}}{dx_{IP}\, dt}\left(\frac{x}{x_{IP}}, Q^2, t\right)$ → diffractive parton density measured in diffraction in DIS

Structure function of nuclear target

$1/2m_N x >> r_{NN}$

$$\frac{1}{A} f_{j/A}(x,Q^2) = f_{j/N}(x,Q^2) - \frac{1}{2}\int_{-\infty}^{\infty} dz_1 \int_{z_1}^{\infty} dz_2 \int_{x}^{x_0} dx_{IP} \int d^2b$$

$$\frac{d f^D_{j/N}}{dx_{IP}\, dt}\left(x/x_{IP}, Q^2, t, x_{IP}\right)\Big|_{k_t^2=0}\; \rho_A(b,z_1)\,\rho_A(b,z_2)$$

$$\cos\left(x_{IP}\, m_N (z_1 - z_2)\right)$$

$\rho_A(r)$ is nuclear density normalized as $\int \rho_A(r)\, d^3r = A$

32)

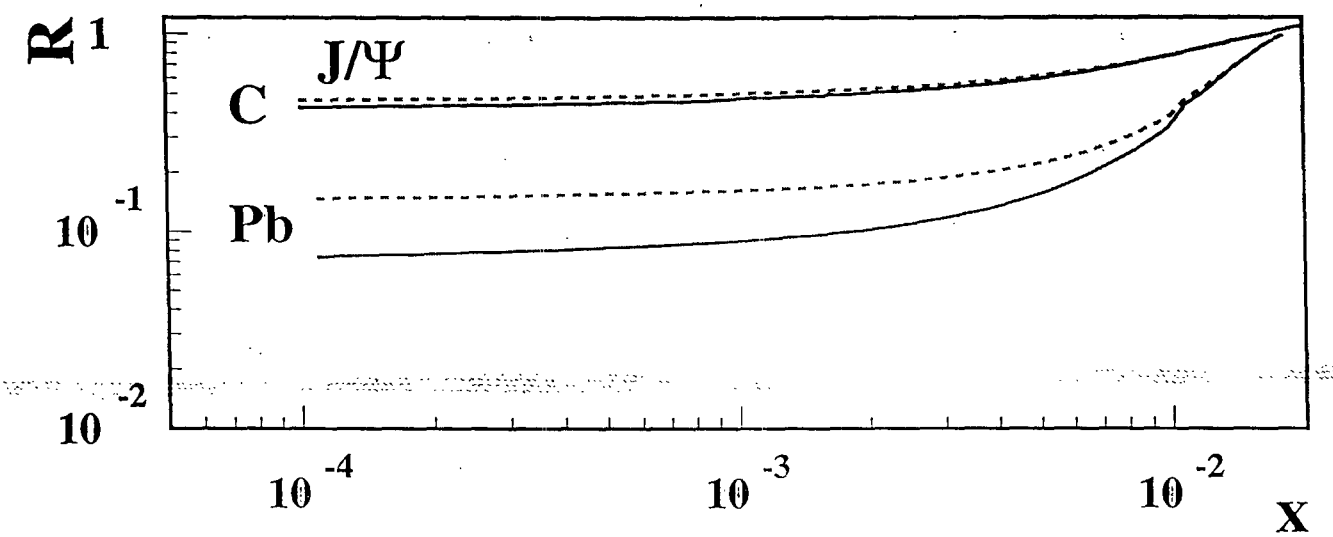

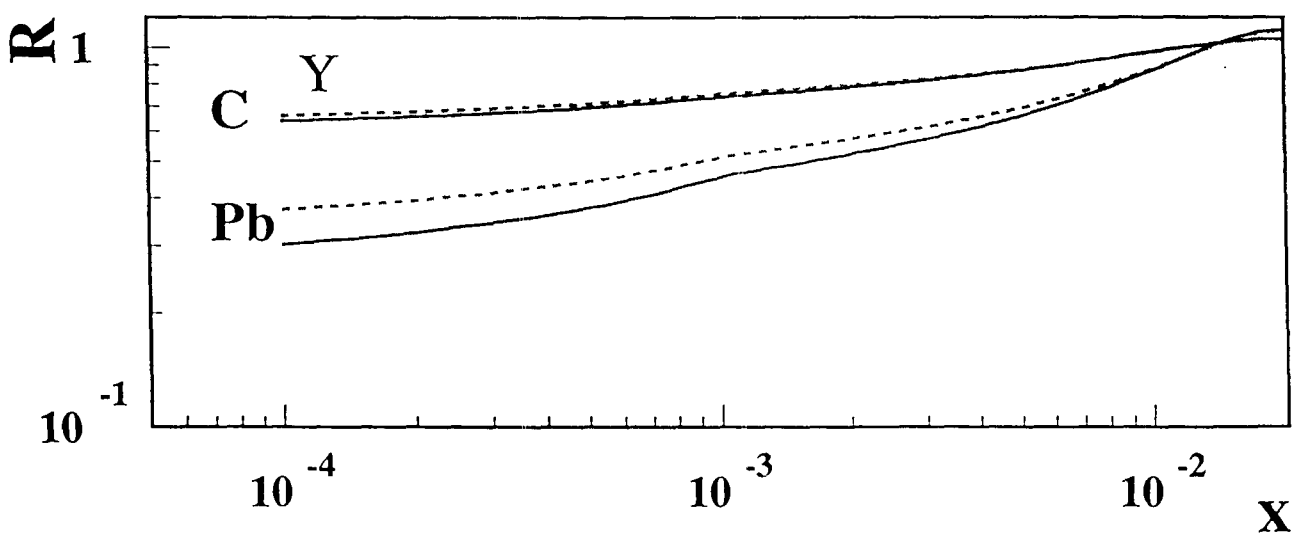

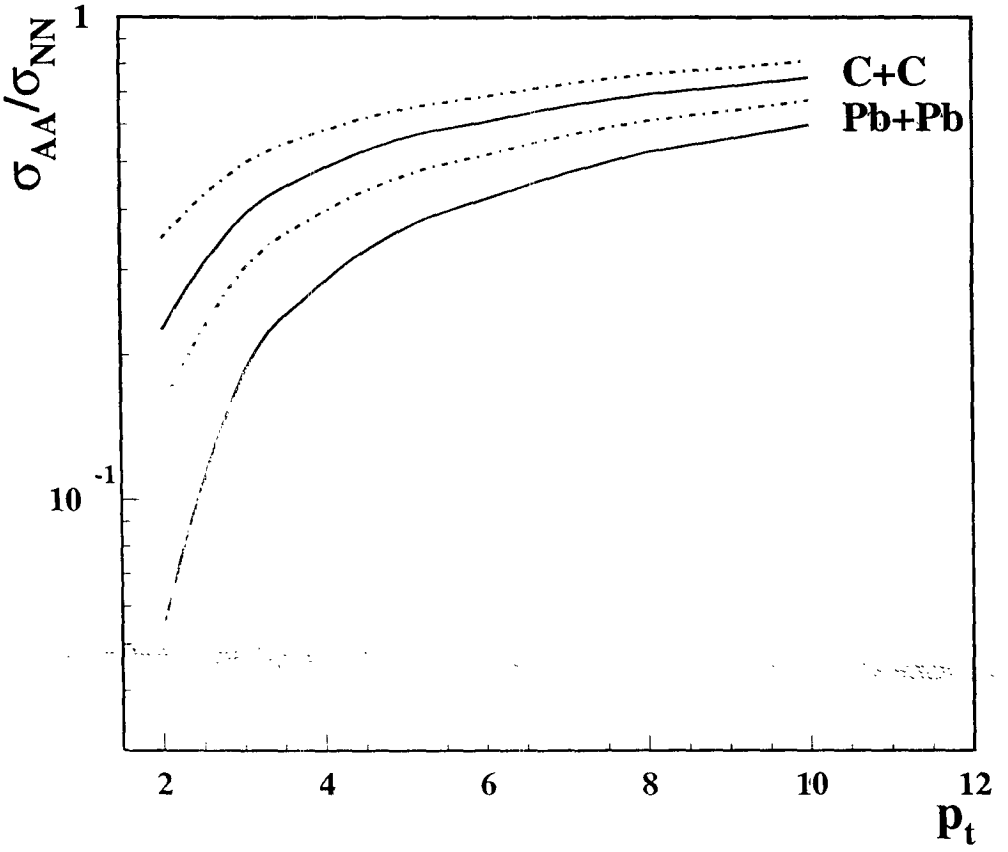

FIG. 5. Suppression of the jet production in $A\,A$ collisions due to gluon shadowing at $y = 0$ calculated in the eikonal and fluctuation models (solid and dashed curves).

Summary.

1. The formulae for nuclear shadowing for gluon distributions have been deduced within the limit of small nucleon density or in black body limit

2. HERA, FNAL data clearly demonstrate existence of soft and hard diffractive phenomena in DIS with the properties predicted by applications of factorization theorems in QCD

3. Use of HERA data on diffractive processes leads to the prediction of large shadowing of gluon distributions, significantly larger than quark distributions. Significant reduction of yields of minijets, heavy quarks ... at AA collisions at LHC

4. Higher twist effects are evaluated

5. New Color Coherent Phenomena in AA collisions are discussed.

Nuclear Shadowing of Gluon Distribution function at RHIC and LHC

Jamal Jalilian-Marian (LBNL)

Using a new evolution equation which takes high gluon density into effect, we investigate the gluon distribution function and show there is a significant depletion for large nuclei.

Effective Action and RGE

$$S = -\frac{1}{4}\int d^4x\, G^2 + i\int d^2x_\perp\, F(\rho(x_\perp))$$

$$+\frac{i}{N_c}\int d^2x_\perp dx^-\, \delta(x^-)\, \mathrm{tr}\,\rho\, W(A)$$

Integrate out high x gluons

$F(\rho)$ changes with x

$$\frac{d}{dy} Z = \alpha_s\left[\frac{1}{2}\frac{\delta^2}{\delta\rho\delta\rho}\chi Z - \frac{\delta}{\delta\rho}\sigma Z\right]$$

$$Z = e^{-F}$$

Weak field $\longrightarrow$ BFKL, DLL DGLAP
GLR

Double Log region

$$\frac{\partial^2}{\partial y \partial \ln \varphi^2} xG(x,\varphi,b_\perp) \sim \left[1 - \frac{1}{K} e^{\frac{1}{K}} E_1(1/K)\right]$$

$$\sim xG\left[1 - \# \frac{xG}{\varphi^2} + \ldots\right]$$

DGLAP

GLR/MQ

$$K \sim \frac{xG(x,\varphi,b_\perp)}{\varphi^2}$$

$$E_1(z) \equiv e^{-z} \int_0^\infty dt \; \frac{e^{-zt}}{1+t}$$

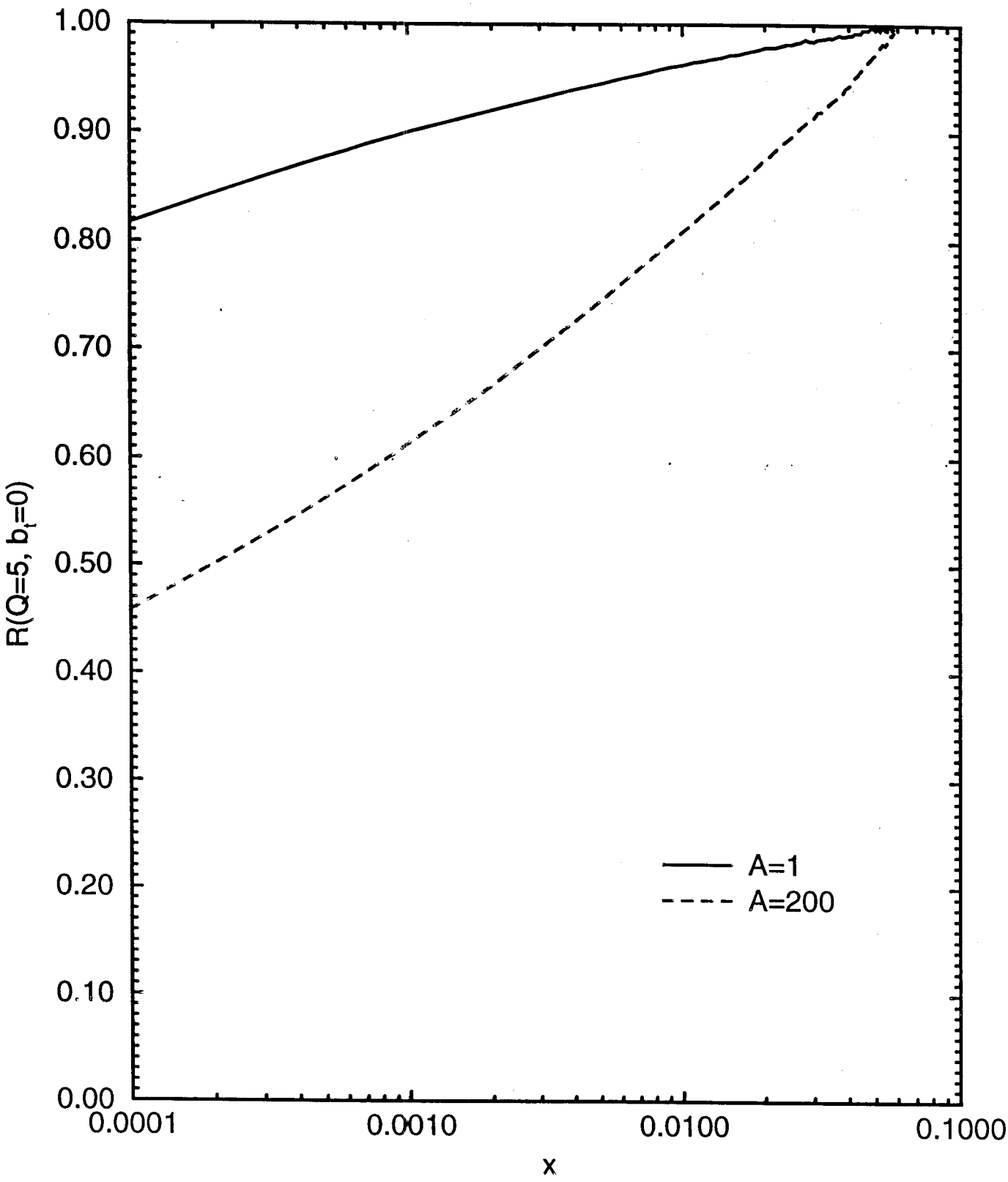
1.00
0.90
0.80
0.70
0.60
0.50
0.40
0.30
0.20
0.10
0.00
R(Q=5, b_t=0)
0.0001
0.0010
0.0100
0.1000
x
A=1
A=200

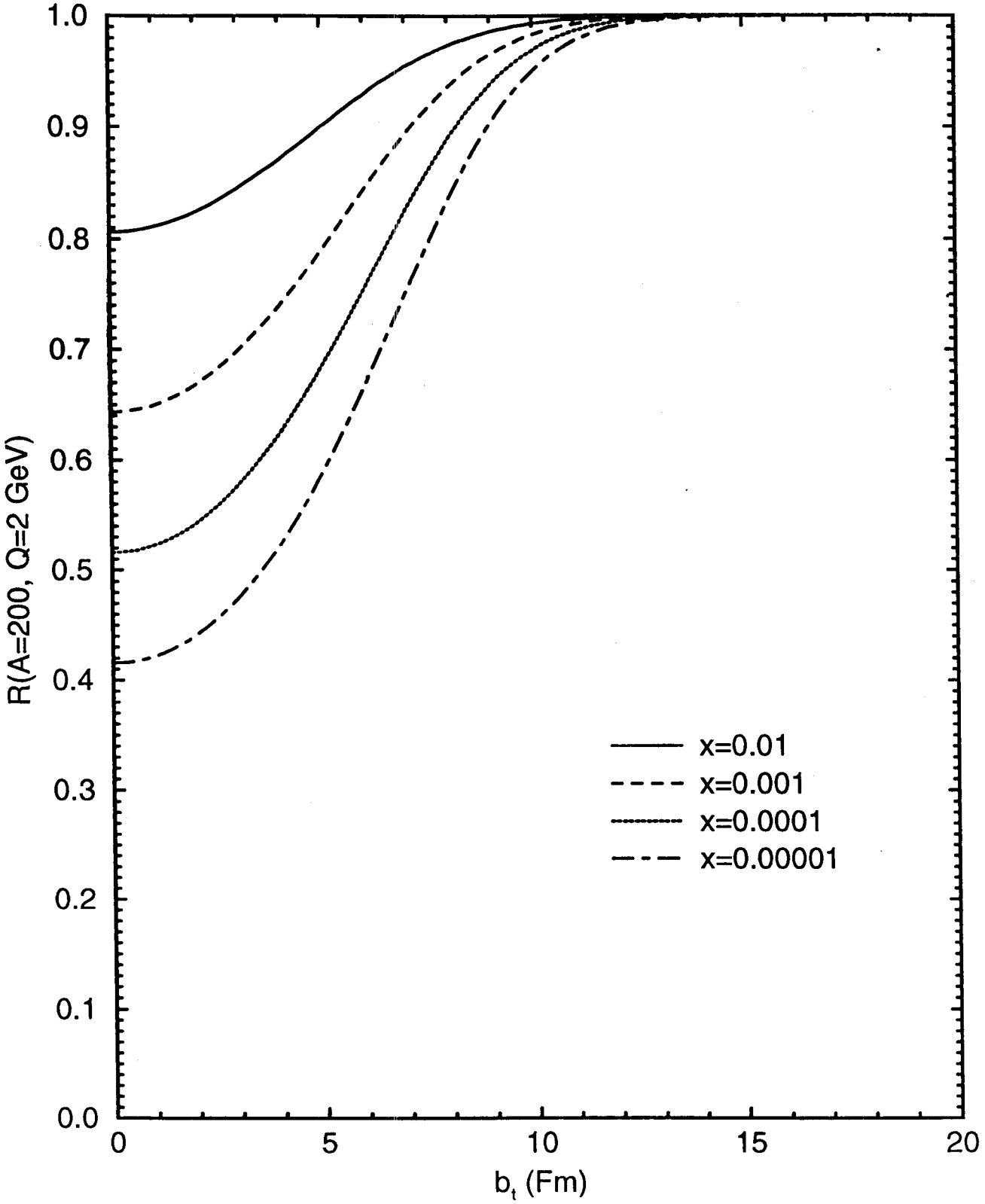
1.0
0.9
0.8
0.7
0.6
0.5
0.4
0.3
0.2
0.1
0.0
R(A=200, Q=2 GeV)
0
5
10
15
20
b_t (Fm)
x=0.01
x=0.001
x=0.0001
x=0.00001

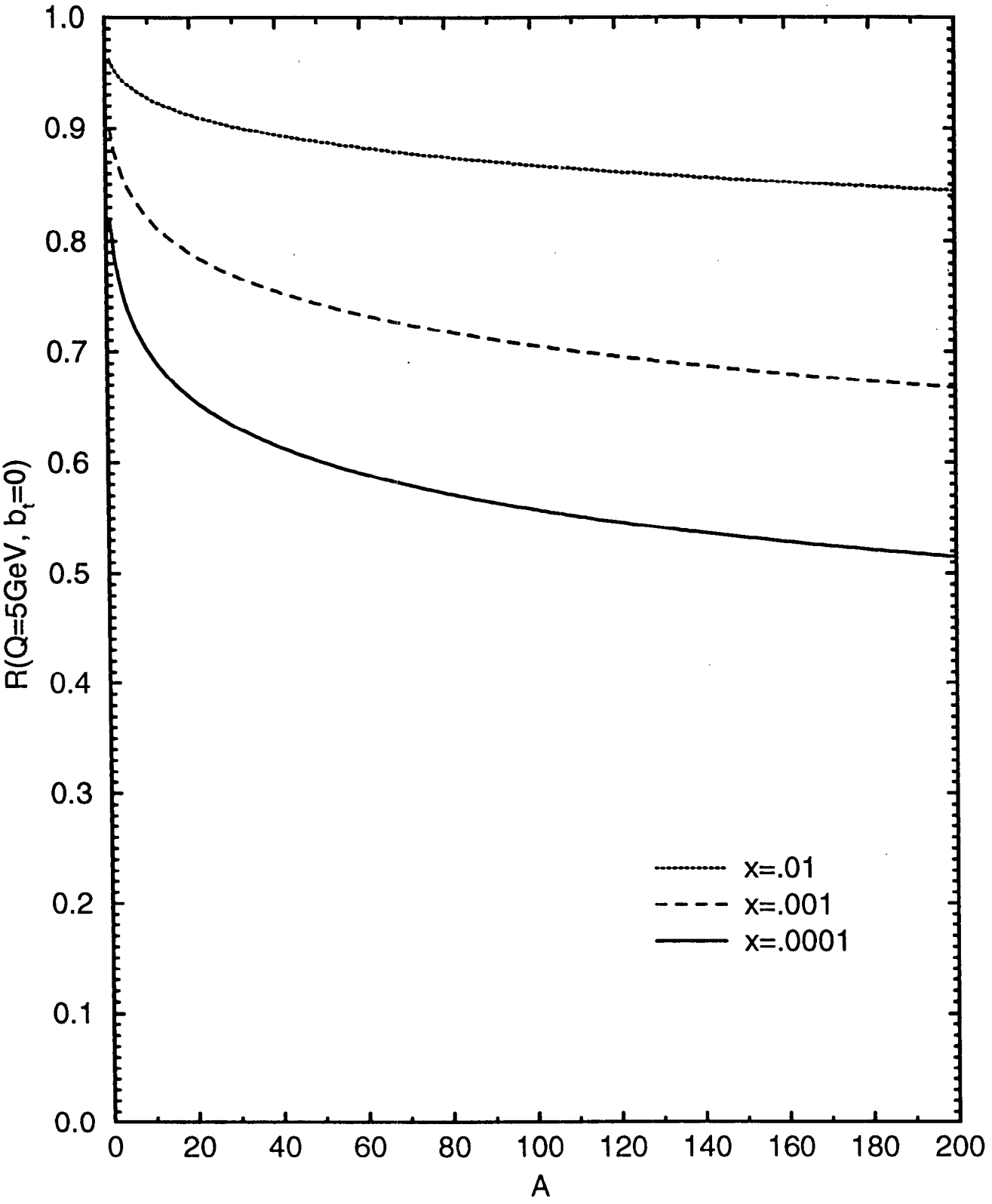
1.0
0.9
0.8
0.7
0.6
0.5
0.4
0.3
0.2
0.1
0.0
R(Q=5GeV, b_t=0)
0
20
40
60
80
100
120
140
160
180
200
A
x=.01
x=.001
x=.0001

Hard scattering in polarized pp collisions at RHIC

W. Vogelsang
Institute for Theoretical Physics, SUNY Stony Brook, NY-11794

We present next-to-leading order QCD corrections to jet and prompt photon production in polarized hadronic collisions. Phenomenological predictions are made for such experiments in $\vec{p}\vec{p}$ at RHIC, analyzing in detail the sensitivity of the spin asymmetries to the spin-dependent gluon density Δg. For prompt photons, an isolation criterion suggested by S. Frixione (Phys. Lett. B429 (1998) 369) is considered, that avoids the need for a fragmentation component in the cross section. Particular attention is paid to uncertainties in the theoretical predictions due to scale dependence.

For further details of the work presented here, see:
D. de Florian, S. Frixione, A. Signer, W. Vogelsang, Next-to-leading order jet cross sections in polarized hadronic collisions, Nucl. Phys. **B539** (1999) 455;
S. Frixione, G. Ridolfi, W. Vogelsang, in preparation.

NEED INDEPENDENT,

MORE DIRECT, INFORM.

ON Δg !

PICK PROCESSES WHICH

- HAVE GLUONIC CONTRIE
  ALREADY AT LO

- HAVE BEEN USEFUL
  IN UNPOLARIZED CASE
  IN PARTICULAR, FOR RHIC

E.G. $pp \to \gamma(+\text{jet})\,X$

$pp \to \text{jet(s)}\,X$

$\mu = \mu_0 \equiv p_T^\gamma$

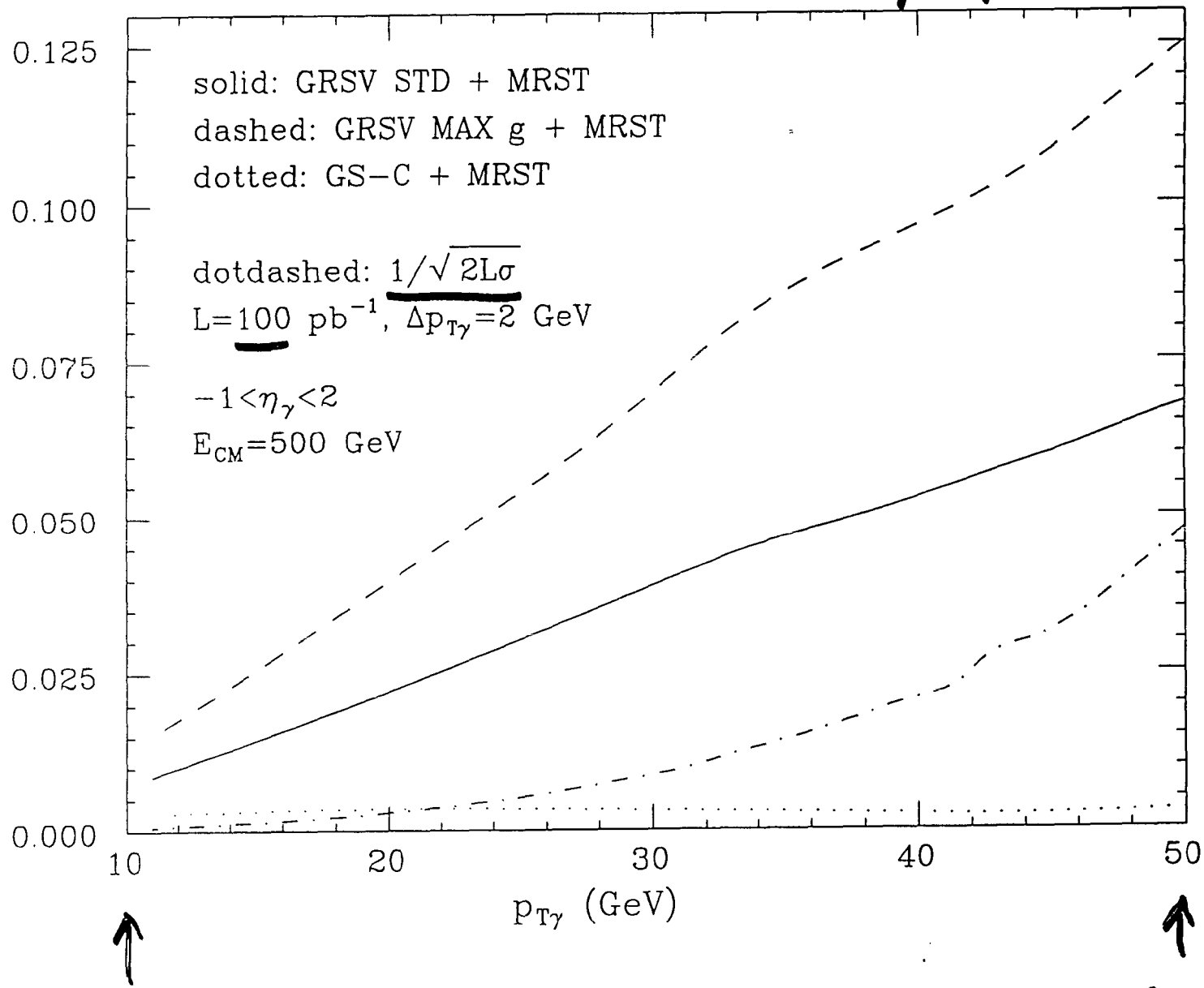

$x_T = 0.04$

$x_T = 0.2$

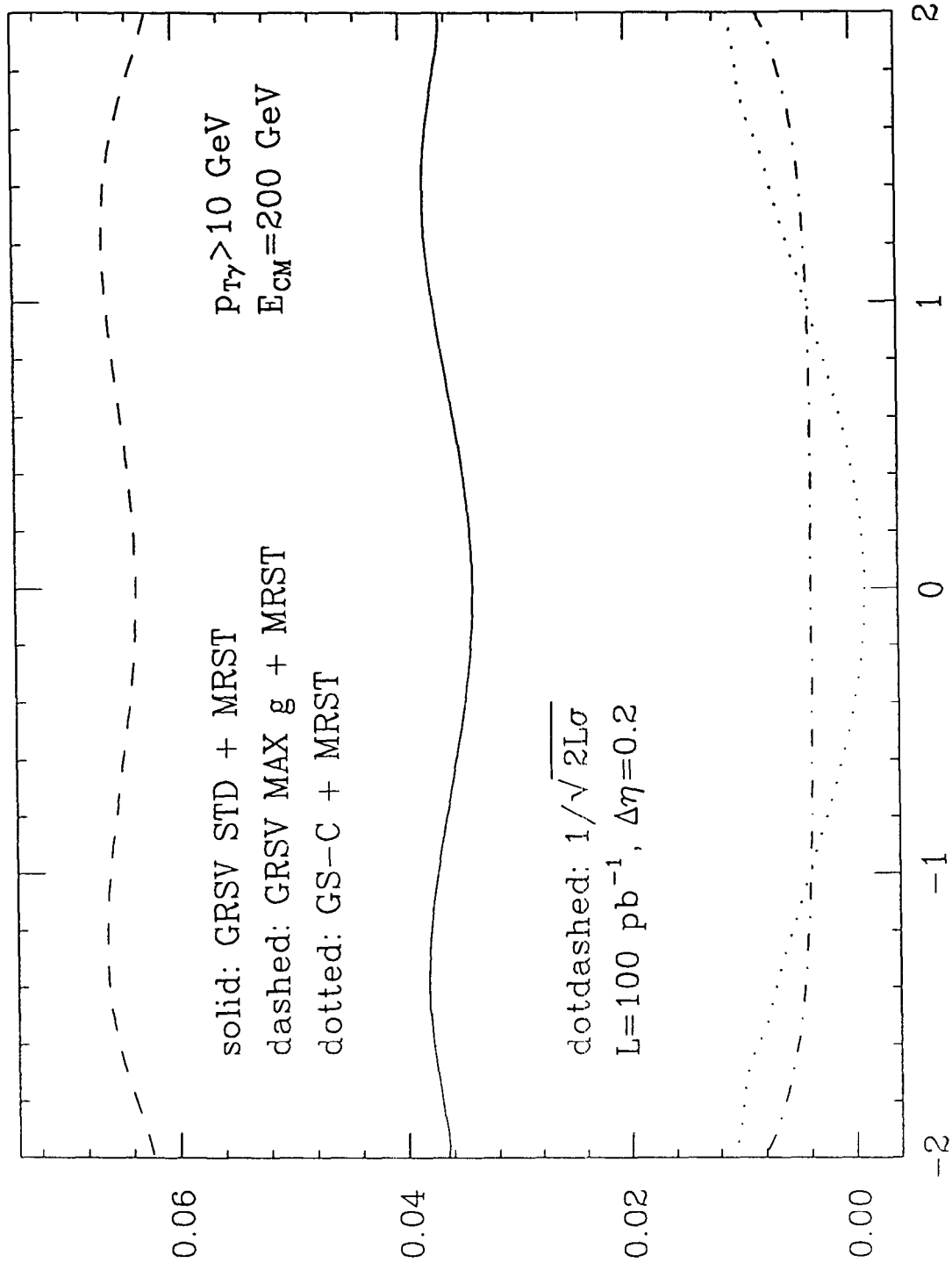
$A = \Delta\sigma/\sigma$
0.06
0.04
0.02
0.00
−2
−1
0
1
2
η_γ
$p_{T\gamma}$>10 GeV
E_{CM}=200 GeV
solid: GRSV STD + MRST
dashed: GRSV MAX g + MRST
dotted: GS−C + MRST
dotdashed: $1/\sqrt{2L\sigma}$
L=100 pb^{-1}, $\Delta\eta$=0.2

JETS:

SCALE DEPENDENCE MORE RELEVANT THAN K-FACTOR!

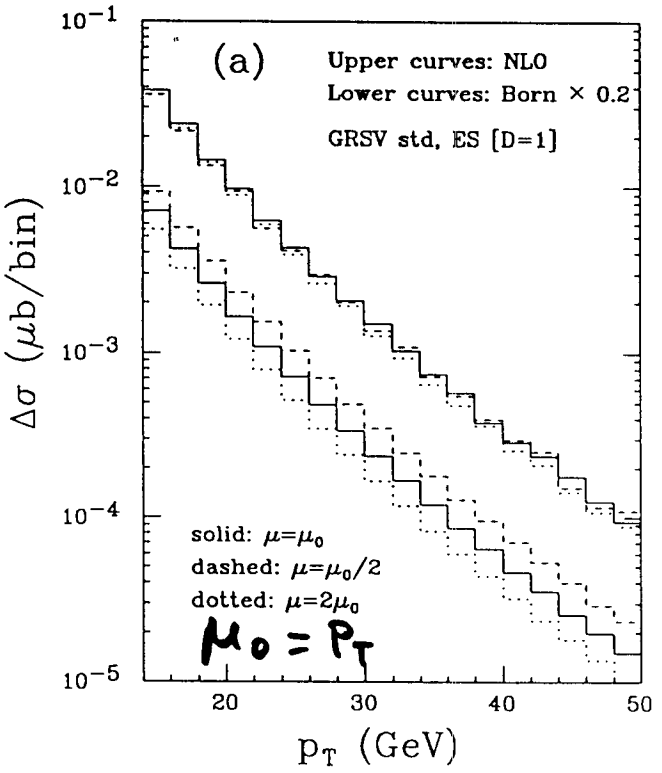

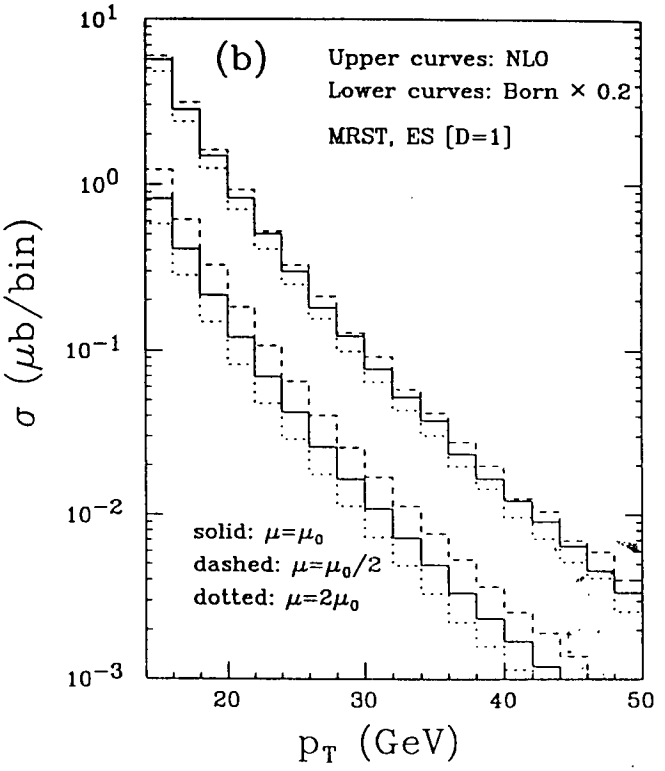

STRONG REDUCTION AT NLO!

FINALLY, ASYMMETRIES:

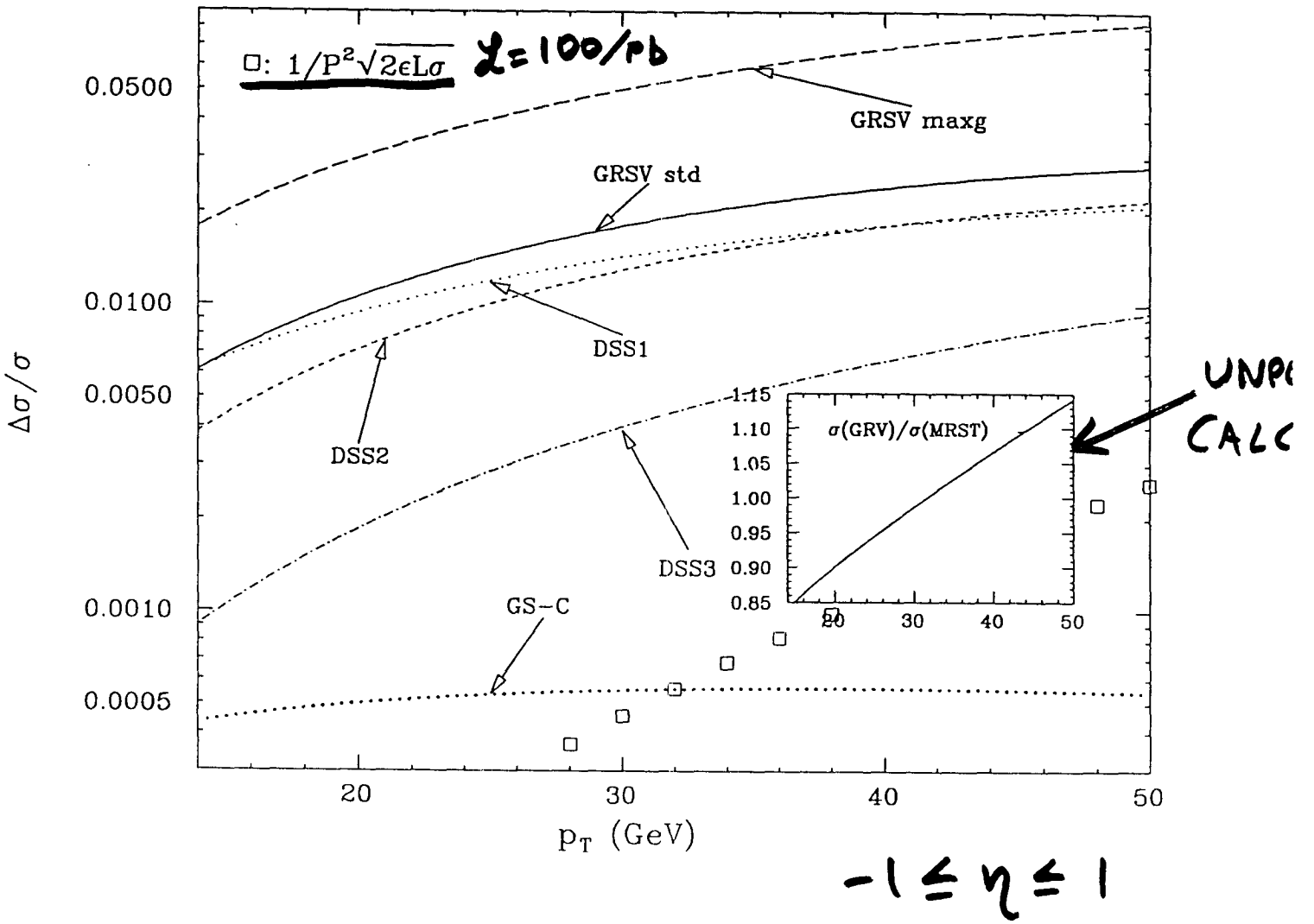

UNPO
CALC

$-1 \leq \eta \leq 1$

Photons in polarized pp collision at PHENIX

Yuji Goto, *RIKEN*

Why do we perform photon physics at PHENIX ? Because one important feature of the PHENIX detector is its high performance EM calorimeter in the central arm. The PHENIX EM calorimeter (EMCal) consists of lead scintillator calorimeters (PbSc) and lead glass calorimeters (PbGl). It covers rapidity region $-0.35 < \eta < 0.35$ and 180° azimuthal angle (PbSc 135° + PbGl 45°). The most important point is its fine granularity about 0.01 radian per tower in both rapidity and azimuthal direction. It gives us good $\pi^0 \rightarrow 2\gamma$ identification up to about 25GeV/c.

What can we do at PHENIX with photons ? We have photons directly produced (direct photon) and photons from π^0 decays. To study the direct photon, photons from π^0 decays are backgrounds. We have good π^0 background reduction capability by the fine granularity of the EMCal. From another viewpoint, it means we have good identification capability of π^0. The π^0 itself is an important probe which is alternative to jet in the small acceptance.

By using these probes, we will study spin physics. Main issue is the spin structure of the proton. Polarized deep inelastic scattering experiments provide precise measurements of the quark polarization in the proton. But it explains about 30% of the proton spin. In the polarized hadron collision, we can directly measure the gluon polarization. For the direct photon production, gluon Compton process is a dominant process. We have clear interpretation of the production mechanism of the direct photon. That's why we can directly probe the gluon structure of the proton, and the gluon polarization, ΔG, in the proton when we perform asymmetry measurement in the polarized hadron collision.

The measurement of the direct photon is experimentally challenging, because we have many background photons from mainly two-photon decay of copious π^0's. We have some methods to distinguish the backgrounds. One is invariant mass reconstruction to identify π^0, and another is isolation cut method. The Monte Carlo simulation study using PYTHIA event generator shows accessible p_T range of the direct photon measurement at PHENIX is 10GeV/c < p_T <30GeV/c for $\sqrt{s}$ =200GeV and 10GeV/c < p_T <40GeV/c for $\sqrt{s}$ =500GeV. Estimation of the asymmetry measurement was also done using polarized parton distribution functions by Soffer–Virey and Gehmann–Stirling which have different ΔG. Statistically, we have enough sensitivity to distinguish these models with full luminosity and $\sqrt{s}$ =200GeV by considering year-3 (2001~) measurement.

The π^0 data is interpreted by gluon–gluon, gluon–quark and quark–quark reactions with jet fragmentation. Advantage of this measurement is its high statistics and clear particle identification of π^0 by detecting two photons. We can perform the measurement in year-2 (2000~). On the other hand, there are uncertainties in the jet fragmentation process and the fraction of contributing processes. The Monte Carlo simulation shows we can compare the asymmetry of the π^0 production between above models and distinguish them well statistically in year-2 with 10% luminosity and $\sqrt{s}$ =200GeV.

Next, we have to understand our results as a parton reaction. Using PYTHIA, we can estimate Bjorken's x value of the gluon in the direct photon production corresponding to its p_T region. But, the result of relation between direct photon p_T and gluon x is very different from naive formula, $x = 2p_T/\sqrt{s}$. We need to know why.

Simulation study - π^0

- Asymmetry measurement
  - year-2 (2000-)
  - sqrt(s)=200GeV, $32pb^{-1}$
  - A_{LL} of inclusive π^0
  - A_{LL} of parton
  - fragmentation - p_T vs z
    - z - splitting fraction of π^0

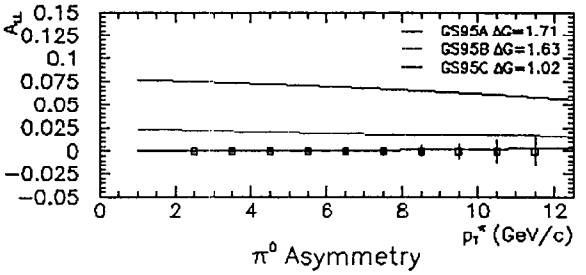

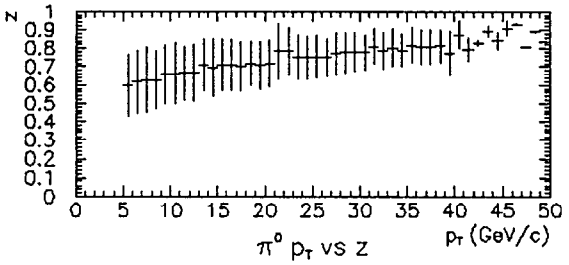

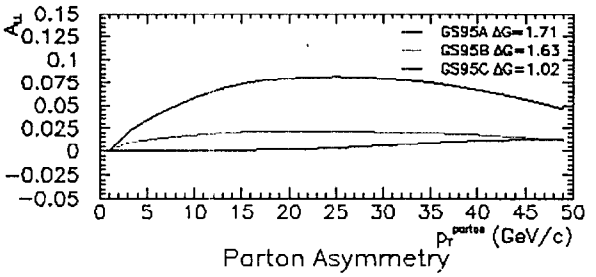

Parton kinematics

- Uncertainies in x estimation
  - PYTHIA prompt photon
  - p_T vs gluon's x
    - naiive formula
      - $x_T=2p_T/\mathrm{sqrt}(s)$
    - evaluation with simulation

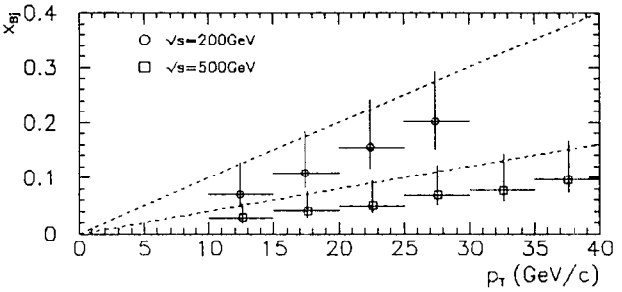

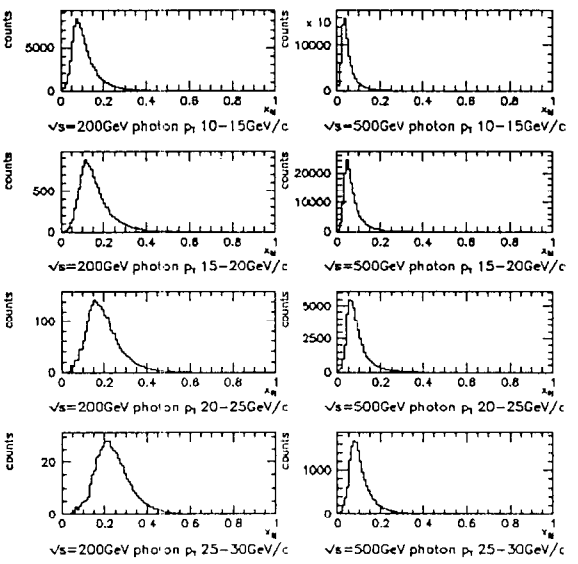

Simulation study - Prompt photon

- Background photon
  - 2γ decay of π^0
    - 1γ escape from detector
    - 2γ merge into 1 cluster
  - other decays
- Background reduction
  - Mass reconstruction
  - Isolation cut
    - R=0.7, fraction=5%
- Accessible p_T range
  - 10GeV/c< p_T<30GeV/c for sqrt(s)=200GeV
  - 10GeV/c< p_T<40GeV/c for sqrt(s)=500GeV

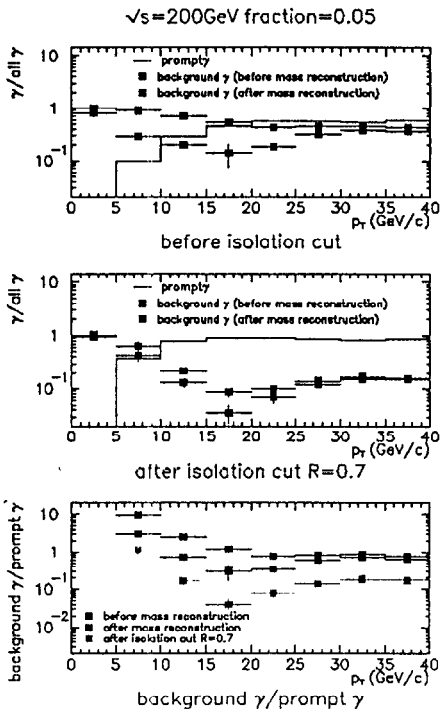

Simulation study - Prompt photon

- Asymmetry measurement
  - year-3 (2001-)
  - sqrt(s)=200GeV, 320pb^{-1}
  - polarized PDF
    - Soffer-Virey
    - GS95
      - (A) ΔG=1.71
      - (B) ΔG=1.63
      - (C) ΔG=1.02

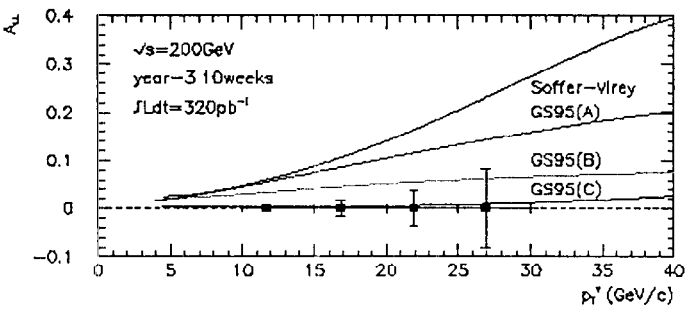

What at PHENIX ?

- Photon
  - good background reduction
- π^0
  - alternative to jet in the small acceptance
- Photon+π^0, π^0+π^0
  - ???
- Spin physics
  - spin structure of the proton
  - polarized DIS experiments - quark polarization - $\Delta\Sigma$=0.3
  - polarized hadron collision - gluon polarization - ΔG =?
    - direct measurement
- Parton kinematics
  - uncertainties in the data interpretation
  - study for QCD reaction itself

Spin physics - Prompt photon

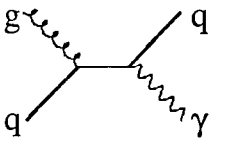

- Gluon Compton process dominant
  - clear interpretation
  - ΔG - gluon polarization measurement in the polarized proton collision
- Asymmetry measurement

$$A_{LL} = \frac{d\sigma^{++} - d\sigma^{+-}}{d\sigma^{++} + d\sigma^{+-}} \Longleftrightarrow A_{LL} = \frac{\Delta G}{G} \cdot A_1^{\,p} \cdot a_{LL}(\, gq \rightarrow \gamma q\,)$$

- Experimentally challenging
  - measure background - 2γ decay of π^0
  - background subtraction
    - mass reconstruction
    - isolation cut

$$A_1^p(x) = \frac{g_1^p(x)}{F_1^p(x)} = \frac{\sum_i e_i^2 \cdot \Delta q_i(x)}{\sum_i e_i^2 \cdot q_i(x)}$$

$$i = u, \bar{u}, d, \bar{d}, s, \bar{s}, \ldots$$

Spin physics - π^0

- gg, gq and qq reactions and jet production
- A_{LL} measurement
  - polarized parton distribution function - ΔG
  - a_{LL} of parton reaction
  - jet - fragmentation function
- Advantage
  - high statistics - 1st-year physics
  - clear particle-ID
- Uncertainties
  - fragmentation function
  - contributing processes - gg + gq + qq

Simulation study

- Simulation study
  - PYTHIA5.7/JETSET7.4
  - PDFLIB GRV94LO
  - prompt photon prodution and QCD jet production for π^0
  - luminosity (full luminosity for 1 year)
    - $320pb^{-1}$ for sqrt(s)=200GeV
    - $800pb^{-1}$ for sqrt(s)=500GeV

Prompt photon yield

	$\sqrt{s}$ = 200GeV			$\sqrt{s}$ = 500GeV		
Photon p_T	Yield	Errors on A_{LL}	Errors on $\Delta G/G$	Yield	Errors on A_{LL}	Errors on $\Delta G/G$
10 – 15 GeV/c	1.0×10^{5}	0.0062	0.046	9.0×10^{5}	0.0022	0.045
15 – 20 GeV/c	1.3×10^{4}	0.0168	0.089	1.8×10^{5}	0.0059	0.059
20 – 25 GeV/c	2.7×10^{3}	0.0376	0.171	5.3×10^{4}	0.0081	0.081
25 – 30 GeV/c	5.9×10^{2}	0.0799	0.309	1.9×10^{4}	0.0115	0.115
30 – 35 GeV/c				7.7×10^{3}	0.0141	0.141
35 – 40 GeV/c				3.3×10^{3}	0.0198	0.198

π^0 yield

π^0 p_T	$\sqrt{s}$ = 200GeV	
	Yield	δA_{LL}
2 – 3 GeV/c	3.3×10^{8}	1.1×10^{-4}
3 – 4 GeV/c	4.3×10^{7}	3.1×10^{-4}
4 – 5 GeV/c	8.8×10^{6}	6.9×10^{-4}
5 – 6 GeV/c	2.3×10^{6}	1.3×10^{-3}
6 – 7 GeV/c	7.4×10^{5}	2.4×10^{-3}
7 – 8 GeV/c	3.5×10^{5}	3.4×10^{-3}
8 – 9 GeV/c	1.3×10^{5}	5.6×10^{-3}
9 – 10 GeV/c	6.8×10^{4}	7.8×10^{-3}
10 – 11 GeV/c	3.1×10^{4}	1.2×10^{-2}
11 – 12 GeV/c	2.1×10^{4}	1.4×10^{-2}

A Direct Extraction of ΔG with STAR

J. Sowinski*
for
The STAR Collaboration

In addition to high energy heavy ion beams RHIC will provide polarized protons colliding at high center of mass energies, up to 500 GeV, for the first time. At these energies hard partonic scattering, where perturbative QCD applies, becomes an important mechanism thus enabling a range of physics studies involving spin. An important part of this program is the spin structure of the nucleon.

Since the "Spin Crisis" was first declared a little more than 10 years ago there have been many more deep inelastic scattering measurements of the quark spin contribution to the nucleon. However the picture has not changed: only about one third of the spin of a nucleon appears to come from the quarks. Ongoing experiments have been investigating the flavor dependence and contributions from sea quarks but one very important component has yet to be measured, the spin carried by the gluons represented by ΔG. However, QCD scaling laws couple the quark and gluon contributions so that they are completely correlated. In fact the statement that quarks account for only about one third of the nucleon spin assumes that $\Delta G=0$. Thus the next important step in understanding the structure of the nucleon is to determine ΔG.

The spin content of the gluons in the proton can be studied at RHIC by viewing the proton as an incoherent collection of partons. The spin dependence of hard parton-parton scattering is understood from perturbative QCD and thus provides a system where the spin of the partons can be measured. In particular the process $q + g \rightarrow \gamma + q$ seems to have many advantages. It is readily identified as a photon-jet coincidence in a near 4π detector such as STAR. The reaction mechanism is expected to be clean and the only competing process has a much smaller cross section in the kinematics of interest. Moreover the polarization of the quarks is large at momentum fraction $x \geq 0.2$ and determined in previous measurements. Thus the polarization of the struck nucleons can be extracted from measured spin dependent asymmetries, the pQCD determined spin dependence and the known quark polarizations.

Star will be able to directly extract $\Delta G(x)$ from the kinematics of the detected photon and jet. Assuming that the partons are co-linear the energy and angle of the photon and the angle of the jet are sufficient to extract the initial momentum fractions of the quark and gluon, x_q and x_g, and the center of mass scattering angle. One must also assume that the larger measured x is associated with the quark, thus allowing the use of previously measured quark polarization distributions and pQCD calculations of the fundamental spin asymmetries. Simulations have been carried out with Pythia and they demonstrate that STAR with an endcap electromagnetic calorimeter can measure $\Delta G(x)$ for $0.01 \leq x \leq 0.3$ with sufficient precision that the integral for $0 \leq x \leq 1$ is determined to $\leq \pm 0.5$. This requires 10 week runs at each of two energies, 200 GeV and 500 GeV. The above assumptions are found to require only small corrections to the integral from simulations. It is expected that these measurements will begin shortly after the endcap calorimeter is installed in 2002.

*The author greatfully acknowledges the help of his IUCF collaborators L.C. Bland, W.W. Jacobs, E.J. Stephenson, S.E. Vigdor and S.W. Wissink in preparing the materials for this talk. Research supported in part by NSF award 9602872.

Nucleon Spin Structure

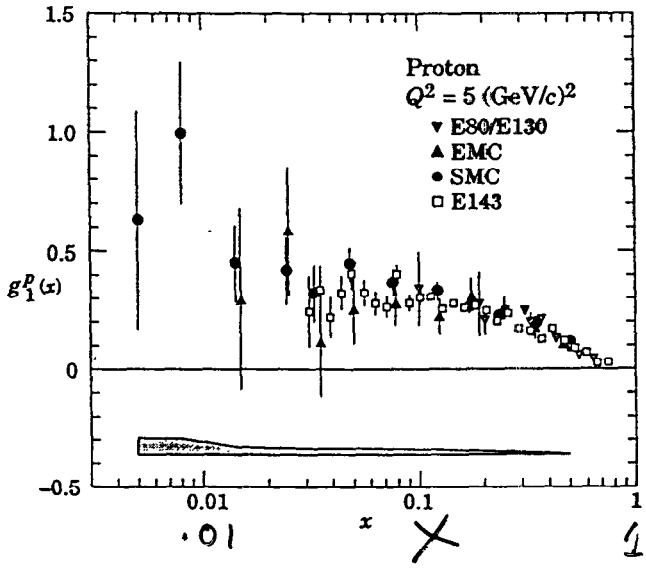

g_1^p

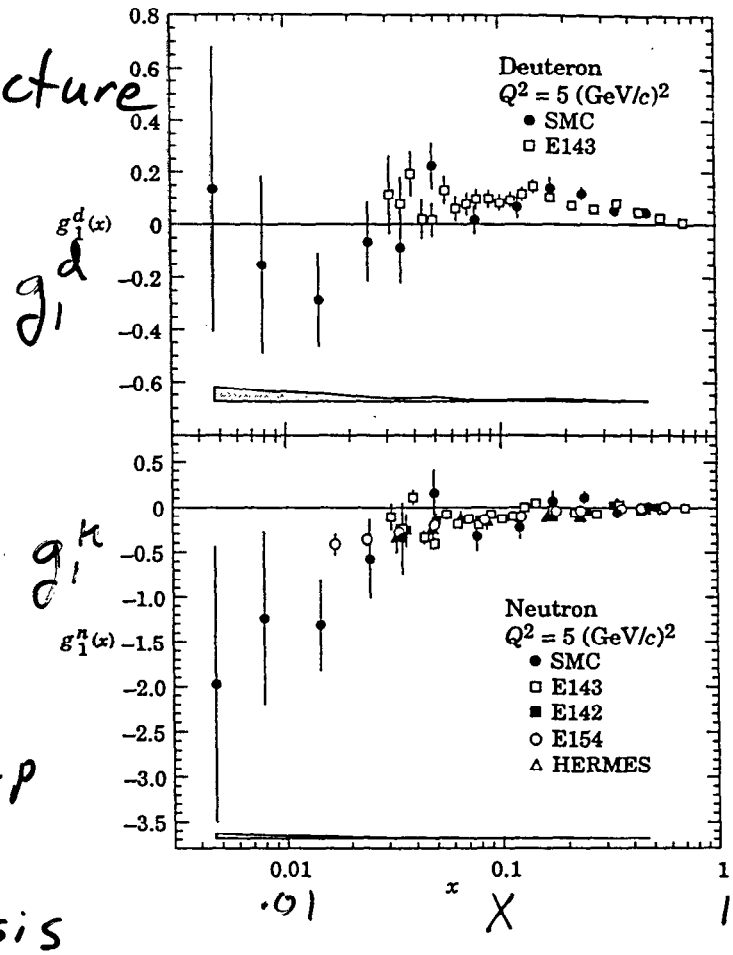

g_1^d g_1^n

Particle Data Group Compilation

Spin Crisis

DIS measure $\frac{g_1}{F_1} \approx \frac{2x\, g_1(x)}{F_2(x)}$

$$g_1(x) = \frac{1}{2}\left\{ \frac{4}{9}\Delta u(x) + \frac{1}{9}\Delta d(x) + \frac{1}{9}\Delta s(x) + \cdots \right\}$$

Integral $\Rightarrow$ quarks account for only small part of the spin of a nucleon

Future exp.

$$\frac{1}{2} = \frac{1}{2}\Delta\Sigma + \Delta G + L_z + L_G$$

$\Delta\Sigma$: Δq, $\Delta\bar{s}$, $\Delta\bar{u}$, Δu, $\Delta\bar{d}$, Δd

Partonic Collisions at a $\vec{p}$ - $\vec{p}$ Collider

1) High c.m. energy $\sqrt{s}$ + hard collisions ($p_T \gtrsim 10$ GeV/c $\Rightarrow$ $\Delta r_T \sim \hbar/p_T \lesssim 0.02$ fm) $\Rightarrow$ pQCD validity for individual parton-parton collisions.

2) $\vec{p}$ beam can be viewed as incoherent ensemble of $\vec{q}$, $\vec{\bar{q}}$, $\vec{g}$:

colliding parton luminosity = $f_1(x_1, Q^2)\, f_2(x_2, Q^2)$ • (pp luminosity)

parton polarization = $\dfrac{\Delta f\,(x, Q^2)}{f\,(x, Q^2)}$ • (proton polarization)

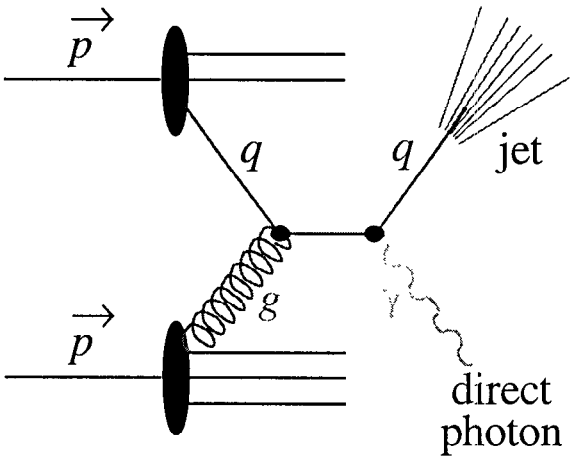

In collider frame, p beams have momentum = $\sqrt{s}/2$; colliding **parton** momenta are then $x_1\sqrt{s}/2$ and $x_2\sqrt{s}/2$

Quark-Gluon Compton scattering

$\vec{p} + \vec{p} \rightarrow \gamma\,(+\,jet) + X$

3) Measure $\vec{p}$ - $\vec{p}$ spin correlation asymmetry with longitudinally polarized protons:

$$P_{b1} P_{b2} A_{LL} = \frac{N_{++} - N_{+-}}{N_{++} + N_{+-}}$$

$P_{b1(2)}$ — beam pol'n (~70%)

N_{++} — equal helicity yield

N_{+-} — opposite helicity yield

4) Interpret A_{LL} via pQCD -- e.g., single LO process $\Rightarrow$

$$A_{LL} = \overbrace{P_{part.\,1} P_{part.\,2}}^{parton\ pol'ns.}\ \hat{a}_{LL} = \overbrace{\frac{\Delta f_1}{f_1}\frac{\Delta f_2}{f_2}}^{pol\ struct\ fncs.}\ \hat{a}_{LL}(\hat{s}, \hat{t}, \hat{u})$$

$\underbrace{\quad}_{unpol\ struct\ fncs.}$

$\hat{a}_{LL}$: pQCD result for specific process

Kinematic Extraction of $\Delta G(x)$

- event-by-event kinematic determination of $x_{1,2}$, θ^* (without reliance on poor resolution p_T(jet)):

$$x_1 = \frac{p_T(\gamma)}{\sqrt{s_{pp}}} \left[\exp(\eta_\gamma) + \exp(\eta_{jet}) \right]$$

$$x_2 = \frac{p_T(\gamma)}{\sqrt{s_{pp}}} \left[\exp(-\eta_\gamma) + \exp(-\eta_{jet}) \right]$$

$$|\cot\theta^*| = \left| \sinh\left(\frac{\eta_{jet} - \eta_\gamma}{2} \right) \right|$$

} neglecting k_T

- $\hat{\sigma}(\theta^*)$, parton distribution functions both favor assignment:

$$x_g = \min\{x_1, x_2\}; \qquad x_q = \max\{x_1, x_2\}$$

$\Rightarrow$ removes ambiguity re sign of $\cot\theta^*$ (preference strongest when $|x_1 - x_2| > 0.1$, $|\cos\theta^*| \gtrsim 0.5$), allows approx. LO direct extraction:

$$\Delta G(x_g) \cong \frac{[N_{++}(x_g) - N_{+-}(x_g)]}{P_{b_1} P_{b_2} \Sigma_{i=1}^{N_{++}+N_{+-}} [A_1^{DIS}(x_{q_i}, Q_i^2)\, \hat{a}_{LL}^{Compton}(\cos\theta_i^*)/G(x_{g_i}, Q_i^2)]}$$

- perform simulations to test effects of neglecting:

$q\bar{q} \to g\gamma$; $x_g \leftrightarrow x_q$ misidentification;
θ^* reconstruction errors; k_T - smearing + g radiation;
eventually, NLO contributions

$\pi^0 + \eta^0$ Background Suppression for $\vec{p} + \vec{p} \rightarrow \gamma + jet + X$ (PYTHIA 5.7 simulations)

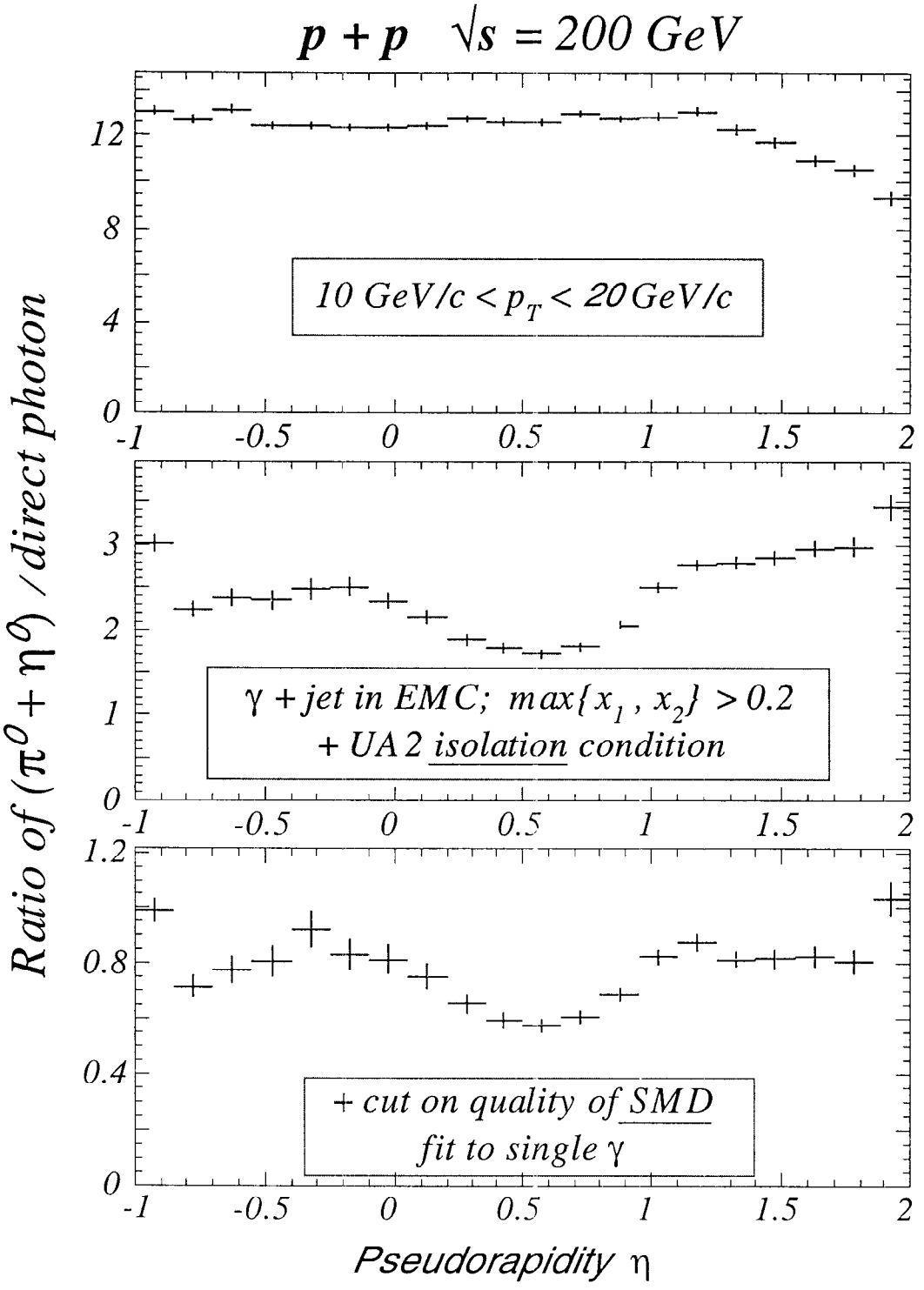

Remaining background to be subtracted by measuring A_{LL} for samples that pass and fail SMD cut

$\Rightarrow$ increased errors on $\Delta G(x)$ by factor 1.5 - 2.0

$\vec{p}\,\vec{p} \rightarrow \gamma + jet + X$ *with STAR + EEMC*

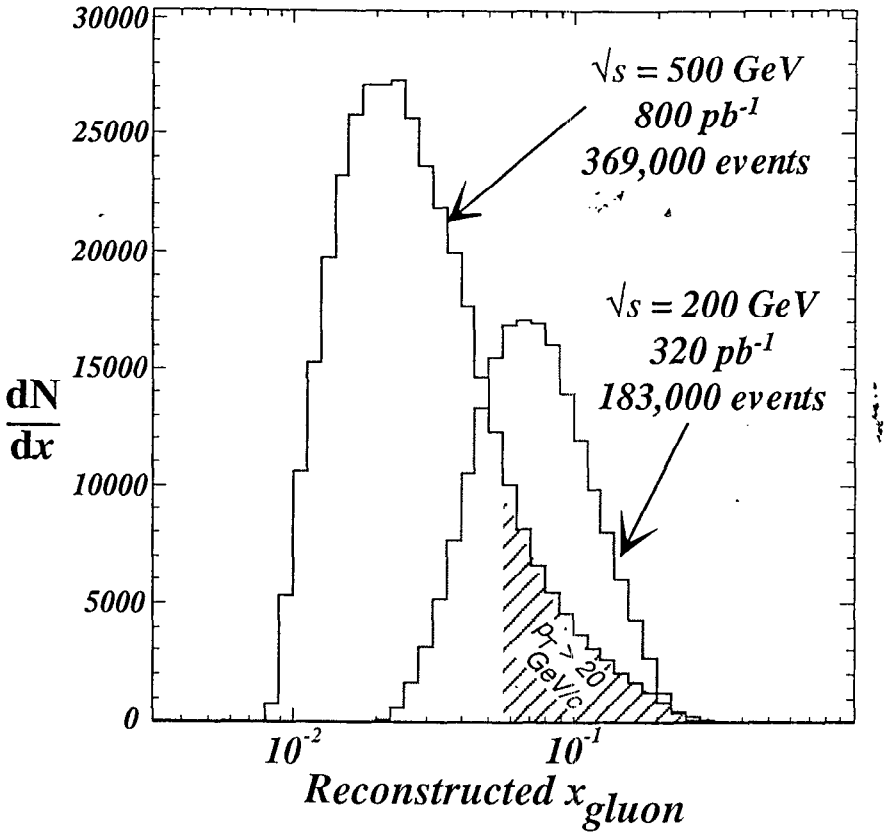

By combining measurements at $\sqrt{s} = 200$ *GeV* and $\sqrt{s} = 500$ *GeV*, STAR γ + jet data will allow a direct determination of $\int \Delta G(x,Q^2)\, dx$ to a precision better than ± 0.5.

Addition of the $\sqrt{s} = 500$ *GeV* results should reduce the $x_g \rightarrow 0$ extrapolation uncertainty by *a factor* ≈ 6.

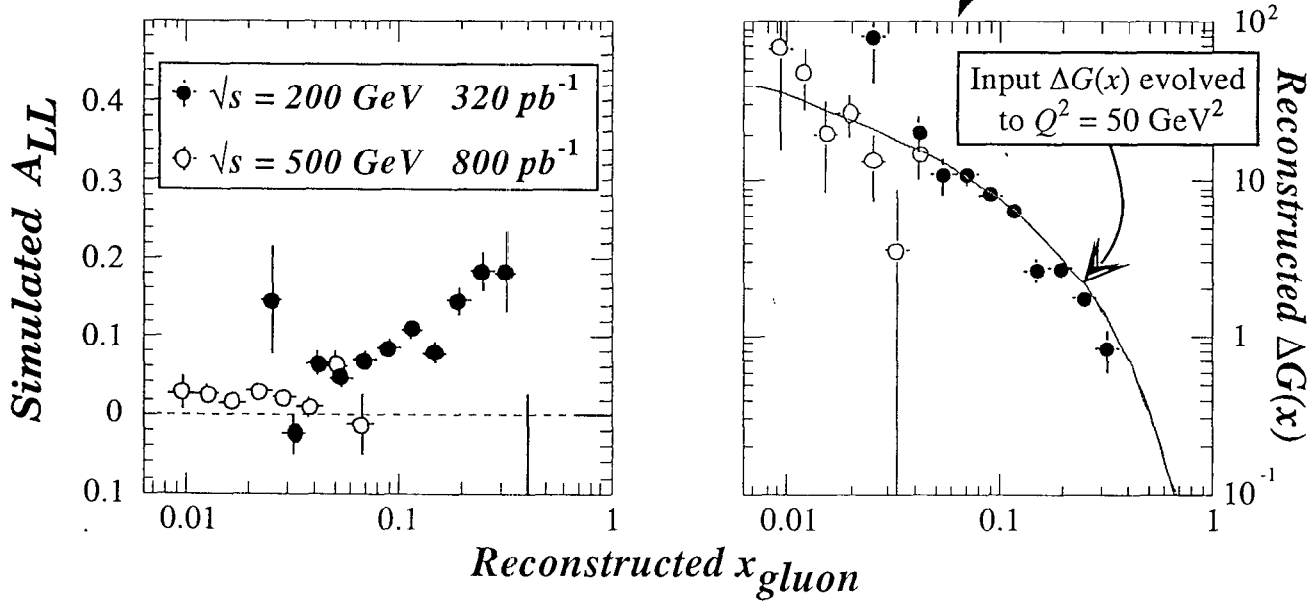

- **Fit uncorrected ΔG(x) reconstructed from 200 + 500 GeV simulations with Gehrmann-Stirling functional form ⇒**

$$\int_0^1 \Delta G_{recon}(x)\, dx = 1.62 \pm 0.23$$

$\rightarrow \approx \pm 0.4$ ***when other syst. errors included***

STUDY OF SPIN-FLAVOR STRUCTURE OF THE NUCLEON WITH PHENIX

NAOHITO SAITO
Radiation Laboratory
The Institute of Physical and Chemical Research (RIKEN)
Hirosawa, Wako, Saitama 351-0198, Japan
and
RIKEN BNL Research Center
Brookhaven National Laboratory
510c Physics Department Upton, NY 11973-5000, USA

The structure of the nucleon has been investigated in lepton scattering from the nucleon target for three decades. However, there remain long-standing problems especially in understanding its spin and flavor structure: namely, what carries the spin of the nucleon, and what fraction of momentum and spin are carried by each flavor?

Production of W in proton-proton collision is very suitable to these studies because W is produced through $V-A$ interaction and the helicity of the initial state quark and anti-quark are fixed, and the flavor contribution is almost fixed, *i.e.* $u\bar{d} \to W^+$, and $d\bar{u} \to W^-$.

The Relativistic Heavy Ion Collider (RHIC) offers very unique opportunity to pursue these studies especially because of its capability to collide polarized proton beams at high energy of 500 GeV at their center-of mass system, high polarization of 70%, and at high luminosity of $2\times10^{32}\mathrm{cm}^{-2}\mathrm{sec}^{-1}$ or more. In addition, the PHENIX detector at RHIC is designed to detect muons at $1.2\leq \eta \leq 2.4$ and electrons at $|\eta| \leq 0.35$ with high momentum/energy resolution and sufficient particle identification.

We can expect about 5,000 signals with PHENIX Muon Arms for each of W^+ and W^- with integrated luminosity of 800 pb^{-1}, which corresponds to 10 weeks with 70% efficiency at the designed luminosity. The estimated statistical errors of 2% for both $\mathcal{A}_L^{W^+}$ and $\mathcal{A}_L^{W^-}$ are precise enough to select one of models on the polarized parton distributions. Furthermore using the decay angular distribution we can estimate the x values carried by the quark and anti-quark so that we can extract x-dependence of the polarized and unpolarized parton distributions from our measurements. Such measurements will contribute much to understand the spin-flavor structure of the nucleon.

Spin Structure of the Nucleon

- Studied with Deep Inelastic Scattering of polarized lepton from polarized nucleon (pol-DIS) → proton spin crisis

$\Delta\Sigma = 0.3$ Δs=-0.10

- Pol-DIS
  - well-defined kinematics
  - sensitive to only e_q^2
    - analysis assume flavor SU(3)

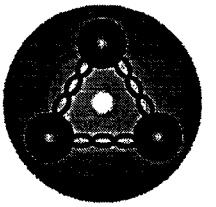

Quark Spin: $\underline{\Delta\Sigma}$
valence quark: $\Delta u_v, \Delta d_v$
sea quark: $\Delta\bar{u}, \Delta\bar{d}, \Delta\bar{s}$
Quark Orbital Motion: $\underline{L_q}$
Gluon Spin: $\underline{\Delta G}$
Gluon Orbital Motion: $\underline{L_g}$

Naohito Saito, RIKEN / RIKEN BNL Research Center

Flavor Structure of the Nucleon

- Charge Symmetry is a good symmetry to describe hadron properties:(u in p and d in n are different?? : C. Boros, J.T. Londergan, A. Thomas:PRL 81 (1998) 4075)
- It is not trivial to assume: $\bar{d} / \bar{u} = 1$

FNAL-E866 results
PRL 80 (1998) 3715

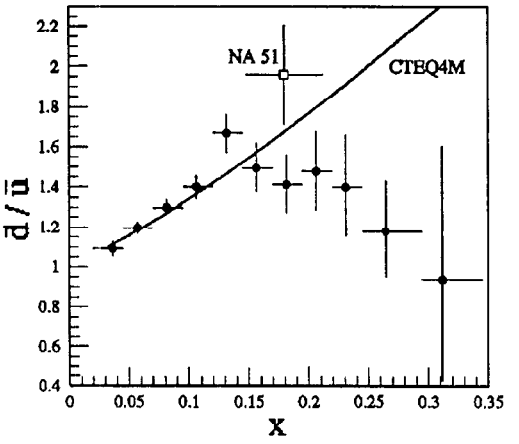

Naohito Saito, RIKEN / RIKEN BNL Research Center

W Production in Polarized pp Collisions

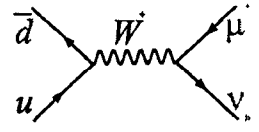

- W is produced through V-A process
  - helicity is fixed →ideal for spin structure studies
- W couples to weak charge ~ flavor
  - flavor is almost fixed →ideal for flavor structure studies
- Parity violating asymmetry in W production

A_L:cross section asymmetry

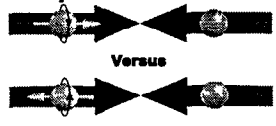

$$A_L^{W^+} = \frac{\Delta u(x_a, M_W^2)\bar{d}(x_b, M_W^2) - \Delta\bar{d}(x_a, M_W^2)u(x_b, M_W^2)}{u(x_a, M_W^2)\bar{d}(x_b, M_W^2) + \bar{d}(x_a, M_W^2)u(x_b, M_W^2)}$$

Naohito Saito, RIKEN / RIKEN BNL Research Center

W yield with 800 pb^{-1}

PYTHIA w/ GRV94LO checked against CDF data

	W^-	W^+
acceptance for muon w/ $p_T > 20$ GeV/c	14%	4%
yield (both muon arms)	5100	5600
ΔA_L (statistical only)	2%	2%
rapidity average	0.78±0.34	0.71±0.41
background from Z-decay	1095(21.5%)	984(17.6%)

Changes with choice of PDF by 20-30%

Acceptance difference between W^- and W^+

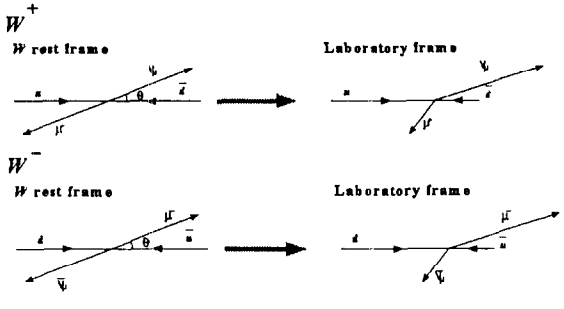

Naohito Saito, RIKEN / RIKEN BNL Research Center

Prediction and Projected Error

- C. Bourrely, J. Soffer Published in Nucl.Phys.B445:341-379,1995

Prediction for the parity violating asymmetry A_L as a function of y^W

solid line: soft gluon
dashed line: hard gluon

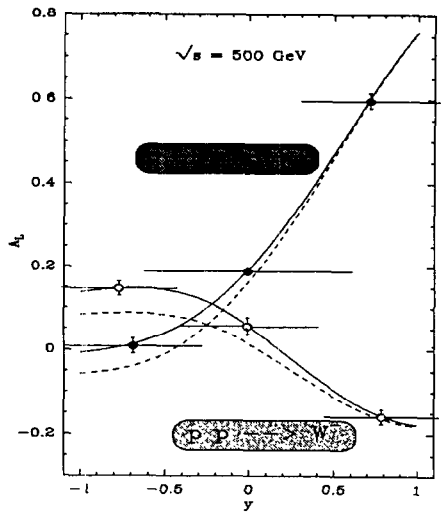

Flavor of Sea Quark in the Proton

- Ratio of Cross Sections for $W+/W-$ production is sensitive to: $\bar{d}/\bar{u}$

$$R_W = \frac{\sigma(W-)}{\sigma(W+)}$$

B . Kamal : PRD 57 (1997) 6663

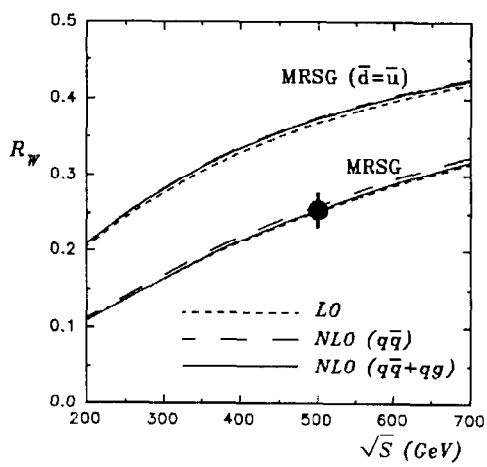

Parton Level Kinematics

- Decay ν cannot be detected: x-determination hard
- but good correlation x vs E^{μ}: V-A requires $(1+\cos\theta)^2$

$$p_{\mu} = \frac{\sqrt{s}}{4}\left[(1+\cos\theta)x_u + (1-\cos\theta)x_{\bar{d}}\right] M_W = \sqrt{x_u x_{\bar{d}} s}$$

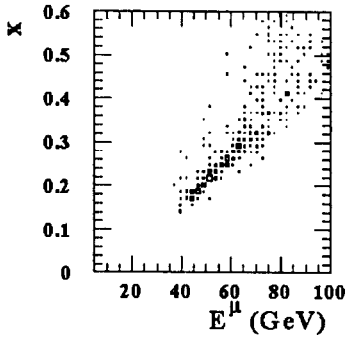

p^{μ} region	x-average W^+
$34 < p^{\mu} < 50$ GeV/c	0.22±0.08
$50 < p^{\mu} < 60$ GeV/c	0.27±0.08
$60 < p^{\mu} < 70$ GeV/c	0.33±0.09
$70 < p^{\mu} < 80$ GeV/c	0.44±0.11
$80 < p^{\mu} < 95$ GeV/c	0.49±0.10
$95 < p^{\mu} < 120$ GeV/c	0.56±0.11

Naohito Saito, RIKEN / RIKEN BNL Research Center

Sensitivity Goal - statistical limit

- Anti-quark polarization measured with A_L^W
- More systematic studies are underway
  - background from π/K decays
  - background from Z^0 decays

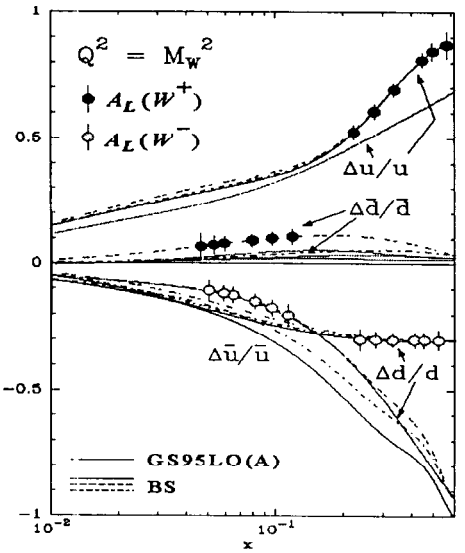

Naohito Saito, RIKEN / RIKEN BNL Research Center

Constraints on Unpolarized PDF

- Ratio of Cross Sections for W-/W+

$$R^W(x_1,x_2)=\frac{\sigma^{W-}(x_1,x_2)}{\sigma^{W+}(x_1,x_2)}$$
$$=\frac{d(x_1)\overline{u}(x_2)+(2\leftrightarrow 1)}{u(x_1)\overline{d}(x_2)+(2\leftrightarrow 1)}$$

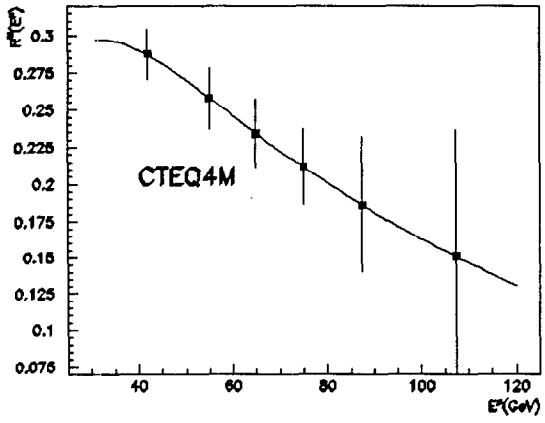

Summary

- RHIC Spin project provides unique opportunity to investigate spin-flavor structure of the nucleon
- Spin Structure Studies
  - $\Delta\overline{q}(x)$ measurement: 2% error for $A_L{}^W$
  - flavor decomposition is possible thru $A_L{}^W$
  - unpolarized PDF can be constrained with R^W
  - further systematic studies are underway...
- RHIC Physics Run will start November, 1999!

Polarization Studies with W's in STAR

OGAWA, Akio for the STAR Collaboration
Pennsylvania State University / Brookhaven National Laboratory
Upton, NY, 11973-5000, U.S.A

The question of how the spin degrees of freedom in the nucleon are organized has still not been fully answered even after recent polarized deep inelastic scattering experiments.

The Relativistic Heavy Ion Collider(RHIC) will accelerate polarized proton beams. The STAR detector, although originally designed for heavy ion physics, has excellent capability for spin physics as well.

STAR will be able to measure the parity violating single spin asymmetry A_L in $\overrightarrow{p}p \rightarrow W^{\pm} + X \rightarrow e^{\pm} + \nu + X$ processes which are sensitive to quark/anti-quark polarization in the nucleon. A big advantage of using $W^{\pm}$ production process is that qurak flavor can be separated. Especially at high η region, where we planning to install Endcap EMC, we will have very clean measurement of d and $\overline{u}$ quark polarizations in the case of W^{-}. A monte Carlo studies using PYTHIA and SPHINX has been done. It shows we will have about 80k and 20k W^{+} and W^{-} at $\sqrt{s} = 500$GeV, $800/pb$. The asymmetries which is calculated using models of polarized parton distributions functions are large(5 to 50%). Our measurement will give much more accurate information about sea quark polarization compare to the one from polarized DIS experiment. Backgrounds from high p_T hadrons, Z^0 and heavy quark decay had been studied and found to be very small. x_{bj} ranges of quarks we will measure are from 0.05 to 0.6. The measured energy of election has a good correlation with x_{bj} of quarks, especially at Endcap EMC region($1 < \eta < 2$) and we will be able to measure x_{bj} dependence of quark polarizations.

$W^{\pm}$ measurement

$$\overrightarrow{p}p \quad \rightarrow \quad W^{\pm} + X \quad \rightarrow \quad e^{\pm} + \nu + X$$

Single spin parity violating asymmetry

$$A_L^{PV} = \frac{N\overrightarrow{p}_p - N\overleftarrow{p}_p}{N\overrightarrow{p}_p + N\overleftarrow{p}_p}$$

Beam "a" polarized $\rightarrow \quad x_a >> x_b$

$$A_L(W^+) = \frac{\Delta u(x_a)\overline{d}(x_b) - \Delta\overline{d}(x_a)u(x_b)}{u(x_a)\overline{d}(x_b) + \overline{d}(x_a)u(x_b)} \quad \rightarrow \frac{\Delta u(x_a)}{u(x_a)}$$

$$A_L(W^-) = \frac{\Delta d(x_a)\overline{u}(x_b) - \Delta\overline{u}(x_a)d(x_b)}{d(x_a)\overline{u}(x_b) + \overline{u}(x_a)d(x_b)} \quad \rightarrow \frac{\Delta d(x_a)}{d(x_a)}$$

Beam "b" polarized

$$A_L(W^+) = \frac{u(x_a)\Delta\overline{d}(x_b) - \overline{d}(x_a)\Delta u(x_b)}{u(x_a)\overline{d}(x_b) + \overline{d}(x_a)u(x_b)} \quad \rightarrow \frac{\Delta\overline{d}(x_a)}{d(x_a)} + \frac{\overline{d}(x_a)\Delta u(x_b)}{u(x_a)\overline{d}(x_b)}$$

$$A_L(W^-) = \frac{d(x_a)\Delta\overline{u}(x_b) - \overline{u}(x_a)\Delta d(x_b)}{d(x_a)\overline{u}(x_b) + \overline{u}(x_a)d(x_b)} \quad \rightarrow \frac{\Delta\overline{u}(x_a)}{u(x_a)} + \frac{\overline{u}(x_a)\Delta d(x_b)}{d(x_a)\overline{u}(x_b)}$$

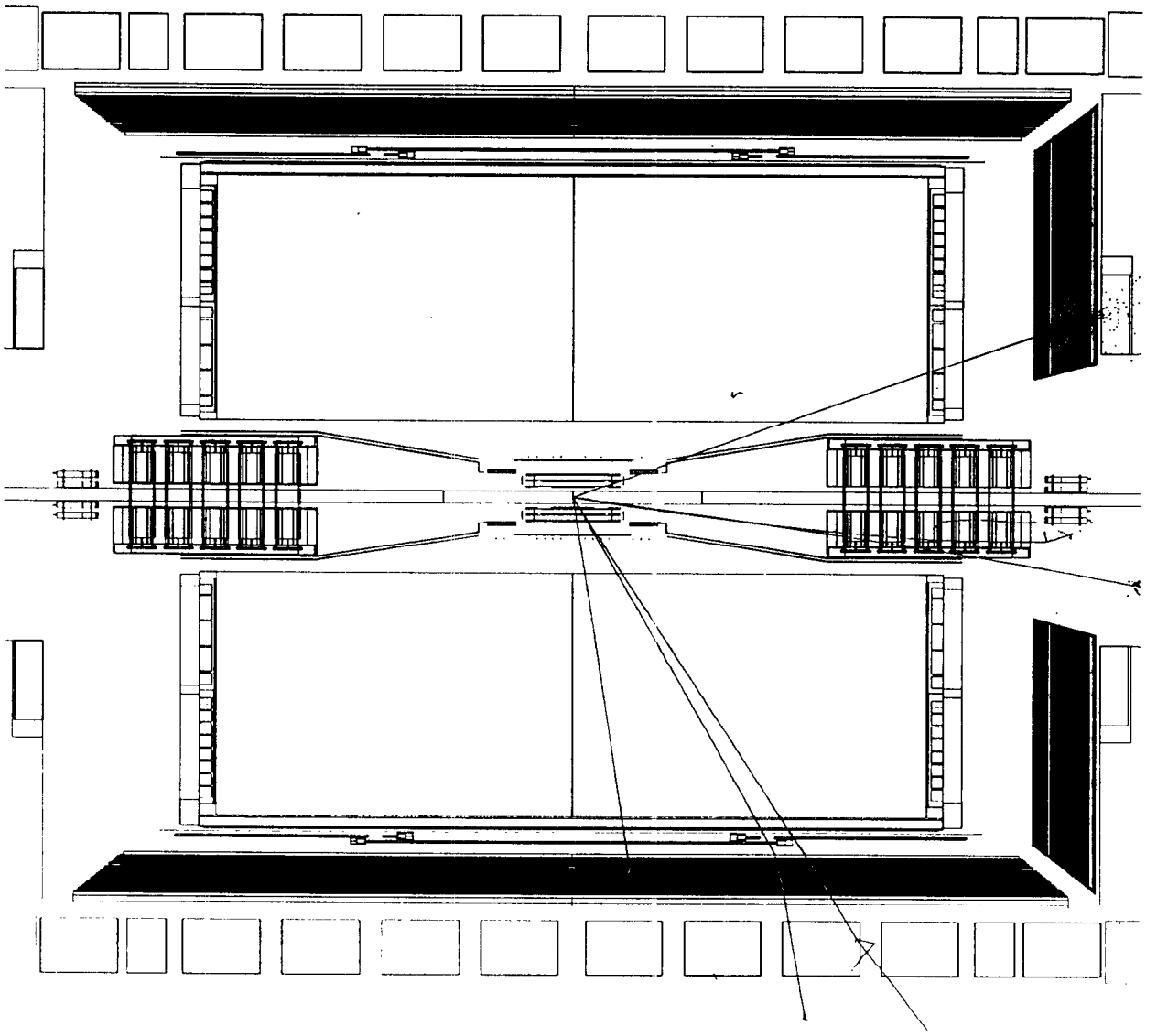

Electron Asymmetry for W^-

$\sqrt{s} = 500GeV$ 800/pb P_b=0.7

Unpol. beam $\rightarrow$ $\leftarrow$ Polarized beam

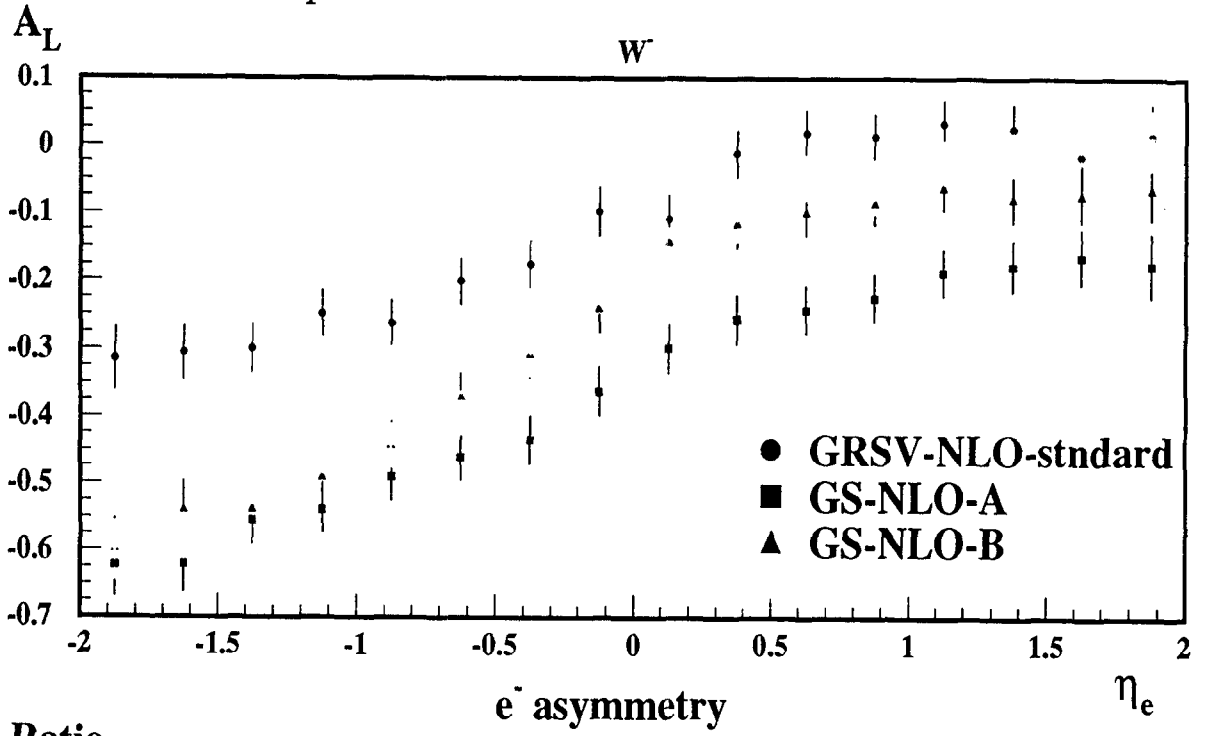

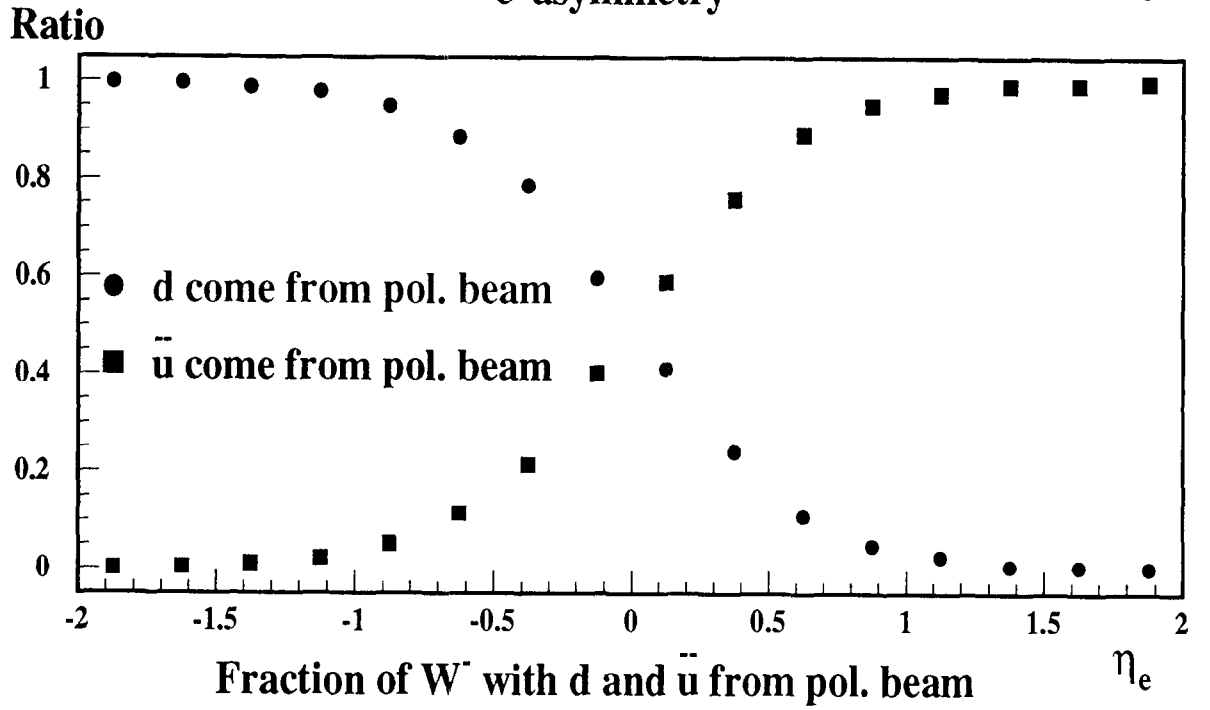

e^- emitted preferentially along W^- momentum
Looking at high η at Endcap gives clean measurement

Background

- High P_T jets

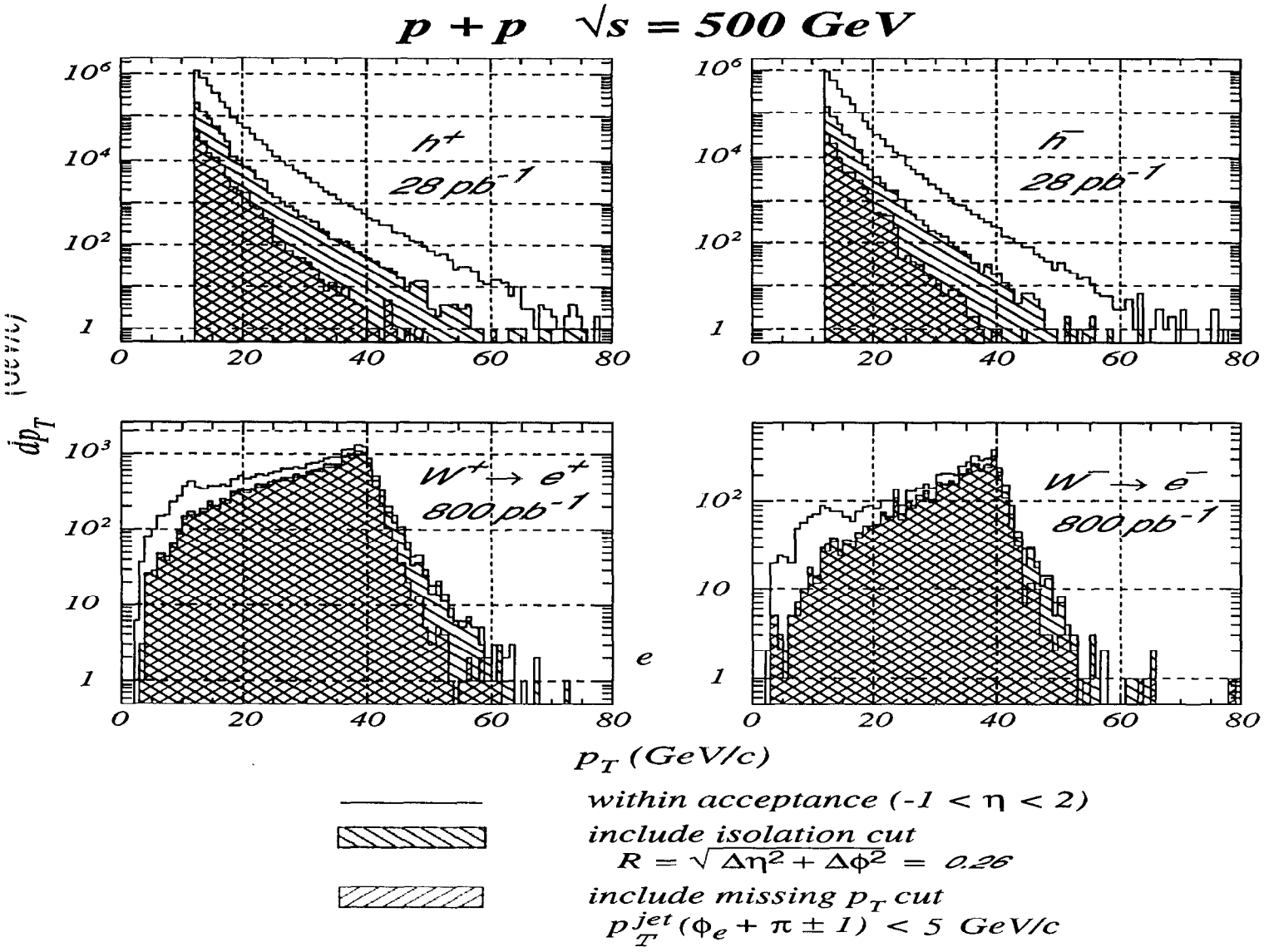

- Z^0 decay and one missing electron
- $b - quark$ decay and one missing electron

x_{bj} range of quarks

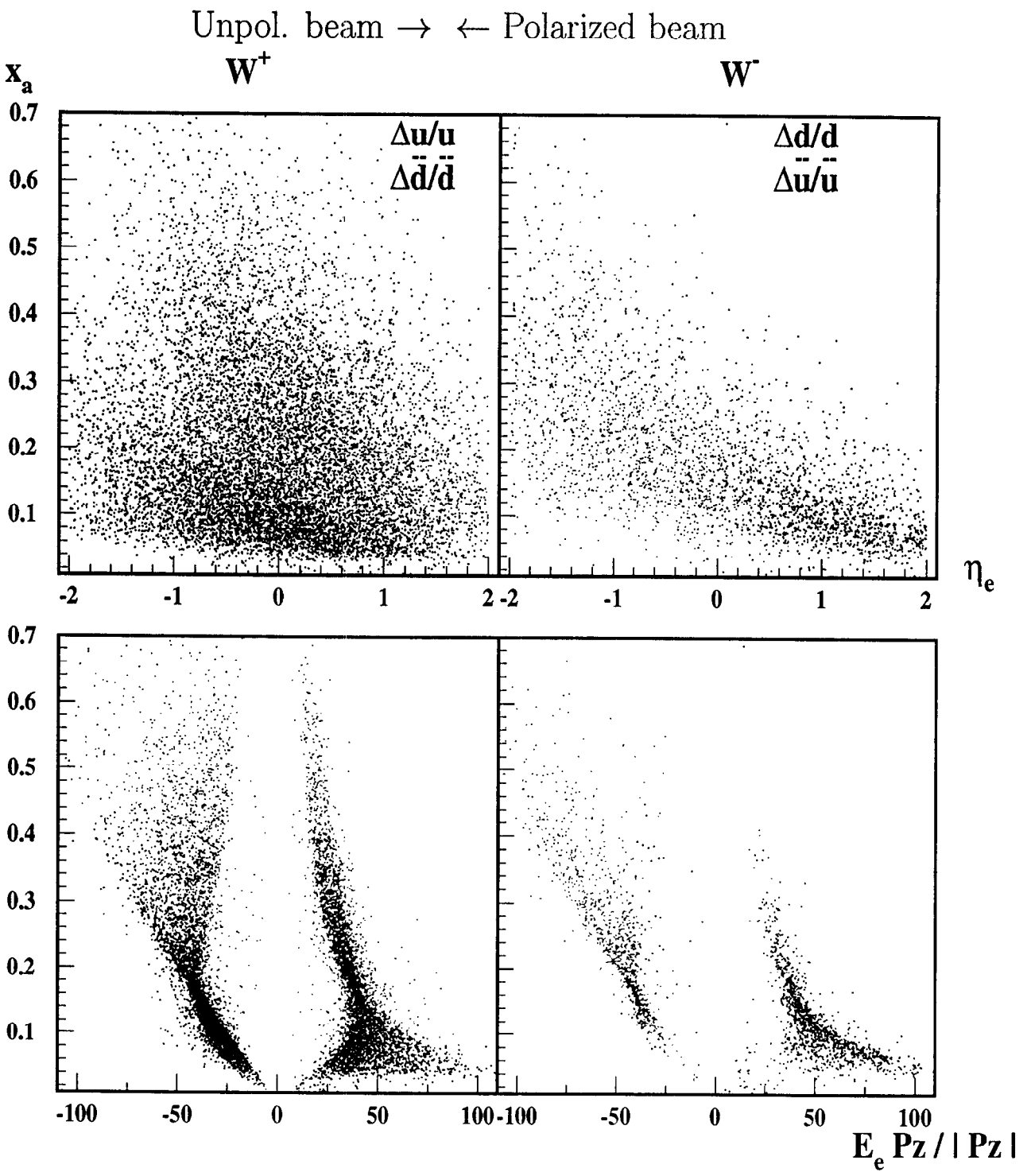

Investigating the origins of transverse spin asymmetries at RHIC

Daniël Boer
RIKEN-BNL Research Center, Brookhaven National Laboratory, Upton, New York 11973

Large single transverse spin asymmetries have been observed experimentally [1] in the process $pp^{\uparrow} \to \pi X$ and many theoretical studies have been devoted to explain the possible origin(s) of such asymmetries. However, one experiment cannot reveal the origin(s) conclusively and one needs comparison to other experiments. The polarized proton-proton collisions to be performed at RHIC can provide important information on transverse spin asymmetries and help to complete the theoretical understanding.

In this talk I will mainly focus on the Drell-Yan process, both on polarized and unpolarized cross sections and investigate what can be learned from studying the angular dependences and their transverse momentum dependence. In other words, the goal is to investigate the consequences and the interplay of the transverse spin and the transverse momentum of quarks. Transverse spin manifests itself through asymmetries and transverse momentum through the transverse momentum dependence of the asymmetries.

I will argue that "conventional" mechanisms which could produce *single* transverse spin asymmetries are expected to fall short in explaining the magnitude and the transverse momentum dependence of the asymmetries in the region where the transverse momentum is (partly) of nonperturbative origin.

Hence, I will discuss possible origins of transverse spin asymmetries in hadron-hadron collisions and propose an explanation in terms of a chiral-odd T-odd distribution function with intrinsic transverse momentum dependence [2], which would signal a correlation between the transverse spin and the transverse momentum of quarks inside an *unpolarized* hadron. Despite its conceptual problems, it can account for single spin asymmetries, in the Drell-Yan process and in principle also, $pp^{\uparrow} \to \pi X$, and at the same time it can account for the large $\cos 2\phi$ asymmetry in the unpolarized Drell-Yan cross section [3], which still lacks understanding too. Therefore, the mechanism provides a relation between unpolarized and polarized asymmetries and this can be tested. One can use the unpolarized asymmetry to arrive at a model for the chiral-odd T-odd distribution function and find explicitly how it relates unpolarized and polarized observables in the Drell-Yan process, as could be measured at RHIC. The relation depends on the transversity distribution function h_1, hence, it would provide an alternative method of measuring or cross-checking the transversity distribution function h_1.

The chiral-odd T-odd distribution function is formally the analog of the fragmentation function that appears in the Collins effect [4], but there is no direct relation between the functions, since they would arise from different physical origins.

[1] E.g. FNAL E704 Collab., A. Bravar *et al.*, Phys. Rev. Lett. 77, 2626 (1996).
[2] D. Boer, hep-ph/9902255.
[3] NA10 Collaboration, S. Falciano *et al.*, Z. Phys. C 31, 513 (1986);
NA10 Collaboration, M. Guanziroli *et al.*, Z. Phys. C 37, 545 (1988);
J.S. Conway *et al.*, Phys. Rev. D 39, 92 (1989).
[4] J.C. Collins, Nucl. Phys. B 396, 161 (1993).

Transverse Momentum Dependent Functions

The leading twist T-even distribution functions:

Pictorially:

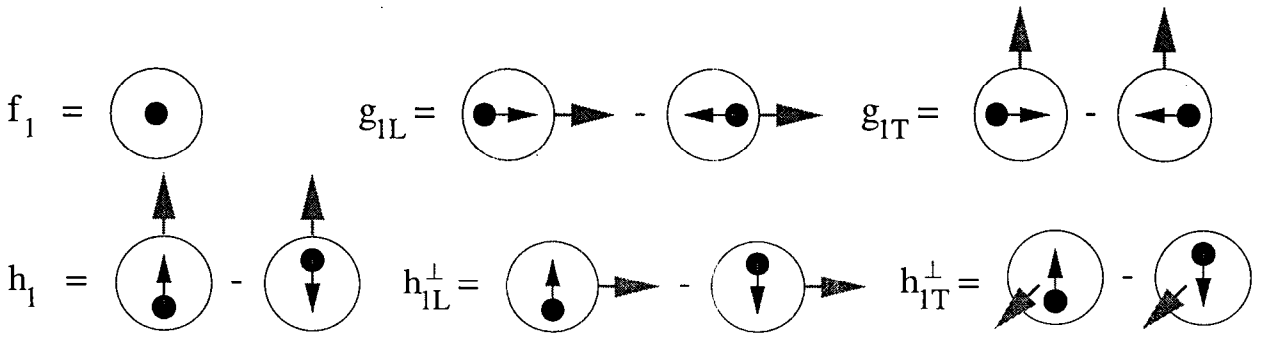

No single spin asymmetries in the angular dependence of the cross section.

Leading twist T-odd distribution functions with transverse momentum dependence can lead to single spin asymmetries.

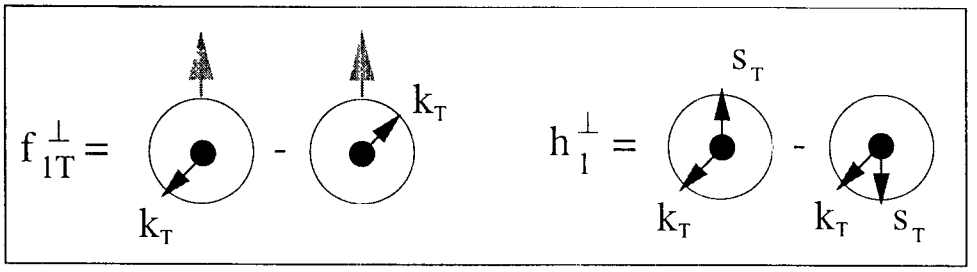

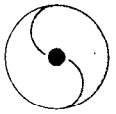

The unpolarized Drell-Yan process

A large angular dependence which is not yet understood

NA10 Collaboration (1988): $\pi^- N \to \mu^+ \mu^- X$, where N is either deuterium or tungsten (no apparent nuclear dependence) and using a π^--beam of 194 GeV.

$$\frac{1}{\sigma}\frac{d\sigma}{d\Omega} \propto \left(1 + \lambda \cos^2\theta + \mu \sin^2\theta \cos\phi + \frac{\nu}{2}\sin^2\theta \cos 2\phi\right)$$

Perturbative QCD prediction (NLO): $\lambda \approx 1, \quad \mu \approx 0, \quad \nu \approx 0$

Brandenburg, Nachtmann & Mirkes (ZPC 60 (1993) 697): large ν arises from a factorization breaking correlation between π and N.

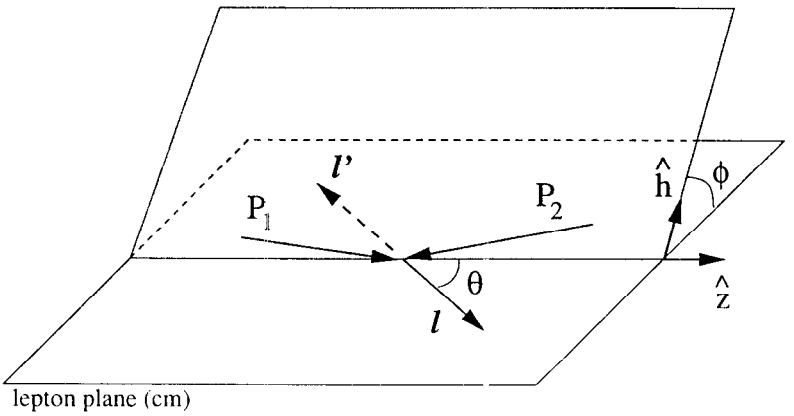

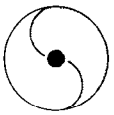

The unpolarized Drell-Yan process

Observation: $\nu \propto h_1^{\perp}(\pi)\, h_1^{\perp}(N)$ [D.B., hep-ph/9902255]

Guided by a model parametrization for $H_1^{\perp}$, we fit the data.

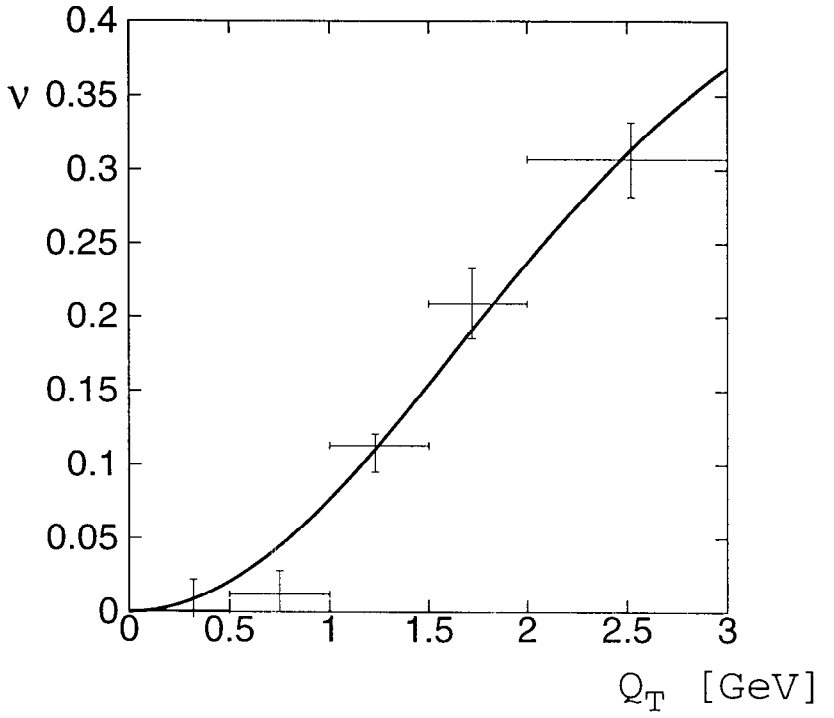

Proposal: measure $\langle \cos(2\phi) \rangle$ in unpolarized $p\,p \to \mu^+\mu^- X$ and the single spin asymmetry $\langle \sin(\phi + \phi_S) \rangle$, which is proportional to $h_1 h_1^{\perp}$.

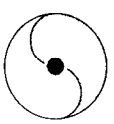

The polarized Drell-Yan process

In the case of a polarized hadron (choosing $\mu = 0$ and $\lambda = 1$):

$$\frac{d\sigma}{d\Omega\, d\phi_{S_1}} \propto 1+\cos^2\theta+\sin^2\theta\left[\frac{\nu}{2}\,\cos 2\phi - \rho\,|\boldsymbol{S}_{1T}|\,\sin(\phi+\phi_{S_1})\right]+\ldots$$

Relation for the case of one flavor: $\rho = \frac{1}{2}\sqrt{\frac{\nu}{\nu_{\max}}}\,\frac{h_1}{f_1}$

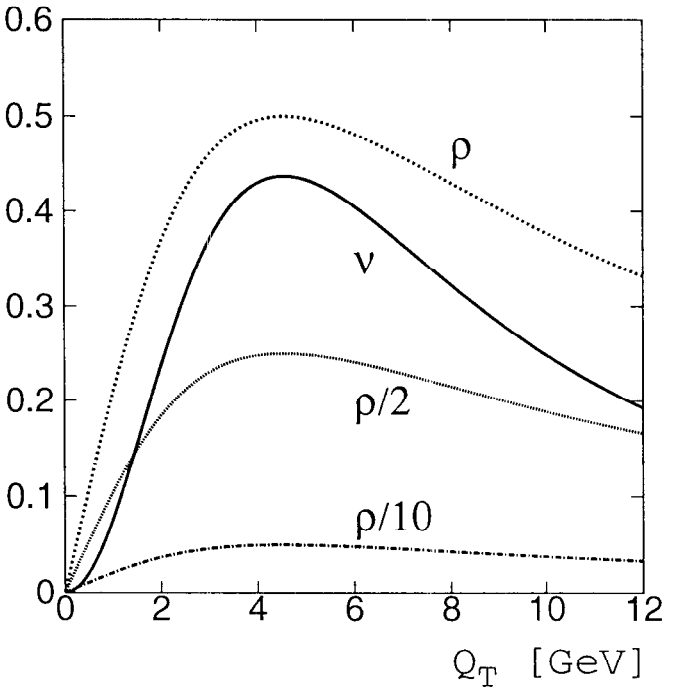

Different angular dependence compared to the other SSA

$$(1+\cos^2\theta)\,|\boldsymbol{S}_{1T}|\,\sin(\phi-\phi_{S_1})\,f_{1T}^{\perp}f_1$$

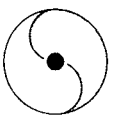

Conclusions

• We have investigated possible origins of transverse spin asymmetries in hadron-hadron collisions

• Single transverse spin asymmetries require some nontrivial mechanism

• Perturbative QCD corrections and higher twist effects are presumably too small

• Time reversal odd distribution and/or fragmentation functions with transverse momentum dependence are leading twist effects:

•The [illegible] effect appears to be small [$e^+e^- \to \pi^+\pi^- X$ data]

•The Sivers effect can fit the $p + p \to \pi + X$ data, but might lead to single spin asymmetries in simple DIS-like processes

•The distribution function $h_1^\perp$, the analog of the Collins effect, can fit unpolarized $\pi^- N \to \mu^+\mu^- X$ data (no other function in this approach can give rise to a $\cos(2\phi)$ asymmetry, unless $1/Q^2$ suppressed). It offers a new possibility to access h_1 in $p\,p(\bar{p}) \to \mu^+\mu^- X$

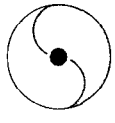

Energy Loss in Thin Plasmas

1) New Twists on Few Glue

- $dN_g/dy\,d^2k_\perp$ 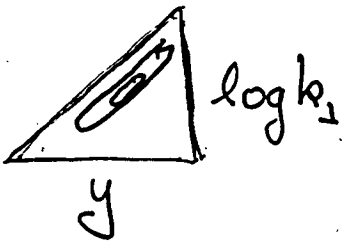

P. Levai
I. Vitev

- $P(n_g)$ and few glue quenching of leading hadrons 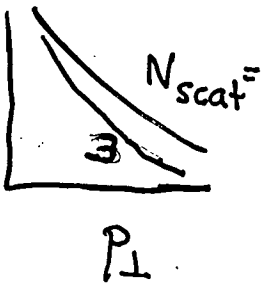

2) Collective Signatures of Thin Plasmas

- hydro $\frac{dE_\perp}{dy\,d\phi}$ 

D. Rischke
S. Vance

- elastic parton cascade
Bin Zhan
C M Ko

- inelastic parton cascade
D. Molna

M. Gyulassy
RBRC Workshop 3/4/99

Probability that a jet of energy E_0 emits

n resolvable gluons with $k^2 > \mu^2$

$$P_n \propto \left(\int_{\mu^2}^{E^2} dt_1 \frac{C_2\,\alpha(t_1)}{\pi\, t_1} \cdots \int_{\mu^2}^{t_{n-1}} dt_n \frac{C_2\,\alpha(t_n)}{\pi\, t_n}\right) \left(\int_{z_0}^{1} \frac{dz_1}{z_1} f(z_1, t_1) \cdots \int_{z_{0/(z_1 \cdots z_{n-1})}}^{1} \frac{dz_n}{z_n} f(z_n, t_n)\right)$$

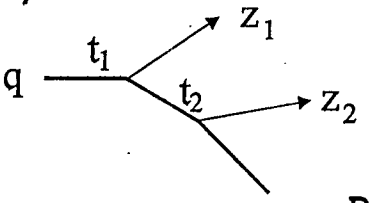

DGLAP

$$P_n = \frac{1}{n!\,n!}\left(\frac{r}{2}\right)^{2n}\left(\frac{1}{I_0(r)}\right) \approx \left(\frac{r^n}{n!\,2^n}\right)^2 \frac{e^{-r}}{\sqrt{2\pi r}} \qquad \langle n\rangle = \frac{r}{2}\frac{I_1(r)}{I_0(r)} \approx \frac{r}{2}$$

$$r = 4\sqrt{\frac{C_2}{\beta_0}\log\left(\frac{\log(E/\Lambda)}{\log(\mu/\Lambda)}\right)\log\left(\frac{E}{\mu}\right)}$$

E=30 GeV $\qquad r = \sqrt{\frac{8\,C_2\,\alpha}{\pi}\log\left(\frac{E}{\mu}\right)}$

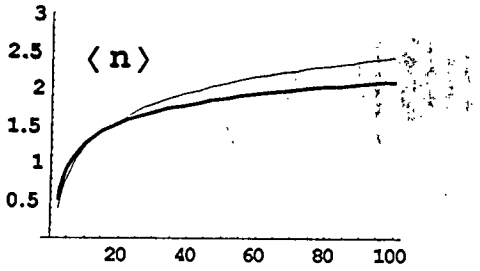

Quark jet of energy E_0 (GeV)

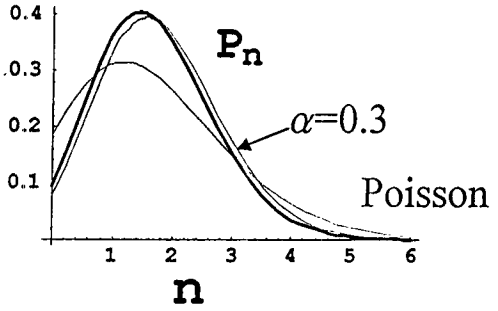

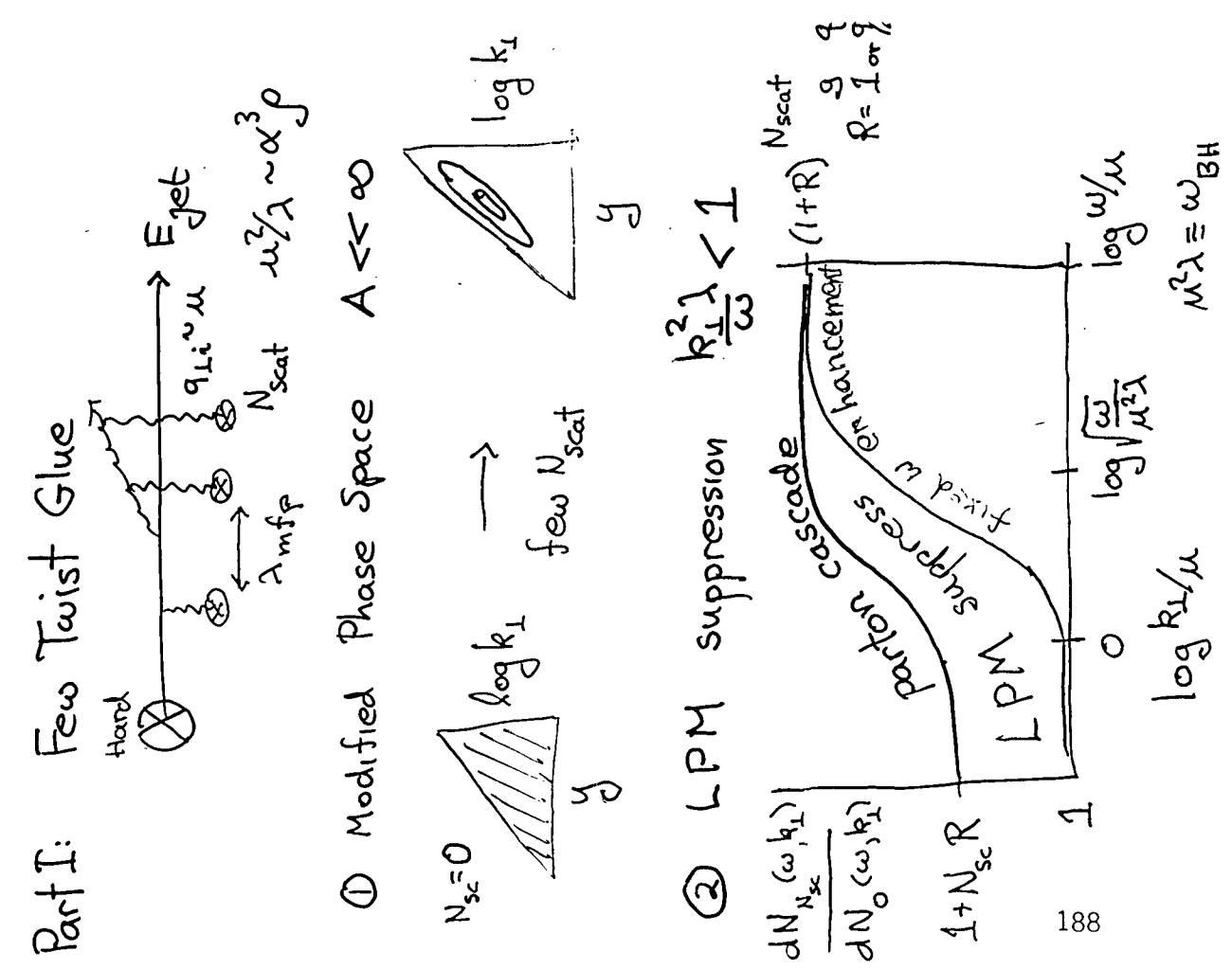

Medium Modified Parton Showers

n_g Phase Space $= du_1 \cdots du_{n_g} \underbrace{\Pi_{n_g, N_s}(u_1 \cdots u_{n_g})}_{\text{distortion } N_{sc} \neq 0}$

$du_i = C\alpha \frac{dk_{\perp i}}{k_{\perp i}} \frac{dz_i}{z_i}$

Product Ansatz (~ mean field)

$$\Pi_{n_g, N_{sc}} \approx \prod_{i=1}^{n_g} (1 + f_{N_{sc}}(u_i))$$

Importance Sampling:

$$\langle \theta \rangle = \frac{\sum_{n_g=0}^{\infty} \int du_1 \cdots du_{n_g} \, \Pi_{n_g, N_{sc}} \theta(u_1 \cdots u_{n_g})}{\sum_{n_g} \int du_1 \cdots du_{n_g} \, \Pi_{n_g, N_{sc}}} \times 1$$

$$= \langle \Pi_{n_g} \theta \rangle / \langle \Pi_{n_g} \rangle$$

Multiplicity Distribution

$$P(n, N_{sc}) = \langle \Pi_{n, N_{sc}} \rangle / \sum_{n=0}^{\infty} \langle \Pi_{n, N_{sc}} \rangle$$

$E_q = 10\,\text{GeV} \rightarrow n_g$ glue + q $\rightarrow$ hadrons

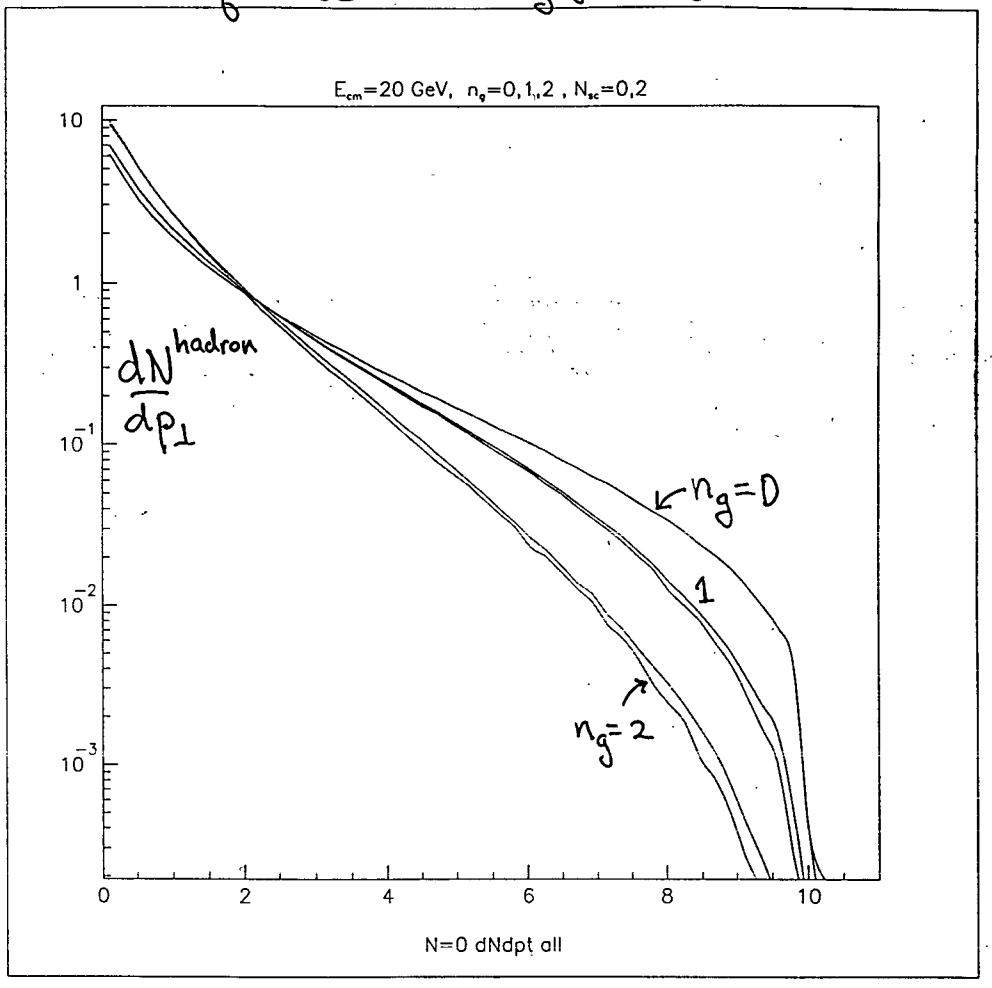

Quenching sensitive to n_g

but insensitive to shape of phase space

$E_q = 50\,GeV$

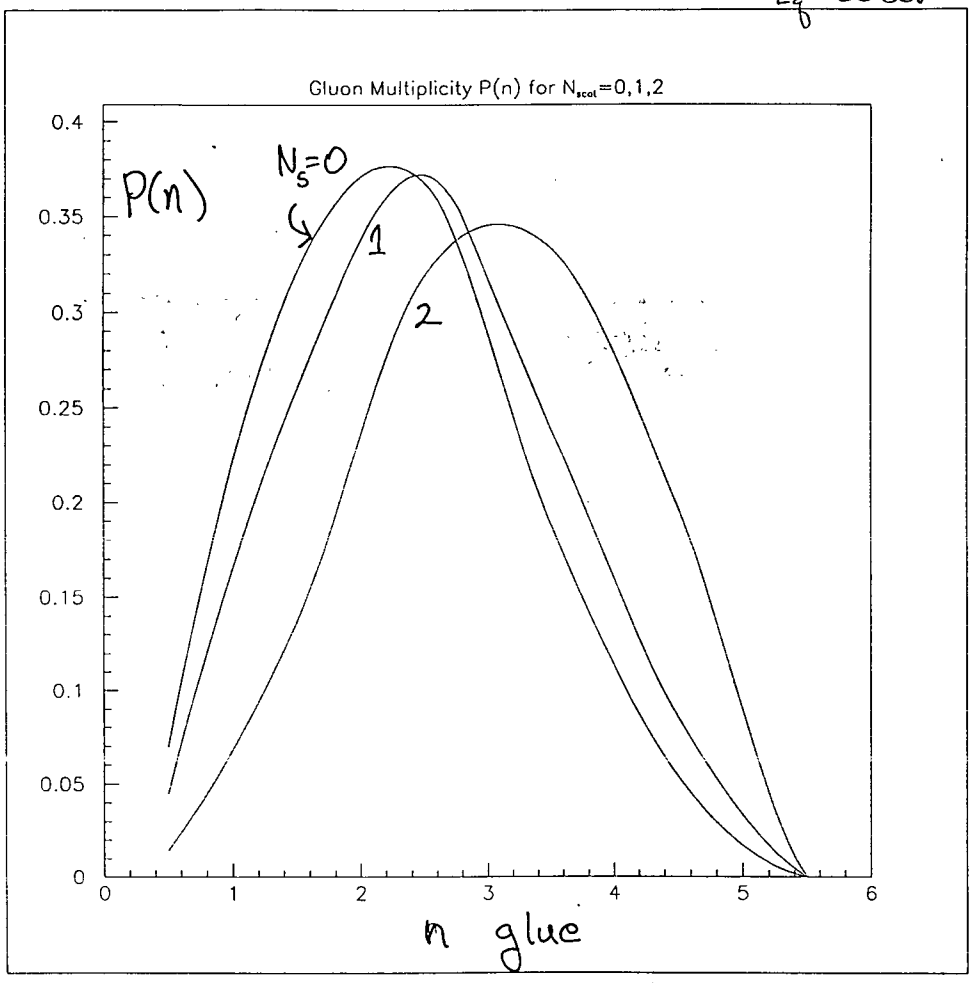

$\langle n \rangle = 2.3 \pm 1.0\ ,\ 2.5 \pm 1.0\ ,\ 3.0 \pm 1.0$

N_{sc} 0 , 1 , 2

$(dN^{had}/dp_\perp)^{N_{scat}=1,2} \;/\; (dN^{had}/dp_\perp)^{N_{scat}=0}$

including $P(n_{gl})$ fluctuations

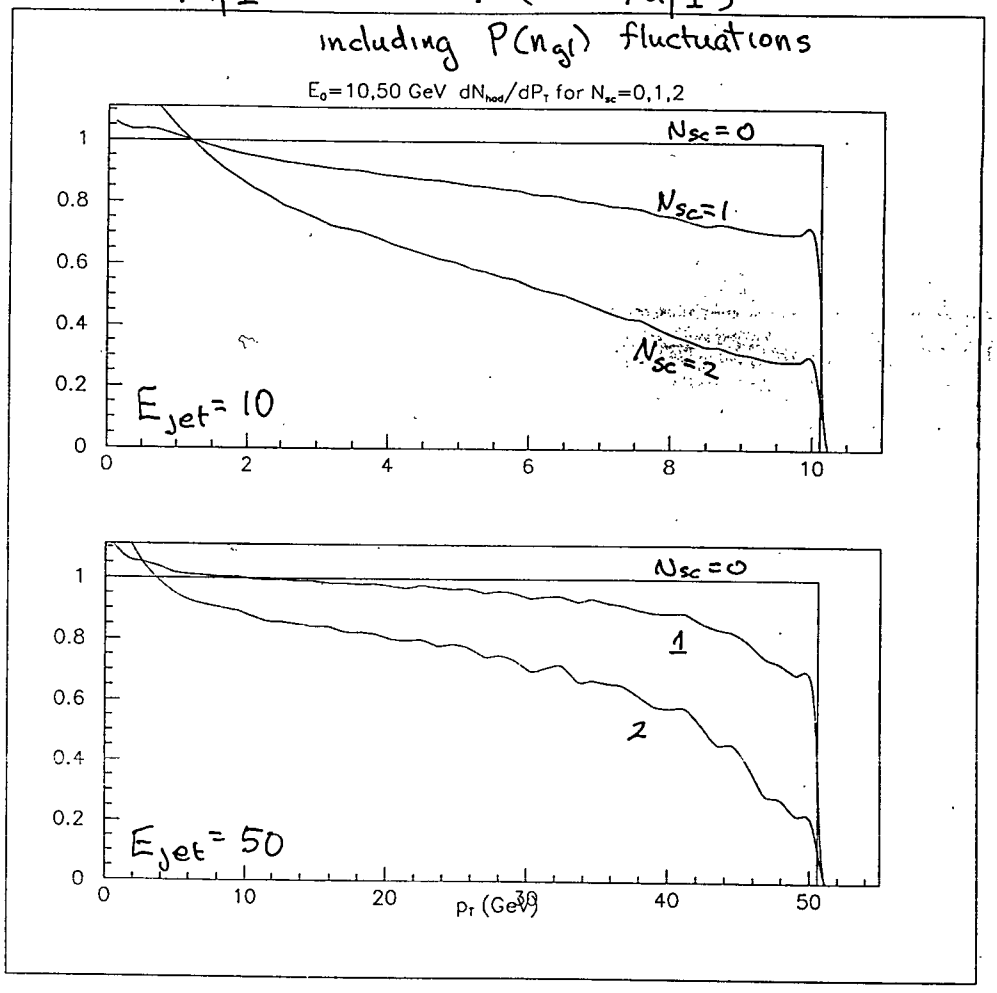

Quenching → 1 slowly with E_{jet} fixed N_{sc}

Part III: Remnants of Collective Signatures from Thin Plasmas

$b \neq 0$ hydro $\Rightarrow$ large $\frac{dE_\perp}{dy d\phi}$ anisotropy

$$\propto 1 + 2v_2 \cos 2\phi + \cdots$$

"Elliptic Flow"

New parton cascade results

$\Rightarrow \sim \frac{1}{2}$ smaller v_2 but still large

$\rightarrow$ strong A dependence

$\rightarrow$ sensitive to $\sigma_{in}^{gg \to ng} / \sigma_{el}$!

* Measurement of A dependence of collective signature critical to sort out dissipative dynamics from equation of state

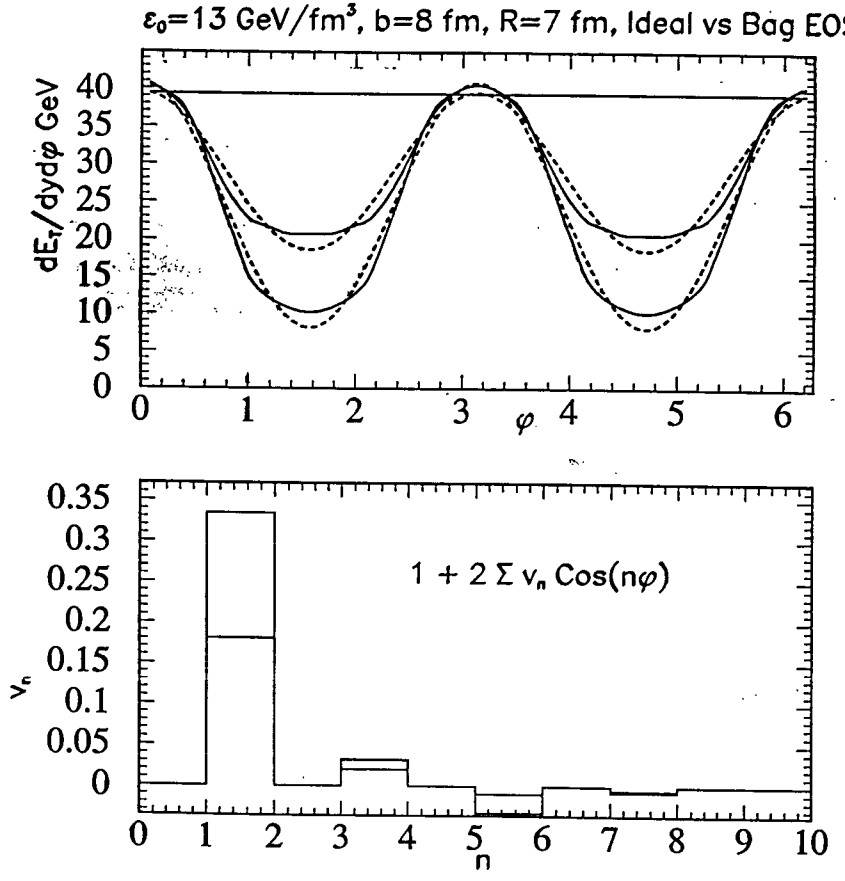

FIGURES

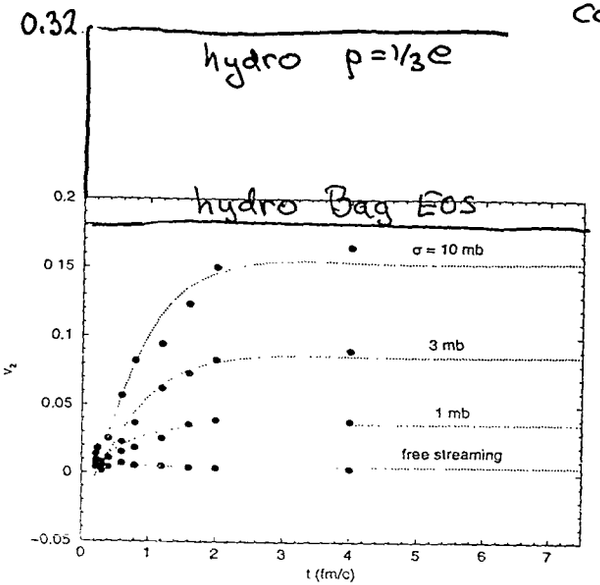

FIG. 1. Time evolution of v_2 coefficient for different effective parton scattering cross sections in Au-Au collisions at $\sqrt{s} = 200$ AGeV with impact parameter 7.5 fm. Filled circles are cascade data, and dotted lines are hyperbolic tangent fits to the data.

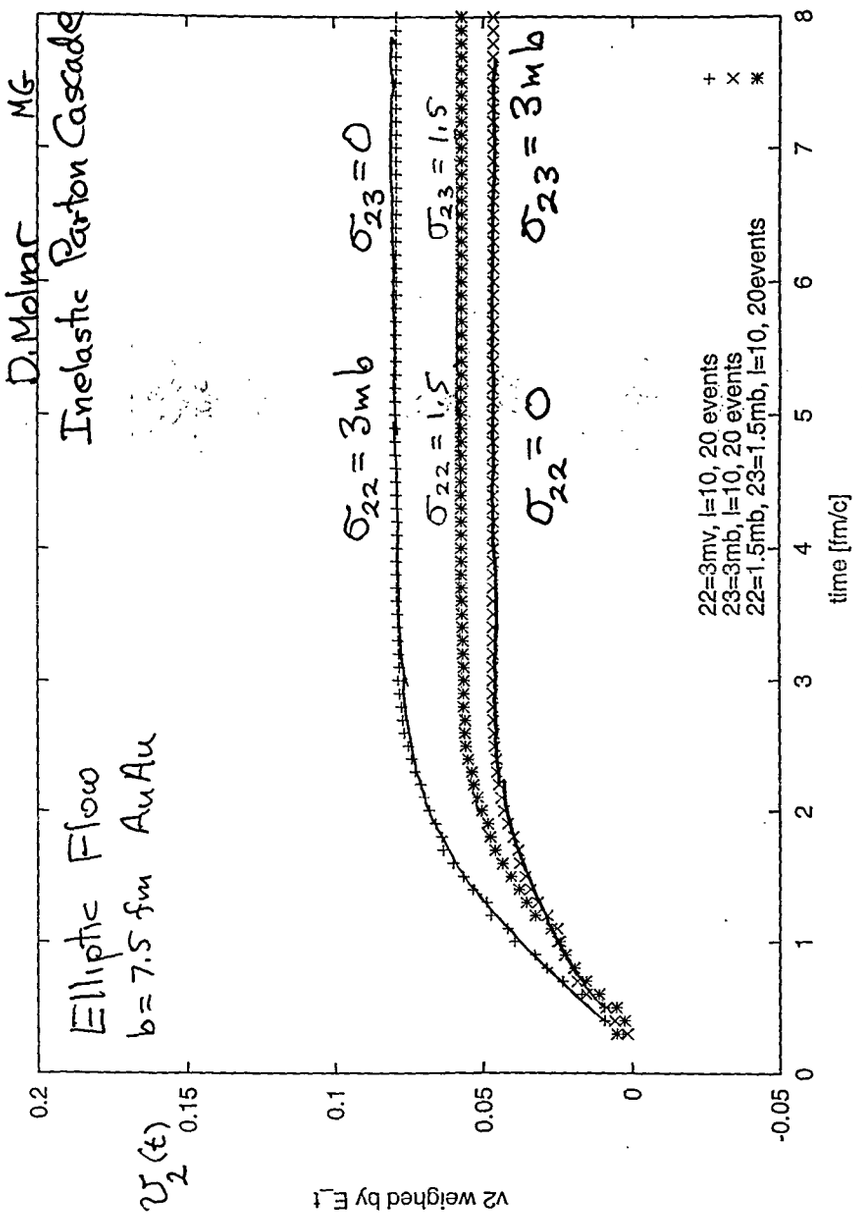

Gluons at low x

Alex Kovner (Oxford)

I discuss the evolution of gluonic observables in a hadron with x.

The Wilson renormalization group technique is discussed and the nonlinear evolution equation is derived. The nonlinearities in the evolution are caused by "recombination" effects at high partonic density.

The doubly logarithmic limit of the evolution is discussed in more detail, and it is shown that the gluon becomes effectively massive in the medium.

I suggest that the evolution in frequency rather than x will be a clean way of separating perturbative and nonperturbative effects.

Gluons at low x

with J. Jalilian-Marian, A. Leonidov, L. McLerran, H. Weigert

Low x structure of hadrons (DIS)

For heavy ions - initial conditions at high energy

High partonic density affects evolution of gluonic observables:

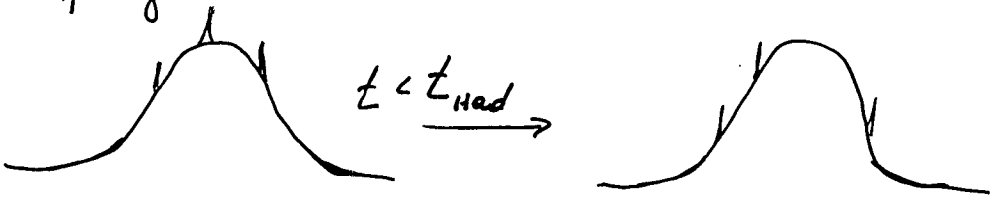

Under boost:

1. fast fluctuations freeze
2. long slow tales grow - acquire more energy

Both components become new players in scattering.

How does this structure evolve in x?

$$\frac{\partial G}{\partial \ln 1/x} \sim G - G^2 + \dots$$

When fields are large the evolution is nonlinear - the emission probability of an extra gluon is inhibited in the presence of large background.

We want to describe the nonlinearity at strong fields and weak coupling.

Remark: The fast fluctuations are hard and perturbative

Slow tales are soft and potentially nonperturbative

The evolution in x does not separate them

(Maybe evolution in $y \sim \frac{Q^2}{x}$?)

Possible way out - soft modes are affected by nonlinearities most and saturate - then we should be OK.

Double log approximation – staying ahead of the soft modes

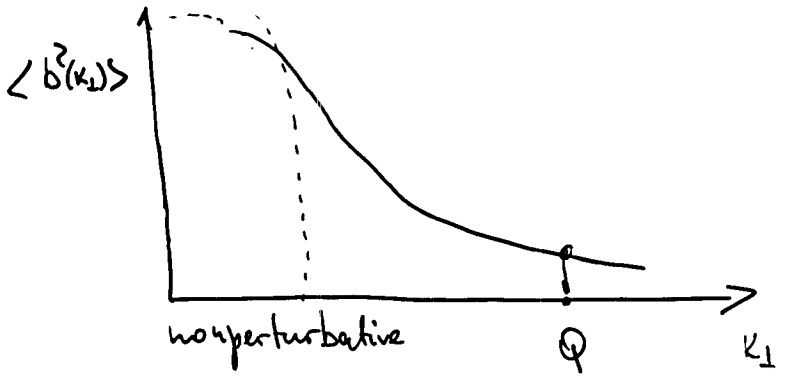

Emission at Q is due to a background with low $k_\perp$.

So we take $b_i(x_\perp) \to b_i$ - constant background

$$\chi^{ij} = 4\left[\frac{D_i D_j}{D^2}\,\frac{b^2}{\partial^2 + 2b^2}\right]$$

Evolution simplifies

$$\frac{d}{d\ln 1/x}\langle b_i(x_\perp)\, b_i(y_\perp)\rangle = 4\alpha_s \langle x_\perp \left|\frac{b^2}{\partial^2+2b^2}\right| y_\perp\rangle$$

Fourier transform brings it to the form of double evolution

$$Q^2\langle b(Q)\, b(-Q)\rangle \sim \frac{\partial}{\partial \ln Q^2} G(Q)$$

$$\langle b^2\rangle \sim \alpha_s G(Q)$$

The physics here - generation of dynamical mass

$$\frac{\partial^2}{\partial \ln 1/x \, \partial \ln Q^2} \langle b^2 \rangle \sim \left\langle \frac{b^2}{Q^2 + z b^2} \right\rangle$$

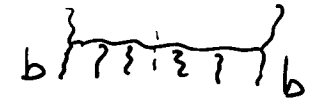

Emission of an extra gluon in the IMF ⟺ propagation of a gluon from the cascade through the hadron (in target rest frame).

Estimated value (from saturation fits to DIS - Levin et.al, Golec-Biernat + Wusthoff) -

$1-2\ \text{GeV}^2$ at $x \sim 10^{-4} - 10^{-5}$

The mass leads to almost saturation at strong fields.

$$\langle b^2 \rangle \sim G(Q) = \frac{N^2-1}{2} \frac{Q^2}{S} \ln 1/x$$

S: area of the hadron

DLA is an overkill - there is more perturbative physics.

The calculation itself gives a clue how to separate perturbative physics

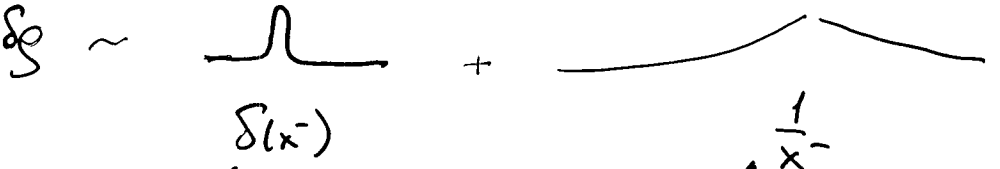

Hard part dominated by fast fluctuations

softer ($k_\perp < p_\perp$) and longer wavelength modes

Scattering of two shock waves and high-energy effective action.

I. Balitsky

S_{eff} for a given interval in rapidity

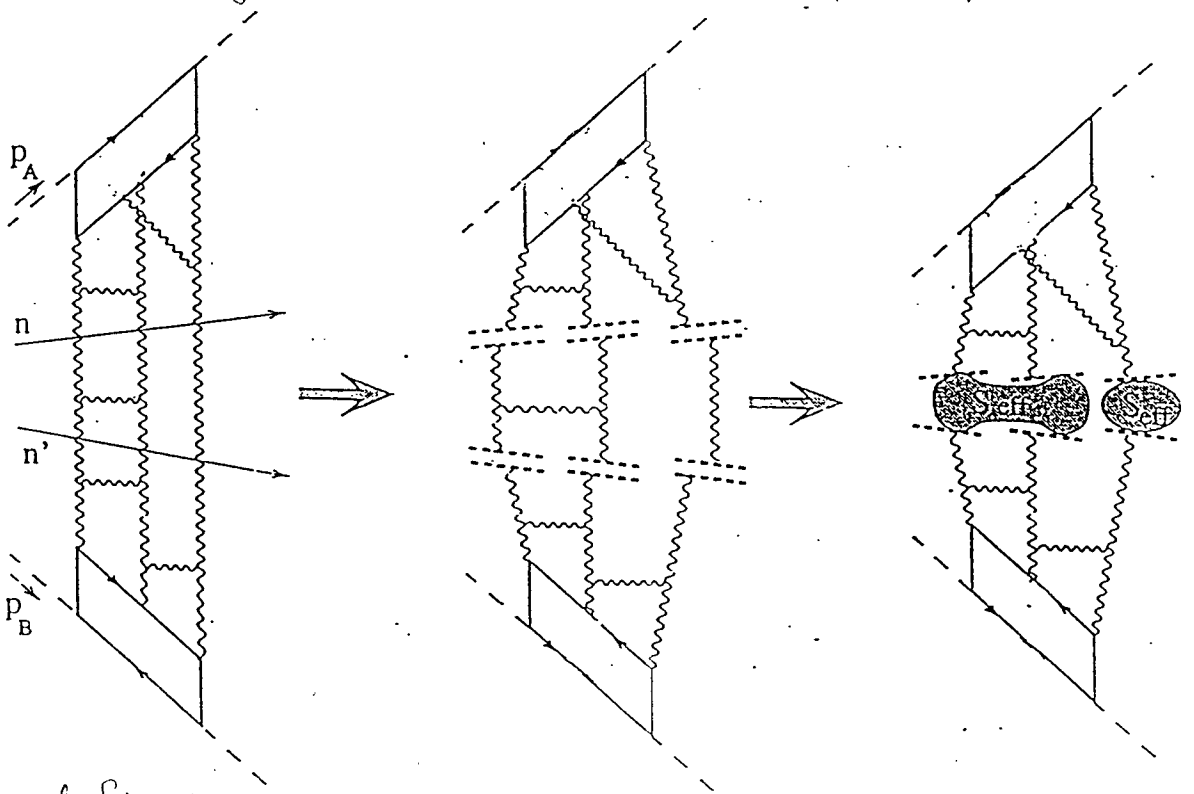

Formal definition

$$e^{iS_{eff}(V,Y;\Delta\eta)} = \int \mathcal{D}A\, e^{iS(A)}\, e^{i\int d^2x_\perp \{V_i(x_\perp)U_i(x_\perp) + W_i(x_\perp)Y_i(x_\perp)\}}$$

$U_i = U^+ i\partial_i U$, $U = [\infty n + x_\perp, -\infty n + x_\perp]$ – Wilson-line operator (infinite gauge link)

$W_i = W^+ i\partial_i W$ $\quad W = [\infty n' + x_\perp, -\infty n' + x_\perp]$

$$[x,y] \equiv P\exp i\int_0^\infty du\,(x-y)_\mu A_\mu(ux+\bar{u}$$

Semiclassical calculation of S_{eff} – scattering of two shock waves

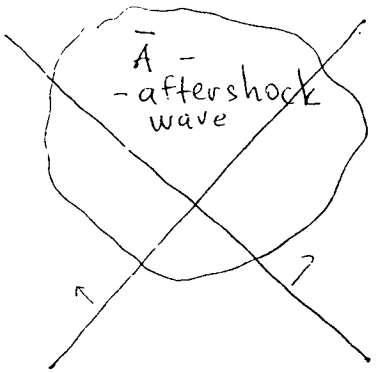

$$\frac{\delta S_{eff}}{\delta A_\mu}\Big|_{A=\bar{A}} = 0 \Rightarrow \text{classical eqs.}$$

Approximate solution:

$$A_i = \psi_i\theta(x_+) + V_i\theta(x_-) + \int dz_\perp \frac{(x-z)_k}{-x_+x_- + (x-z)_\perp^2}\, ik(z$$

$$L_{ik} \equiv [V_i, Y^i]\,\delta_{ik} + [V_i, Y_k]$$

$$\Rightarrow S_{eff} \simeq \frac{\alpha_s}{2\pi}(\Delta\eta)\int d^2x_\perp\, d^2y_\perp \Big\{L_{ik}(x_\perp)\ln(x-y)_\perp^2 L_{ik}(y_\perp) + (Y_i(x_\perp)V_i(y_\perp) - Y_i(x_\perp)\cdot V_i(x_\perp))\frac{1}{(x-y)_\perp^2}\Big\}$$

← contains BFKL, three-pomeron vertex

Formal definition of S_{eff}:

$$e^{iS_{eff}(V_i,Y_i)} = \int \mathcal{D}A\, e^{iS(A)} \exp\Big[-2i\,\mathrm{Tr}\int d^2x_\perp\, V_i(x_\perp)\cdot$$

$$\int du\,[-\infty p_1+x_\perp, up_1+x_\perp]\,F_{\cdot i}(up_1+x_\perp)\,[up_1+x_\perp, -\infty p_1+x_\perp] -$$

$$-2i\,\mathrm{Tr}\int d^2x_\perp\, Y_i(x_\perp)\int dv\,[-\infty p_2+x_\perp, vp_2+x_\perp]\,F_{*i}(v)\,[vp_2+x_\perp, -\infty p_2+x_\perp$$

(with power accuracy, $e \leftrightarrow p_1$ and $e' \leftrightarrow p_2$)

How we can actually compute S_{eff}?

1. Pert. theory
2. Semiclassical approach
3. Conformal symmetry (?).

Perturbation theory:

$e^{iS_{eff}} =$ 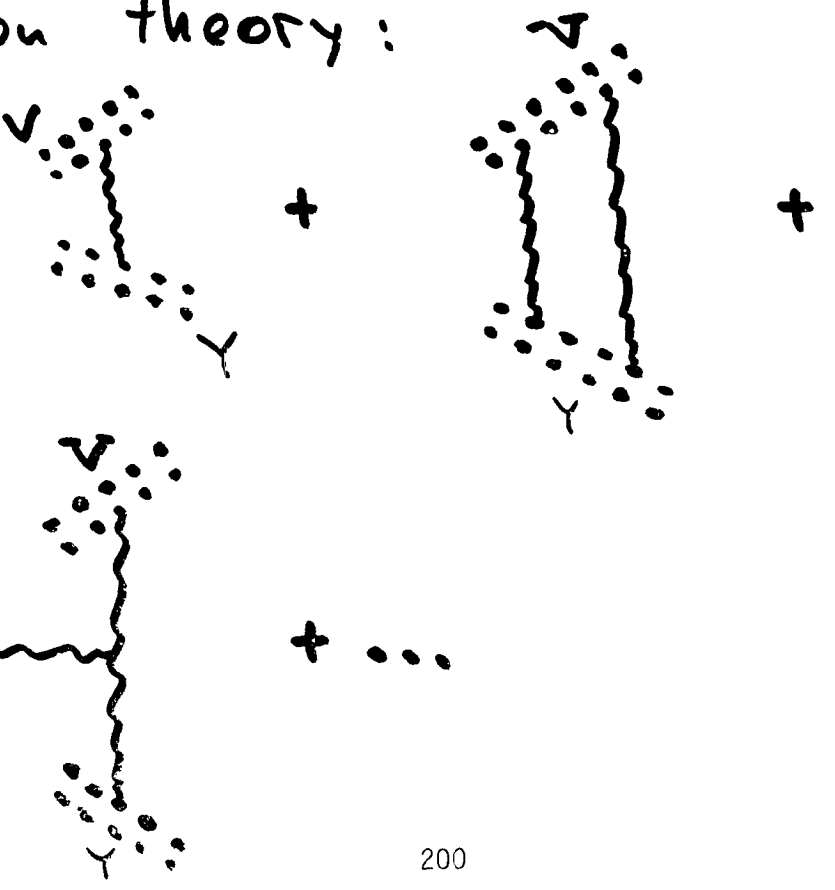

Semiclassical approach is relevant when $\alpha_s \ll 1$ but the fields are strong ($V_i \sim Y_i \sim \frac{1}{g} \Rightarrow [\infty, -\infty] \sim 1$) ⟹

Collision of two shock waves

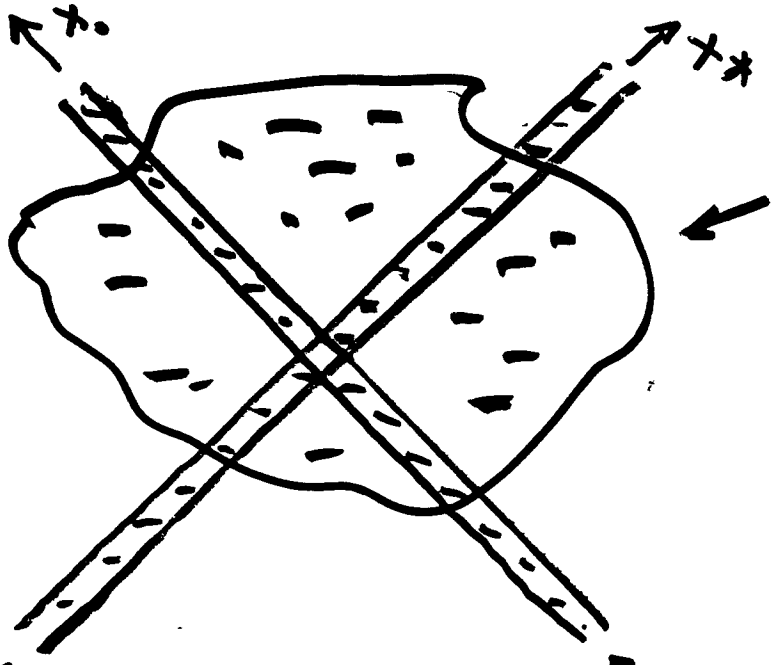

„classical" c
field generate
by the colli'si

„A" fields
(„left movers")

„B" fields („right-
-movers")

For the effective action, the boundary conditions at $t = \infty$ are Feynman-type (no production of particles ≡ outgoing wave

Possible way to solve classical eqs:

Take a trial configuration = sum of shock waves

$$A_i^{(0)} = Y_i\,\theta(x_*) + V_i\,\theta(x_-) \;;\; A_- = A_* = 0$$

and improve it order by order in pert theory

$$(D^2\delta_{\mu\nu} - 2iG_{\mu\nu})^{(0)}\,\delta A_\nu^{(1)} = \frac{\delta S_{eff}}{\delta A}\Big|_{A=A'}$$

$$\vdots$$

Parameter of the expansion is

$$\sim [Y_i, V_j]\, g^2 \ln\frac{\sigma}{\sigma_1}$$ → sort of leading log approximation

In the first nontrivial order

$$F_{-*}^{(1)} \simeq g\int dz_\perp \frac{1}{-x_{11}^2 + (x-z)_\perp^2}\,[Y_k, V^k](z_\perp)$$

$$F_{ik}^{(1)} \simeq g\int dz_\perp \frac{1}{-x_{11}^2 + (x-z)_\perp^2}\,([Y_i, V_k] - i\partial_k)$$

$$F_{*i}^{(1)} = \left(\frac{1}{x_+ + i\epsilon}\right) g\int dz_\perp \frac{(x-z)_\perp^k}{-x_{11}^2 + (x-z)_\perp^2}\,L_{ik}$$

$$x_{11}^2 \sim x_* x_-$$

$$L_{ik} \equiv \delta_{ik}[Y_j, V_j] + [Y_i, V_k] - [Y_k, V_i]$$

This corresponds to Lipatov's eff. vertex

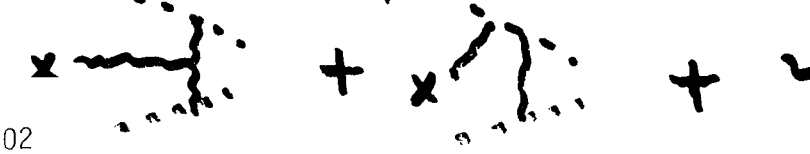

Conclusions

1. Factorization formula $\Rightarrow$ definition of S_{eff} (for a given $\Delta\eta$)
2. Semiclassical approach to S_{eff} $\Leftrightarrow$ $\Leftrightarrow$ scattering of two shock waves
3. „Aftershock" field $\bar{A}$ (solution of classical eqs. for S_{eff}) is logarithmic in energy $\Rightarrow$
4. The fields inside the scattering region will be large (at large E) even for weak initial sources (like virtual photons (or nucleons)

Outlook

1. Take into account particle production $\Leftrightarrow$ S_{eff} for inclusive cross section
2. Aftershock field $\bar{A}$ in LLA (conformal symmetry?)
3. Reggeized gluons in terms of Wilson lines $\Leftrightarrow$ Lipatov's effective action

Small–x F_2 Structure Function of a Nucleus Including Multiple Pomeron Exchanges

Yuri V. Kovchegov

School of Physics and Astronomy, University of Minnesota,

Minneapolis, MN 55455

We derive an equation determining the small-x evolution of the F_2 structure function of a nucleus or a hadron which includes all multiple pomeron exchanges in the leading logarithmic approximation using Mueller's dipole model. In the linear limit the equation reproduces the BFKL evolution. In the non–linear regime the equation sums up the so–called "fan" diagrams. We show that in the double leading logarithmic limit this evolution equation reduces to the GLR equation. We discuss the cancelation of pomeron loop diagrams, which employs an analogue of the AGK cutting rules in dipole model. Finally, we urge people to try fitting recent HERA data employing the proposed evolution equation.

I. Saturation of the hadronic structure functions and BFKL equation.

* Goal ~ study high density gluon states.

$F_{\mu\nu}^2 \sim \frac{1}{\alpha}$ saturation

BFKL is a way of getting to high density regime

rapidity $Y = \ln \frac{s}{4M^2} \sim \ln \frac{1}{x}$

BFKL equation resums leading log's of s:

$(\alpha \ln s)^n$ or $(\alpha Y)^n$

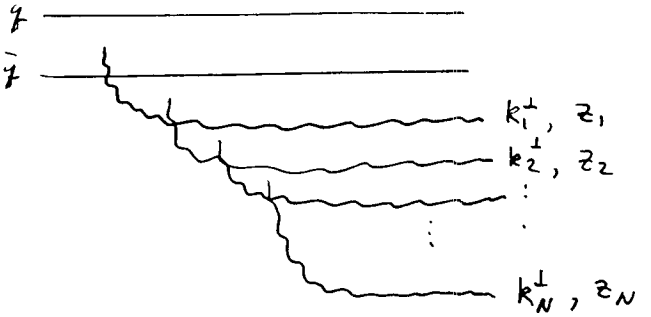

$k_1^\perp \sim k_2^\perp \sim \ldots \sim k_N^\perp$

$z_1 >> z_2 >> \ldots >> z_N$

Solution to BFKL equation yields

$$\sigma \sim \alpha^2 e^{(\alpha_P - 1) Y}$$

$\alpha_P - 1 = \frac{4\alpha N_c}{\pi} \ln 2$.

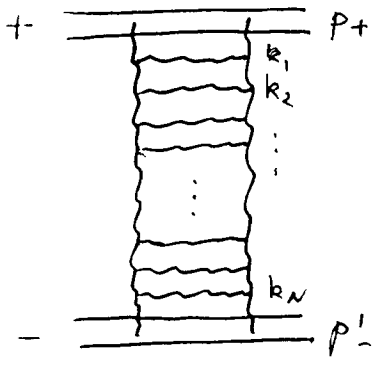

It corresponds to 1 pomeron exchange.

BFKL (hard) pomeron $\sigma \sim s^{(\alpha_P - 1)}$

$k_i = \alpha_i p_+ + \beta_i p'_- + k_i^\perp$

$\alpha_1 >> \alpha_2 >> \alpha_3 >> \ldots >> \alpha_N$ Regge kinematics

$\beta_1 << \beta_2 << \ldots << \beta_N$

II. Large N_c limit of BFKL: the dipole model of A.H. Mueller.

NPB 415, 373 (1994)
NPB 425, 471 (1994)
NPB 437, 107 (1995)

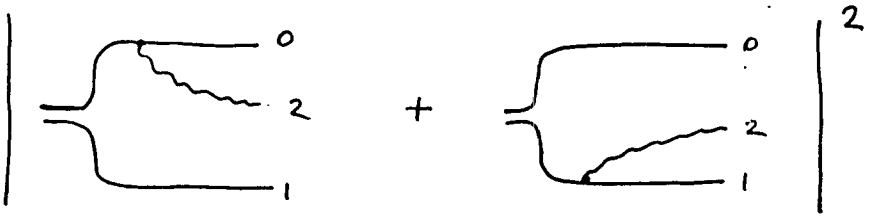

$$\Phi^{(1)}(\underline{x}_1, z_1) = \frac{\alpha C_F}{\pi^2} \int_{z_0}^{z_1} \frac{dz_2}{z_2} d^2x_2 \frac{x_{01}^2}{x_{02}^2 x_{12}^2} \Phi^{(0)}(\underline{x}_1, z_1)$$

Large N_c :

next step:

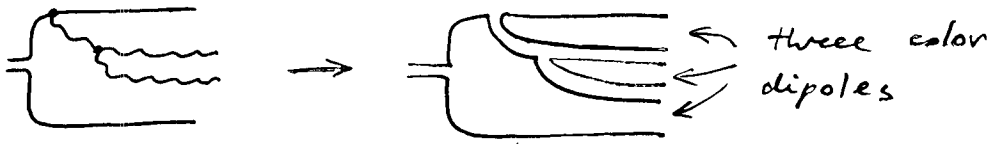

etc.

At each step in rapidity we produce a gluon, i.e. create an extra dipole.

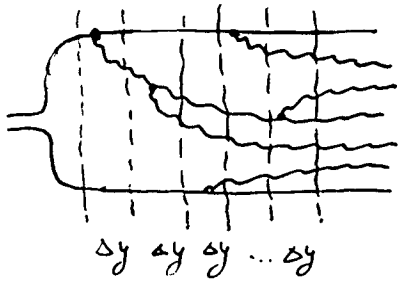

$(\alpha \Delta y)^{n}$ → leading logarithm

$\alpha Y \sim \alpha \ln \frac{1}{x}$

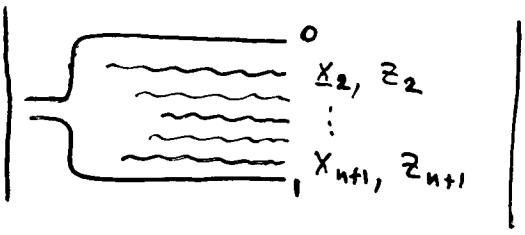

$\equiv \Phi^{(n)}(\underline{x}_1, \underline{x}_2, \ldots, \underline{x}_{n+1}; z_1, \ldots, z_{n+1})$

n-dipole or n-gluon wave function

Define the generating functional for dipoles $Z(\underline{x}_{01}, u)$:

$$\Phi^{(n)}_{1,2,\ldots,n+1} = \frac{1}{n!}\left[\frac{\delta}{\delta u(\underline{x}_2, z_2)}\frac{\delta}{\delta u(\underline{x}_3, z_3)}\cdots\frac{\delta}{\delta u(\underline{x}_{n+1}, z_{n+1})} Z(\underline{x}_{01}, u(x,z))\right]_{u=0} \Phi^{(0)}(\underline{x}_{01})$$

$u(\underline{x}, z)$ ~ some arbitrary function (dipole's S-matrix)

For Z one can write down the following equation:

$$Z(\underline{b}, \underline{x}_{01}, Y, u) = u(\underline{b}_0, \underline{x}_{01})\, e^{-\frac{4\alpha C_F}{\pi}\ln\left(\frac{x_{01}}{\rho}\right)Y} +$$

A.H. Mueller

$$+ \frac{\alpha C_F}{\pi^2}\int_0^Y dy\, e^{-\frac{4\alpha C_F}{\pi}\ln\left(\frac{x_{01}}{\rho}\right)(Y-y)} \int d^2x_2 \frac{x_{01}^2}{x_{02}^2 x_{12}^2} \cdot Z(\underline{b}+\tfrac{1}{2}\underline{x}_{12}, \underline{x}_{02}, y, u) \cdot$$

$$\times Z(\underline{b}-\tfrac{1}{2}\underline{x}_{20}, \underline{x}_{12}, y, u)$$

The most important equation of the dipole model and, probably, all multiple pomeron physics!!!

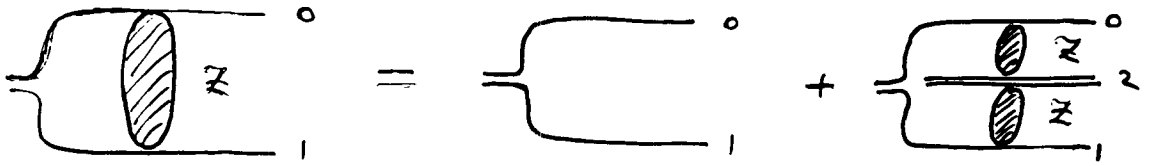

$Z = \text{inhomogeneous term} + K \otimes Z\, Z$

$e^{-\frac{4\alpha C_F}{\pi}\ln\left(\frac{x_{01}}{\rho}\right)Y}$ ~ virtual corrections

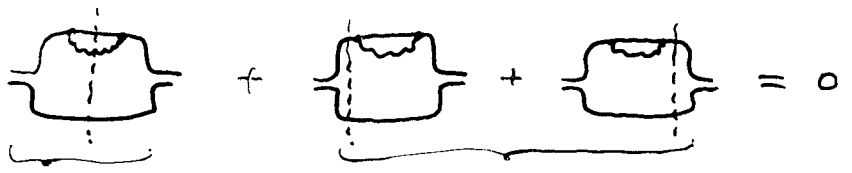

$\Phi^{(1)}_{real}$ ~ know $\qquad \Phi^{(1)}_{virt}$

III. Summation of the multiple pomeron exchanges.

The idea is very simple: since there is a one to one correspondence between pomerons and fast dipoles, we can just consider a scattering of a cascade of dipoles on the nucleus at rest:

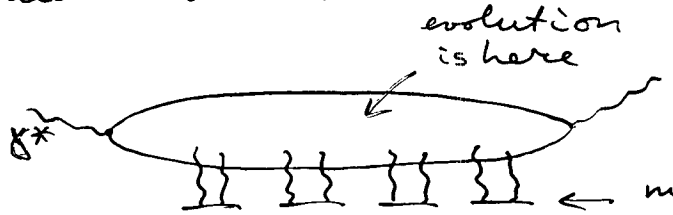

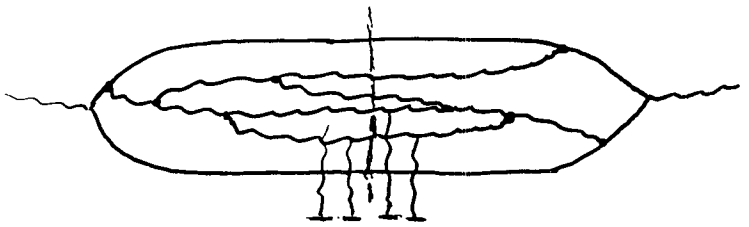

the incoming γ^* develops a cascade of gluons, which then rescatter on the nucleus.

Large N_c : gluon cascade $\Rightarrow$ dipole wave function

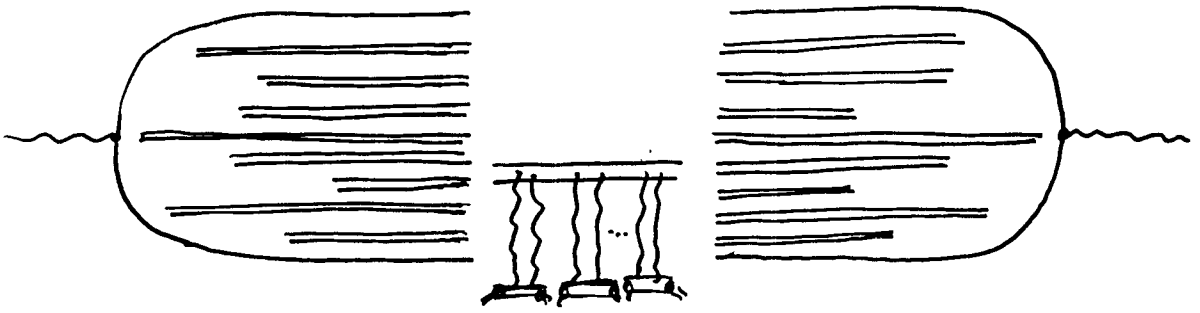

dipole (gluon) BFKL evolved cascade

each dipole undergoes a Glauber-type rescattering in the nucleus

$\Rightarrow$ cascade in ... amplitude

Defining $q\bar{q}$ scattering x-section

$$N = \quad \otimes \gamma \; + \frac{1}{2!} \; \otimes\gamma \; \otimes\gamma \; + \ldots$$

$$N = \frac{\delta Z}{\delta u} \otimes \gamma + \frac{1}{2!} \frac{\delta^2 Z}{\delta u \, \delta u} \otimes \gamma^2 + \ldots$$

1 pomeron 2 pomerons etc.

$\gamma =$  $\gamma = e^{-\frac{\alpha_s^2}{2R^2 S_\perp} x_\perp^2 A\, xG} - 1$ (Glauber propagator)

One can see that $N = 1 - Z(1+\gamma)$, i.e. $U = 1 + \gamma$.

(U: S-matrix, T: T-matrix)

We obtain an equation for N:

$$N(\underline{x}_{01}, \underline{b}_0, Y) = -\gamma(\underline{x}_{01}, \underline{b}_0)\, e^{-\frac{4\alpha C_F}{\pi} \ln\left(\frac{x_{10}}{\rho}\right) Y} + \frac{\alpha C_F}{\pi^2} \int_0^Y dy\, e^{-\frac{4\alpha C_F}{\pi} \ln\left(\frac{x_{10}}{\rho}\right)(Y-y)}$$

$$\cdot \int_\rho d^2 x_2 \, \frac{x_{01}^2}{x_{02}^2 x_{12}^2} \left[2N\left(\underline{x}_{02}, \underline{b}_0 + \tfrac{1}{2}\underline{x}_{12}, y\right) - N\left(\underline{x}_{02}, \underline{b}_0 + \tfrac{1}{2}\underline{x}_{12}, y\right) N\left(\underline{x}_{12}, \underline{b}_0 + \tfrac{1}{2}\underline{x}_{02}, y\right) \right]$$

This equation resums multiple pomeron exchanges in the LLA ($\ln \frac{1}{x}$). This is the main result!

$$F_2(x, Q^2) = \frac{Q^2}{4\pi^2 \alpha_{EM}} \int \frac{d^2 x_{01}\, dz}{4\pi} \, \Phi(x_{01}, z) \cdot 2N(\underline{x}_{01}, \underline{b}_0, Y)$$

Easily connected to an experimentally measurable quantity, avoiding all the problems associated with xG.

$\Rightarrow$ Crucial assumption: the dipoles scatter independently!

$\Rightarrow$ need large nucleus, formally does not work for a hadron, however it probably does since many "nuclear" assumptions somehow work out for hadrons.

$\Rightarrow$ [illegible]

Effects of Shadowing on Initial Conditions and Hard Probes in Nuclear Collisions*

R. Vogt

The modification of nucleon structure functions in nuclei, a depletion at small and medium x and an enhancement at intermediate x, is well established in nuclear deep-inelastic scattering. However, the source of the modification, or shadowing, is not completely understood. Two primary models are (1) recombination of long wavelength partons; and (2) multiple interactions of the incoming parton along the path length through the nucleus. In case (2), when $x < 0.016$, the coherence length l_c is larger than any nuclear radius.

Shadowing should depend on the location of the parton in the nucleus since partons in nucleons closer to the nuclear surface should be less shadowed because there is a lower probability to either recombine with partons in neighboring nucleons or to be part of a multiple interaction chain. However, the exact spatial dependence is a function of the origin of the shadowing. In case (2) above and at small x, since $l_c > R_A$, the shadowing should be proportional to the path length through the nucleus. For $l_c < R_A$ and in case (1), the shadowing should be proportional to the local nuclear density. The spatial dependence over the entire x range is difficult to parameterize in case (2) since the crossover between the relevant formulation is A dependent and occurs at x values typical for $p_T \sim 2$ GeV at RHIC.

Because no model of shadowing can explain the effect over all x, we use three parameterizations of nuclear shadowing to explore the its effects on the initial conditions at RHIC and LHC. Unfortunately, the nuclear gluon distribution is least constrained by data and most important for particle production in hard interactions. The behavior of the gluon distribution is significantly different in the three parameterizations. We have also studied two spatial parameterizations of shadowing, one proportional to the local nuclear density and the other to the path length through the nucleus. Both are normalized so that an integration over the nuclear volume reproduces the spatial average results reported in nuclear deep-inelastic scattering. The impact parameter dependence is stronger than the average in central collisions and disappears as $b \to \infty$.

We have calculated minijet production and the corresponding E_T moments at RHIC and LHC energies assuming hard production for $p_T \geq p_0 = 2$ GeV. We use these moments, along with the expected soft component to estimate the effect of shadowing on the initial conditions for further evolution of the hot system created in Au+Au collisions at $\sqrt{s_{NN}} = 200$ GeV and Pb+Pb collisions at $\sqrt{s_{NN}} = 5.5$ TeV. As expected, at the higher energy, the semihard minijets dominate particle production. The energy and number densities calculated at 5.5 TeV without shadowing result in a ratio ϵ_i/n_i close to that expected for an ideal gas with a temperature of ≈ 1.1 GeV. One can then imagine fast thermalization at $\tau_i \sim 1/p_0$, even if the system is not yet isotropic. However, when shadowing is included, this 'temperature' is reduced by $\approx 10\%$ so that $\epsilon_i/n_i > \epsilon_{\rm th}/n_{\rm th} \sim 2.7 T_{\rm th}$. At RHIC, minijet production is on the level of the soft particle production so that the hard component is responsible for only $\approx 40\%$ of the particle production. Thus the system is even further from equilibrium.

Finally, we note that shadowing effects can smear the $E_T - b$ correlation, particularly at RHIC, making the determination of b from E_T less precise.

*from V. Emel'yanov, A. Khodinov, S.R. Klein and R. Vogt, LBNL-42900, in preparation for Phys. Rev. C.

Nuclear Parton Distributions

parton i in nucleus A:

$$F_i^A(x, Q^2, \vec{r}, z) = \rho_A(s)\, S^i(A, x, Q^2, \vec{r}, z)\, f_i^N(x, Q^2)$$

$f_i^N(x, Q^2)$: free proton parton distributions

GRV 94 LO and MRS A' (fig)

Woods-Saxon nuclear density distribution

$$\rho_A(s) = \rho_0 \frac{1 + w(s/R_A)^2}{1 + \exp\left[\frac{s - R_A}{d}\right]} \qquad s = \sqrt{r^2 + z^2}$$

Shadowing parameterizations based on fits to nuclear DIS

-- measures b-average modification (fig)

$S_1 \equiv S_1(A, x)$ $q, \bar{q}, g$ same, no Q^2 evolution (Eskola, Qiu, Czyzewski)

$S_2 \equiv S_2^i(A, x, Q^2)$ based on Duke-Owens, $q_V = u_V + d_V$, $q_S = \bar{u} + \bar{d} + \bar{s}$ and G evolved over $2 < Q < 10$ GeV (Eskola)

$S_3 \equiv S_3^i(A, x, Q^2)$ based on GRV LO, each parton density evolved separately $1.5 < Q < 100$ GeV (Eskola, Kolhinen, Ruuskanen)

Impact parameter dependence

- local nuclear density

$$S_{WS}^i = 1 + N_{WS}\left[S^i(A, x, Q^2) - 1\right] \frac{\rho_A(s)}{\rho_0}$$

- parton path

$$S_R^i = \begin{cases} 1 + N_R\left[S^i(A, x, Q^2) - 1\right]\sqrt{1 - (r/R_A)^2} & r \le R_A \\ 1 & r > R_A \end{cases}$$

- normalized so that $\frac{1}{A}\int d^2r\, dz\, \rho_A(s)\, S_{WS,R}^i = S^i$
- larger than average modifications for $b = 0$
- $s \gg R_A$, nucleons are like free protons

Shadowing Parameterizations

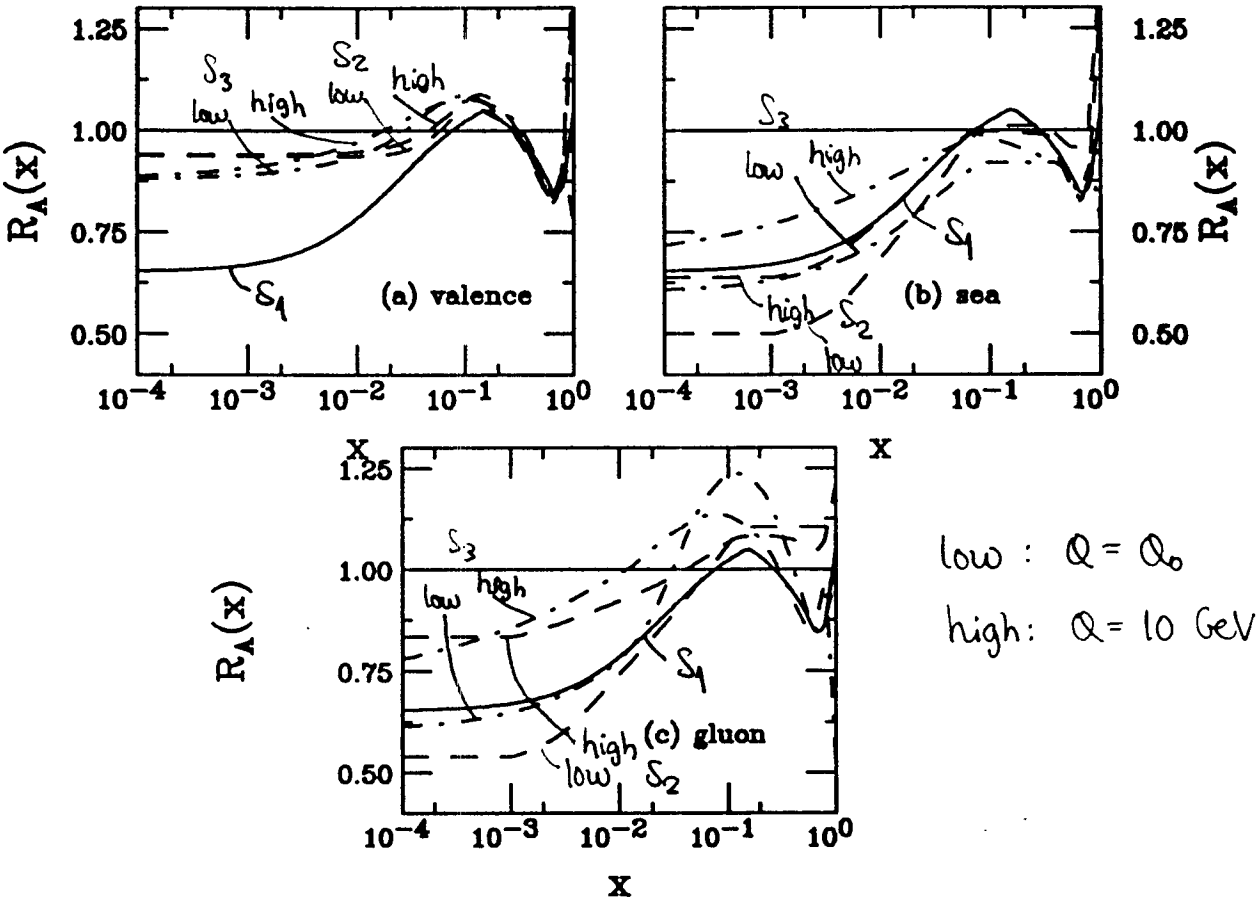

low : $Q = Q_0$

high: $Q = 10$ GeV

- 'saturation' in ratio at low x in S_1 and S_2, not S_3
- evolution strongest for gluon
- sea quarks shadowed around $x \sim 0.1$ in S_3, unmodified with S_2
- gluon antishadowing in all parameterizations – most significant for S_3
- gluon ratio mainly determined by conservation rules, not data

Impact Parameter Dependence of Shadowed first E_T moments relative to $S=1$ GRV 94 LO STAR acceptance → PHENIX similar

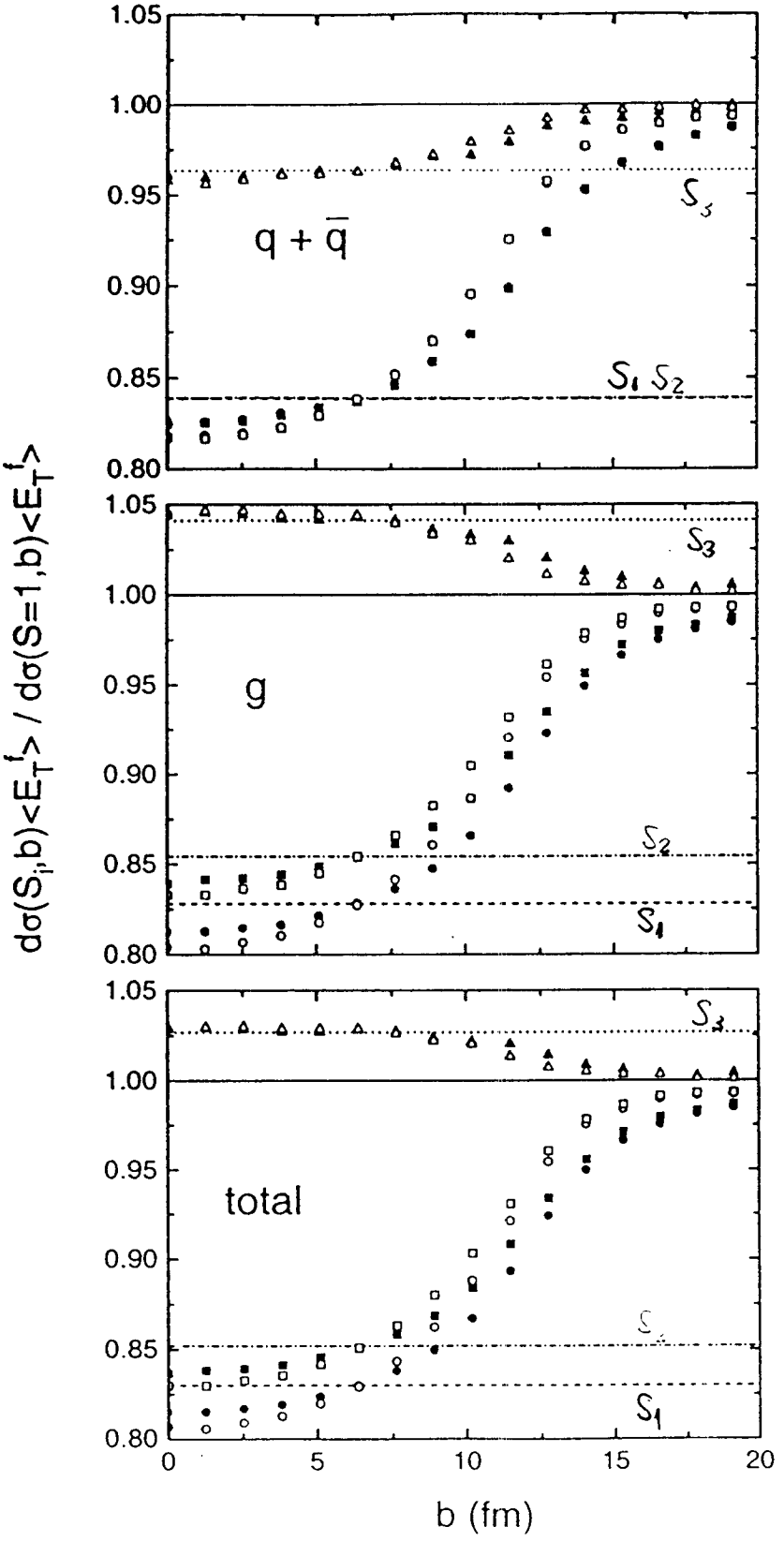

Thermalization ?

- Minijet moments depend strongly on p_0, may be determined from transverse saturation

$$\frac{\pi \bar{N}_{AB}}{b^2} > \pi R_A^2$$

$$\sigma_{PbPb}(\sqrt{s_{NN}}, p_0) > 74 \left(\frac{p_0}{2\,GeV}\right)^2 mb$$

$$\sigma_{AuAu}(\sqrt{s_{NN}}, p_0) > 71 \left(\frac{p_0}{2\,GeV}\right)^2 mb$$

transverse saturation at $\sqrt{s_{NN}} = 5.5$ TeV with $p_0 = 2$ GeV

$p_0 \approx 1$ GeV needed for RHIC (200 GeV) → sof physics still dominates

- Initial energy and number densities

$$\varepsilon_i^f(b, \sqrt{s_{NN}}, p_0) = \frac{\bar{E}_T^f(b, \sqrt{s_{NN}}, p_0)}{V_i}$$

$$n_i^f(b, \sqrt{s_{NN}}, p_0) = \frac{\bar{N}_{AB}^f(b, \sqrt{s_{NN}}, p_0)}{V_i}$$

$$\frac{\varepsilon_i^f}{n_i^f} \approx 3\,GeV > p_0$$

- What about an ideal gas?

$$\varepsilon_{th} = 3a T_{th}^4$$

$$n_{th} = \frac{s_{th}}{3.6} = \frac{4a T_{th}^3}{3.6}$$

$a = 16\pi^2/90$ gluons

$47.5\pi^2/90$ gluons + 3 quark flavors

$$\frac{\varepsilon_{th}}{n_{th}} = 2.7\, T_{th}$$

T_{th} extracted from calculations with $p_0 = 2$ GeV, GRV 94 LO

	LHC		RHIC	
	g	tot.	g	tot.
$S=1$	1.1 GeV	800 MeV	410 MeV	330 MeV
$S \neq 1$	reduced 10-17%		reduced < 5%	

$\frac{\varepsilon_i^g}{n_i^g}\Big|_{S=1} \approx \frac{\varepsilon_{th}}{n_{th}}$ but $S \neq 1$ $\frac{\varepsilon_i^g}{n_i^g} > \frac{\varepsilon_{th}}{n_{th}} = 2.7$

Shadowing makes equilibration less likely, even at LHC

Conclusions

- Semihard minijet production dominates production at LHC, even with shadowing included
- At RHIC minijets are only responsible for $\approx 40\%$ of particle production
- Shadowing is stronger in central collisions, weaker in peripheral collisions so it is difficult to compare data from different regions without taking this into account
- Shadowing drives system away from thermalization at LHC no early thermalization at RHIC
- E_T distributions strongly influenced by shadowing at LHC, weaker at RHIC
- Impact parameter dependence of shadowing could smear E_T-impact parameter correlation, particularly at RHIC

Small x, Hard Subcollisions and Hard-Soft Interface

Gösta Gustafson
Coll. with B. Andersson, J. Samuelsson, H. Kharraziha
L. Lönnblad, M. Rignér, P. Edén, P. Sutton

Summary

The **Linked Dipole Chain** model interpolates smoothly between large x and small x

A unified treatment of "normal" DIS, boson-gluon fusion, hard γp or hh scattering

Suitable for MC simulations. It can include running α_s and some non-leading effects

$\sigma_{incl.}(\text{jet})$ expressed in terms of non-integrated structure fcns, $\mathcal{F}(x, k_t^2)$, does not blow up for small p_t.

Can describe multiple hard collisions in a single chain. These correlated subcollisions contribute significantly to the multiple collision rate, and for larger p_t they are correlated in rapidity.

Hard-Soft transition:

Flux tube ~ helix ~ massive string ?

Linked Dipole Chain model

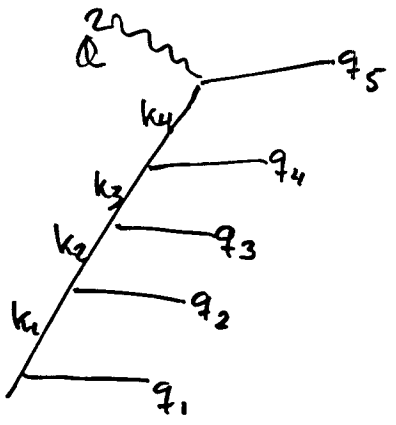

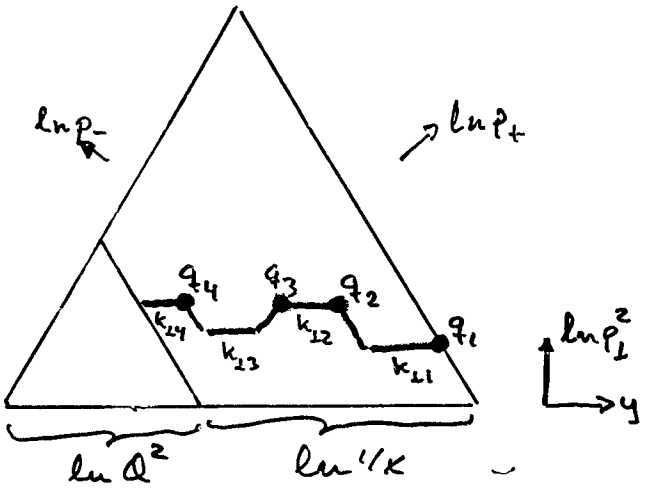

Allowed initial state rad. chains have $q_{\perp i} \approx \max(k_{\perp i}, k_{\perp i-1})$ and are ordered in q_+ and q_-.

Contribution from each such chain:

$$\mathcal{P}_i \sim \frac{dz_i}{z_i} \frac{d^2 q_{\perp i}}{\pi q_{\perp i}^2}$$

Expressed in link momenta k_i we have

$$d^2 q_{\perp i} = d^2 k_{\perp i} \quad ; \quad q_{\perp i}^2 = \max(k_{\perp i}^2, k_{\perp i-1}^2)$$

$\Rightarrow$ step up, $k_{\perp i} > k_{\perp i-1} \Rightarrow \dfrac{d^2 q_{\perp i}}{q_{\perp i}^2} \approx \dfrac{d^2 k_{\perp i}}{k_{\perp i}^2}$

step down, $k_{\perp i} < k_{\perp i-1} \Rightarrow \dfrac{d^2 q_{\perp i}}{q_{\perp i}^2} \approx \dfrac{d^2 k_{\perp i}}{k_{\perp i}^2} \cdot \underbrace{\dfrac{k_{\perp i}^2}{k_{\perp i-1}^2}}_{\text{extra suppr. factor}}$

Note: 1) Fully left-right symmetric

2) Local maximum 

$\Rightarrow \dfrac{1}{k_{\perp max}^4}$

Hard subcollision

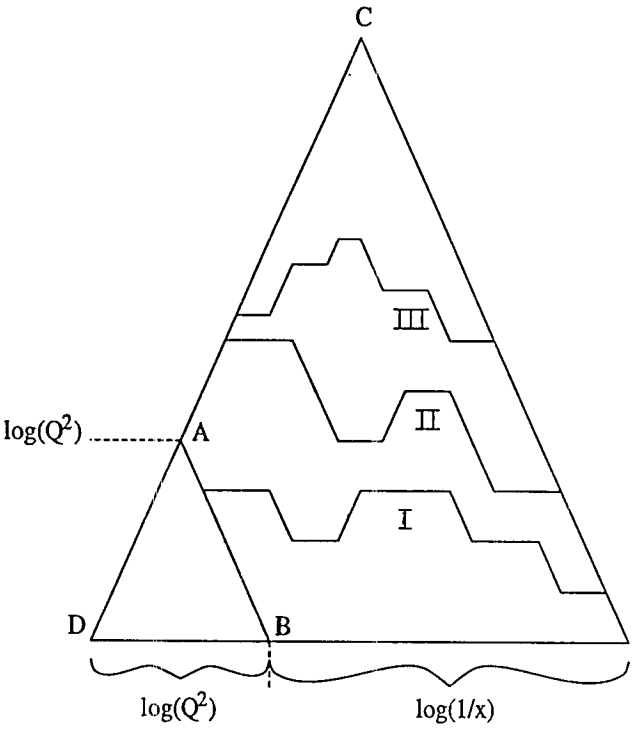

Figure 16: *Three different types of gluon chains.*

Different types of reactions described in the same formalism

I: "Normal" DIS

II: Boson-gluon fusion. $k_{\perp final}^2 > Q^2$

III: Hard γp scattering.

$$k_{\perp max}^2 > k_{\perp final}^2 \; (> Q^2)$$

MC program developed by Leif Lönnblad and Hamid Kharraziha

Inclusive jet cross section properly expressed in terms of non-integrated structure functions $\mathcal{F}(x, k_\perp^2)$

$$F(x, Q^2) = \int^{Q^2} \frac{dk_\perp^2}{k_\perp^2} \mathcal{F}(x, k_\perp^2) + \text{suppressed contrib. for } k_\perp^2 > Q^2$$

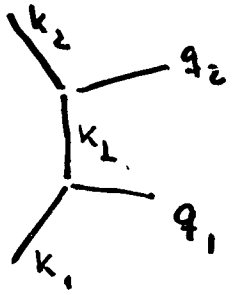

Suppressed for small $k_\perp$

$$\frac{d\sigma^{incl}}{dq_\perp^2} \sim \int \tilde{\mathcal{F}}(x_1, k_{\perp 1}^2)\, \tilde{\mathcal{F}}(x_2, k_{\perp 2}^2)\, \frac{d\hat{\sigma}}{dq_\perp^2}(q_\perp^2, k_{\perp 1}^2, k_{\perp 2}^2, \hat{s} = s x_1 x_2)$$

For $k_{\perp 2} > k_{\perp 1}$ we get:

$$\frac{d\hat{\sigma}}{dq_\perp^2} \sim \frac{2}{q_\perp^4} \cdot \Theta(q_\perp^2 - k_{\perp 2}^2)\, \Theta(\hat{s} - q_\perp^2) +$$

$$+ \frac{1}{q_\perp^2 k_{\perp 2}^2} \cdot \Theta(q_\perp^2 - k_{\perp 1}^2)\, \Theta(k_{\perp 2}^2 - q_\perp^2) +$$

$$+ \delta(q_\perp^2 - k_{\perp 2}^2) \left[\frac{1}{k_{\perp 2}^2} \ln \frac{k_{\perp 2}^2}{k_{\perp 1}^2} + \frac{1}{k_{\perp 2}^2} - \frac{1}{\hat{s}} \right] +$$

$$+ \delta(q_\perp^2 - k_{\perp 1}^2) \left[\frac{1}{k_{\perp 2}^2} - \frac{1}{\hat{s}} \right]$$

Multiple scattering in single chain

Only preliminary results

For a purely gluonic chain at $x \sim 10^{-4}$:

5-10% of the chains contain

2 or more hard Rutherford subcollisions with $k_\perp > 1$ GeV

Deep valleys suppressed => For larger $k_\perp$ the hard subcollisions get more correlated and come closer in rapidity

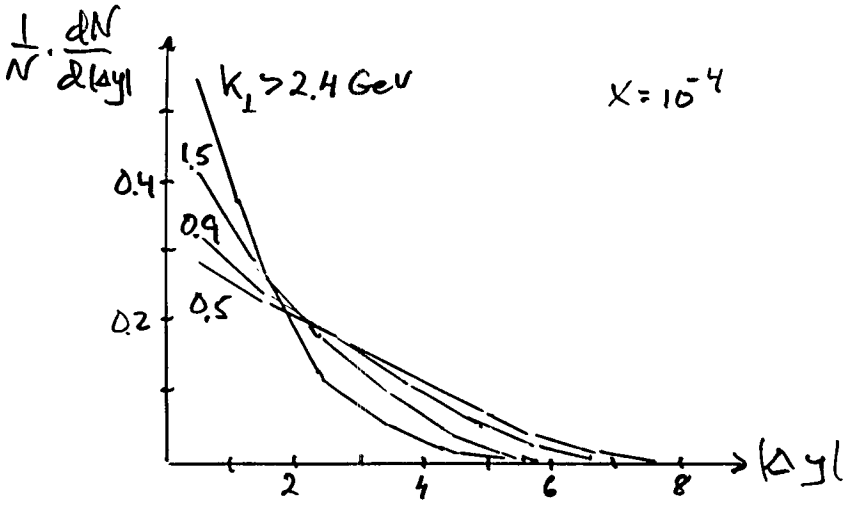

Perturbative - nonpert. interface

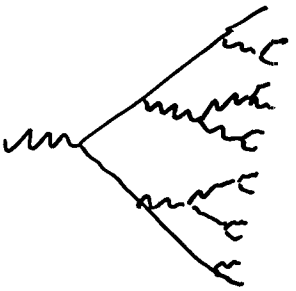

End of cascade: α_s large

⇒ emitted gluons harder than emitters after recoils.

⇒ A different tree diagram should be more important.

⇒ Interference and non-tree diagrams essential.

Coherent state? Ladder-like cascade?

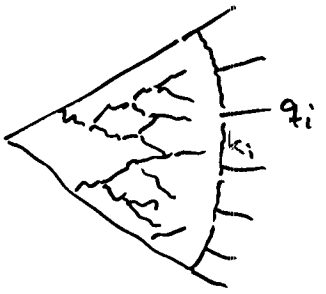

$q_i^2 = 0$; $k_i^2 \approx -m^2$

Simple solution: Helix

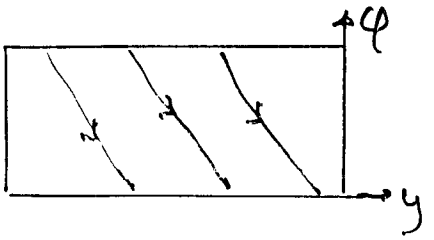

Similarities to a massive string or a string coupled to a gauge field

Observable "screwiness". Appears to be too simple

X.N. Wang

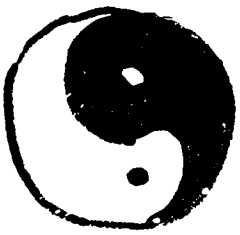

HIJING Monte Carlo

Modeling pp . pA . AtA Collisions

1) purpose & limitation

2) modeling hard & semi-hard & soft processes

3) Uncertainty & parameters

4) "Redictions" for RHIC

With M. Gyulassy. 90

Y. Pang 92 (cascade)

S. Vance 97 (Baryon)

What's New:

1) Latest PDF's

originally used DO Set.

2) Re-adjust parameters

$\sqrt{s} = 200$ GeV	DC1	GRV	MRSD'
P_0	2.0	2.2	2.1c
σ_{jet}	11.50 (mb)		
σ_{tot}	51.3 (mb)		

3) push to SPS (almost its limit)

4) new shadowing

(bomb shell from Fiala

5) Jet quenching (improved)*

6) Baryon Junction & hadron cascade

$b \leq 3$ fm Au+Au

$b \leq 3$ fm

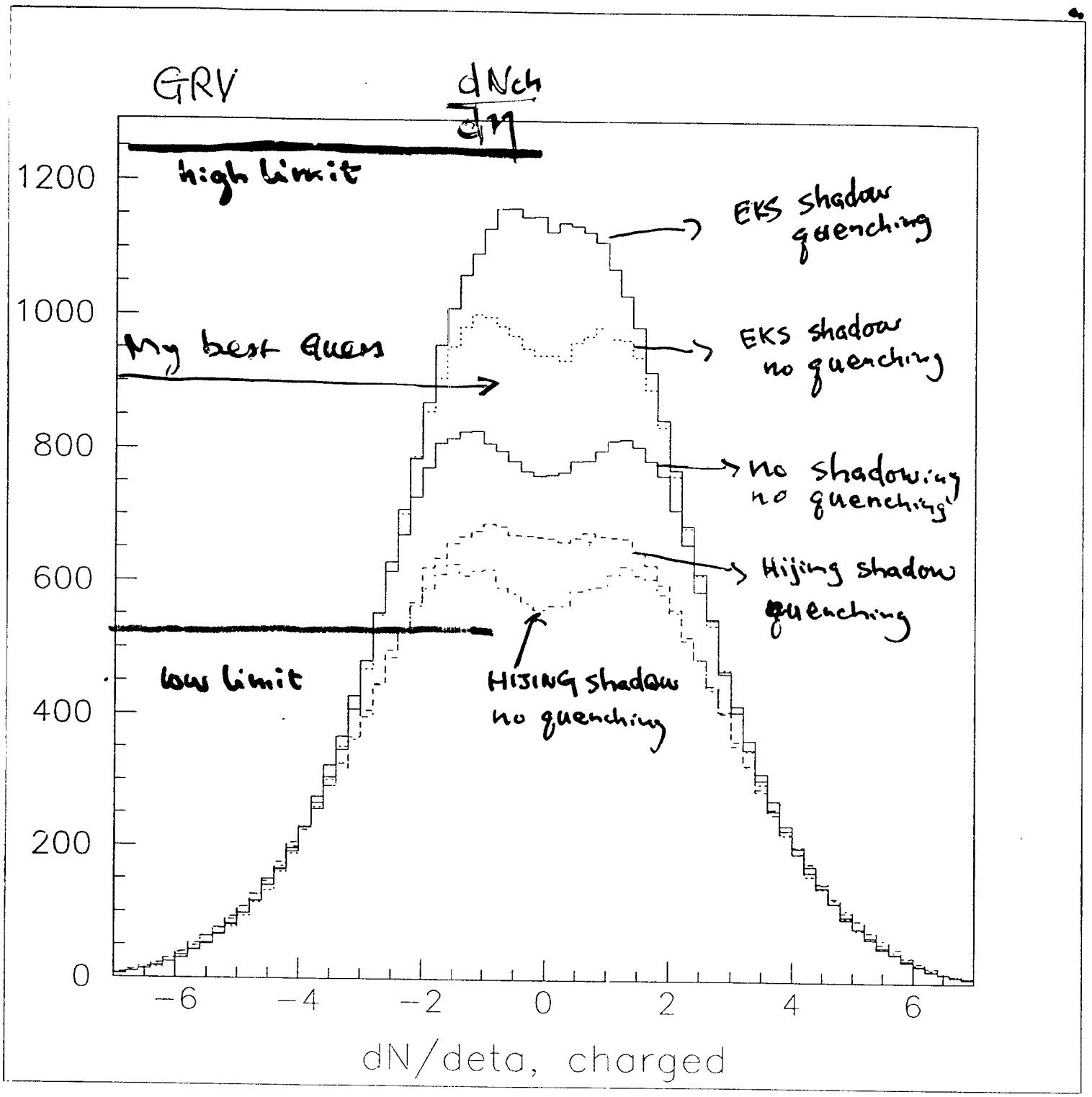

no plateau in $\frac{dN_{ch}}{dy}$

Lowest limit on $\frac{dn_{ch}}{d\eta}$

$$\frac{dn_{ch}^{AA}}{d\eta} \Big/ \frac{dn_{ch}^{pp}}{d\eta}(\sqrt{s}=200) = \frac{dn_{ch}^{AA}}{d\eta} \Big/ \frac{dn_{ch}^{pp}}{d\eta}(\sqrt{s}=20)$$

$$\frac{dn_{ch}^{Au+Au}}{d\eta} \cong 550$$

High limit

$$\frac{dn_{ch}^{AA}}{dy} = \frac{N_{wound}}{2} n_{soft}^{pp} + N_{binary} n_{hard}^{pp}$$

$$\simeq 1250$$

VNI

- Version 4.1 -

Simulation of high-energy particle collisions in QCD:

Space-time evolution of collision dynamics with

- parton-cascades -
- cluster-hadronization -
- final-state hadron cascades-

Klaus Geiger - Ron Longacre - Dinesh Srivastava

Physics Department, Brookhaven National Laboratory, Upton, N.Y. 11973, U.S.A.

Variable Energy Cyclotron Centre, 1/AF Bidhan Nagar, Calcutta 700 064, India

e-mail: klaus@bnl.gov, longacre@bnl.gov, dks@vecdec.veccal.ernet.in

phone: (516) 344-3791
fax: (516) 344-2918

c) parton-cluster formation, hadronization, hadron cascade development

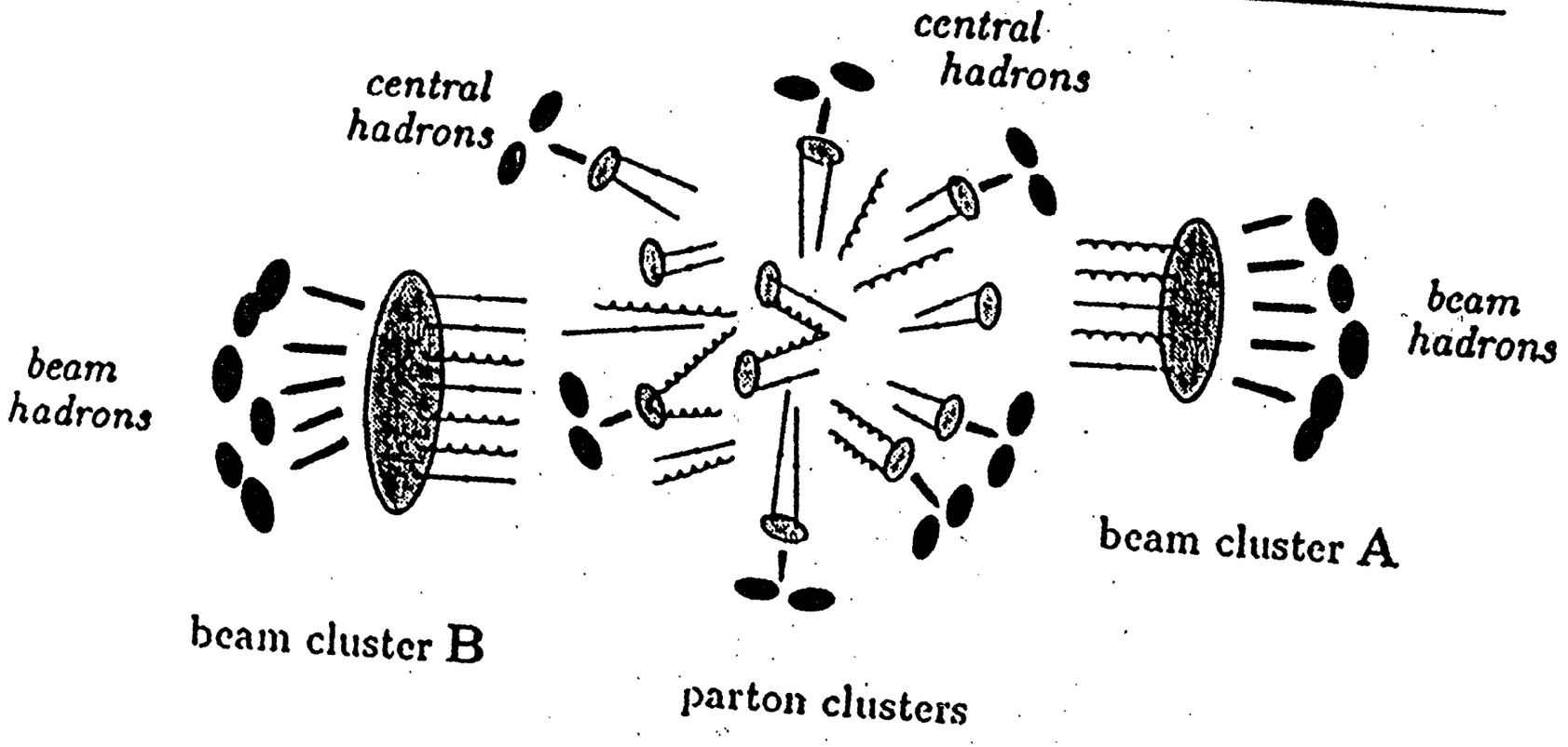

$$k \cdot \frac{\partial}{\partial r} F_h \;=\;$$

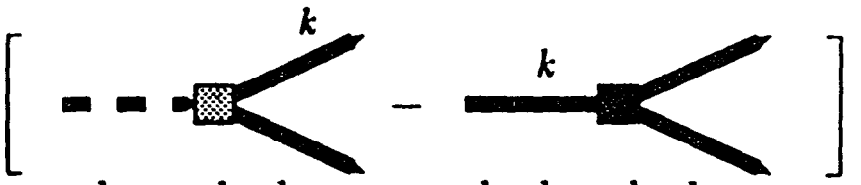

cluster-hadron decay — hadron-hadron decay

$+$

hadron-cluster scattering

$+$

hadron-hadron scattering

$+$

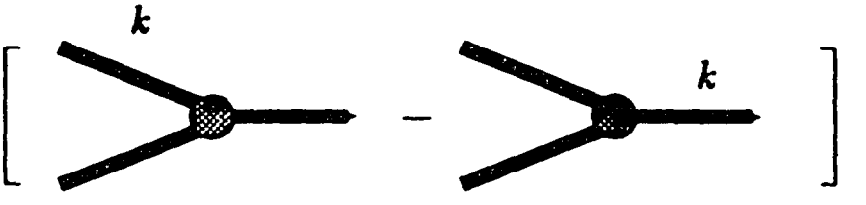

hadron-resonance formation

$+ \;\ldots\ldots\ldots\ldots$

$$k^2 \frac{\partial}{\partial k^2} F_h \;\approx\; 0$$

$$k \cdot \frac{\partial}{\partial r} F_c \;=\;$$

parton-cluster coalescence — cluster-hadron decay

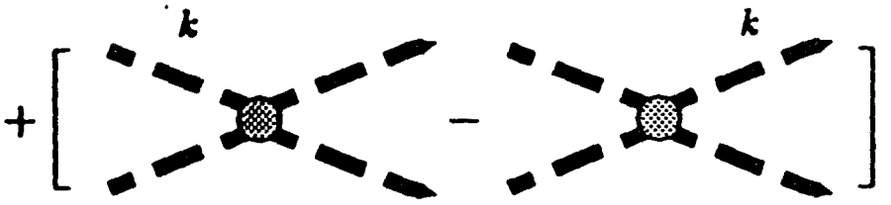

cluster-cluster scattering

cluster-hadron scattering

$+ \;\ldots\ldots\ldots\ldots$

$$k^2 \frac{\partial}{\partial k^2} F_c \;\approx\; 0$$

$NN \rightarrow NN$
$NN \rightarrow N\Delta$
$NN \rightarrow \Delta\Delta$

.
.
.

$\Delta N \rightarrow \Delta N$
$\Delta N \rightarrow NN$
$\Delta N \rightarrow \Delta\Delta$

.
.
.

$\Lambda N \rightarrow \Lambda N$
$\Lambda N \rightarrow \Sigma N$
$\Lambda N \rightarrow \Xi KN$
$\Sigma N \rightarrow \Xi KN$

.
.
.

<u>Isobars</u>

$\pi N \rightarrow N^*$	$KN \rightarrow Y^*$	$K\Delta \rightarrow Y^*$	$\rho\pi \rightarrow a_1$
$\Delta\pi \rightarrow N^*$	$\Lambda\pi \rightarrow Y^*$	$\Lambda\rho \rightarrow Y^*$	
$\rho N \rightarrow N^*$	$\Sigma\pi \rightarrow Y^*$	$\Sigma\rho \rightarrow Y^*$	

$N^*N \rightarrow NN$	$NN \rightarrow N^*N$
$N^*N \rightarrow \Delta N$	$\Delta N \rightarrow N^*N$
$Y^*N \rightarrow \Lambda N$	$\Lambda N \rightarrow Y^*N$
$Y^*N \rightarrow \Sigma N$	$\Sigma N \rightarrow Y^*N$

$N\pi \rightarrow N\pi$
$N\pi \rightarrow \Delta$
$N\pi \rightarrow \Delta\pi$
$N\pi \rightarrow N\rho$
$N\pi \rightarrow N\eta$
$N\pi \rightarrow \Lambda K$
$N\pi \rightarrow \Sigma K$

$\Delta\pi \rightarrow N\pi$
$\Delta\pi \rightarrow \Delta\pi$
$\Delta\pi \rightarrow N\rho$
$\Delta\pi \rightarrow \Lambda K$
$\Delta\pi \rightarrow \Sigma K$

$N\rho \rightarrow N\pi$
$N\rho \rightarrow N\rho$
$N\rho \rightarrow \Lambda K$
$N\rho \rightarrow \Sigma K$

$KN \rightarrow KN$
$KN \rightarrow K\Delta$
$KN \rightarrow KN\pi$
$K\Delta \rightarrow KN$
$K\Delta \rightarrow K\Delta$
.
.
.
.
.

$\bar{K}N \rightarrow \bar{K}N$
$\bar{K}N \rightarrow \Lambda\pi$
$\bar{K}N \rightarrow \Lambda\pi\pi$
$\bar{K}N \rightarrow \Sigma\pi$
$\bar{K}N \rightarrow \Sigma\pi\pi$
$\bar{K}N \rightarrow \bar{K}N\pi$
$\bar{K}N \rightarrow \bar{K}\Delta$
$\bar{K}\Delta \rightarrow \bar{K}N$
$\bar{K}\Delta \rightarrow \bar{K}\Delta$
$\bar{K}\Delta \rightarrow \Lambda\pi$
$\bar{K}\Lambda \rightarrow \Xi N$
$\bar{K}N \rightarrow \Xi K$

.
.
.

$\pi^+\pi^- \rightarrow \pi^+\pi^-$
$\pi^+\pi^- \rightarrow \pi^0\pi^0$
$\pi^+\pi^- \rightarrow K^0\bar{K}^0$
$\pi^+\pi^- \rightarrow \eta\eta$

$\pi^0\pi^0 \rightarrow \pi^0\pi^0$

$\pi^+\pi^0 \rightarrow \pi^+\pi^0$

$\pi^-\pi^0 \rightarrow \pi^-\pi^0$

$\pi^- p \rightarrow \pi^+\pi^- n$ (OPE) ;
$\pi^- p \rightarrow K^+K^- n$ (OPE);
$\pi^- p \rightarrow K_s K_s n$ (OPE);
$\pi^- p \rightarrow \eta\eta n$ (OPE);

$\pi K \to K\pi$	$K^- p \to K^- \pi^+ n$ (OPE)
$\pi K \to K\pi\pi$	$K^- p \to K_s \pi^+ \pi^- n$ (OPE)
$\pi K \to K\pi\pi\pi$	$K^- p \to K^- \pi^+ \pi^- \pi^+ n$ (OPE)

$K\bar{K} \to K\bar{K}$	
$K\bar{K} \to \pi\pi$	
$K\bar{K} \to \eta\eta$	$\underline{K\bar{K}}$ form $f_0(975)$, $a_0(980)$, $\phi(1020)$, $f_2(1270)$
$K\bar{K} \to \eta\pi$	$a_2(1320)$, $f_2(1525)$
$K\bar{K} \to \rho\pi$	

$\rho\pi \to \rho\pi$	
$\rho\pi \to K\bar{K}$	$\underline{\rho\pi}$ form $h_1(1170)$, $a_1(1260)$, $a_2(1320)$
$\rho\pi \to \eta\pi$	

$K^*\pi \to K^*\pi$	$\underline{K^*\pi}$ form $K^*(1420)$
$K^*\pi \to K\pi$	

$a_1\pi \to \pi\pi$	$\underline{a_1\pi}$ form $\rho(1700)$, $f_2(1800)$
$a_1\pi \to a_1\pi$	

$\omega\pi \to \omega\pi$	$\underline{\omega\pi}$ form $b_1(1235)$

$\eta\pi \to \eta\pi$	$\underline{\eta\pi}$ form $a_0(980)$, $a_2(1320)$
$\eta\pi \to K\bar{K}$	

Interplay between hard and soft physics in AA collisions at RHIC

H. Sorge
Department of Physics and Astronomy , SUNY at Stony Brook

Abstract

I discuss uncertainties of the initial entropy production in central nucleus-nucleus collisions at collider energies. Independent whether one considers dominance of soft or semi-hard production of particles estimates may vary in a wide range, between $\sim A$ up to $A^{4/3}$. Dynamics depends strongly on this number, because it determines how deep in the quark-gluon phase initial state at RHIC is produced. Non-central collisions and a novel "jettiness" observable may provide clues about hard versus soft reaction mechanisms, e.g. jet (non-)quenching versus hydrodynamic flow and amount of equilibration achieved in the reactions.

charged hadrons

RHIC

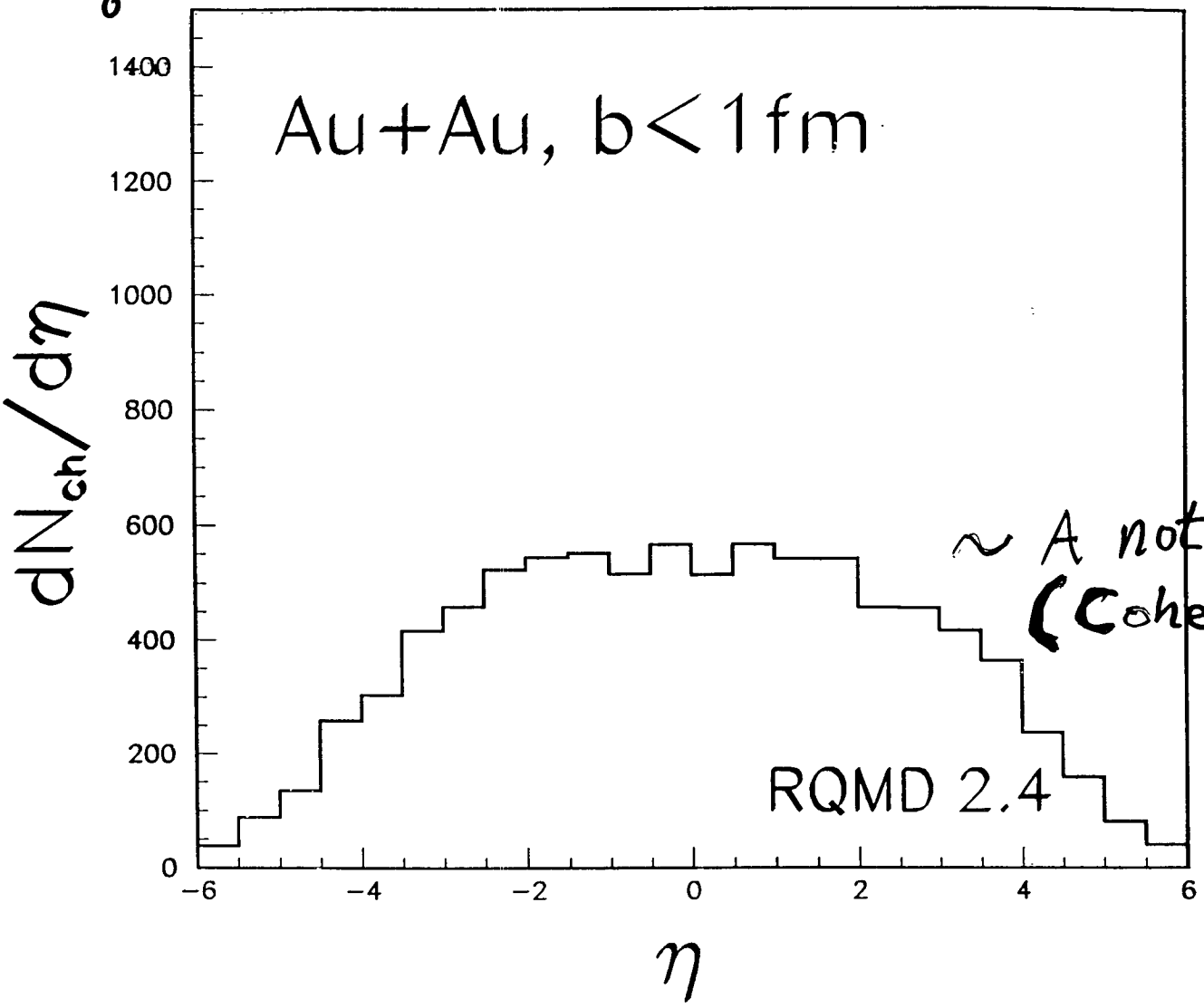

$\sim A$ not $A^{4/3}$ (Coherence)

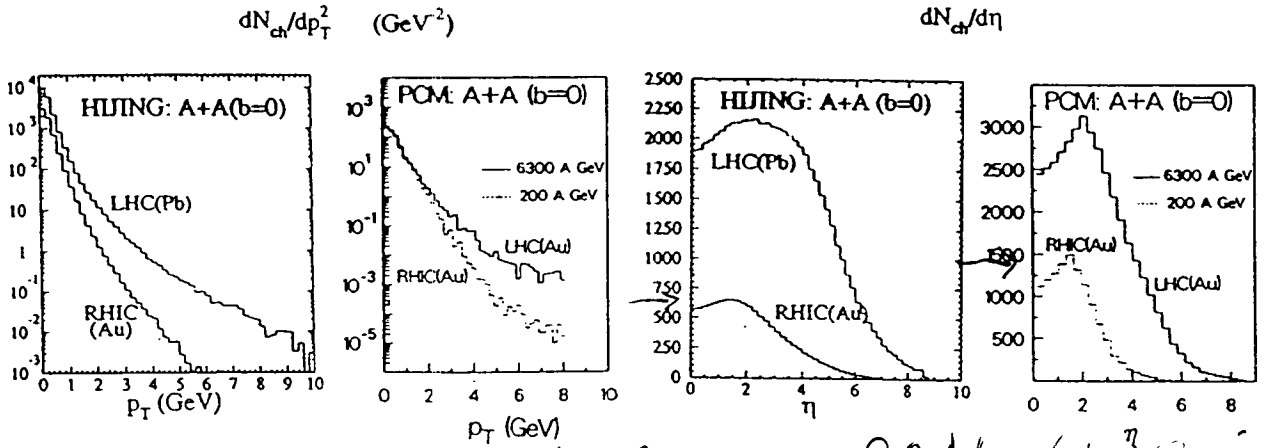

HIJING (X.N. Wang)

PCM (K. Geiger B. Mueller)

In AA:
responsible for
$\sim A^{4/3}$

$$\frac{d\sigma}{dy\,d^2p_t} = \sum_{\substack{a,b \\ c,d}} \int dx_a \int dx_b \; f_a(x_a, Q^2)\, f_b(x_b, Q^2) \cdot \frac{d\hat{\sigma}}{d\hat{t}}(ab \to cd)\, D_{h/c}(\,)$$

most of produced partons are rather soft:

$2 \to 2$

$2 \to 3$

$2 \to 4$

$\vdots$

convergence?

cross section

$gg \to (n-2)\,g$

tree diagrams (PT)

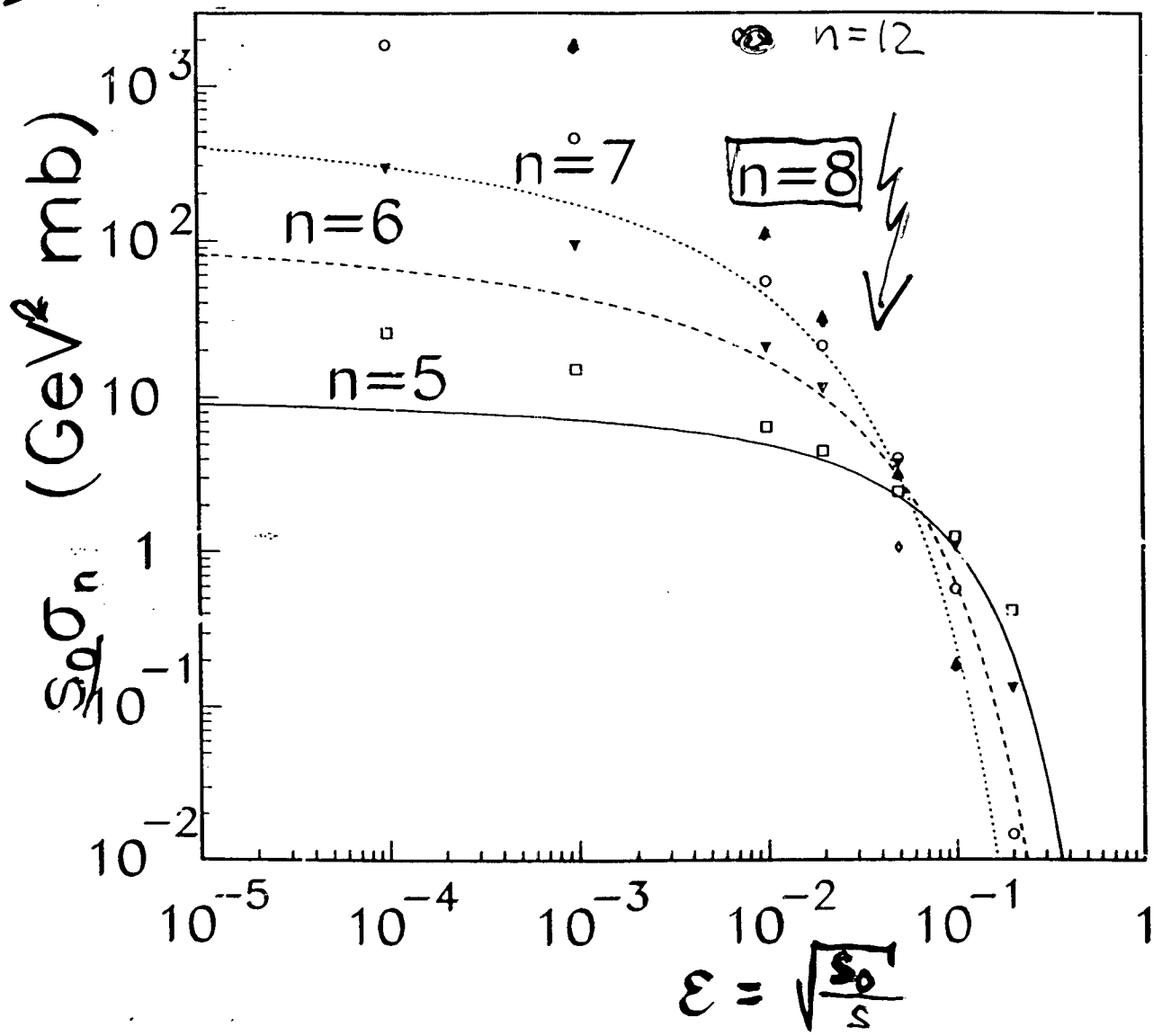

s_0 : the only dimensionful parameter

Cutoff : subenergies $s_{gg} > s_0$

Jet quenching scenario

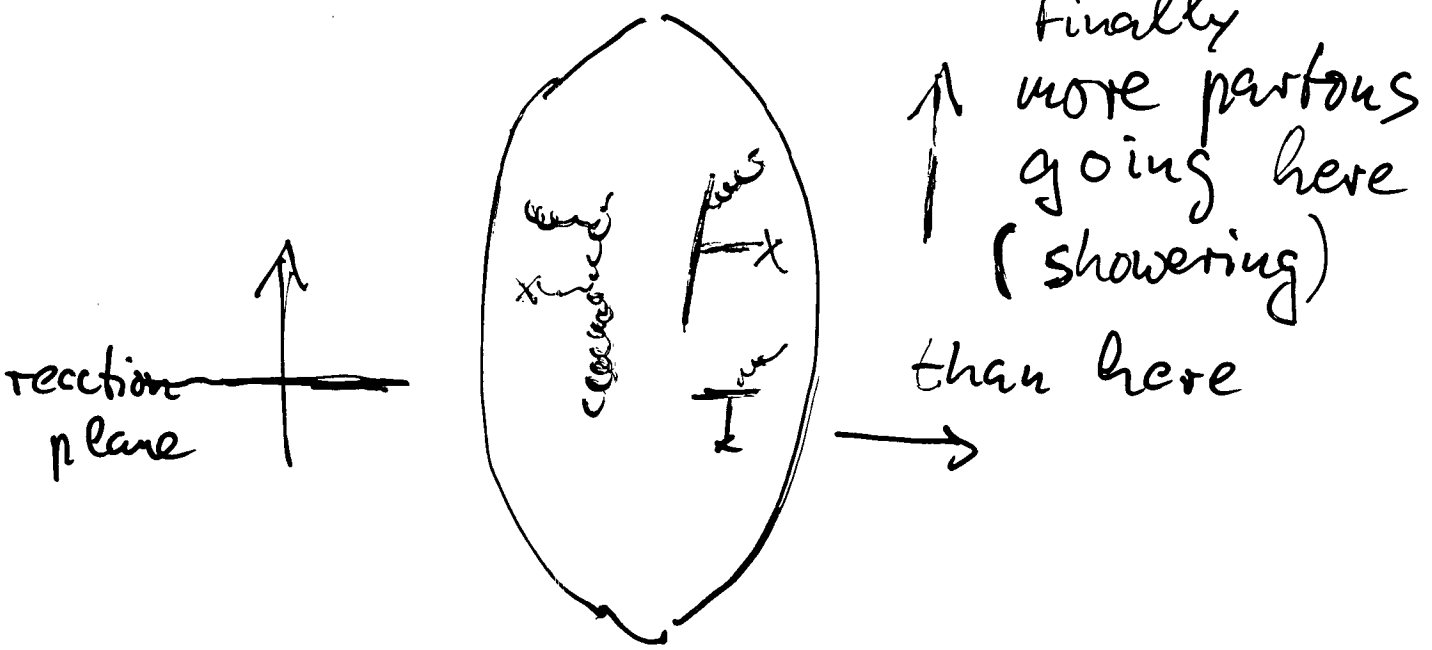

↳ azimuthal asymmetry in momentum space

$$\frac{dN}{d^2p_t} \sim 1 + \sum_{n=1}^{\infty} 2v_n \cos(n\phi)$$

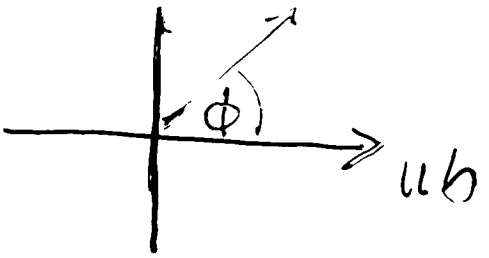

"Jettiness" of Heavy-Ion State: How to measure

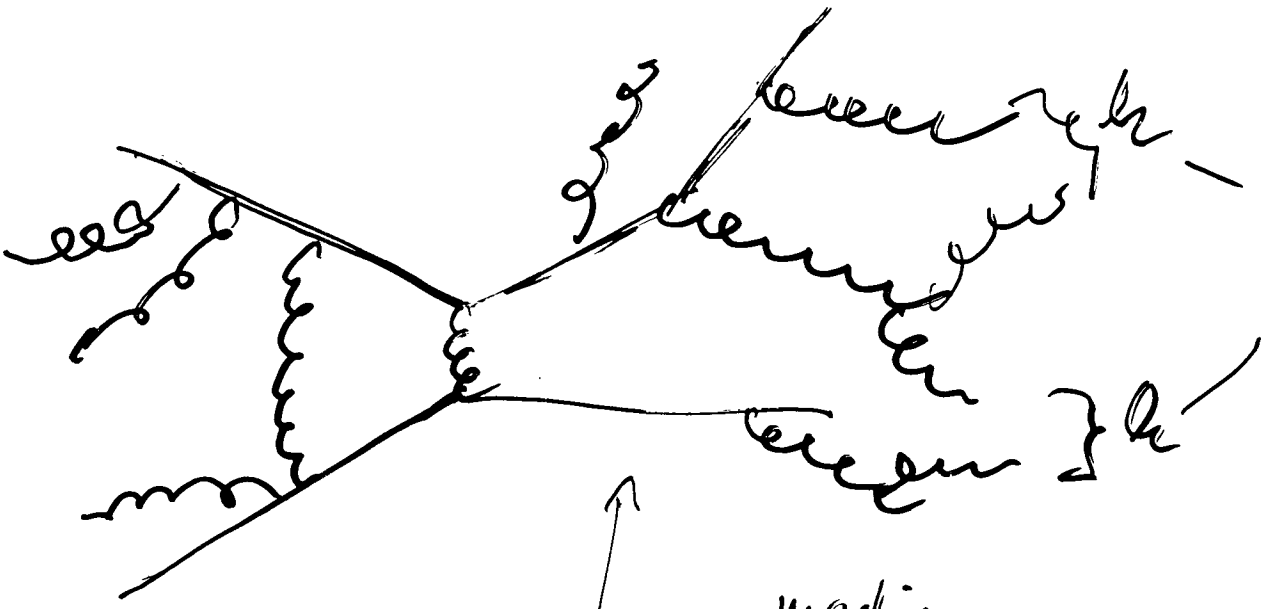

initial state (under "control")

medium effect

Question: How local in (η, ϕ) is large p_t of final hadron compensated? How many hadrons are involved

Measure:

$$x_{comp} = \frac{1}{p_t^{\wedge}} \sum_{h}^{\text{cut in } \eta} \left(|p_t^{\perp}| - |p_t''| \right)(h)$$

trigger particle

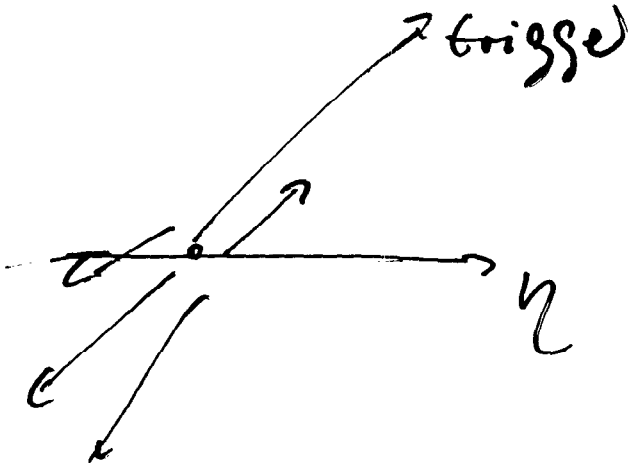

$x_{comp} < 0$

Surprise : RQMD looks "jettier" than HIJING

Examples:

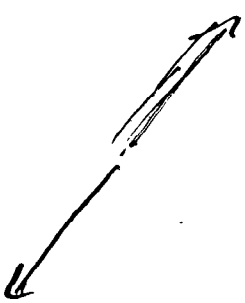

$x_{comp} = -1$

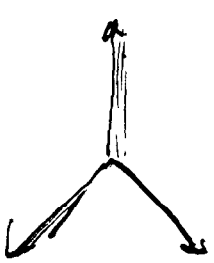

$x_{comp} = 0$

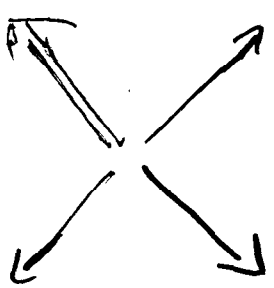

$x_{comp} > 0$

A Low-brow Look at the Centrality Dependence of Hard Scattering Rates and Quenching in A-A and p-A Collisions

Brian A. Cole
Columbia University

Riken Hard-Scattering Workshop
March 5, 1999

Outline

1. Introduction
2. A+A Hard scattering rates
3. Quenching & Geometry
4. Measuring centrality in p-A collisions

Hard Scattering Rates

Calculation

- Calculate an "unnormalized" rate: $R = \iint dxdy T_A(x,y) T_B(x,y)$
  - Independent of process, multiply by σ to get actual rate
- Plot vs b for various A

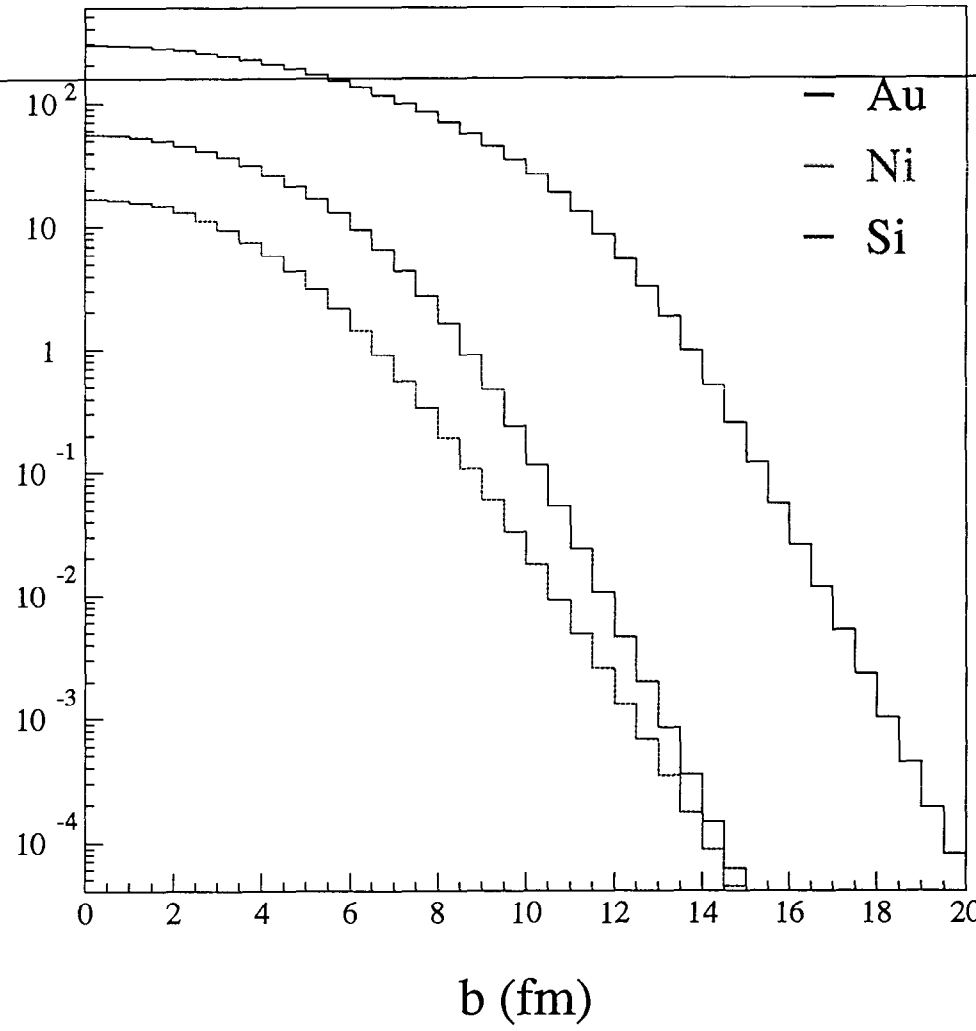

Observations

- Rates relatively flat
  - for Au up to 10 fm
  - for Si up to 5 fm
- Feasible to study centrality dependence out to large b
- Factor ~ 10 difference between Au, Si at b=0
  - more than x A

Hard Scattering Rates vs # spectators

Study vs experimental centrality measure: E^0

- At point (x,y) in transverse plan, a projectile nucleon has probability to be spectator $P^A_{spec} \approx e^{-\bar{\nu}} = e^{-\sigma_{NN} T_B(x,y)}$
- So, the total number of projectile spectators is
  - $N^A_{spec} \approx \iint dx dy T_A(x,y) e^{-\sigma_{NN} T_B(x,y)}$

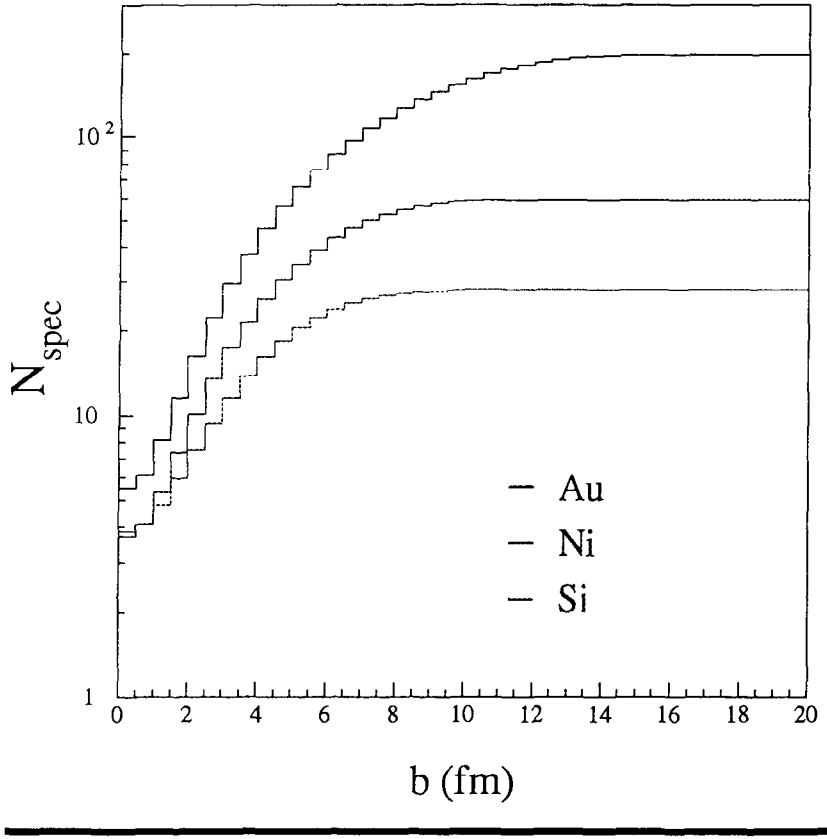

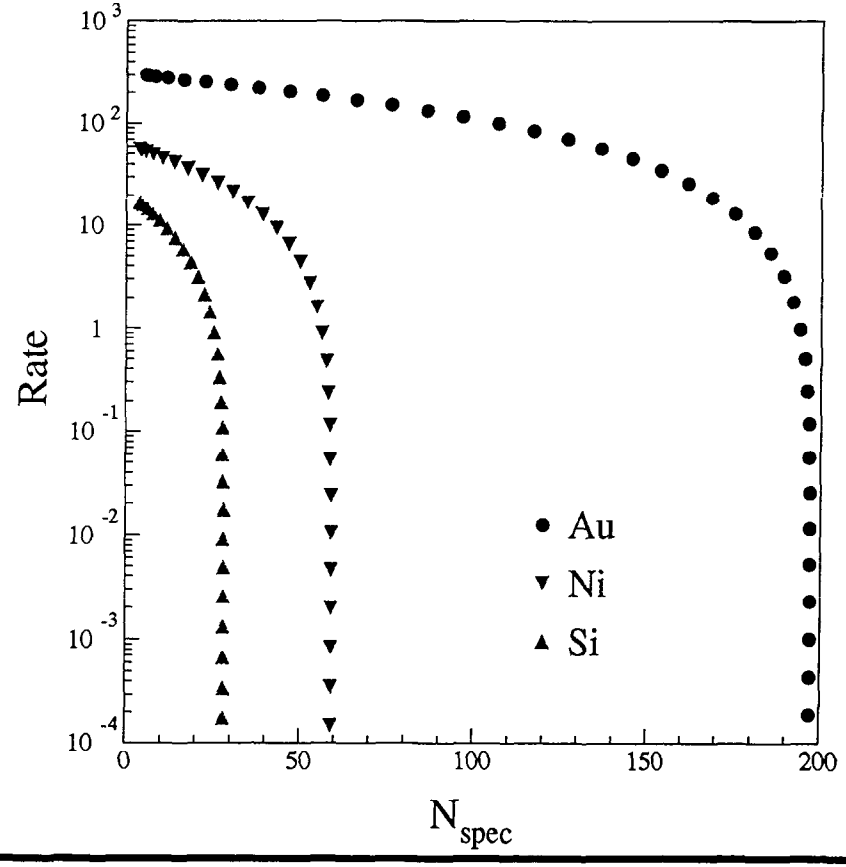

Geometry of Jets and Quenching (2)

Study paths of Quarks out of System

- Study only propagation in the transverse plane
- Use simplest possible set of physically sensible assumptions
  - Assume all hard processes including mini-jets occur instantaneously
  - $dE/dx \propto \varepsilon$ - energy density , $\varepsilon(x, y) \propto (T_A \bullet T_B)(x,y)$
- So, for a quark leaving system $\Delta E \propto \int ds T_A T_B(s)$

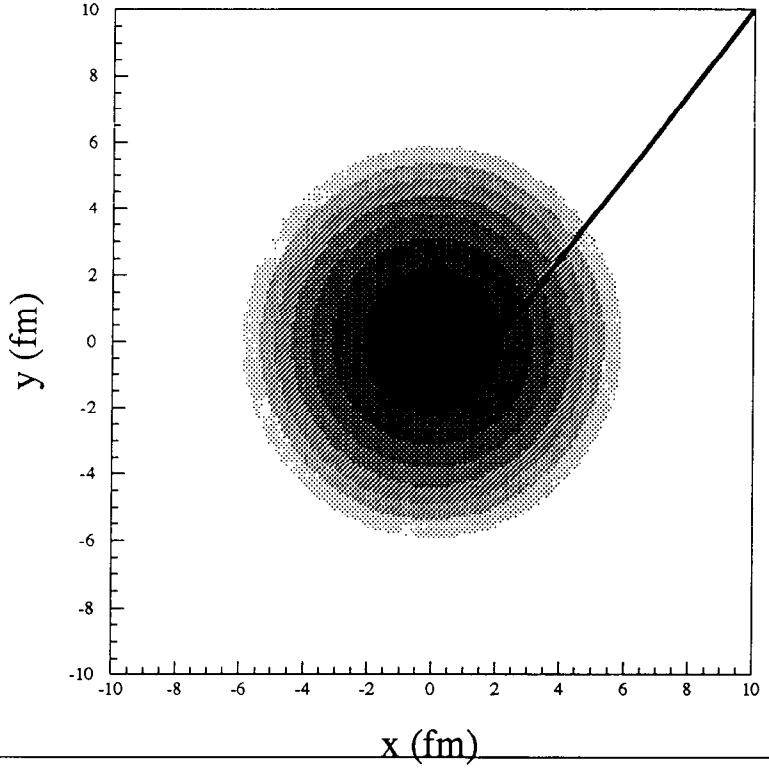

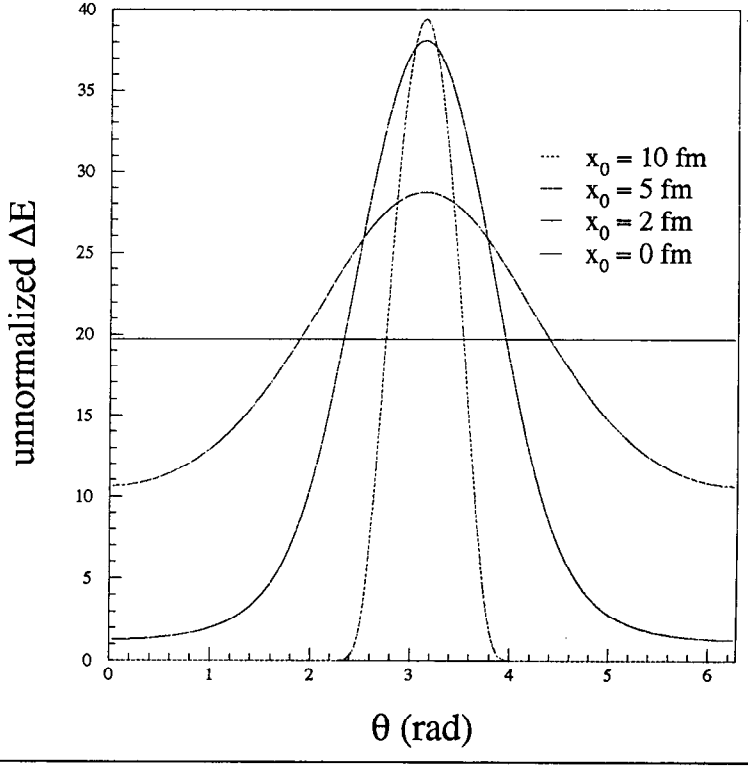

Geometry of Jets and Quenching (3)

Now look at ΔE distribution vs b

- Use $T_A T_B$ weighting for production points

Observations

- Results consistent with intuition
- Get large ΔE's even at b=5
- Quenching should disappear by b=10 fm
- BUT, there's a problem
  - From previous slide a quark starting at r = 0 has ΔE=20
  - where do the larger values come from ?
  - Quarks going "back" into system
- Need to include time dependence of ε

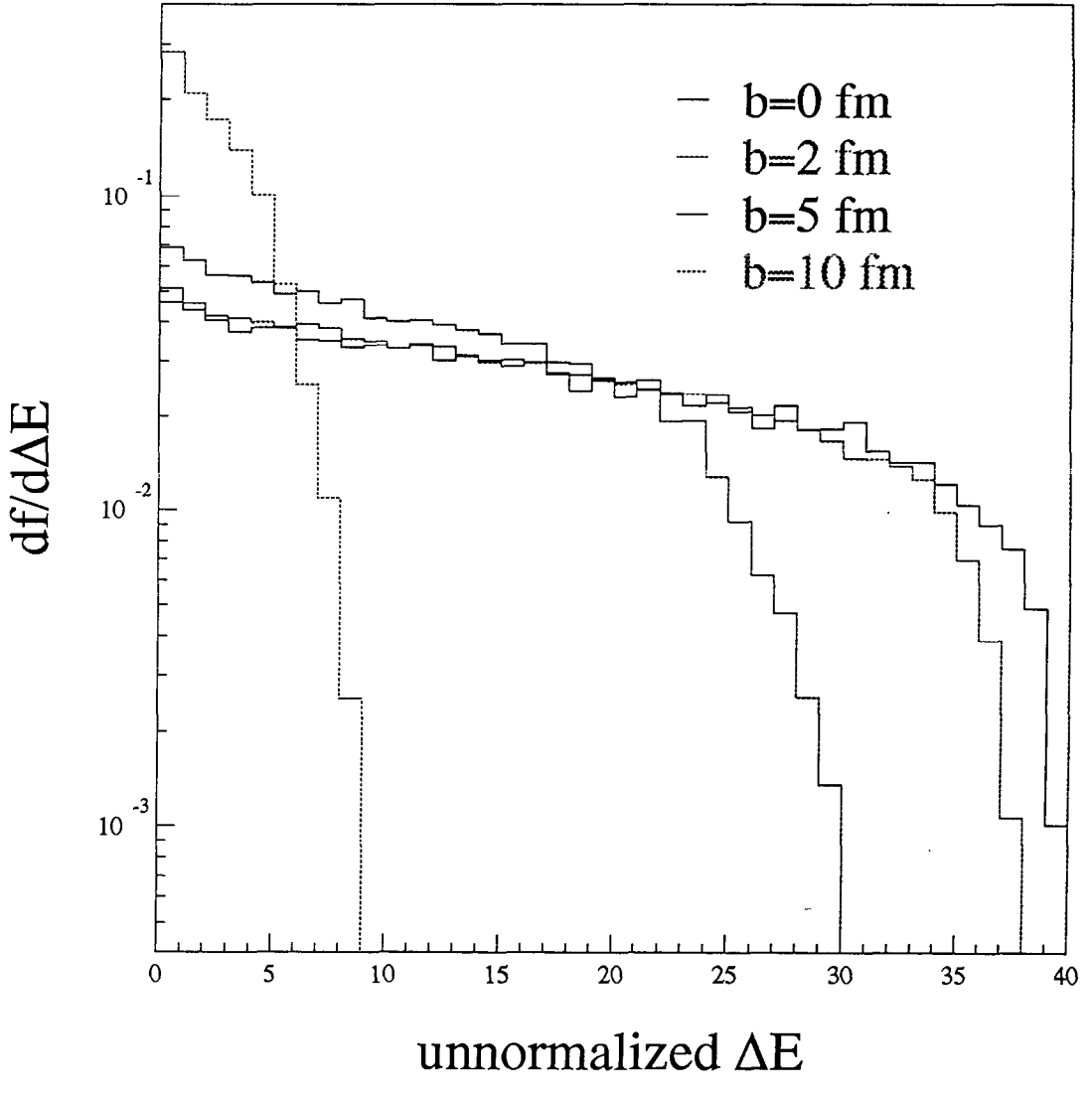

Geometry of Jets & Quenching (4)

Put in simplest time dependence

- Assume $\varepsilon = \varepsilon_0(x, y)(\tau_0 / \tau)$, for $\tau > \tau_0$
- Now comes the fun … Try τ_0 = 0.3, 0.5, 1.0, 2.0 fm
  - 1 fm is "standard", 2 fm mostly just cuts off very late contributions
- Look at distributions of ΔE for different τ_0

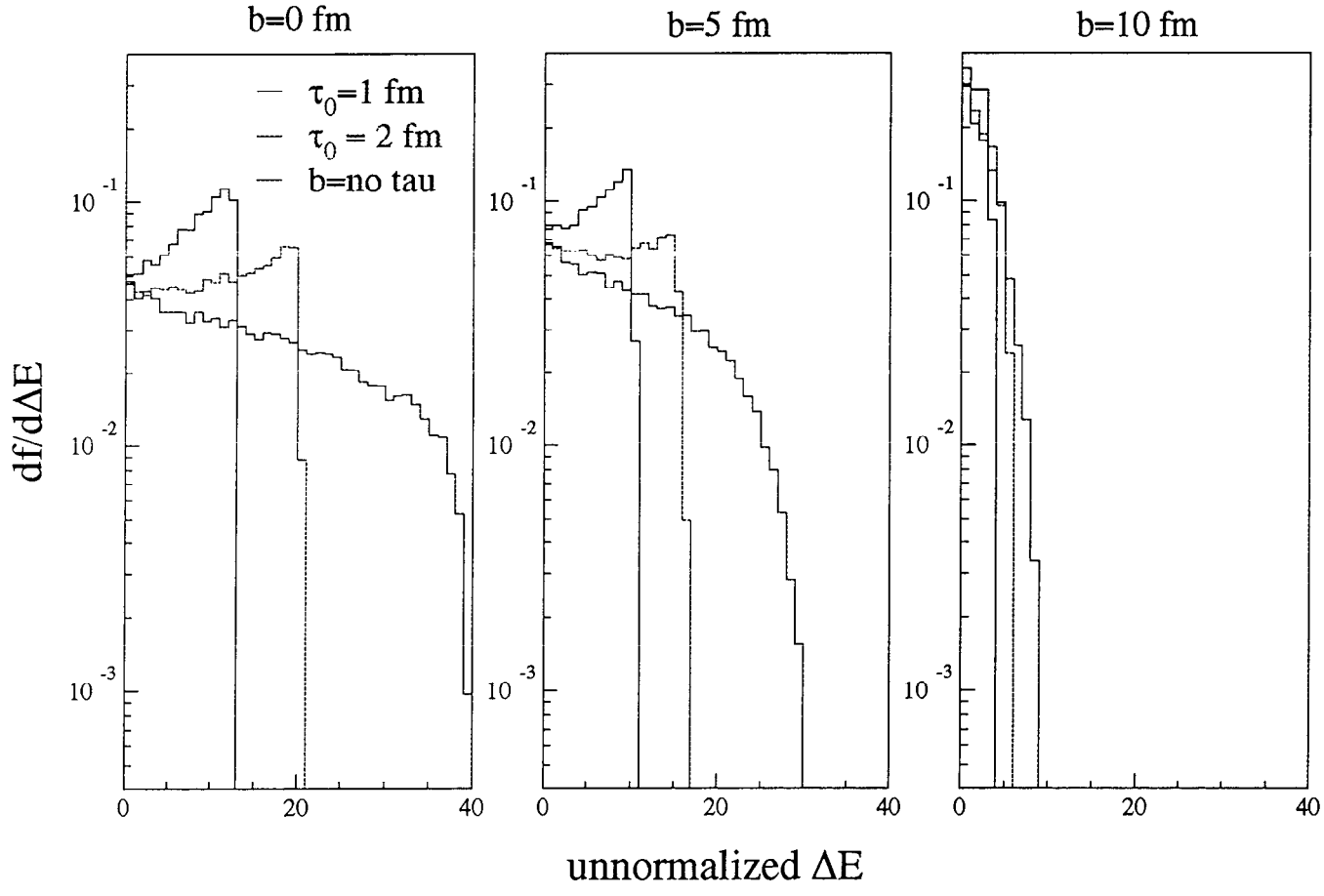

Hidden and Open Charm at RHIC

Dmitri Kharzeev

RIKEN-BNL Research Center,
Brookhaven National Laboratory,
Upton, New York 11973, USA

I discuss some aspects of the physics of hidden and open charm at RHIC. Polarization and spin asymmetries in charmonium production can be used to determine both the production mechanism and the polarized gluon distributions in the nucleon. In particular, the study of angular distributions in the $\chi_2 \to J\psi + \gamma$ decays of charmonium produced in pp collisions provides a unique possibility to distinguish clearly between the color singlet and color octet production mechanisms [1]. Once the production mechanism is known, the angular distribution in the polarized case can be used to measure the polarized gluon distribution in the proton, ΔG [1].

Recent theoretical studies [2] of charmonium interaction with low-energy pions show that the elastic and inelastic cross sections of $\pi J/\psi$ interaction are extremely small, on the order of 0.01 mb. This is important for the interpretations of charmonium suppression in nuclear collisions. New additional arguments are given to support the idea that heavy quarkonium is a sensitive probe of gluon fields, and the low-energy quarkonium scattering amplitudes are evaluated explicitly with the help of QCD theorems [2]. The study of heavy quarkonium production in nuclear collisions will constitute a very important part of the RHIC program.

Acoplanarity in the production of open charm in nuclear collisions can be used to study the growth of "intrinsic" transverse momenta of gluons in the nuclei due to saturation effects.

References

[1] R.L. Jaffe and D. Kharzeev, HEP-PH 9903280; Phys.Lett.B, *in press.*

[2] H. Fujii and D. Kharzeev, HEP-PH 9903495; HEP-PH 9807383; Proc of the 3rd Workshop "Continuous Advances in QCD", Minneapolis, 1998.

- <u>Heavy quarks</u> are heavy: $m_Q \gg \Lambda_{QCD}$,

and perturbation theory is meaningful

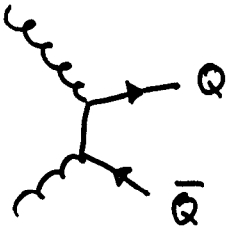

$$\tau_{Q\bar{Q}} \sim \frac{1}{2m_Q} \ll \Lambda_{QCD}^{-1}$$

$\Rightarrow$ a good probe of gluon densities

- <u>Heavy quarkonia</u> are small:

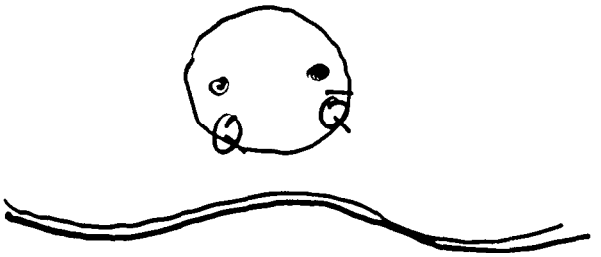

$$\tau_{(Q\bar{Q})} \sim \frac{1}{m_Q v} < \Lambda_{QCD}^{-1}$$

v ↑ velocity

non-perturbative effects can be systematically taken into account using multipole/OPE expansion

$\Rightarrow$ a good probe of softer gluon fields

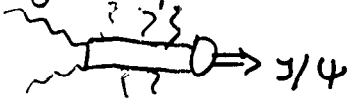

$\Rightarrow$ a test of hadronization

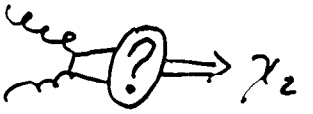

Mechanisms of quarkonium production

- color singlet model

C.H. Chang, NPB172(80)425
E.L. Berger, D. Jones, PRD23(81)1521
R. Baier, R. Rückl, PLB102(81)364, Z. Phys. C19(83)251
.....

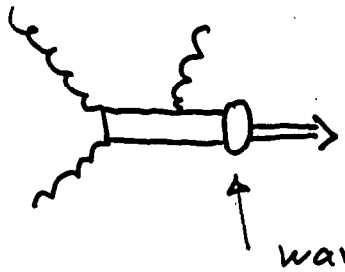

wave function at the origin, extracted from $J/\psi \to e^+e^-$

$\Rightarrow$ everything can be computed

- But: fails in describing the integrated cross sections and high p_T production at the Tevatron (CDF, DØ) $\longrightarrow$ figures

- color octet model

G. Bodwin
E. Braaten
G. Lepage
PRD51(95)1125
....

three scales:

$m_Q \gg$
$\gg m_Q v = r_{Q\bar{Q}}^{-1} \gg$
$\gg m_Q v^2 = \epsilon_{Q\bar{Q}}$

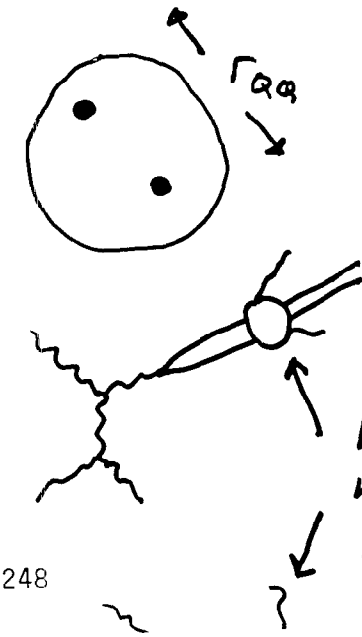

at high p_T

non-perturbative matrix elements, to be extracted from the data

at small p_T

- χ_2 wave function

composite tensor field $\eta^{\mu\nu}$

irreducible: symmetric $\eta^{\mu\nu} = \eta^{\nu\mu}$

traceless $\eta^{\mu}_{\mu} = 0$

transverse $\partial_\mu \eta^{\mu\nu} = 0$

the w.f.:

$$\langle P, \lambda | \eta^{\mu\nu} | 0 \rangle = H^{\mu\nu}(P, \lambda)$$

(λ: helicity; P: momentum)

- Interaction with external gauge fields

effective Lagrangian $\mathcal{L}_{int} = \psi^+_\mu D_\nu \eta^{\mu\nu} \sim \psi^+_\mu A_\nu \eta^{\mu\nu}$

(ψ_μ: massive vector field)

- apply first to angular distributions

in $\chi_2 \to J/\psi + \gamma$ decay

amplitude $A \sim \epsilon^+_k(\lambda_\psi)\, \epsilon^+_\ell(\lambda_\gamma)\, H^{k\ell}(\lambda)$ (λ: helicity state of χ_2)

$$\sum_{\lambda_\psi} \epsilon^m(\lambda_\psi)\epsilon^{k+}(\lambda_\psi) = \delta^{km} \qquad \sum_{\lambda_\gamma} \epsilon^n(\lambda_\gamma)\epsilon^{\ell+}(\lambda_\gamma) = \delta^{n\ell} - \hat{k}^n \hat{k}^\ell$$

cross section

$$\sigma \sim \sum_{\lambda_\psi, \lambda_\gamma} A^+ A \sim H^{+k\ell}(\lambda)(\delta^{\ell n} - \hat{k}^\ell \hat{k}^n) H^{kn}(\lambda)$$

$$H^{jk}(\lambda) = \sum_{\mu\mu'} (1\mu 1\mu' | 2\lambda)\, V^j(\mu)\, V^k(\mu')$$

Example:

consider $pp \longrightarrow \chi_2 + X$

$\chi_2 \longrightarrow J/\psi + \gamma$

- What is the angular distribution of the photon?

χ_2 : $J^{PC} = 2^{++}$ $\quad {}^3P_2$ 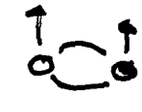

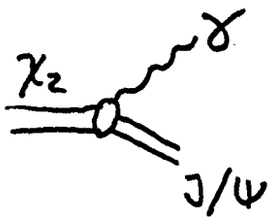

effective coupling

vector potential

$\mathcal{L} \sim \psi_\mu^+ D_\nu \eta^{\mu\nu} \sim \psi_\mu^+ A_\nu \eta^{\mu\nu}$

ψ_μ^+: J/ψ field; $\eta^{\mu\nu}$: χ_2 field

(QED multipole expansion)

$$W^{2,\pm 2}(\theta) = \frac{1}{2} + \frac{1}{2}\cos^2\theta$$

$$W^{2,\pm 1}(\theta) = \frac{3}{4} - \frac{1}{4}\cos^2\theta$$

$$W^{2,0}(\theta) = \frac{5}{6} - \frac{1}{2}\cos^2\theta$$

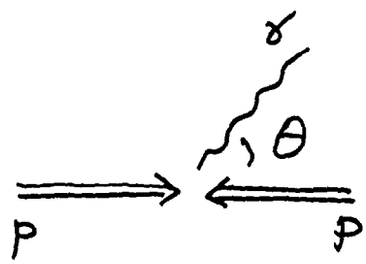

$\Rightarrow$ angular distribution of the photon can be used to determine the helicity of the χ_2

R.L. Jaffe, D.K.
hep-ph/9903280

$\Downarrow$

The angular distribution in the decay $\chi_2 \to J/\psi + \gamma$ determines the ratio of octet/singlet amplitudes:

$$\frac{d\sigma}{d\Omega} \sim g(x_1, M_\chi^2)\, g(x_2, M_\chi^2) \left\{ \left(\frac{1}{2} + \frac{1}{2}\cos^2\theta\right) \underline{A}^1 + \left(\frac{3}{4} - \frac{1}{4}\cos^2\theta\right) \underline{A}^8 \right.$$

- Once A^8/A^1 is measured in polarized $\vec{p}\vec{p}$ one can measure ΔG!

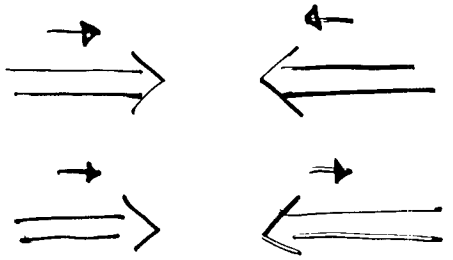

$$\frac{d\sigma^{\uparrow\uparrow} - d\sigma^{\uparrow\downarrow}}{d\sigma^{\uparrow\uparrow} + d\sigma^{\uparrow\downarrow}} = - \frac{\Delta g(x_1, M_\chi^2)}{g(x_1, M_\chi^2)} \frac{\Delta g(x_2, M_\chi^2)}{g(x_2, M_\chi^2)} \times$$

$$\times \frac{\frac{1}{2} + \frac{1}{2}\cos^2\theta - \frac{A^8}{A^1}\left(\frac{3}{4} - \frac{1}{4}\cos^2\theta\right)}{\frac{1}{2} + \frac{1}{2}\cos^2\theta + \frac{A^8}{A^1}\left(\frac{3}{4} - \frac{1}{4}\cos^2\theta\right)}$$

Understanding Global features – 1

- Cross-section for high mass Drell-Yan pairs scale like A in pA collision
  - * Q: How do you get

$$\sigma_{pA}^{X} = A\sigma_{pN}^{X} \ ?$$

    That is, count the target nucleons?
  - * A: The number of X produced in a single pA collision is always the same as the number of X produced in pN regardless of where it is made.
  - * How can that be?
    - ○ The production cross-section for X is a constant and is not a function of $\sqrt{s}$. – Not true for DY.
      Or
    - ○ The projectile loses no or very little energy until it produces X – Coherence time.
      Or
    - ○ Multiple collision – Rescattering = 0 – Remote possibility at best

Coherence Time – 3

- A daughter particle needs at least

$$\Delta t \sim E/k_\perp^2$$

to be separated from the mother – Landau-Pomeranchuck-Migdal effect.

- For a typical pion in N-N CMS frame with $E \sim k_\perp \sim 500$ MeV,

$$\Delta t_{\rm cms} \sim 1/500 \text{ MeV} \sim 0.4 \text{ fm}$$

In the nucleus rest frame with $p_{\rm lab} = 800$ GeV,

$$\Delta t_{\rm A\ rest} \approx \Delta t_{\rm cms} \sqrt{\gamma_{\rm lab}/2} \sim 5 \times l_{\rm free}$$

where $l_{\rm free} = (1/\sigma_{NN}\rho_N) = 1.6$ fm.

- For small nucleus where $2R/l_{\rm free} < 5$ or $A < 50$,

$$\sigma_{pA} \propto A^\alpha \quad \text{with} \quad \alpha = 1$$

For larger nucleus with $A \geq 50$, $\alpha < 1$ due to energy loss.

LEXUS Results with $4 \leq n_{\text{shift}} \leq 6$

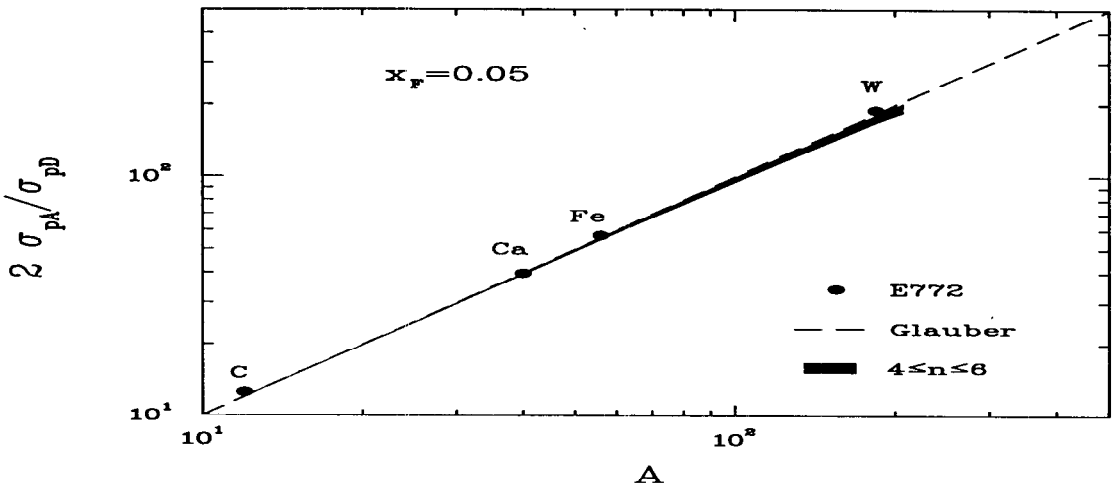

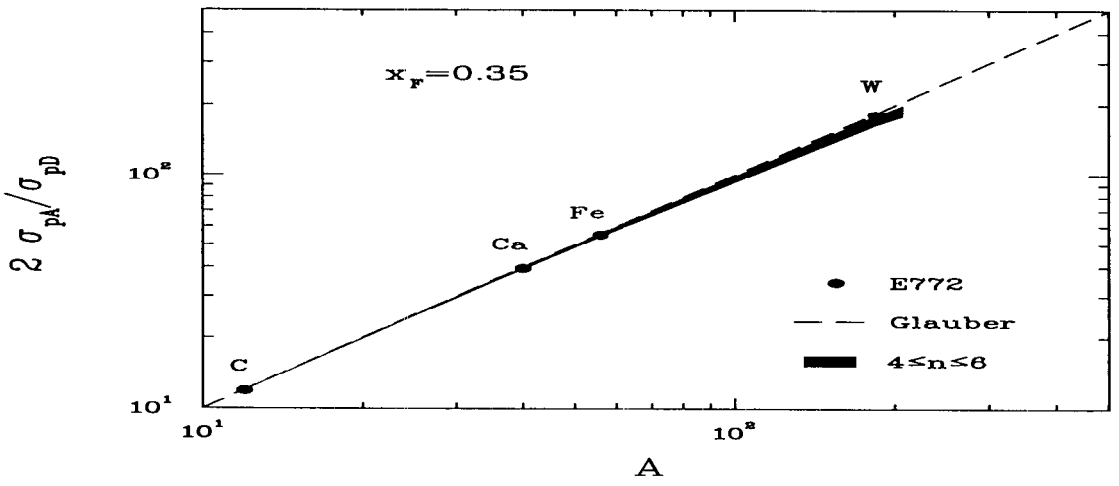

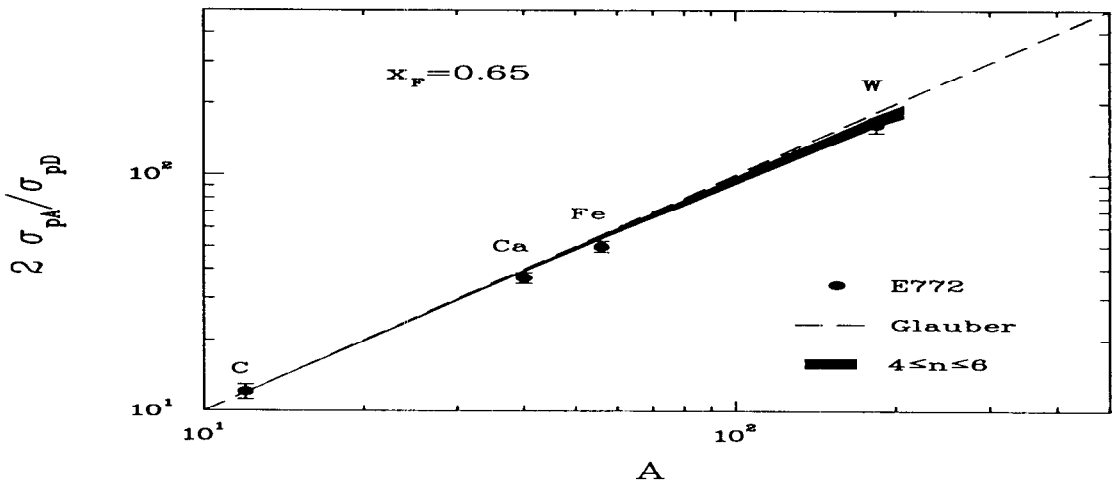

- With $\sigma_{\rm abs} = 3.6$ mb,

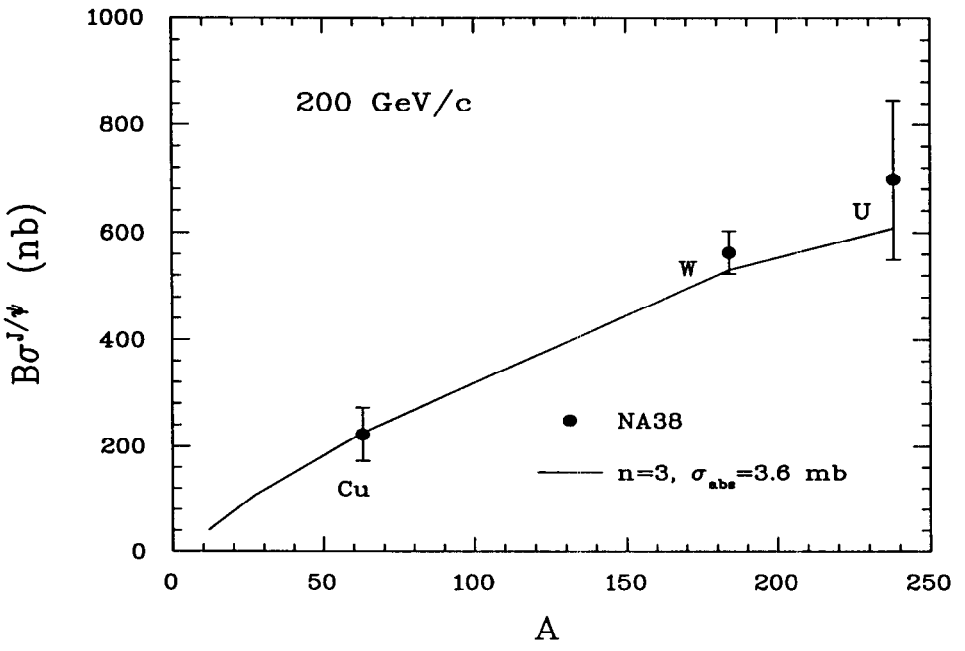

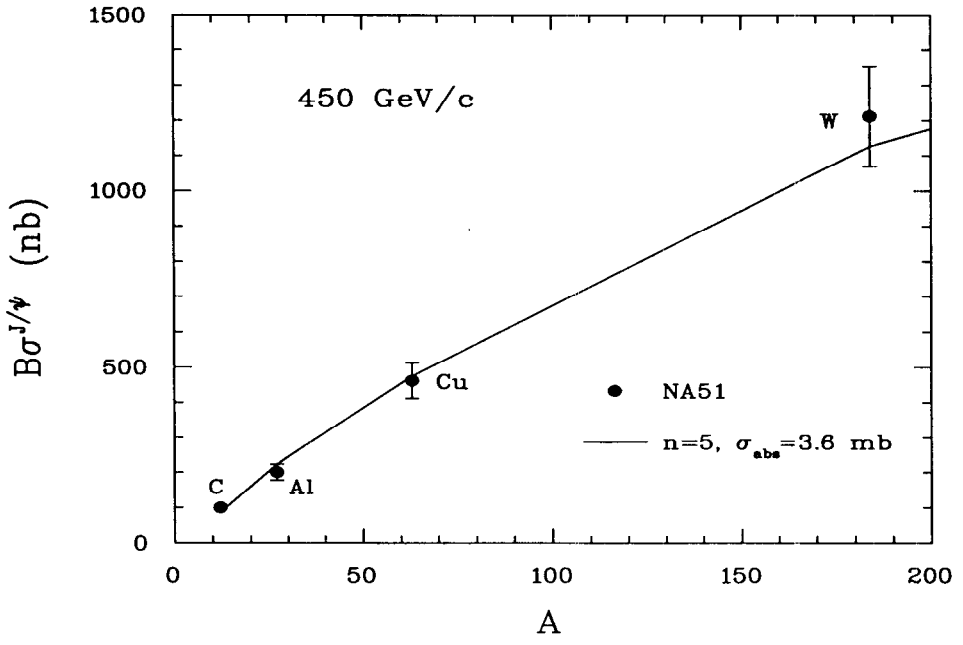

Conclusions

- Implemented an approximation to adding QM amplitudes for multiple scattering within LEXUS
- pA Drell-Yan cross-section very well reproduced with the coherence time of $t_{\text{coherence}} = \tau\sqrt{\gamma_{\text{lab}}/2}$ with $\tau \approx 0.4$ fm
- pA J/ψ cross-section well reproduced with the same τ and a small absorption cross-section of 3.6 mb.
- AB J/ψ cross-section calculation on the way. Preliminary result suggests NA50 $Pb-Pb$ data is not inconsistent with energy loss + absorption.

L. McLerran
BNL - March 1999

(1)

Summary - Perspectives
Hard Partons @ RHIC

Three separate sets of interest:

1. QCD Tests
   - High $p_\perp$ jets + minijets
   - High $p_\perp$ γ's
     - Not fully understood
     - Intrinsic $k_\perp$?
   - Polarized structure functions
     - Not understood
     - Great interest in past → future
   - A dependence of structure functions
   - A dependent higher twist?

Any of the above have + will continue to generate intense interest

2. Quark-gluon plasma

- Much discussed & central theme for RHIC
- To begin: first must know what is not QGP

- Must understand environment in which it is formed

3. Asymptotic QCD

- Cross sections as $E \to \infty$
- Universality of particle spectra
- How are particles produced & can one explain it quantitatively
- Where do structure functions come from?

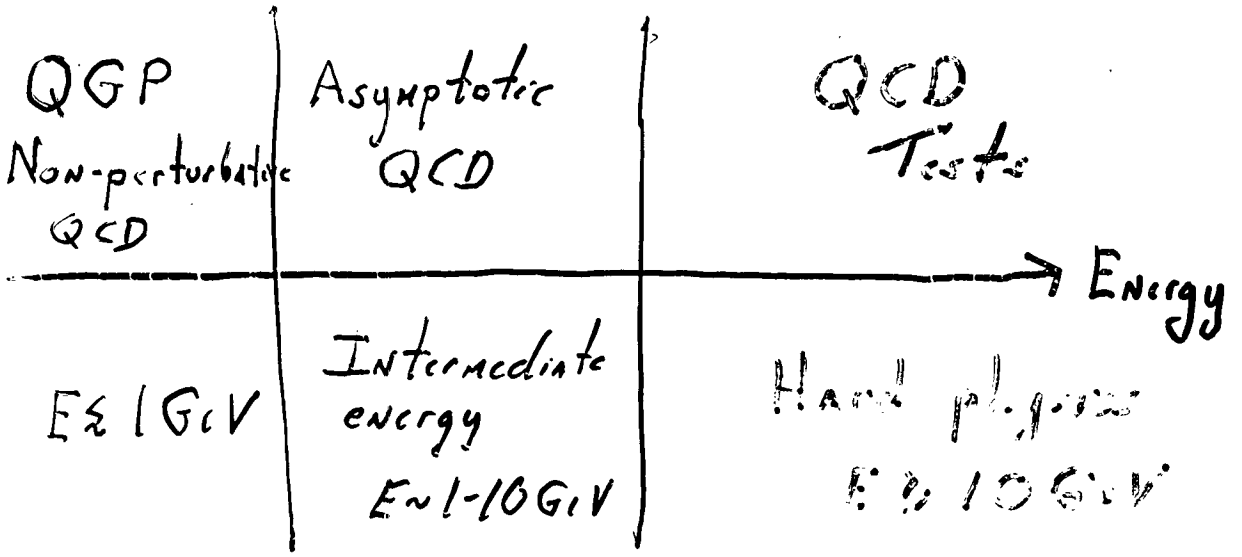

Optomism strong; Risk/Return about right

In RHIC, will appear as deviations from hard physics

This we understand (more or less)

Will discuss RHIC in context of asymptotic QCD. What can we hope for from experiment?

Why do we think we can understand asymptotic QCD?

Minnesota Mob Authorized Version

Hera + BFKL

Work in frame where hadron is fast

$$y = y_{hadron} - \ln \frac{1}{x}$$

$$p^{\pm} = \frac{p^0 \pm p^3}{\sqrt{2}} \qquad x^{\pm} = \frac{t \pm z}{\sqrt{2}}$$

$$x = \frac{p^+_{constituent}}{p^+_{Hadron}}$$

$$x^- \cong 1/p^+ \qquad (p \cdot x = p_\perp \cdot x_\perp - p^+ x^- - p^- x^+)$$

$$y_{space\text{-}time} = y_{hadron} - \ln x^- p^+$$

$$\cong \ln x^- \Lambda_{QCD} \cong y$$

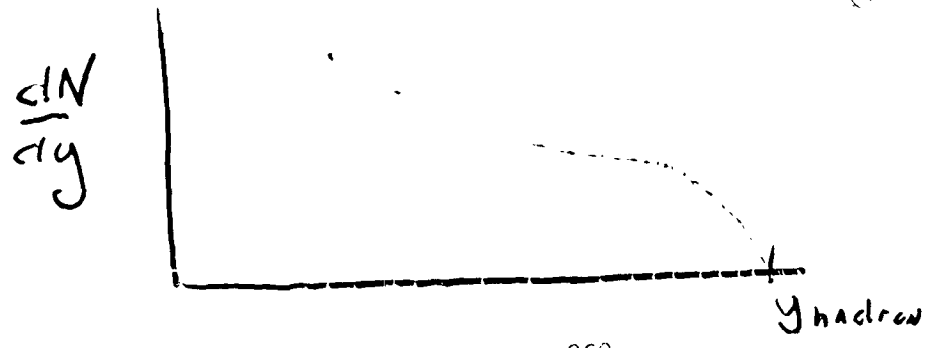

$$\frac{dN}{dy} \simeq \frac{dN}{dy}_{\text{gluons}} \quad \text{AS}$$

$$|y - y_{had}| \to \infty$$

$$\Lambda^2 = \frac{dN}{dy}\Big/_{\pi R^2} \gg \Lambda^2_{QCD}$$

$$\alpha_s(\Lambda) \ll 1$$

Small x physics $\Rightarrow$ weak coupling

For particle scattering & gluon production

$$y = \frac{1}{2} \ln \frac{E + p_z}{E - p_z} = \ln \frac{E}{m_\perp} \simeq y_{had} \simeq \ln \frac{1}{x}$$

$$y_{cm} = \frac{1}{2} \ln \frac{x_1}{x_2} = \ln \frac{1}{\sqrt{\tau}}$$

All rapidities roughly equal.

Hello? Is pp the same as AA at fixed $\frac{dN}{dy}/\pi R^2$?

Distributions of particles same at fixed $dN/dy\,/\pi R^2$?

Al Mueller's talk: Even QGP issues the same! (See later discussion)

Why bother with nuclei?

$$\frac{dN}{dy} \sim \frac{A^{1/3}}{x^{0.2\text{--}0.3}}$$

$A^{1/3}: 1 \to 10 \Rightarrow x: 1 \to 10^{-3} \times x_0$

!!

10^3 more energy!!

Theory of small x:

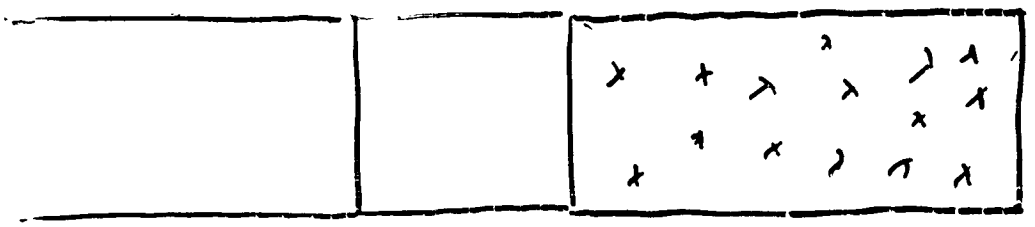

theory dominated by quantum noise

classical gluon field, little quantum noise

sources of color

Effective theory good for

$\alpha_s y_n \lesssim y \lesssim y_n$

Renormalization group allows redefining theory at smaller and smaller y_n

BFKL, DGLAP, GLR +
NON-linear generalizations
follow.

Hello?

Classical field slowly varies
in y: $\Delta y \sim 1/\alpha_s$

Rapidity correlations ~ $1/\alpha_s$ units

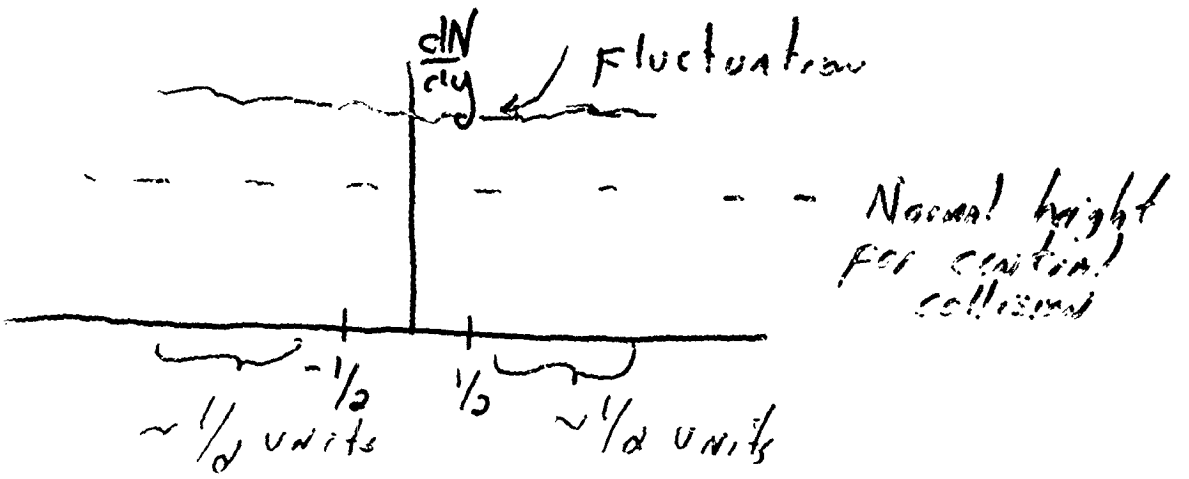

Structure of gluon field:

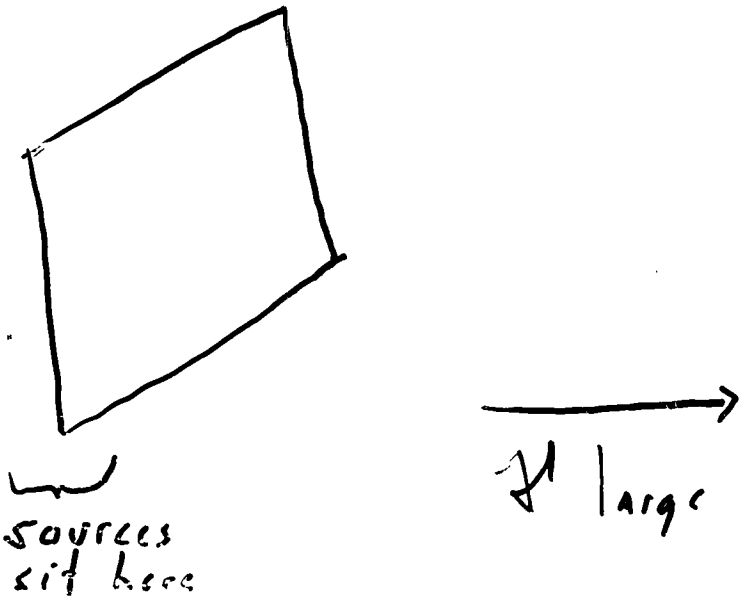

size is e^{-y_A} in x

Natural size per parton is $e^{-y} \gg e^{-y_A}$

A dipole field:

At rest

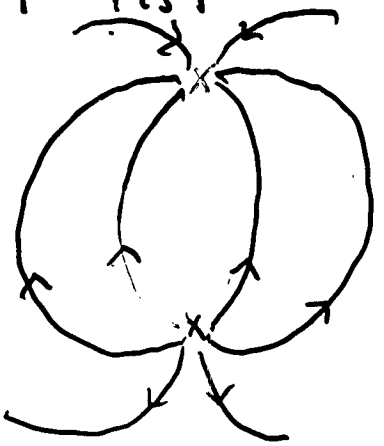

Boosted:

Head on view

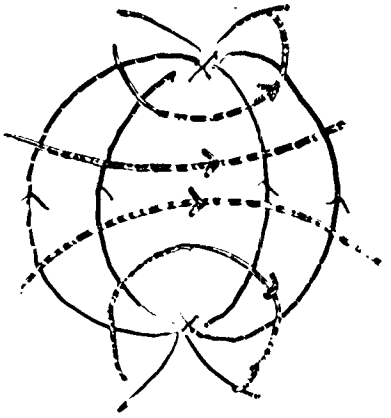

Sidewise

Lorentz contracted

$F^{i0}_{\perp} B^{i}_{\perp} \hat{z}$, $\delta(t-z) F(x_\perp)$

Head on view of nucleus:

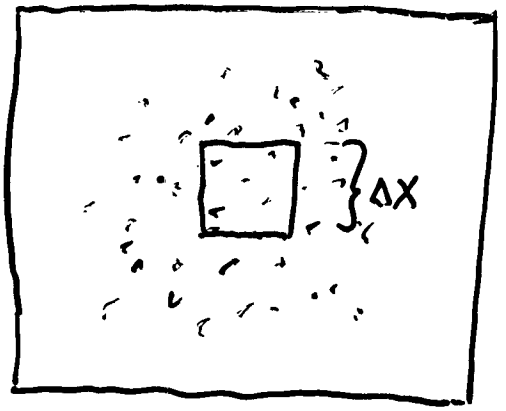

$\Delta X \gtrsim 1\,F_M$ colour neutral

$E, B = 0$

$\frac{1}{\sqrt{s}} \ll \Delta X \ll 1\,F_M$

$\vec{E} \perp \vec{B}$

Random on the surface

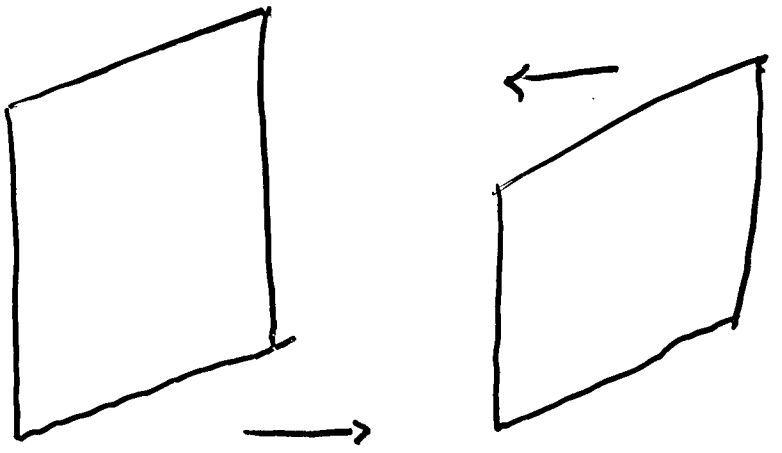

AA collisions

$t = x = 0$

Classical field evolves

- Strength:

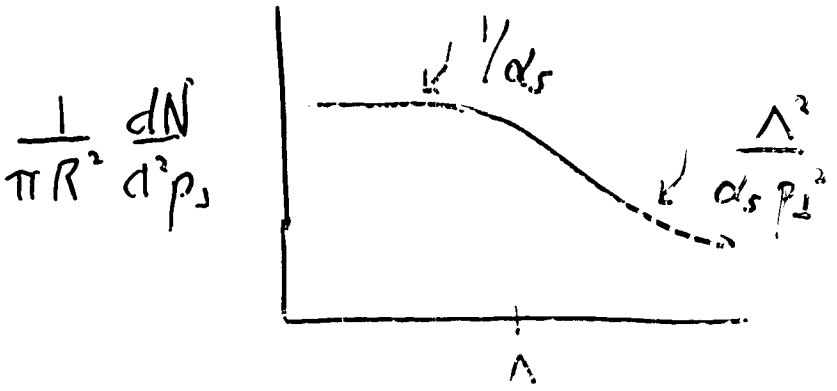

Classical fields have $\sim 1/\alpha_s$ quanta of $p_\perp \sim \Lambda$

Very strong initial color field

Bjorken like expansion:

$B^2 \sim 1/t \sim E^2$

At $t \sim 1/\Lambda$, linearities disappear, equations linearize

⇓

Classically produce gluon radiation

$$\mathcal{E}\Big|_{t=1/\Lambda} \sim \Lambda^4 \sim \left(\frac{dN}{dy}/\pi R^2\right)^2 \sim A^{2/3}$$

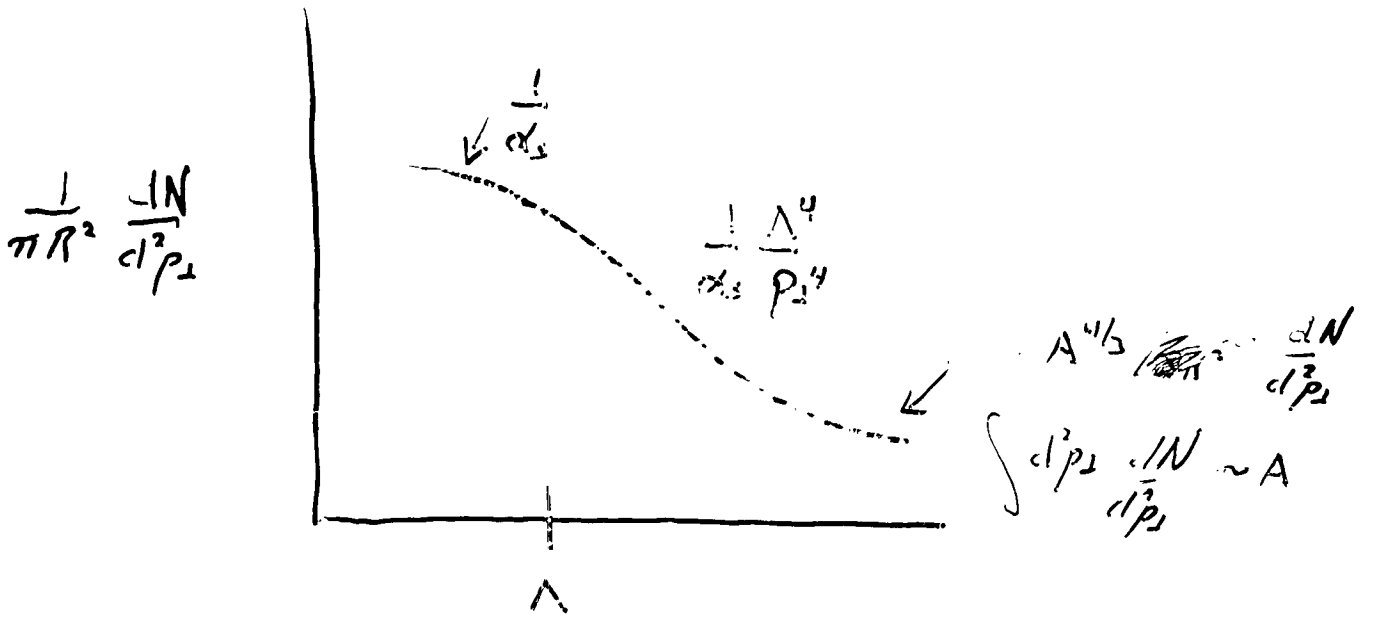

Al Mueller

$$N_{sc} \sim \int_{\tau_i}^{\tau_f} d\tau \; \sigma n$$

$$\sim \int_{\tau_i}^{\tau_f} d\tau \, (\alpha^2/\Lambda^2) \left(\frac{\Delta^2}{\alpha t}\right)$$

$$\sim \alpha \ln \frac{\tau_f}{\tau_i}$$

$$\alpha \sim \frac{1}{\ln Q^2/\Lambda_{QCD}^2} \sim \ln^{-1} \frac{R\tilde{\Lambda}^2}{\Lambda_{QCD}^2}$$

$$\ln \tau_f/\tau_i \sim \ln \sqrt{R\tilde{\Lambda}}/\Lambda_{QCD}$$

N_{sc} a pure number independent of R

∴ Some fixed fraction of high $p_\perp$ stuff thermalizes independent of A!

Some fraction thermalizes:

$$\tau T^3 \sim \tau_i T_i^3 \sim \Lambda^2$$

$$\tau \sim \frac{1}{T}\left(\frac{\Lambda^2}{T^2}\right)$$

$\Lambda \sim 1\,GeV$, $T \sim 200\,MeV$

$\tau \sim 1\,Fm \times 25$

to cool to 200 MeV if only longitudinal

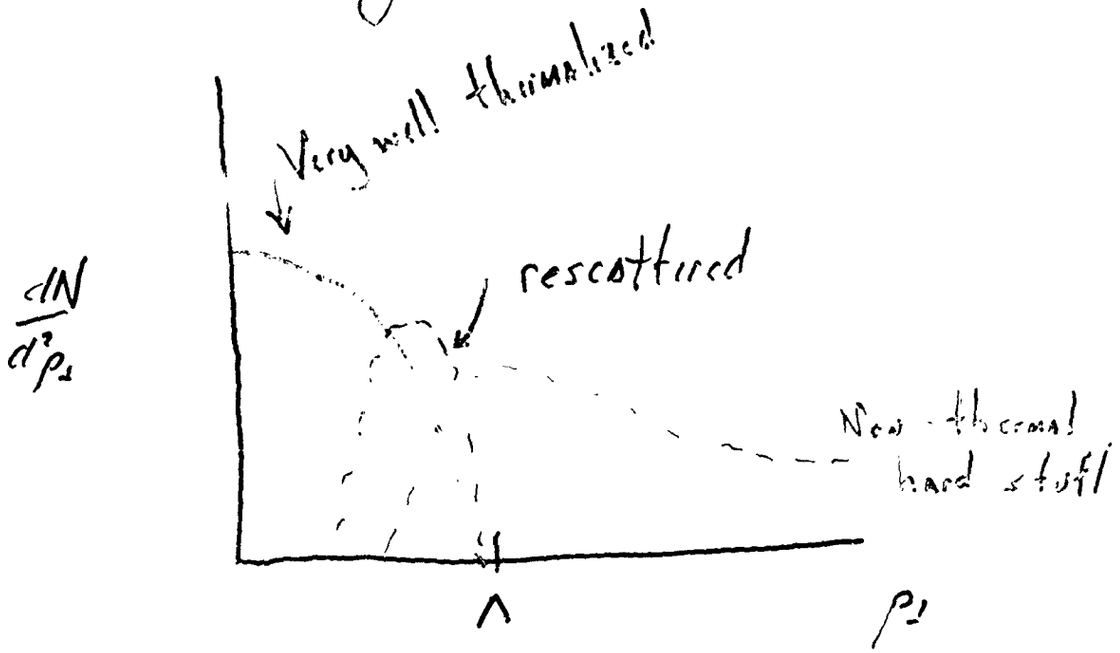

Crucial issues:

Λ:

- DIS on nuclei
- Hard $\not{q}$ production
- $\frac{dN}{d^3p_J}$

Very important to have
↓ understand eA !!

Hard Parton Physics in High Energy Nuclear Collisions

March 1-5, 1999

Organizers: Jim Carroll (LBL), Charles Gale (McGill), Mike Tannenbaum (BNL), and Raju Venugopalan (BNL)

List of Registered Participants

Name	Affiliation	Mailing Address	E-mail address
Patrick Aurenche	LAPTH	LAPTH B.P. 110 F-74941 Annecy-Le-Vieux Cedex, France	aurenche@lapp.in2p3.fr
Terry Awes	ORNL	Building 6003, MS-6372 Oak Ridge National Laboratory Oak Ridge, TN 37831 USA	awes@mail.phy.ornl.gov
Ian Balitsky	Jefferson Lab.	Theory Group Jefferson Lab. 12000 Jefferson Avenue Newport News, VA 23606 USA	balitsky@jlab.org
Anthony Baltz	BNL	Physics Department, Bldg. 510A Brookhaven National Laboratory Upton, NY 11973 USA	baltz@bnl.gov
Steffen Bass	Duke Univ.	Department of Physics Duke University Durham, NC 27708-0305 USA	bass@phy.duke.edu
Stefan Bathe	Univ. of Muenstr	Institut fuer Kernphysik Wilhelm-Klemm-Strasse 9 48149 Muenster, Germany	bathe@ikp.uni-muenster.de
Michael Begel	Univ. of Rochester	University of Rochester Box 500 Fermilab Batavia, IL 60510 USA	begel@fnal.gov
Gerald Blazey	Northern Illinois Univ.	Physics Department Northern Illinois University DeKalb, IL 60115 USA	blazey@niuhep.physics.niu.edu
Daniel Boer	RIKEN Center	Physics Department, Bldg. 510A Brookhaven National Laboratory Upton, NY 11973 USA	dboer@bnl.gov
Henner Buesching	Univ. of Muenster	Institut fuer Kernphysik Wilhelm-Klemm-Strasse 9 48149 Muenster, Germany	buschin@uni-muenster.de
Jim Carroll	LBL	Nuclear Science, MS 50A 1148 Lawrence Berkeley Laboratory Berkeley, CA 94720 USA	jbcarroll@lbl.gov
William Christie	BNL	Physics Department, Bldg. 510A Brookhaven National Laboratory Upton, NY 11973 USA	christie@bnl.gov
Brian Cole	Columbia Univ.	Physics Department Columbia University Nevis Labs, P.O. Box 137 Irvington, NY 10533 USA	cole@nevis.columbia.edu
Thomas Cormier	Wayne State Univ.	Department of Physics Wayne State University Detroit, MI 48202 USA	cormier@physics.wayne.edu
Sally Dawson	BNL	Physics Department, Bldg. 510A Brookhaven National Laboratory Upton, NY 11973 USA	dawson@bnl.gov
Hughes Delagrange	SUBATECH	SUBATECH, Ecole des Mines La Chantrerie 4, rue Alfred Kastler BP 20722 - 44307 Nantes Cedex-3, France	Hugues.Delagrange@subatech.in2p3.fr
Abhee Dutt-Mazumder	McGill Univ.	Physics Department McGill University 3600 University Street Montreal, QC Canada H3A 2T8	abhee@hep.physics.mcgill.ca

Hard Parton Physics in High Energy Nuclear Collisions

March 1-5, 1999

Organizers: Jim Carroll (LBL), Charles Gale (McGill), Mike Tannenbaum (BNL), and Raju Venugopalan (BNL)

List of Registered Participants

Name	Affiliation	Mailing Address	E-mail address
George Fai	Kent State Univ.	Department of Physics Kent State University Kent, OH 44242 USA	fai@cnrred.kent.edu
Leonid Frankfurt	Tel Aviv Univ.	Tel Aviv University Ramat-Aviv 69978 Tel Aviv, Israel	frankfur@lev.tau.ac.il
Hirotsugu Fujii	RIKEN Center	Physics Department, Bldg. 510A Brookhaven National Laboratory Upton, NY 11973 USA	hfujii@bnl.gov
Charles Gale	McGill Univ.	Physics Department McGill University 3600 University Street Montreal, QC Canada H3A 2T8	gale@physics.mcgill.ca
Yuji Goto	RIKEN	Physics Department, Bldg. 902C Brookhaven National Laboratory Upton, NY 11973 USA	goto@bnl.gov
Xiaofeng Guo	Univ. of Kentucky	Dept. of Physics & Astronomy University of Kentucky Lexington, KY 40506 USA	gxf@ruthless.pa.uky.edu
Wlodek Guryn	BNL	Physics Department, Bldg. 510 Brookhaven National Laboratory Upton, NY 11973 USA	guryn@bnl.gov
Gosta Gustafson	Lund Univ.	Dept. of Theoretical Physics Lund University Solvegatan 14A S-22362 Lund, Sweden	gosta@thep.lu.se
Vadim Guzey	Penn State Univ.	104 Davey Lab., Box 191 The Pennsylvania State University University Park, PA 16801 USA	guzey@phys.psu.edu
Miklos Gyulassy	Columbia Univ.	Columbia Univ., MS5202 550 West 120th Street New York, NY 10027 USA	gyulassy@mail-cunuke.phys.columbia.edu
Tim Hallman	BNL	Physics Department, Bldg. 510 Brookhaven National Laboratory Upton, NY 11973 USA	hallman@bnl.gov
Yong-Bin He	Univ. of Heidelberg	Institute for Theoretical Physics University of Heidelberg Philosophenweg 19 D-69120 Heidelberg, Germany	hyb@frodo.tphys.uni-heidelberg.de
Peter Jacobs	LBL	MS 70-319, LBNL 1 Cyclotron Road Berkeley, CA 94720 USA	pmjacobs@lbl.gov
Jamal Jalilian-Marian	LBL	Nuclear Science Division LBNL, MS 70A-3307 One Cyclotron Road Berkeley, CA 94720 USA	jjmarian@lbl.gov
Sangyong Jeon	LBL	Nuclear Science Division LBNL, MS 70A-3307 One Cyclotron Road Berkeley, CA 94720 USA	jeon@nta2.lbl.gov
Dmitri Kharzeev	RIKEN Center	Physics Department, Bldg. 510A Brookhaven National Laboratory Upton, NY 11973 USA	kharzeev@bnl.gov
Yuval Kluger	LANL	Theoretical Division, T8, MS B285 LANL Los Alamos, NM 87545	yuval@schwinger.lanl.gov

Hard Parton Physics in High Energy Nuclear Collisions

March 1-5, 1999

Organizers: Jim Carroll (LBL), Charles Gale (McGill), Mike Tannenbaum (BNL), and Raju Venugopalan (BNL)

List of Registered Participants

Name	Affiliation	Mailing Address	E-mail address
Boris Kopeliovich	Max-Planck-Inst.	Max-Planck-Institut fuer Kernphysik Postfach 103980 69029 Heidelberg, Germany	bzk@dxnhdl.mpi-hd.mpg.de
Yuri Kovchegov	Univ. of Minnesota	School of Physics and Astronomy University of Minnesota 148 Tate Laboratory of Physics 116 Church Streeet., SE Minneapolis, MN 55455 USA	yuri@tpi1.hep.umn.edu
Alex Kovner	Oxford Univ.	Theoretical Physics Oxford University 1 Keble Road Oxford OX1 3NP, United Kingdom	kovner@thphys.ox.ac.uk
Mieczyslaw Krasny	Paris VI Univ. & Oxford Univ.	Particle and Nuclear Physics Laboratory University of Oxford Keble Road Oxford OX1 3RH, United Kingdom	w.krasny@physics.ox.ac.uk
Shunzo Kumano	Saga Univ.	Department of Physics Saga University Saga 840-8502, Japan	kumanos@cc.saga-u.ac.jp
Gerd Kunde	Yale Univ.	Yale University 272 Whitney Avenue New Haven, CT 06520 USA	g.j.kunde@yale.edu
Andrei Leonidov	P.N. Lebedev Physics Inst.	Theoretical Physics Institute University of Minnesota 431 Physics 116 Church Street S.E. Minneapolis, MN 55455 USA	leonidov@tpi2.hep.umn.edu
Peter Levai	KFKI RMKI	KFKI RMKI POB 49 Budapest, 1525, Hungary	plevai@rmki.kfki.hu
Qun Li	LBL	LBNL, MS 70-319 1 Cyclotron Road Berkeley, CA 94720 USA	qli@lbl.gov
Igor Lokhtin	Moscow State Univ.	RU-119899, Vorobievy Gory Nuclear Physics Institute Moscow State University Moscow, Russia	igor@lav1.npi.msu.su
Ronald Longacre	BNL	Physics Department, Bldg. 510A Brookhaven National Laboratory Upton, NY 11973 USA	longacre@bnl.gov
Leon Madansky	Johns Hopkins Univ.	Department of Physics The Johns Hopkins University 3400 North Charles Street Baltimore, MD 21218 USA	lm@jhup.pha.jhu.edu
Alexander Makhlin	Wayne State Univ.	Department of Physics & Astronomy Wayne State University 666 West Hancock Detroit, MI 48201 USA	makhlin@physics.wayne.edu
Larry McLerran	Univ. of Minnesota	Physics Department University of Minnesota Minneapolis, MN 55445 USA	mclerran@tpi2.hep.umn.edu
Alfred Mueller	Columbia Univ.	Physics Department Columbia University 538 West 120th Street New York, NY 10027 USA	arb@physics.columbia.edu

Hard Parton Physics in High Energy Nuclear Collisions

March 1-5, 1999

Organizers: Jim Carroll (LBL), Charles Gale (McGill), Mike Tannenbaum (BNL), and Raju Venugopalan (BNL)

List of Registered Participants

Name	Affiliation	Mailing Address	E-mail address
Akio Ogawa	Penn State Univ. & BNL	Physics Department, Bldg. 510A Brookhaven National Laboratory Upton, NY 11973 USA	akio@bnl.gov
Craig Ogilvie	MIT	24-410, MIT 77 Mass Avenue Cambridge, MA 02139 USA	ogilvie@mitlns.mit.edu
Shigemi Ohta	RIKEN Center	Physics Department, Bldg. 510A Brookhaven National Laboratory Upton, NY 11973 USA	shigemi.ohta@kek.jp
Frank Paige	BNL	Physics Department, Bldg. 510A Brookhaven National Laboratory Upton, NY 11973 USA	paige@bnl.gov
Jen-Chieh Peng	LANL	MS H846, LANL Los Alamos, NM 87545 USA	peng@lanl.gov
Jan Rak	Max-Planck-Inst.	MPI fuer Kernphysik Saupfercheckweg 1 69 117 Heidelberg Germany	rak@fossy2.mpi-hd.mpg.de
Dirk Rischke	RIKEN Center	Physics Department, Bldg. 510A Brookhaven National Laboratory Upton, NY 11973 USA	rischke@bnl.gov
Naohito Saito	RIKEN	Physics Department, Bldg. 510C Brookhaven National Laboratory Upton, NY 11973 USA	saito@bnl.gov
Ina Sarcevic	Univ. of Arizona	Physics Department University of Arizona Tucson, AZ 85721 USA	ina@gluon.physics.arizona.edu
Juergen Schaffner-Bielich	RIKEN Center	Physics Department, Bldg. 510A Brookhaven National Laboratory Upton, NY 11973 USA	jschaffner@bnl.gov
Heinz Sorge	SUNY, Stony Brook	Department of Physics & Astronomy State University of NY, Stony Brook Stony Brook, NY 11794-3800 USA	sorge@alba.physics.sunysb.edu
James Sowinski	Indiana Univ. Cyclotron Facility	Indiana University Cyclotron Facility 2401 Milo B. Sampson Lane Bloomington, IN 47408 USA	sowinski@iucf.indiana.edu
Paul Stankus	ORNL	Oak Ridge National Laboratory B 6003, MS 6372 Oak Ridge, TN 37831-6372 USA	stankus@mail.phy.ornl.gov
Peter Steinberg	Columbia Univ.	Nevis Laboratories Columbia Universitiy P.O. Box 137 Irvington, NY 10533 USA	steinber@nevis1.columbia.edu
George Sterman	SUNY, Stony Brook	Institute for Theoretical Physics State University of NY, Stony Brook Stony Brook, NY 11794-3840 USA	sterman@insti.physics.sunysb.edu
Michael Sumbera	Nuclear Physics Institute ASCR	Nuclear Physics Institute ASCR 250 68 Rez Czech Republic	sumbera@ujf.cas.cz
Michael Tannenbaum	BNL	Physics Department, Bldg. 510C Brookhaven National Laboratory Upton, NY 11973 USA	mjt@bnl.gov
Hisayuki Torii	Kyoto Univ.	Building 902C Brookhaven National Laboratory Upton, NY 11973 USA	htorii@bnl.gov

Hard Parton Physics in High Energy Nuclear Collisions

March 1-5, 1999

Organizers: Jim Carroll (LBL), Charles Gale (McGill), Mike Tannenbaum (BNL), and Raju Venugopalan (BNL)

List of Registered Participants

Name	Affiliation	Mailing Address	E-mail address
Kathleen Turner	BNL	Physics Department, Bldg. 510A Brookhaven National Laboratory Upton, NY 11973 USA	kathy@bnl.gov
Raju Venugopalan	BNL	Physics Department, Bldg. 510A Brookhaven National Laboratory Upton, NY 11973 USA	raju@bnl.gov
Werner Vogelsang	SUNY, Stony Brook	Institute for Theoretical Physics State University of NY, Stony Brook Stony Brook, NY 11794-3840 USA	vogelsan@insti.physics.sunysb.edu
Ramona Vogt	LBNL and UC Davis	Mail Stop 70A-3307, LBNL One Cyclotron Road Berkeley, CA 94720 USA	vogt@lbl.gov
Xin-Nian Wang	LBL	Nuclear Science Division LBNL, MS 70A-3307 One Cyclotron Road Berkeley, CA 94720 USA	xnwang@lbl.gov
Urs Wiedemann	Columbia Univ.	Columbia Univ., MS5202 550 West 120th Street New York, NY 10027 USA	awiedema@nt3.phys.columbia.edu
Nu Xu	LBNL	LBNL, MS 50A-1148 One Cyclotron Road Berkeley, CA 94720 USA	nxu@lbl.gov

RIKEN BNL Research Center

Workshop on Hard Parton Physics in High-Energy Nuclear Collisions

March 1–5, 1999

Physics Department - Large Seminar Room

Organizers:

Jim Carroll, Charles Gale, Mike Tannenbaum and Raju Venugopalan

AGENDA

Monday 1 March

Morning

8:30		Registration - Seminar Lounge
Chairman: Raju Venugopalan		
9:00	M. Murtagh	*Welcome and Introduction*
9:15	G. Sterman	*Overview of Hard Parton Physics for RHIC*
10:15	K. Lokhtin	*In-medium Energy Loss and Jet Characteristics in Nuclear Collisions*
10:55		Coffee Break
11:25	X.-N. Wang	*Energy Loss at the SPS*
12:15	B. Kopeliovich	*Phenomenology of Energy Loss and Light Cone Formalism for Bremsstrahlung in Multiple Scattering*
13:05		Lunch

Afternoon

Chairman: Jim Carroll		
14:30	M. Tannenbaum	*Using Leading Particles to Measure Hard Scattering at RHIC*
15:10	M.W. Krasny	*Jets at HERA*
16:00		Coffee
16:30	G. Blazey	*Jets at the Tevatron*
17:10	K. Turner	*Jets and Photon Results from the Tevatron* (30min)

Tuesday 2 March

Morning

Chairman: Dima Kharzeev		
9:00	P. Stankus	*Partons in AA Collisions at RHIC with PHENIX*
9:50	C. Ogilvie	*Angular Correlations Among High p_t Particles in STAR*
10:40		Coffee
11:10	A. H. Mueller	*Parton Equilibration in Nuclear Collisions*

12:00	W. Christie	*STAR Data Sets and Analyses Required to Search for QGP*
12:30	X. Guo	*Gluon Mini-Jet Production in High Energy Nuclear Collisions*
13:00		Lunch

Afternoon

Chairman: Mike Tannenbaum

14:30	U. Weidemann	*Transverse momentum dependence of the Landau-Pomeranchuk-Migdal Effect*
15:00	A. Leonidov	*New Results on Mini-Jet Production in Hadron and Nuclear Collisions*
15:30		Coffee
16:00	T. Cormier	*High p_t π^0's in the First Year at STAR*
16:40	I. Sarcevic	*Partonic Picture of Nuclear Shadowing at Small x* (30min)

Wednesday 3 March

Morning

Chairman: Shigemi Ohta

9:00	J. Peng	*Dilepton Production at Fermilab and at RHIC*
9:50	S. Kumano	*Parton Distributions in Nuclei*
10:40		Coffee
11:10	M. Begel	*Direct Photons from E706*
11:50	P. Aurenche	*Critical Phenomenological Study of Inclusive Photon Production in Hadronic Collisions*
12:30	P. Levai	*Hard Photon vs Neutral Pion Production at RHIC*
13:00		Lunch

Afternoon

Chairman: Rob Pisarski

14:30	T. Awes	*Pion and Direct Photon Production in Pb+Pb Collisions*
15:20	G.J. Kunde	*High p_t Physics with the STAR Ring Imaging Cerenkov Detector*
15:50		Coffee
16:20	L. Frankfurt	*Nuclear Shadowing of Gluon Distribution and Related QCD Phenomena*
17:10	J. Jalilian-Marian	*Nuclear Gluon Shadowing at RHIC and LHC Energies* (30min)
18:30		Conference Dinner

Thursday 4 March

Morning

Chairman: Gerry Bunce

9:00	W. Vogelsang	*Hard Scattering in Polarized pp at RHIC*
9:50	Y. Goto	*Photons in Polarized pp Collisions at PHENIX*

10:20	J. Sowinski	*A Direct Extraction of ΔG at STAR*
10:50		Coffee
11:20	N. Saito	*Study of the Spin-Flavor Structure of the Nucleon with PHENIX*
11:50	A. Ogawa	*Polarization Studies with W 's in STAR*
12:20	D. Boer	*Investigating the Origins of Transverse Spin Asymmetries at RHIC*
12:50		Lunch

Afternoon

Chairman: Dirk Rischke

14:30	Miklos Gyulassy	*Jet Quenching in Thin Plasmas*
15:20	A. Kovner	*Gluons at Small x*
15:50		Coffee
16:10	I. Balitsky	*Scattering of Two Shock Waves and High Energy Effective Action*
1640	Y. Kovchegov	*Multiple Pomeron Exchanges in Nuclear Structure Functions*
17:10	R. Vogt	*Effect of Shadowing on Initial Conditions and Hard Probes in Nuclear Collisions* (30min)

Friday 5 March

Morning

Chairman: Charles Gale

9:00	G. Gustafson	*Multiple Hard Sub-Collisions in Small x Events and Correlations in the Hadronization Process*
9:50	X-N. Wang	*Predictions from HIJING for RHIC*
10:30		Coffee
11:00	R. Longacre	*VNI: Status Update*
11:30	H. Sorge	*Interplay Between Hard and Soft Physics in AA Collisions at RHIC*
12:00	B. Cole	*Impact Parameter Dependence in Hard Scattering*
12:50		Lunch

Afternoon

Chairman: Larry Trueman

14:30	D. Kharzeev	*Hidden and Open Charm at RHIC*
15:20	S. Jeon	*Coherence Time in High Energy Proton–Nucleus Collisions*
16:00	L. McLerran	*Summary talk*
17:00	Wine and Cheese Party	

Forthcoming RIKEN BNL Center Workshops

Title:	**Event Generator for RHIC Spin Physics**
Organizers:	N. Saito/A. Schaefer
Dates:	Mar. 15-19, 1999

Title:	**Numerical Algorithms at Non-Zero Chemical Potential**
Organizers:	T. Blum/M. Creutz
Dates:	Apr. 27–May 1, 1999

Title:	**Gauge Invariant Observables in Gauge Theories**
Organizers:	P. Orland/P. van Baal
Dates:	May 25–29, 1999

Title:	**OSCAR II: Predictions for RHIC**
Organizers:	Y. Pang/M. Gyulassy
Dates:	July 8–16, 1999

Title:	**Coulomb and Pion-Asymmetry Polarimetry and Hadronic Spin Dependence at RHIC Energies**
Organizer:	E. Leader
Date:	August 18, 1999

Title:	**RHIC Spin**
Organizer:	G. Bunce
Dates:	Oct. 6–8, 1999

For information please contact:

Ms. Pamela Esposito
RIKEN BNL Research Center
Building 510A, Brookhaven National Laboratory
Upton, NY 11973, USA
Phone: (516)344-3097 Fax: (516)344-4067
E-Mail: rikenbnl@bnl.gov
Homepage: http://penguin.phy.bnl.gov/www/riken.html

RIKEN BNL RESEARCH CENTER

HARD PARTON PYSICS IN HIGH-ENERGY NUCLEAR COLLISIONS

MARCH 1–5, 1999

Li Keran

Nuclei as heavy as bulls
Through collision
Generate new states of matter.
T. D. Lee

Speakers:

P. Aurenche	T. Awes	I. Balitsky	M. Begel	G. Blazey	D. Boer
W. Christie	B. Cole	T. Cormier	L. Frankfurt	Y. Goto	X. Guo
G. Gustafson	M. Gyulassy	J. Jalilian-Marian	S. Jeon	D. Kharzeev	B. Kopeliovich
Y. Kovchegov	A. Kovner	M.W. Krasny	S. Kumano	G.J. Kunde	A. Leonidov
P. Levai	K. Lokhtin	R. Longacre	L. McLerran	A. Ogawa	C. Ogilvie
J. Peng	N. Saito	I. Sarcevic	H. Sorge	J. Sowinski	P. Stankus
G. Sterman	M. Tannenbaum	K. Turner	W. Vogelsang	R. Vogt	X.-N. Wang
U. Weidemann					

Organizers: Jim Carroll, Charles Gale, Mike Tannenbaum and Raju Venugopalan